

CONSTANT-FREQUENCY, CLAMPED-MODE RESONANT CONVERTERS

by

Fu-Sheng Tsai

Dissertation submitted to the Faculty of the
Virginia Polytechnic Institute and State University
in partial fulfillment of the requirements for the degree of
Doctor of Philosophy
in
Electrical Engineering

APPROVED:

Fred C. Lee, Chairman

Bo H. Cho

Vatche Vorperian

Kwa S. Tam

Ronald D. Riess

December 13, 1989

Blacksburg, Virginia

CONSTANT-FREQUENCY, CLAMPED-MODE RESONANT CONVERTERS

by

Fu-Sheng Tsai

Fred C. Lee, Chairman

Electrical Engineering

(ABSTRACT)

Two novel clamped-mode resonant converters are analyzed. These clamped-mode converters operate at a constant frequency while retaining many desired features of conventional resonant converters such as fast responses, zero-voltage turn-on or zero-current turn-off, and low EMI levels, etc. The converters are able to regulate the output from no load to full load and are particularly suitable for off-line, high-power applications.

To provide insights to the operations and derive design guidelines for the clamped-mode resonant converters, a complete dc characterization of both the clamped-mode series-resonant converter and the clamped-mode parallel-resonant converter, operating above and below resonant frequency, is performed. State-plane analysis techniques are employed. By portraying the converters' operation on a state-plane diagram, various circuit operating modes are identified. The boundaries between different operating modes are determined. The regions for natural and force commutation of the active switches are defined. Important dc characteristics, such as control-to-output transfer ratio, rms inductor current, peak capacitor voltage, rms switch currents, average diode currents, switch turn-on currents, and switch turn-off currents, are derived to facilitate the converter designs.

To illustrate the converter designs in different operating regions, several design examples are given. Finally, three prototype circuits are built to verify the analytical results.

Acknowledgements

I would like to express my sincere appreciation to my advisor, Dr. Fred C. Lee, for his guidance, support, and encouragement during the course of this research work. His extensive knowledge, creative thinking, and patience have been invaluable help and are very much appreciated.

I also owe my gratitude to Dr. Bo H. Cho, Dr. Vatchè Vorperian, Dr. Kwa S. Tam, and Dr. Ronald D. Riess for their teaching, suggestions, and discussions, and their kindness to serve as my committee members.

I am thankful to my old colleagues, _____, _____, and my fellow student, _____, for their help in obtaining the experimental results used in this thesis.

Thanks also extend to all the VPEC members for their friendship which has made my stay at Virginia Tech an enjoyable one.

Special thanks go to VPEC secretary _____, who is always kind and ready to help, and _____, who has done excellent jobs in editing my manuscripts.

I would like to give my heartfelt appreciation to my parents, _____ and _____, for their never-ending efforts to provide me with good education opportunities, and my sisters, _____, _____, _____, for helping me taking care of my mother while I was away. Most of all, I would like to thank my beloved wife, _____, for her continuous support and understanding during the course of my study and my daughter, _____, who has brought so much joyfulness into my life.

Finally, I would like to thank EG&G Almond Instruments, NASA Lewis Research Center, and Rocketdyne Division, Rockwell International for their financial support during my stay.

TABLE OF CONTENTS

CHAPTER 1. INTRODUCTION

1.1 General Background	1
1.2 Derivation of Clamped-Mode Resonant Converters	10
1.3 State-Plane Analysis Techniques	14

CHAPTER 2. ANALYSIS OF CLAMPED-MODE SERIES-RESONANT CONVERTER

2.1 Introduction	15
2.2 Circuit Operation	17
2.3 State-Plane Analysis	22
2.3.1 Assumptions	22
2.3.2 Circuit topological modes	22
2.3.3 State trajectories for circuit topological modes	25
2.3.4 Equilibrium trajectories	27
2.3.5 Circuit operating modes	32
2.3.6 Regions of operation	55
2.3.7 DC characteristics	64
2.4 Design Examples	85
2.4.1 Example 1 - Design in natural-commutation region	86
2.4.2 Example 2 - Design in mixed-commutation region	93

2.4.3 Example 3 - Design in force-commutation region	101
2.5 Hardware Verifications	109
2.5.1 Circuit operating modes below resonant frequency	109
2.5.2 Circuit operating modes above resonant frequency	123
2.6 Conclusions	130

CHAPTER 3. ANALYSIS OF CLAMPED-MODE PARALLEL-RESONANT CONVERTER

3.1 Introduction	132
3.2 Circuit Operation	134
3.3 State-Plane Analysis	139
3.3.1 Assumptions	139
3.3.2 Circuit topological modes	139
3.3.3 State trajectories for circuit topological modes	145
3.3.4 Equilibrium trajectories	148
3.3.5 Circuit operating modes	151
3.3.6 Regions of operation	179
3.3.7 DC characteristics	183
3.4 Design Examples	195
3.4.1 Example 1 - Design in natural-commutation region	196
3.4.2 Example 2 - Design in mixed-commutation region	201
3.4.3 Example 3 - Design in force-commutation region	203
3.5 Hardware Experiments	211
3.6 Conclusions	215
CHAPTER 4. CONCLUSIONS	217

APPENDIX A. DERIVATION OF CLAMPED-MODE, PARALLEL-RESONANT CONVERTER	225
--	------------

APPENDIX B. SUPPLEMENTS TO CHAPTER 2

B.1 Rules for Constructing Equilibrium State Trajectories of a CM-SRC	228
B.2 Prediction of Mode Transitions of a CM-SRC Operating Below Resonant Frequency	232
B.3 Prediction of Mode Transitions of a CM-SRC Operating Above Resonant Frequency	249
B.4 Calculation of Trajectory Parameters of a CM-SRC Operating Below Resonant Frequency	257
B.5 Expressions for Circuit Salient Features of a CM-SRC Operating Below Resonant Frequency	271
B.6 DC Characteristics of a CM-SRC Operating Below Resonant Frequency ...	279
B.7 Calculation of Trajectory Parameters of a CM-SRC Operating Above Resonant Frequency	285
B.8 Expressions for Circuit Salient Features of a CM-SRC Operating Above Resonant Frequency	294
B.9 DC Characteristics of a CM-SRC Operating Above Resonant Frequency ...	297
B.10 Generation of Circuit Waveforms of a CM-SRC	303

APPENDIX C. SUPPLEMENTS TO CHAPTER 3

C.1 Rules for Constructing Equilibrium State Trajectories of a CM-PRC	318
---	-----

C.2 Prediction of Mode Transitions of a CM-PRC Operating Below Resonant	
Frequency	323
C.3 Prediction of Mode Transitions of a CM-PRC Operating Above Resonant	
Frequency	334
C.4 Calculation of Trajectory Parameters of a CM-PRC	344
C.5 Calculations of Circuit Salient Features of a CM-PRC	377
C.6 DC Characteristics of a CM-PRC Operating Below Resonant Frequency ...	388
C.7 DC Characteristics of a CM-PRC Operating Above Resonant Frequency ..	391
C.8 Generation of Circuit Waveforms of a CM-PRC	397

CHAPTER 1.

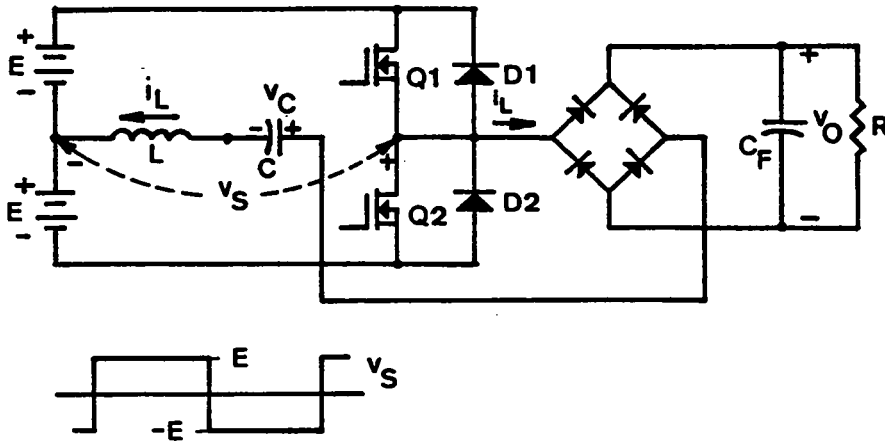
INTRODUCTION

1.1 GENERAL BACKGROUND

In recent years, resonant power conversion technology has gained much attention in power conversion applications [1-32]. Due to their distinct advantages, such as fast response, high efficiency, reduced switch stresses, and low EMI (electromagnetic interference) levels, resonant power processors have gradually taken over roles previously dominated by the pulse-width-modulated (PWM) converters.

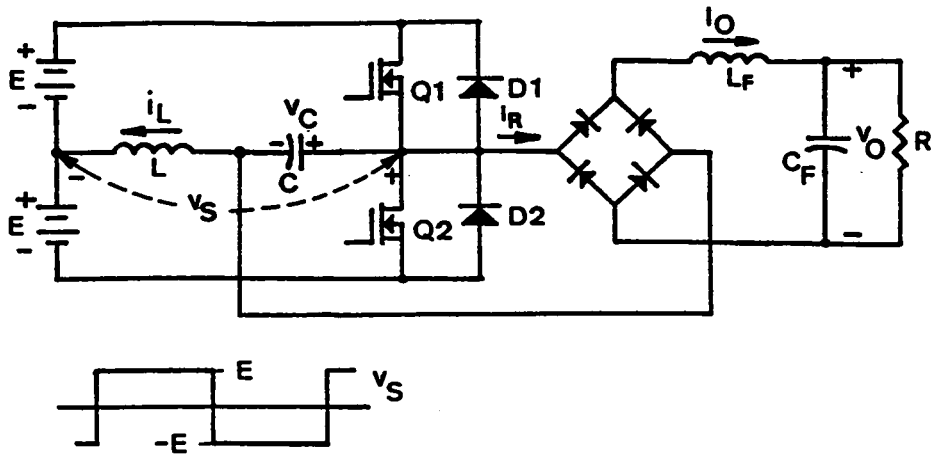
The major advantage of resonant converters, as compared to PWM converters, is their ability to eliminate switching losses by commutating the switches at zero voltage and/or zero current. As a result, resonant converters can be operated at much higher frequencies than PWM converters. The increase in operating frequency reduces the size of magnetic components, thus increasing the converters' power density.

Conventional resonant converters have bridge configurations, as illustrated in Figure 1.1. An LC resonant tank is used to transfer energy from input to the load. The two controlled switches are triggered with 50%-duty-cycle gating signals such that a square-wave voltage, v_S , is generated across the resonant tank. The output is obtained by rectifying and filtering the sinusoidal-like resonant inductor current (series-resonant



(a) Series-resonant converter (SRC)

Figure 1.1 Conventional Series- and Parallel-Resonant Converters



(b) Parallel-resonant converter (PRC)

Figure 1.1 Continued

converter) or resonant capacitor voltage (parallel-resonant converter). The output voltage regulation is achieved by varying the operating frequency.

Depending upon the operating frequency and the load, the controlled switches in the resonant converters can be naturally commutated or force commutated [18,19,31]. In general, natural commutation of the switches occurs when the converter operates below the resonant frequency of the LC tank, while force commutation occurs when the converter operates above the tank's resonant frequency.

When natural commutation is achieved, the switches' turn-off losses are eliminated. However, since the diodes are commutated at high currents fast antiparallel diodes are required to minimize the cross conductions in the totem-pole switch-diode pairs caused by the reverse recovery of the diodes. When force-commutation is achieved, the power switches operate with zero-voltage turn-on and the switches' turn-on losses are eliminated. Slow antiparallel diodes and simple losseless capacitor snubbers can be used for the switches since the diodes are commutated at zero current and the switches always turn on at zero voltage.

Due to the line and/or load variations, the operating frequency of the conventional resonant converters usually has to vary over a wide range to regulate their outputs. This results in a penalty in the magnetics and filter design and lowers the overall conversion efficiency.

To optimize the design of magnetic components and filters, several circuit topologies and control techniques able to operate at a constant frequency were proposed [33-46].

Figure 1.2 shows a parallel-resonant converter (PRC) with a controlled output rectifier. The converter's operating frequency is fixed. Its output is controlled by varying the conduction intervals of the output controlled switches [33,34]. Although the converter is able to regulate its output over a wide load range and is bidirectional, it is only suitable for low-current, high-voltage applications since the output controlled switches introduce additional losses.

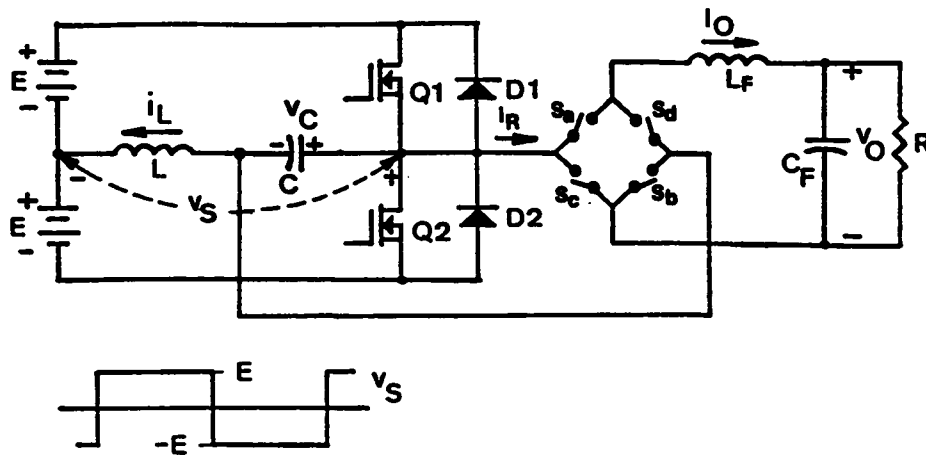
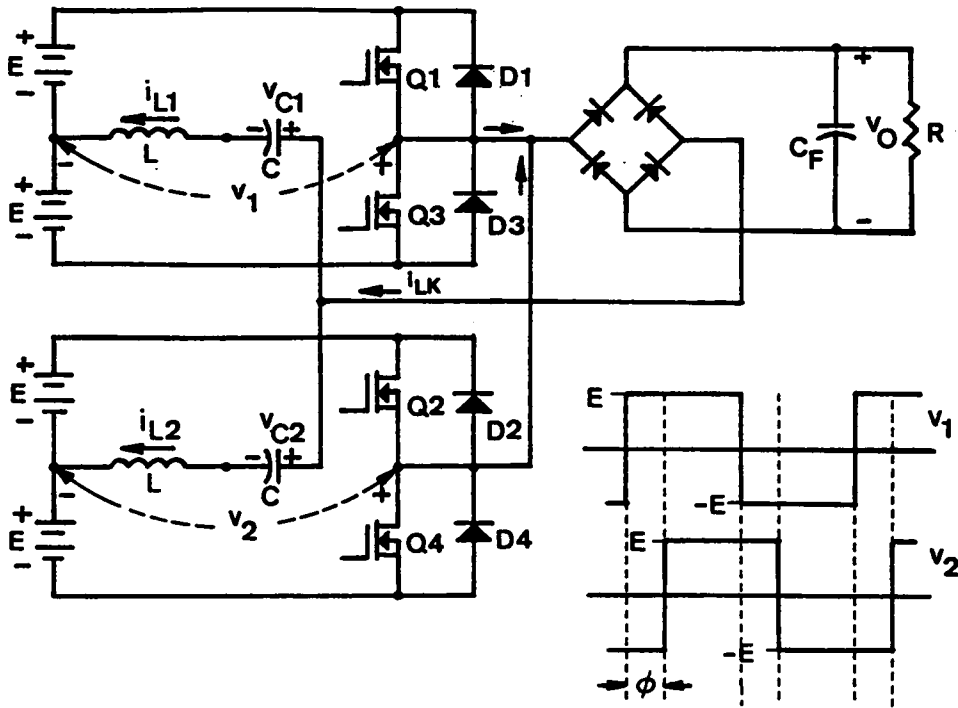


Figure 1.2 A Parallel-Resonant Converter with a Controlled Output Rectifier

A phase-control scheme was introduced which employs two identical series- or parallel- resonant inverters with their outputs connected in parallel or in series, respectively, to a common load [35,36,37], as shown in Figure 1.3. The two resonant inverters are driven by gating signals which have the same frequency but have different phases. The outputs of the converters are controlled by varying the phase displacement between the gating signals. These phase-controlled converters are able to regulate their outputs from no load to full load. However, due to the phase displacement of the two inverters, the effective load power factor seen by each inverter is different. As a result, the inductor currents and capacitor voltages in the resonant tanks of the inverters are unbalanced. This introduces high component stresses in one of the resonant inverters [37]. Also, high circulating currents exist in the inverters under light load since the exciting frequency of the inverters remains unchanged.

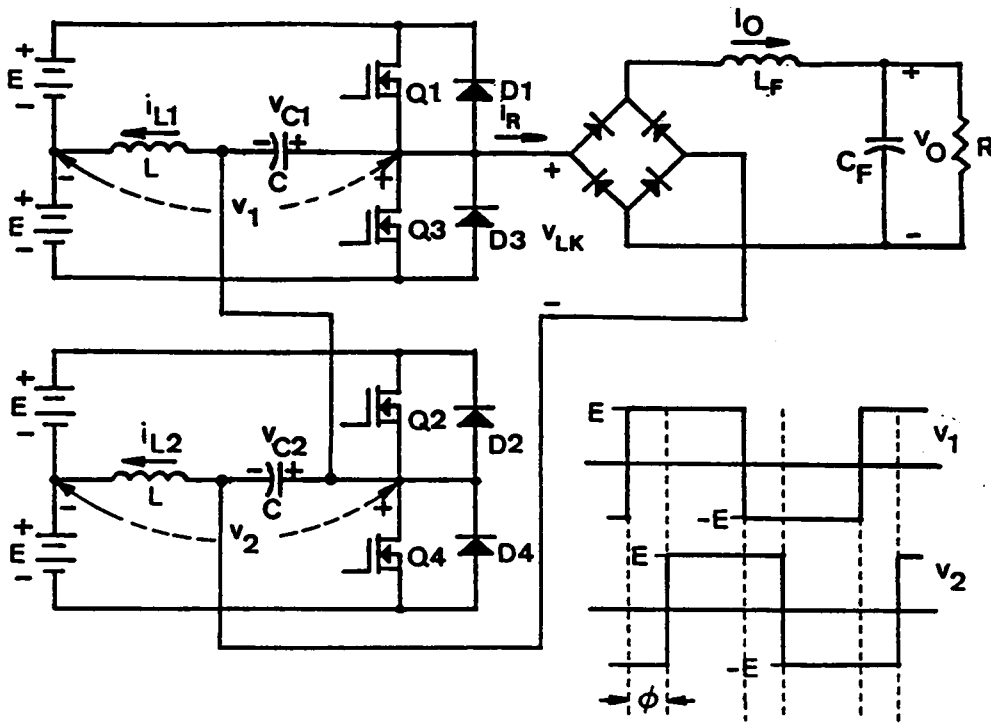
The pseudo-resonant converter proposed in Reference [38] is an analogy to the phase-controlled converters.

To alleviate the current and voltage imbalance and reduce the circulating currents under light load, the two phase-controlled resonant inverters can be combined. This results in two new clamped-mode, resonant converters which are functional equivalence to their phase-controlled counterparts. The circuit topologies of the clamped-mode resonant converters are the same as those of conventional full-bridge resonant converters. However, they operate under a quite different principle. As illustrated in Figure 1.4(d) and 1.4(e), the switched input voltage v_S to the resonant tank of a clamped-mode resonant converter is a fixed-frequency, duty-cycle-modulated, quasi-square wave, instead of a frequency-modulated square wave in the conventional resonant converters. The output of the converter is controlled by varying the time interval, ϕ_S/ω_S as shown in Figure 1.4(e), during which voltage v_S is "clamped" at zero volt. These converters are therefore referred in the text as "*clamped-mode resonant converters*". The fact that clamped-mode resonant converters possess the same desired output characteristics as the



(a) Phase-controlled series-resonant converter

Figure 1.3 Phase-Controlled Resonant Converters



(b) Phase-controlled parallel-resonant converter

Figure 1.3 Continued

phase-controlled converters while alleviating their aforementioned shortcomings makes these converters very attractive. It is a major goal of this research to fully characterize the dc behaviors of these two clamped-mode resonant converters and provide systematic design guidelines.

1.2 DERIVATION OF CLAMPED-MODE RESONANT CONVERTERS

Figure 1.4 illustrates how the clamped-mode series-resonant converter is derived by combining the two phase-controlled resonant inverters. The outputs of the inverters are connected in parallel. Viewing tank voltages v_1 and v_2 as new voltage sources, a simplified equivalent circuit is shown in Figure 1.4(b). The circuit equations for the phase-controlled, series-resonant converter (PC-SRC) are

$$v_1 = v_O + v_{C1} + L \frac{di_{L1}}{dt}, \quad (1.1)$$

$$i_{L1} = C \frac{dv_{C1}}{dt}, \quad (1.2)$$

$$v_2 = v_O + v_{C2} + L \frac{di_{L2}}{dt}, \quad (1.3)$$

$$i_{L2} = C \frac{dv_{C2}}{dt}, \quad (1.4)$$

and

$$i_O = i_{L1} + i_{L2}. \quad (1.5)$$

Adding (1.1) to (1.3) and (1.2) to (1.4), we obtain

$$(v_1 + v_2) = 2v_O + (v_{C1} + v_{C2}) + L \left(\frac{di_{L1}}{dt} + \frac{di_{L2}}{dt} \right), \quad (1.6)$$

and

$$(i_{L1} + i_{L2}) = C \left(\frac{dv_{C1}}{dt} + \frac{dv_{C2}}{dt} \right). \quad (1.7)$$

Rewriting (1.6) and (1.7), we have

$$\frac{(v_1 + v_2)}{2} = v_o + \frac{(v_{C1} + v_{C2})}{2} + \left(\frac{L}{2} \right) \frac{d}{dt} (i_{L1} + i_{L2}), \quad (1.8)$$

$$(i_{L1} + i_{L2}) = (2C) \frac{d}{dt} \left(\frac{v_{C1} + v_{C2}}{2} \right). \quad (1.9)$$

From Eqs. (1.5),(1.8), and (1.9), viewing $(v_{C1} + v_{C2})/2$ and $(i_{L1} + i_{L2})$ as new state variables, an equivalent circuit can be derived, as shown in Figure 1.4(c), where

$$v_C = \frac{(v_{C1} + v_{C2})}{2}, \quad (1.10)$$

$$i_L = (i_{L1} + i_{L2}), \quad (1.11)$$

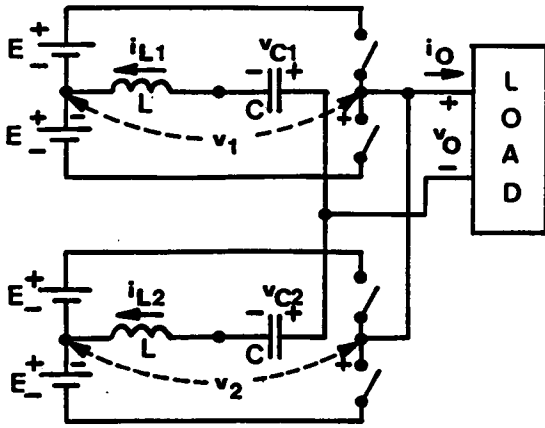
and

$$v_S = \frac{(v_1 + v_2)}{2}. \quad (1.12)$$

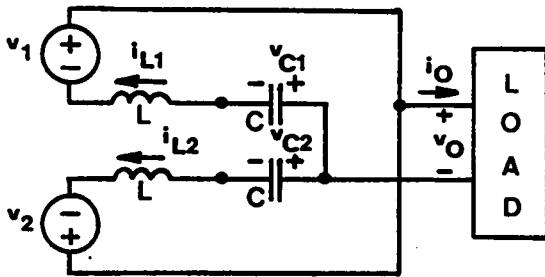
The voltage, v_S , as shown in Figure 1.4(c), is a quasi-square wave with pulse width, β_S , determined by the phase displacement between v_1 and v_2 . The zero-voltage period of v_S is equal to the phase displacement, ϕ_S , between v_1 and v_2 . Such a voltage can be realized using a full-bridge circuit, as shown in Figure 1.4(d), by operating switches S1,S2,S3, and S4 in a fashion illustrated in Figure 1.4(f). When switches S1 and S4 or S2 and S3 are both on, v_S is clamped at zero volts. Otherwise, v_S is equal to either $+E$ or $-E$. A full-

bridge, series-resonant converter is referred to as "*clamped-mode, series-resonant converter (CM-SRC)*" when it is operated in such a fashion.

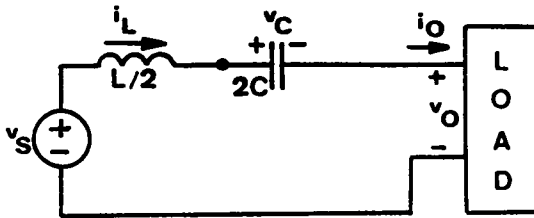
Following a similar manner, a "*clamped-mode, parallel-resonant converter (CM-PRC)*" can be derived from a phase-controlled, parallel-resonant converter (PC-PRC), as illustrated in Appendix A.1.



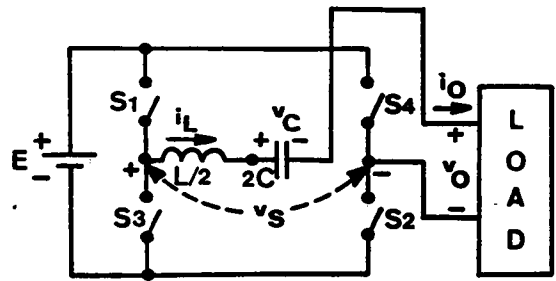
(a) A PC-SRC



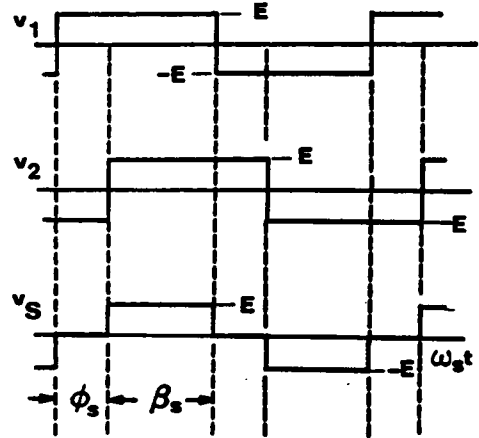
(b) Simplified circuit



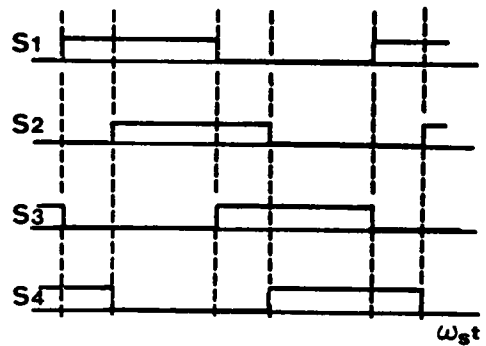
(c) Equivalent circuit



(d) A CM-SRC



(e) Equivalent source voltage



(f) Switch conduction sequence

Figure 1.4 Derivation of Clamped-Mode Series-Resonant Converter (CM-SRC)

1.3 STATE-PLANE ANALYSIS TECHNIQUES

Many different analysis techniques have been used to characterize the dc behaviors of resonant converters [1,14-15,18-19,33-34]. Due to the complexity of the circuit operation, most analytical work presented to date are numerical in nature. In general, a computer method numerically calculates the instantaneous current and voltage in the resonant tank and determines the steady state by comparing the values of inductor current and capacitor voltage a half switching period away [1]. This approach, although simple and straightforward, provides no physical insights to the converter's behaviors.

A piece-wise linear circuit approach divides a steady-state operation into several switching intervals and derive expressions for the current and voltage during each interval. Boundary conditions are matched to determine the steady-state values for the current and voltage [33,34]. This approach, however, has to assume the phase relationship between certain circuit waveforms which is sometimes unpredictable.

Graphical techniques have recently been employed in the analysis of resonant converters [14-15,18-19,31]. The advantage of these approaches is their ability to illustrate graphically the converter's behavior on a planar diagram. The complex circuit operation can be easily visualized and many less familiar operating modes uncovered. Important circuit features can be derived from the geometrical relationship easily identified in the diagram.

Among the two graphical approaches, the state-plane analysis technique is more powerful than the output-plane technique. The state-plane technique monitors the instantaneous resonant inductor current and the instantaneous resonant capacitor voltage and provides better insights to the converter operation.

In Chapter 2 and Chapter 3, state-plane techniques are employed to characterize the dc behaviors of the clamped-mode, series-resonant and the clamped-mode, parallel-resonant converters.

CHAPTER 2.

ANALYSIS OF CLAMPED-MODE SERIES RESONANT CONVERTER

2.1 INTRODUCTION

In designing a conventional series-resonant converter(SRC), two operating frequency ranges are usually considered. One is below the resonant frequency (often between 50% and 100% of the resonant frequency) where zero-current turn-off (natural commutation) of the controlled switches is achieved, thus eliminating the turn-off losses and stresses of the switches. The other is above resonant frequency where zero-voltage turn-on of the switches is achieved, thus eliminating the turn-on losses of the switches. When an SRC operates below resonant frequency, fast antiparallel diodes are required for the switches since these diodes are commutated at high currents. While, when an SRC operates above the resonant frequency, slower antiparallel diodes can be used for the switches since the diodes turn off at zero current. A simple lossless capacitor snubber can be employed for the switches to reduce their turn-off losses since the switches always turn on at zero voltage.

Similar to SRC, a clamped-mode series-resonant converter (CM-SRC) can be designed to operate either below or above the resonant frequency to obtain either zero-current turn-off or zero-voltage turn-on. The design is, however, more complicated.

For a CM-SRC, three modes of commutation can exist: (1) all the controlled switches are naturally commutated; this mode is referred to as "*natural commutation*"; (2) two of the switches in one leg of the bridge are naturally commutated and the other two switches are force commutated; the two switches which are force commutated are nevertheless operating with zero-voltage turn-on; this mode is referred to as "*mixed commutation*"; (3) all the switches are force commutated (or zero-voltage turn on); this mode is referred to as "*forced commutation*". It should be noticed that in the context of this thesis, the forced commutation mode is always associated with zero-voltage turn-on property. This is, however, not necessarily the case in general. When a CM-SRC operates below the resonant frequency, the switches may be operated under natural commutation or mixed commutation. When a CM-SRC operates above the resonant frequency, the switches may be operated under forced commutation or mixed commutation.

To provide insights to the converter's operation and derive guidelines for the converter design, a complete dc characterization of the CM-SRC is presented in this chapter. Graphical state-plane techniques are employed to identify various circuit operating modes for the converter. The boundaries between different operating modes are determined. The regions for natural, mixed, and force commutation are specified. Important dc control-to-output characteristics are derived. Three design examples are given. Finally, the analytical results are verified using two breadboard circuits.

2.2 CIRCUIT OPERATION

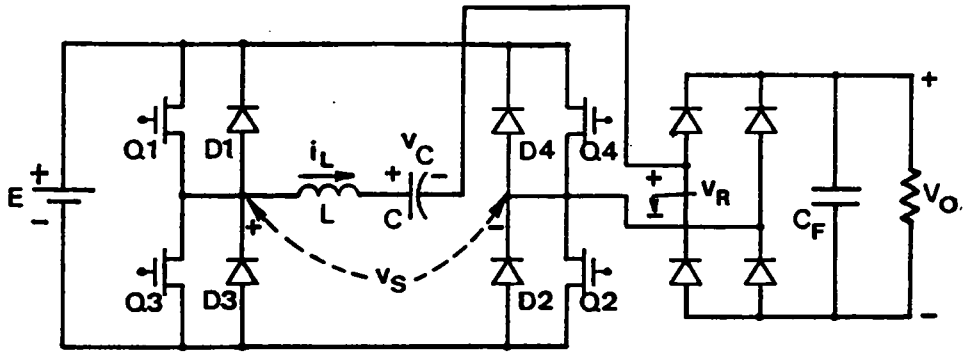
Figure 2.1(a) shows a clamped-mode, series-resonant converter with the controlled switches S1,S2,S3,S4 in Figure 1.4(d) implemented by transistors Q1,Q2,Q3,Q4 and their antiparallel diodes D1,D2,D3,D4, respectively. The transistors are triggered in a timing sequence as illustrated in Figure 2.1(b). All the transistors are driven with 50% duty-cycle gating signals. Transistors Q1,Q3 are triggered according to a clock signal whose frequency determines the converter's operating frequency. Transistors Q2,Q4 are triggered with a controllable time delay, $\frac{\phi_S}{\omega_S}$, with respect to the triggering of Q1,Q3, respectively. The time delay is the interval during which the resonant tank is clamped as a short circuit. By controlling the time delay, the pulse-width, β_S , of the quasi-square-wave voltage, v_S , is controlled and the converter's output voltage, V_O , is regulated.

Depending upon the operating conditions, a CM-SRC can result in different modes of operation. Each mode of operation represents a unique conduction sequence of the switching devices, and is characterized by different circuit waveforms and device commutation requirements.

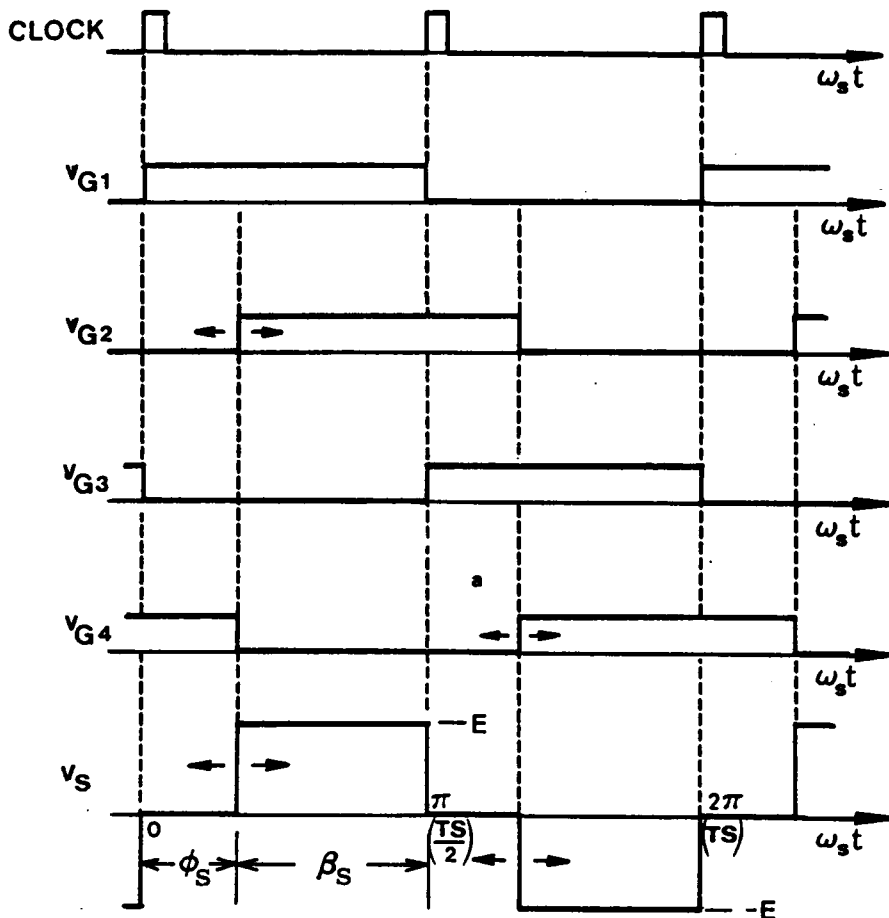
A typical circuit operation of a CM-SRC operating below the resonant frequency is illustrated in Figure 2.2. Prior to $t = 0$, diodes D3,D4 are conducting. At $t = 0$, transistor Q1 turns on and diode D3 is commutated and the inductor current, i_L , resonates through Q1,D4. At $t = t_1$, transistor Q2 is triggered. Diode D4 is commutated and i_L resonates through Q1,Q2. At $t = t_2$, i_L decreases to zero due to resonance. Transistors Q1,Q2 turn off naturally and diodes D1,D2 conduct subsequently. The inductor current, i_L , resonates through D1,D2. At the end of the half switching cycle, $t = \frac{T_S}{2}$, transistor Q3 turns on, commutating diode D1 and a similar process repeats with the roles of Q1,Q2,D1,D2 and Q3,Q4,D3,D4 interchanged, respectively. The reflected load voltage, v_R , changes polarity whenever i_L crosses the zero-axis.

A typical circuit operation of a CM-SRC operating above the resonant frequency is illustrated in Figure 2.3. At $t=0$, transistor Q3 is forced off and Q1 is triggered. Since the inductor current i_L is negative, Q1 cannot conduct. Instead, diode D1 conducts. The inductor current, i_L , resonates through Q4 and D1. At $t=t_1$, transistor Q4 is forced off and Q2 is triggered. Transistor Q2 cannot conduct since i_L is still negative. Instead, diode D2 conducts. The inductor current i_L resonates through D1 and D2. At $t=t_2$, i_L increases to zero. Diodes D1 and D2 commute naturally and transistors Q1 and Q2 conduct subsequently. The inductor current, i_L , resonates through Q1 and Q2. At the end of the half switching cycle, $t = \frac{T_s}{2}$, transistor Q1 is forced off. and Q3 is triggered. A similar process occurs with the roles of Q1,Q2,D1,D2 and Q3,Q4,D3,D4 interchanged, respectively. The reflected load voltage, v_R , changes polarity whenever i_L crosses the zero-axis.

In the examples discussed above, the commutation features of the transistors Q1,Q2,Q3,Q4, and the diodes D1,D2,D3,D4 are the same as those in a conventional SRC. The commutation feature for the devices, however, can be different if the operating condition of the converter changes, as shall be discussed in later sections.



(a) Circuit diagram



(b) Gating Signals

Figure 2.1 A Clamped-Mode Series-Resonant Converter

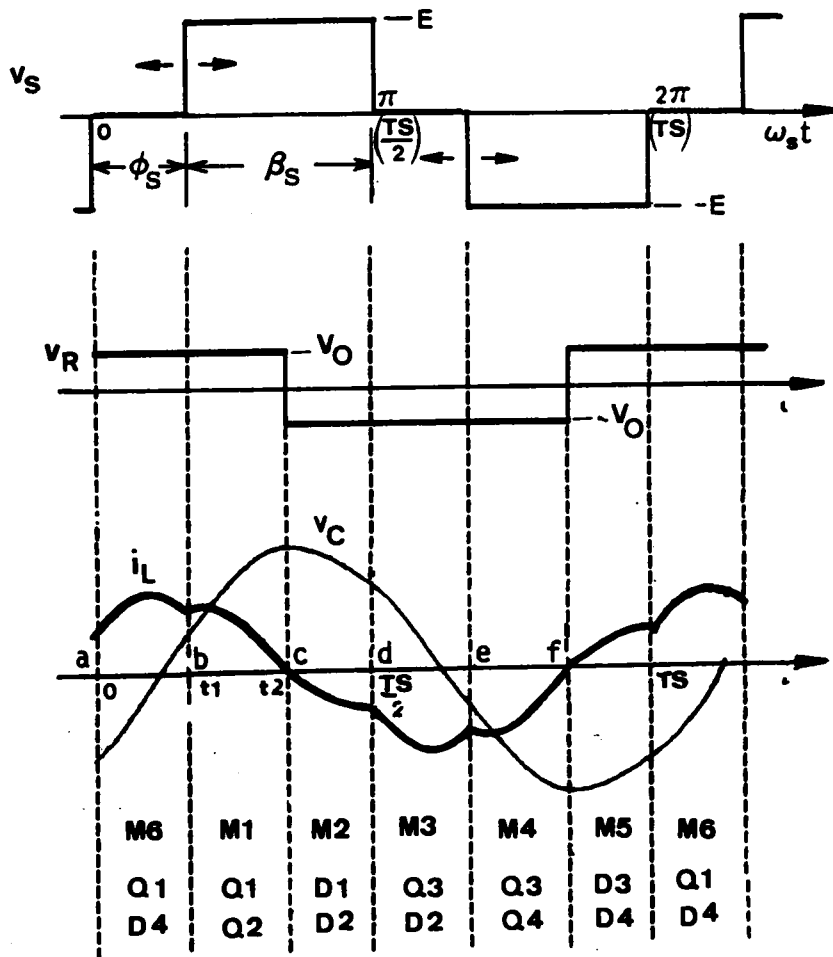


Figure 2.2 A Typical Circuit Operation Below Resonant Frequency

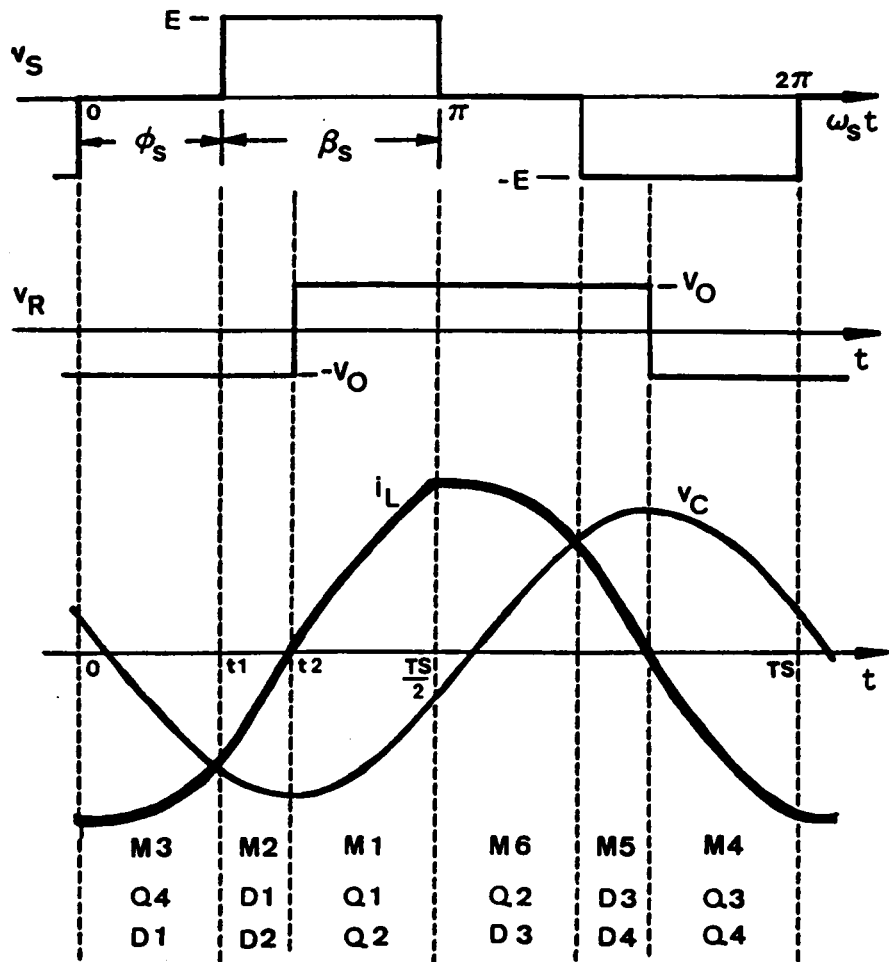


Figure 2.3 A Typical Circuit Operation Above Resonant Frequency

2.3 STATE-PLANE ANALYSIS

In this section, graphical state-plane techniques are employed to characterize the CM-SRC. The state-plane analysis enables one to visualize the converter's complex behavior from a state portrayal and derive various important circuit features such as control-to-output transfer ratio, rms inductor current, peak capacitor voltage, rms switch currents, average diode currents, etc. from the state trajectory, which significantly simplifies the analysis.

2.3.1 Assumptions

The following assumptions are made during the analysis:

1. all the transistors are ideal, with zero switching time and no conduction drop;
2. the quality factor of the resonant tank is infinite; in other words, there is no loss in the tank circuit;
3. the output filter is large enough such that the output voltage, V_O , can be assumed constant during several switching cycles;
4. the transistors are driven with ideal 50%-duty-cycle gating signals;
5. the switching frequency of the converter is greater than 50% of the resonant frequency.

2.3.2 Circuit Topological Modes

As illustrated in Figures 2.2 and 2.3, the one-cycle operation of a CM-SRC is composed of a sequence of linear circuits, each corresponding to a particular switching interval. There are seven linear circuit topologies for a CM-SRC, as shown in Figure 2.4. These circuit topologies are referred to as **circuit topological modes** of a CM-SRC. The topological modes M1,M2,M3,M4,M5, and M6 are called "resonant modes" and topological mode M0 is called "recess mode". The circuit behaviors of a CM-SRC under each topological mode can be described using the following differential equations.

For resonant modes M1,M2,M3,M4,M5, and M6,

$$\begin{aligned} L \frac{di_L}{dt} + v_C &= v_E, \\ C \frac{dv_C}{dt} &= i_L, \end{aligned} \tag{2.1}$$

where,

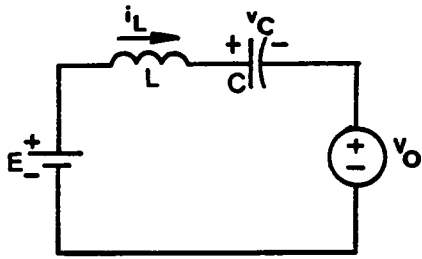
$$v_E = \begin{cases} E - V_O & \text{for M1,} \\ E + V_O & \text{for M2,} \\ V_O & \text{for M3,} \\ -E + V_O & \text{for M4,} \\ -E - V_O & \text{for M5,} \\ -V_O & \text{for M6.} \end{cases}$$

For recess mode M0,

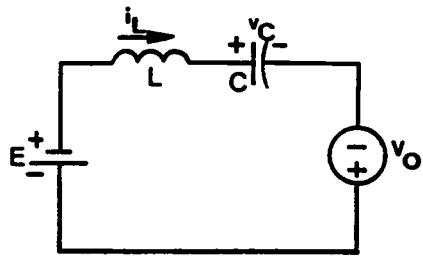
$$\begin{aligned} L \frac{di_L}{dt} &= 0, \\ C \frac{dv_C}{dt} &= 0. \end{aligned} \tag{2.2}$$

By solving these differential equations, expressions for i_L and v_C in each topological mode can be derived. The expressions are normalized and shown in the following.

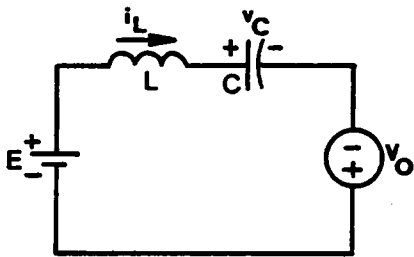
For resonant modes M1,M2,M3,M4,M5, and M6,



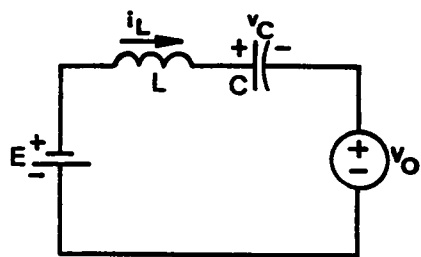
• M1: Q1, Q2 on ($i_L > 0$)



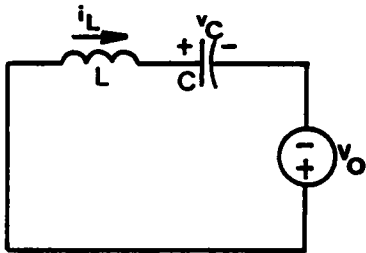
• M4: Q3, Q4 on ($i_L < 0$)



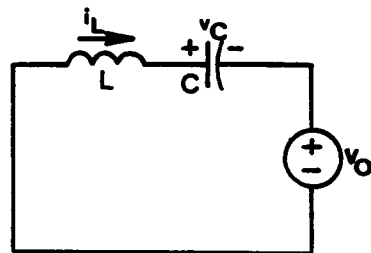
• M2: D1, D2 on ($i_L < 0$)



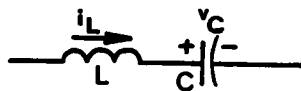
• M5: D3, D4 on ($i_L > 0$)



• M3: Q3, D2 or Q4, D1 on ($i_L < 0$)



• M6: Q1, D4 or Q2, D3 on ($i_L > 0$)



• M0: None of the devices on ($i_L = 0$)

Figure 2.4 Circuit Topological Modes of a CM-SRC

$$\begin{aligned}
i_{LN} &= -(V_{CON} - v_{EN}) \sin \omega_0(t - t_0) + I_{LON} \cos \omega_0(t - t_0) \\
v_{CN} &= (V_{CON} - v_{EN}) \cos \omega_0(t - t_0) + I_{LON} \sin \omega_0(t - t_0) + v_{EN}
\end{aligned} \tag{2.3}$$

where, t_0 is the initial time and

$$\begin{aligned}
\omega_0 &= \frac{1}{\sqrt{LC}} && \text{is the angular resonant frequency,} \\
Z_0 &= \sqrt{\frac{L}{C}} && \text{is the characteristic impedance,} \\
v_{CN} &= \frac{v_C}{E} && \text{is the normalized capacitor voltage,} \\
i_{LN} &= \frac{i_L}{E/Z_0} && \text{is the normalized inductor current,} \\
V_{CON} &= \frac{V_{CO}}{E} && \text{is the normalized initial capacitor voltage,} \\
I_{LON} &= \frac{I_{LO}}{E/Z_0} && \text{is the normalized initial inductor current,} \\
v_{EN} &= \frac{v_E}{E}.
\end{aligned}$$

For recess mode M0,

$$\begin{aligned}
i_{LN} &= 0, \\
v_{CN} &= V_{CON}.
\end{aligned} \tag{2.4}$$

The normalizing factors for the voltages and currents are E and E/Z_0 , respectively.

2.3.3 State Trajectories for Circuit Topological Modes

Table 2.1 Trajectory Equations for Various Circuit Topological Modes

Topo'l Modes	State Trajectory Equations	Trajectory Centers (v_{CN}, i_{LN})
M1	$i_{LN}^2 + (v_{CN} - (1 - V_{ON}))^2 = I_{LON}^2 + (1 - V_{ON} - V_{CON})^2$	$(1 - V_{ON}, 0)$
M2	$i_{LN}^2 + (v_{CN} - (1 + V_{ON}))^2 = I_{LON}^2 + (1 + V_{ON} - V_{CON})^2$	$(1 + V_{ON}, 0)$
M3	$i_{LN}^2 + (v_{CN} - V_{ON})^2 = I_{LON}^2 + (V_{ON} - V_{CON})^2$	$(V_{ON}, 0)$
M4	$i_{LN}^2 + (v_{CN} + (1 - V_{ON}))^2 = I_{LON}^2 + (-1 + V_{ON} - V_{CON})^2$	$(-1 + V_{ON}, 0)$
M5	$i_{LN}^2 + (v_{CN} + (1 + V_{ON}))^2 = I_{LON}^2 + (-1 - V_{ON} - V_{CON})^2$	$(-1 - V_{ON}, 0)$
M6	$i_{LN}^2 + (v_{CN} + V_{ON})^2 = I_{LON}^2 + (-V_{ON} - V_{CON})^2$	$(-V_{ON}, 0)$
M0	$i_{LN} = 0, \quad v_{CN} = V_{CON}$	<i>None</i>

The trajectories for resonant modes M1, M2, M3, M4, M5, and M6, when plotted in the state plane (v_{CN} versus i_{LN} plane), are circular arcs with centers located at $(v_{EN}, 0)$ and radii $R = \sqrt{(v_{EN} - V_{CON})^2 + I_{LON}^2}$. Table 2.1 summarizes the trajectory equations. A family of trajectories for each resonant topological mode is plotted in Figure 2.5, where the centers of M1-M6 are indicated by m1-m6, respectively. These trajectories are half-circles since the polarity of i_L in each topological mode is either positive or negative. The state trajectory corresponding to a particular switching interval is a segment of these trajectories determined by the topological mode, the initial conditions of the inductor current and the capacitor voltage, and the duration of the interval. Time is implicit in these trajectories. The time elapsed in a trajectory segment is measured by the angle subtended by the segment with respect to its center. For example, the time elapsed from point **a** to point **b** in topological mode M1 in Figure 2.5 is $\Delta t = \gamma/\omega_0$. As time advances, the state trajectories travel clockwise as indicated by the arrows.

The trajectory for the recess mode M0 is a stationary point lying on the v_{CN} -axis. The coordinate of the stationary point is either $(V_{CON}, 0)$ or $(-V_{CON}, 0)$. A finite amount of time elapses at the stationary point since both i_{LN} and v_{CN} are independent of time. A circle is used in the state plane to indicate such a stationary point, as illustrated in Figure 2.5. This topological mode occurs when none of the switching devices are conducting. In other words, all the switching devices are either reverse-biased or not triggered.

2.3.4 Equilibrium Trajectory

A steady-state operation of a CM-SRC can be represented by an equilibrium trajectory in the state plane [18,19,31]. An equilibrium trajectory is a closed contour composed of several trajectory segments. It is symmetric with respect to the origin and is constructed via a particular sequence of circuit topological modes determined by the circuit operation. An equilibrium trajectory constructed via a different topological mode

sequence represents a different device conducting sequence, thus corresponding to a different circuit operating mode.

An equilibrium state trajectory of a CM-SRC can be constructed using a composite diagram generated by overlapping the families of trajectories in Figure 2.5 on the same i_{LN} , v_{CN} axes, as shown in Figure 2.6. The rules for constructing an equilibrium trajectory on the composite diagram are summarized in Appendix B.1. Figure 2.7 shows an example illustrating the construction of an equilibrium trajectory on the composite diagram. The constructed trajectory corresponds to the circuit operation described in Figure 2.2, where M6(M3) is initiated when Q1(Q3) is triggered at point a(d), M1(M4) is initiated when Q2(Q4) is triggered at point b(e), and M2(M5) is initiated when i_L reverses polarity at point c(f).

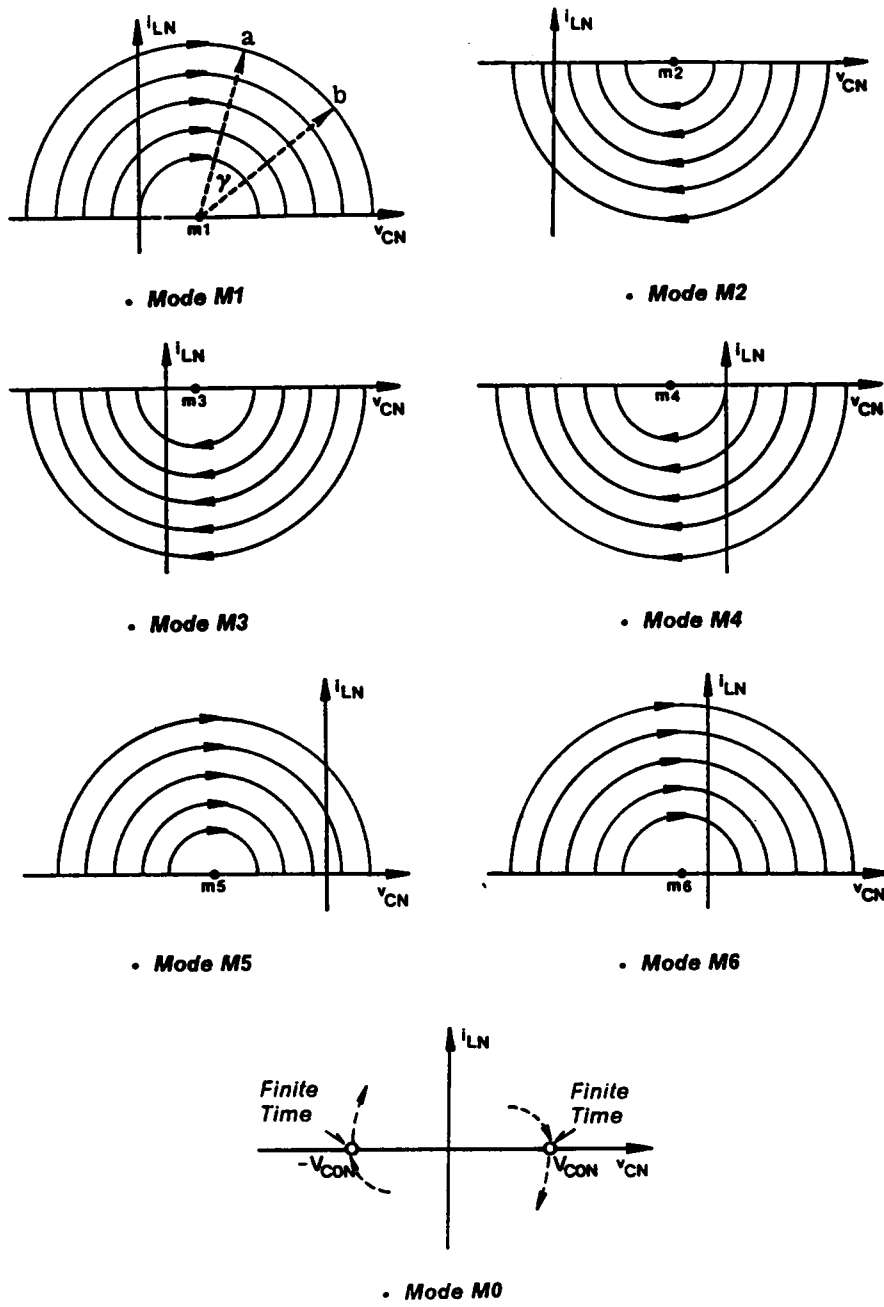


Figure 2.5 Families of State Trajectory for Various Circuit Topological Modes

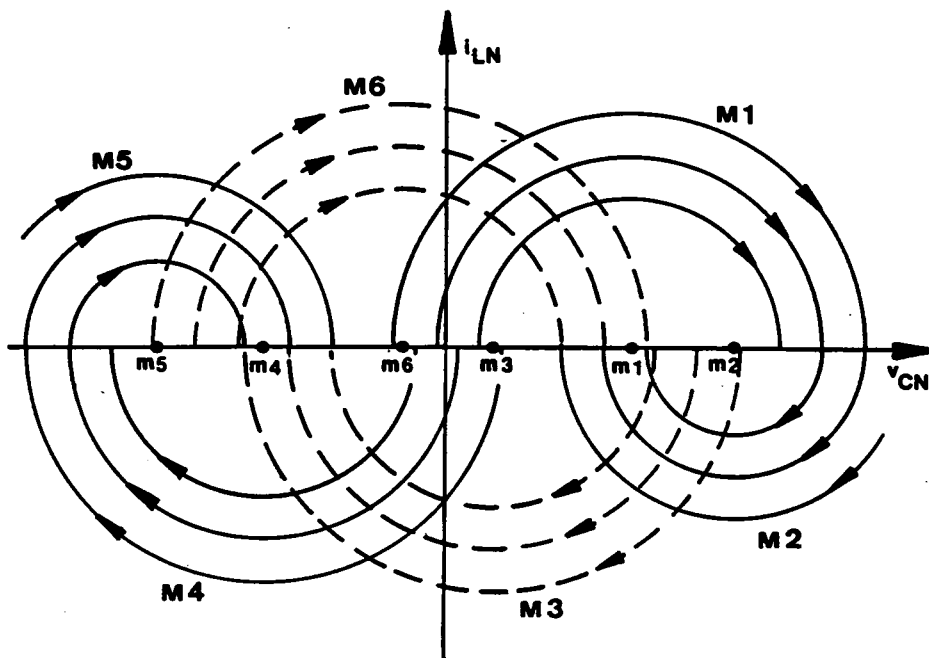


Figure 2.6 A Composite State Diagram for Constructing Equilibrium State Trajectories

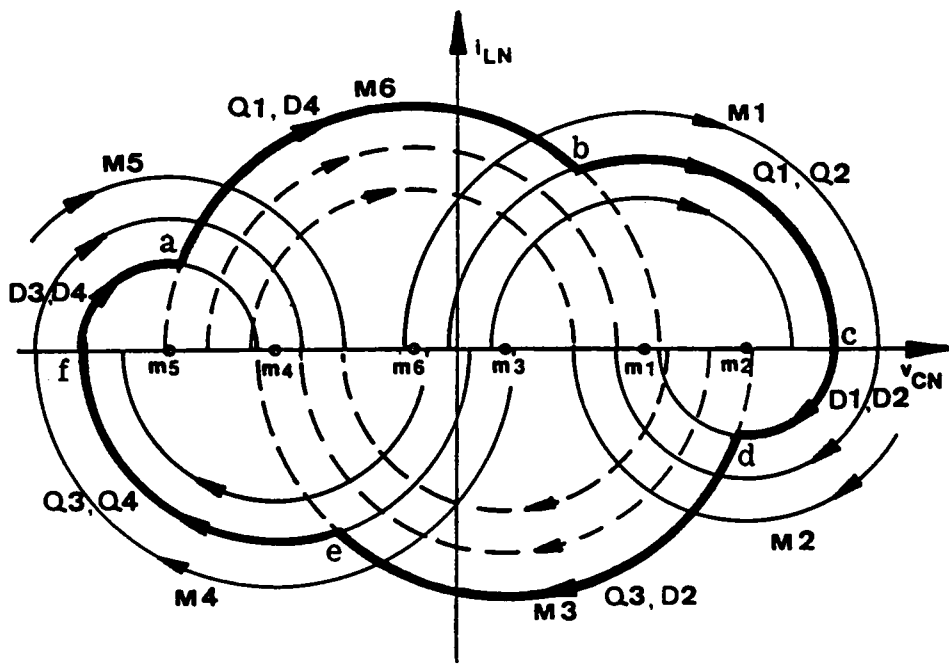


Figure 2.7 An Example Illustrating Construction of an Equilibrium State Trajectory on the Composite Diagram

2.3.5 Circuit Operating Modes

Many equilibrium trajectories, each representing a circuit operating mode, have been constructed. These trajectories are categorized into two frequency ranges and discussed in the following.

2.3.5.1 Operating modes below the resonant frequency

Figure 2.8 shows a series of equilibrium state trajectories which illustrate all the possible operating modes of a CM-SRC operating below the resonant frequency. The corresponding circuit waveforms for the trajectories are also included in the figure to help explain the converter's operation.

Trajectory 0: This trajectory represents the case when the converter operates as a conventional SRC. In other words, no zero-voltage interval exists in voltage v_S . As shown in Figure 2.8(a), at $t = a$, transistors Q1 and Q2 turn on commutating diodes D3 and D4. The inductor current, i_{LN} , resonates through Q1 and Q2(M1). At $t = b$, i_{LN} reverses polarity due to resonance. Transistors Q1 and Q2 *turn off naturally* and diodes D1 and D2 conduct subsequently. The inductor current resonates through D1 and D2(M2). At $t = c$, transistors Q3 and Q4 turn on commutating diodes D1 and D2 and a similar process occurs with the roles of Q1,Q2,D1,D2 and Q3,Q4,D3,D4 interchanged, respectively. The topological mode sequence of this trajectory is M1-M2-M4-M5.

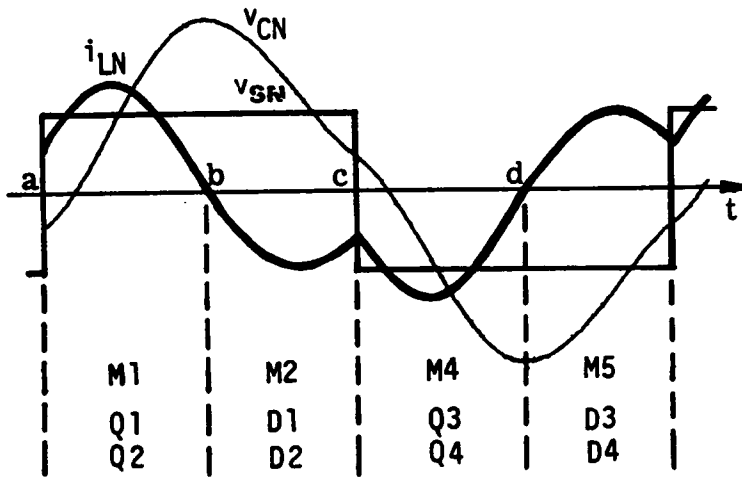
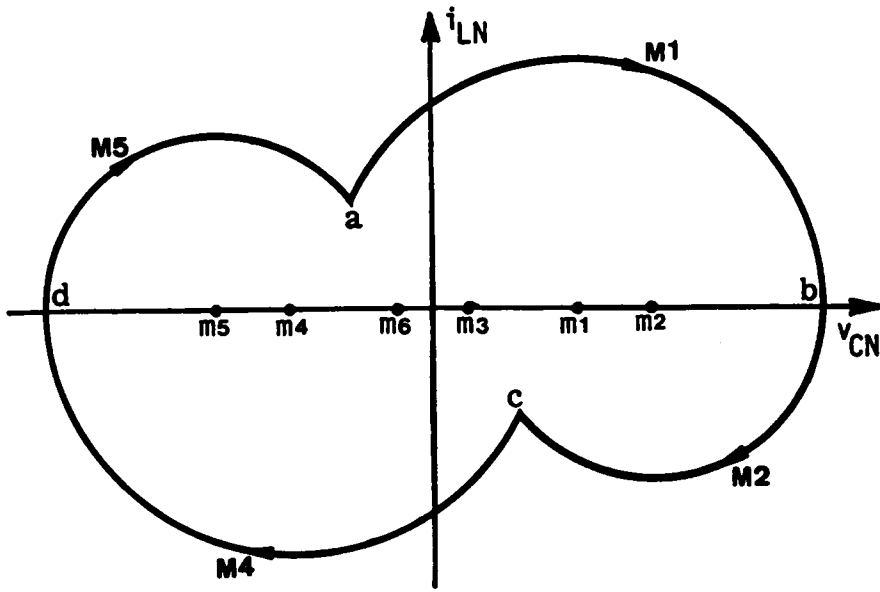
Trajectory 1: When a zero-voltage interval is introduced into v_S , topological modes M3 and M6 will be present in the trajectory. As shown in Figure 2.8(b), at $t = a$, transistor Q1 turns on commutating diode D3. The inductor current, i_{LN} , resonates through Q1 and D4(M6). At $t = b$, transistor Q2 turns on commutating diode D4. The inductor current, i_{LN} , resonates through Q1 and Q2(M1). At $t = c$, i_{LN} reverses polarity. Transistors Q1 and Q2 *turn off naturally* and diodes D1 and D2 conduct subsequently. The inductor current resonates through D1 and D2(M2). At $t = d$, transistor Q3 turns on

commutating diode D1 and a similar process occurs with the roles of Q1,Q2,D1,D2 and Q3,Q4,D3,D4 interchanged, respectively. The topological mode sequence of this trajectory is $M6-M1-M2-M3-M4-M5$, which is defined as "mode-I operation" of CM-SRC. Obviously, Trajectory 0 is a special case of Trajectory 1.

Trajectory 1': As the zero-voltage interval in v_s increases, natural commutation of all the transistors no longer can be achieved. In this trajectory, the natural-commutation boundary for transistors Q1 and Q3 is reached. As shown in Figure 2.8(c), transistors Q1,Q3 are triggered at the instants i_{LN} reverses polarity ($t=a$ and c). As a result, no D1,D2 or D3,D4 conduction period exists. The topological mode sequence for this trajectory is $M6-M1-M3-M4$, which is also a special case of Trajectory 1.

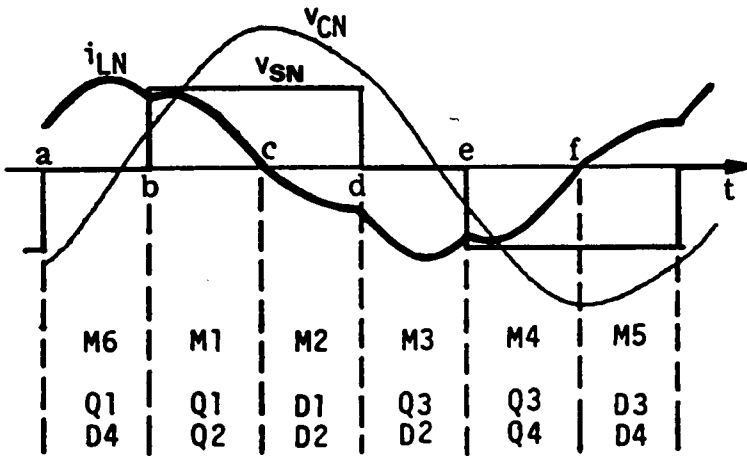
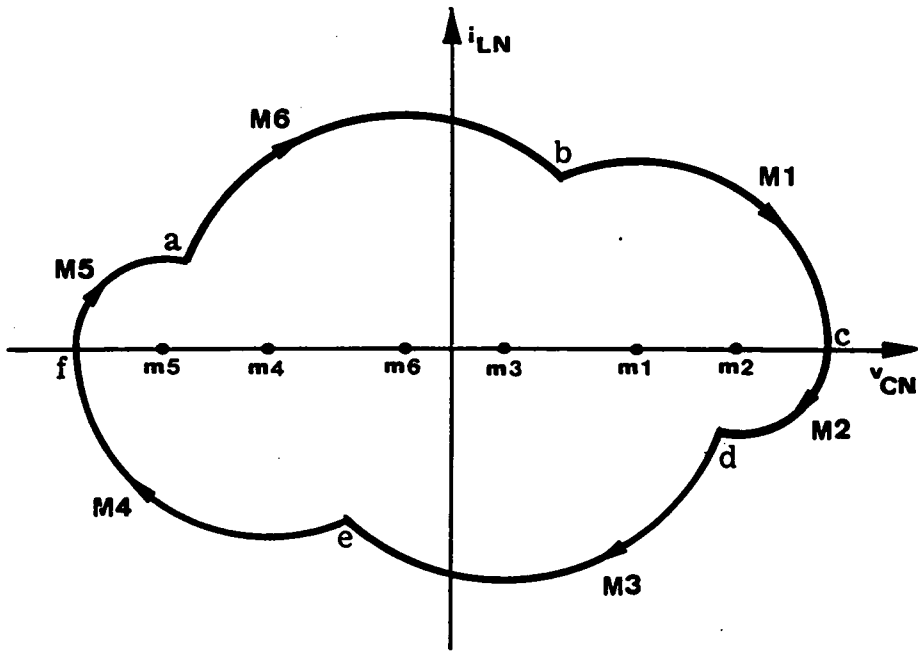
Trajectory 2: In Trajectory 1, it is possible that the magnitude of the capacitor voltage, $|v_{CN}|$, is less than the sum of the input voltage and the output voltage, $1 + V_{ON}$, when i_{LN} reverses polarity at $t=c$ (or f), as shown in Figure 2.8(d). As a result, diodes D1,D2 (or D3,D4) are reverse biased and none of the switching devices conducts. The circuit stays in a recess mode(M0) until transistor Q3 (or Q1) is triggered at $t=d$ (or a) to initiate another resonant mode. The topological mode sequence of this trajectory is $M6-M1-M0-M3-M4-M0$, which is defined as "mode-II operation".

Trajectory 3: When the zero-voltage interval in v_s is further increased, natural commutation of Q1 and Q3 is no longer possible. As illustrated in Figure 2.8(e), at $t=a$, Q3 is *forced off* and Q1 is triggered. Diode D1 conducts since i_{LN} is negative. The inductor current resonates through D1 and Q4(M3). At $t=b$, i_{LN} reverses polarity. Diode D1, transistor Q4 *turn off naturally* and transistor Q1, diode D4 conduct subsequently. The inductor current resonates through Q1 and D4(M6). At $t=c$, transistor Q2 turns on commutating diode D4. The inductor current resonates through Q1 and Q2(M1). At $t=d$, Q1 is *forced off* and Q3 is triggered. A similar process occurs with the roles of Q1,Q2,D1,D2 and Q3,Q4,D3,D4 interchanged, respectively. The topological



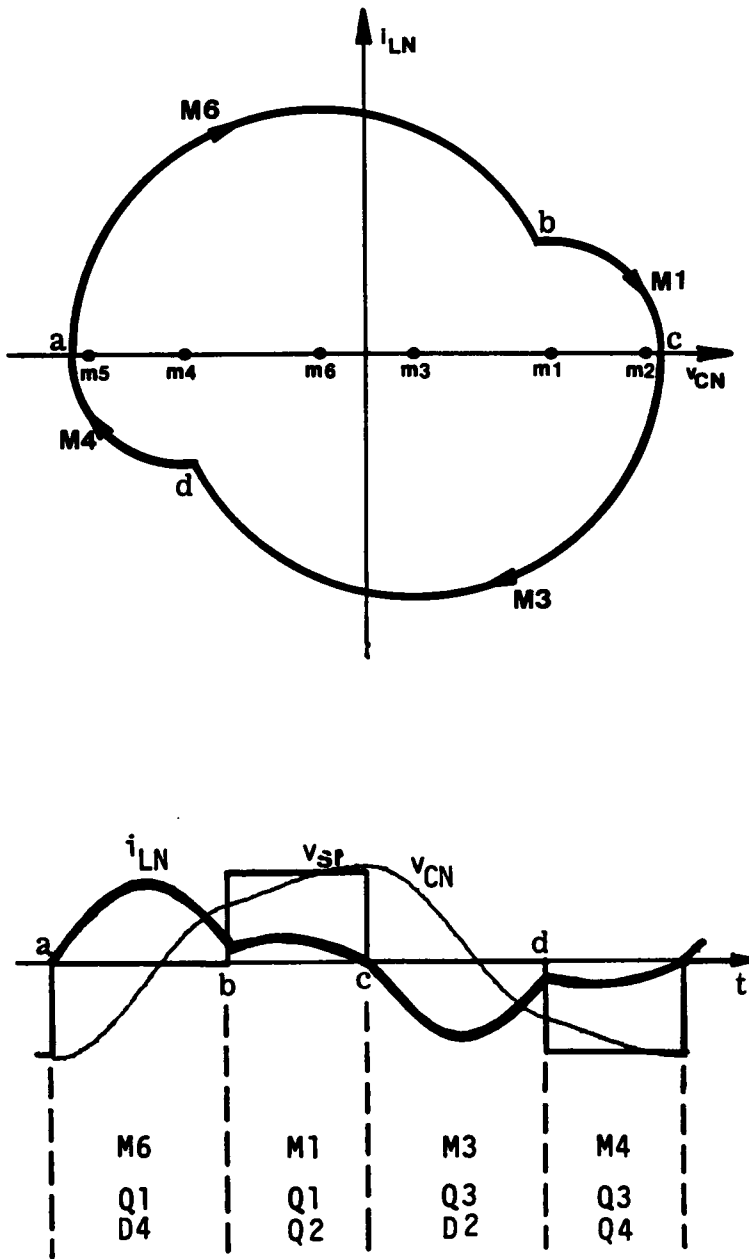
(a) Trajectory 0 and its corresponding circuit waveforms (SRC operation)

Figure 2.8 Equilibrium Trajectories of a CM-SRC Operating Below Resonant Frequency



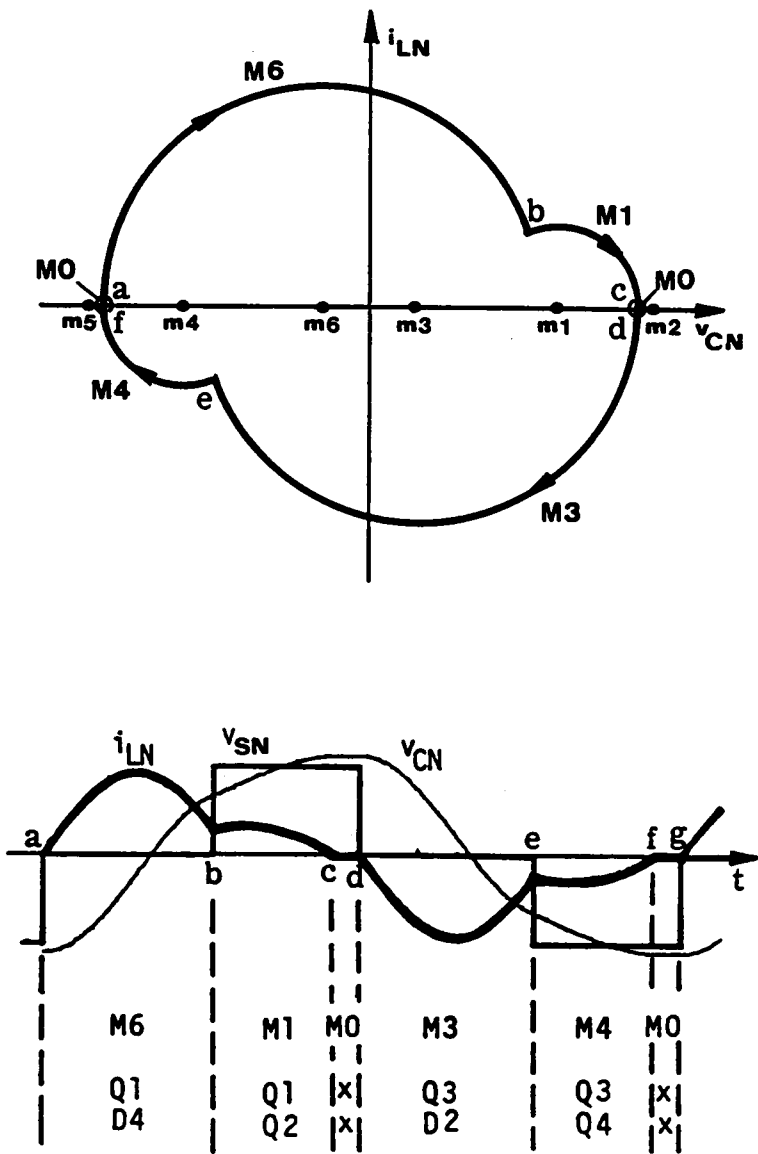
(b) Trajectory 1 and its corresponding circuit waveforms (Mode-I operation)

Figure 2.8 Continued



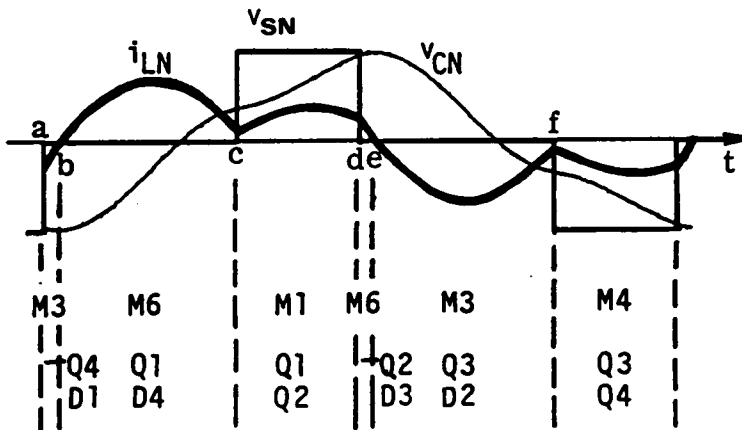
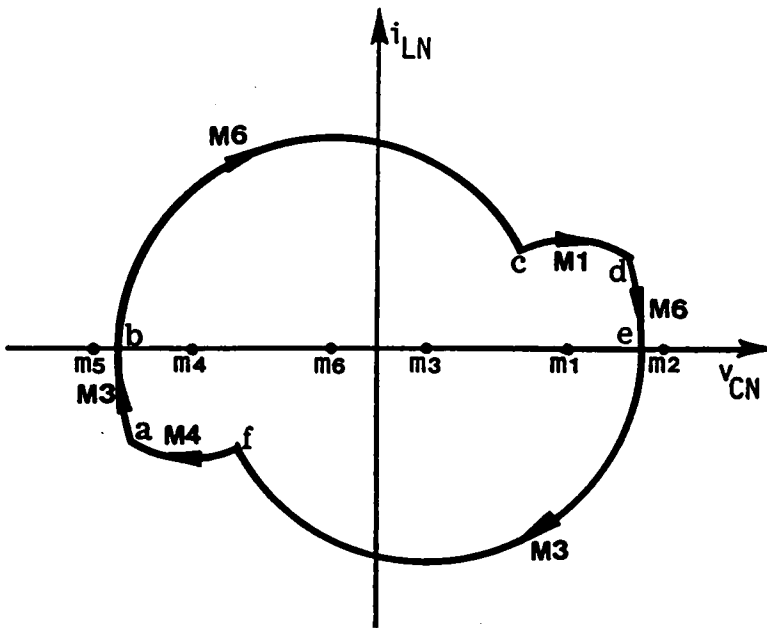
(c) Trajectory I' and its corresponding circuit waveforms (Mode-I operation)

Figure 2.8 Continued



(d) Trajectory 2 and its corresponding circuit waveforms (Mode-II operation)

Figure 2.8 Continued



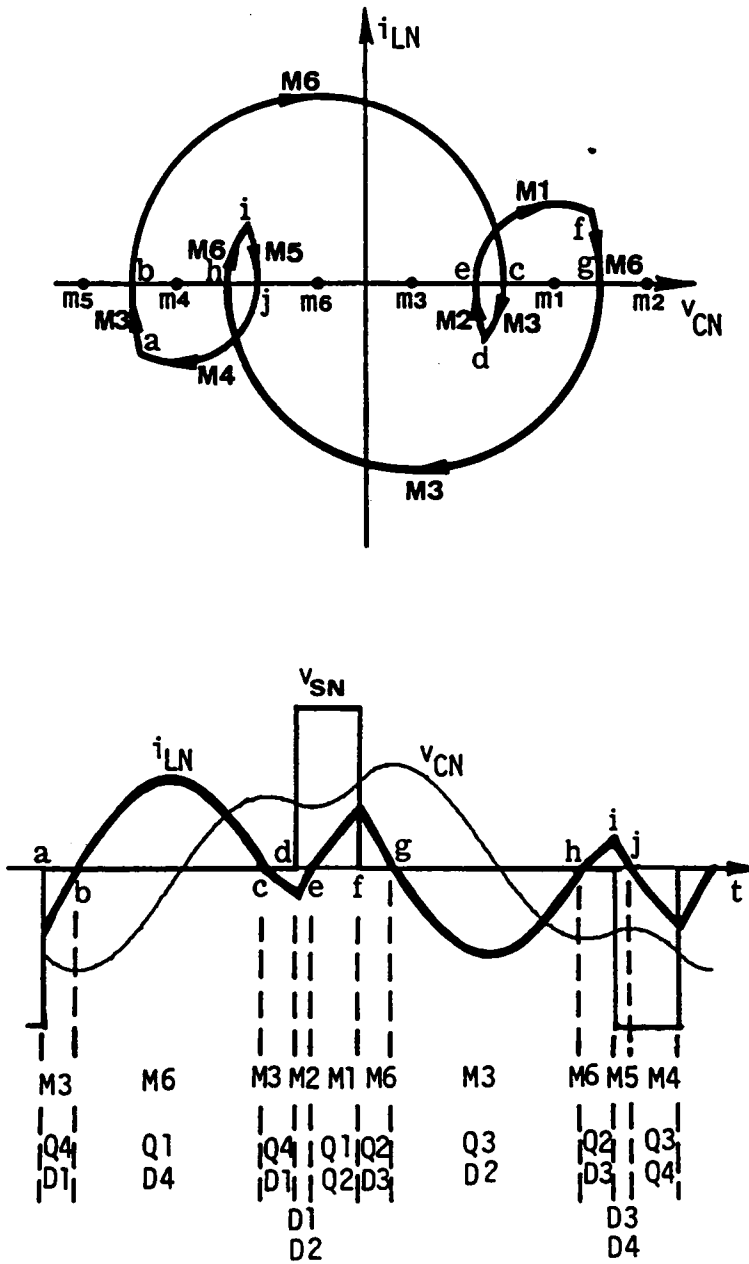
(e) Trajectory 3 and its corresponding circuit waveforms (Mode-III operation)

Figure 2.8 Continued

mode sequence for this trajectory is $M3-M6-M1-M6-M3-M4$, which is defined as “mode-III operation”.

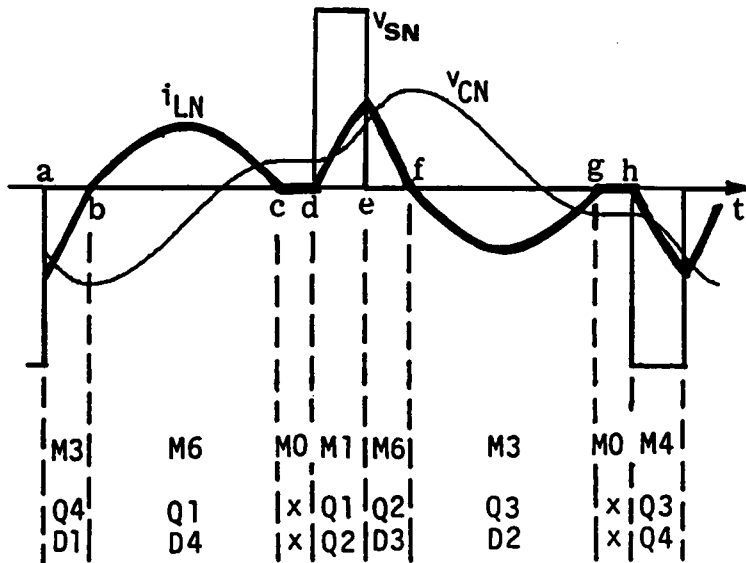
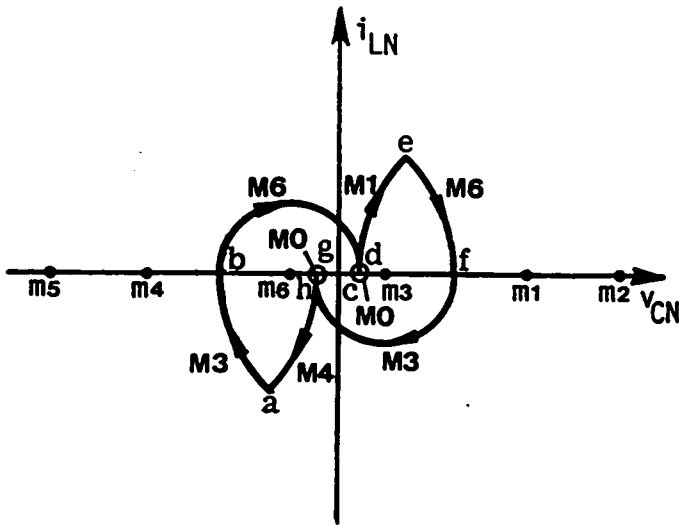
Trajectory 4: In Trajectory 3, if i_{LN} reverses polarity for the second time before Q2 (or Q4) is triggered at $t=c$ (or f) and the magnitude of v_{CN} is greater than V_{ON} at both instants i_{LN} reverses polarity, transistors Q1,Q2,Q3,Q4 will conduct twice during an operating cycle. As illustrated in Figure 2.8(f), at $t=a$, Q3 is *forced off* and Q1 is triggered. Diode D1 conducts since i_{LN} is negative. The inductor current resonates through D1 and Q4(M3). At $t=b$, i_{LN} reverses polarity. Diode D1, transistor Q4 *turn off naturally* and transistor Q1, diode D4 conduct subsequently. The inductor current resonates through Q1 and D4(M6). At $t=c$, i_{LN} reverses polarity again. Transistor Q1, diode D4 *turn off naturally* and diode D1, transistor Q4 conduct for the second time. The inductor current resonates through D1 and Q4(M3). At $t=d$, Q4 is *forced off* and Q2 is triggered. Diode D2 conducts since i_{LN} is negative. The inductor current resonates through D1 and D2(M2). At $t=e$, i_{LN} reverses polarity. Diodes D1,D2 *turn off naturally* and transistors Q1,Q2 conduct subsequently. The inductor current resonates through Q1 and Q2(M1). At $t=f$, Q1 is *forced off* and Q3 is triggered. Diode D3 conducts since i_{LN} is positive and a similar process occurs with the roles of Q1,Q2,D1,D2 and Q3,Q4,D3,D4 interchanged, respectively. The topological mode sequence for this trajectory is $M3-M6-M3-M2-M1-M6-M3-M6-M5-M4$, which is defined as “mode-IV operation”.

Trajectory 5: This trajectory evolves either from Trajectory 3 or from Trajectory 4 as the zero-voltage interval in v_S is increased. Consider Trajectory 4. At $t=c$ (or h), if the magnitude of v_{CN} is less than V_{ON} , diode D1 and transistor Q4 (or D3 and Q2) will be reverse-biased. As a result, the circuit will stay in a recess mode(M0) until transistor Q2 (or Q4) is triggered to initiate another resonant mode. The circuit’s operation for this trajectory is illustrated in Figure 2.8(g). The topological mode sequence is $M3-M6-M0-M1-M6-M3-M0-M4$, which is defined as “mode-V operation”.



(f) Trajectory 4 and its corresponding circuit waveforms (Mode-IV operation)

Figure 2.8 Continued



(g) Trajectory 5 and its corresponding circuit waveforms (Mode-V operation)

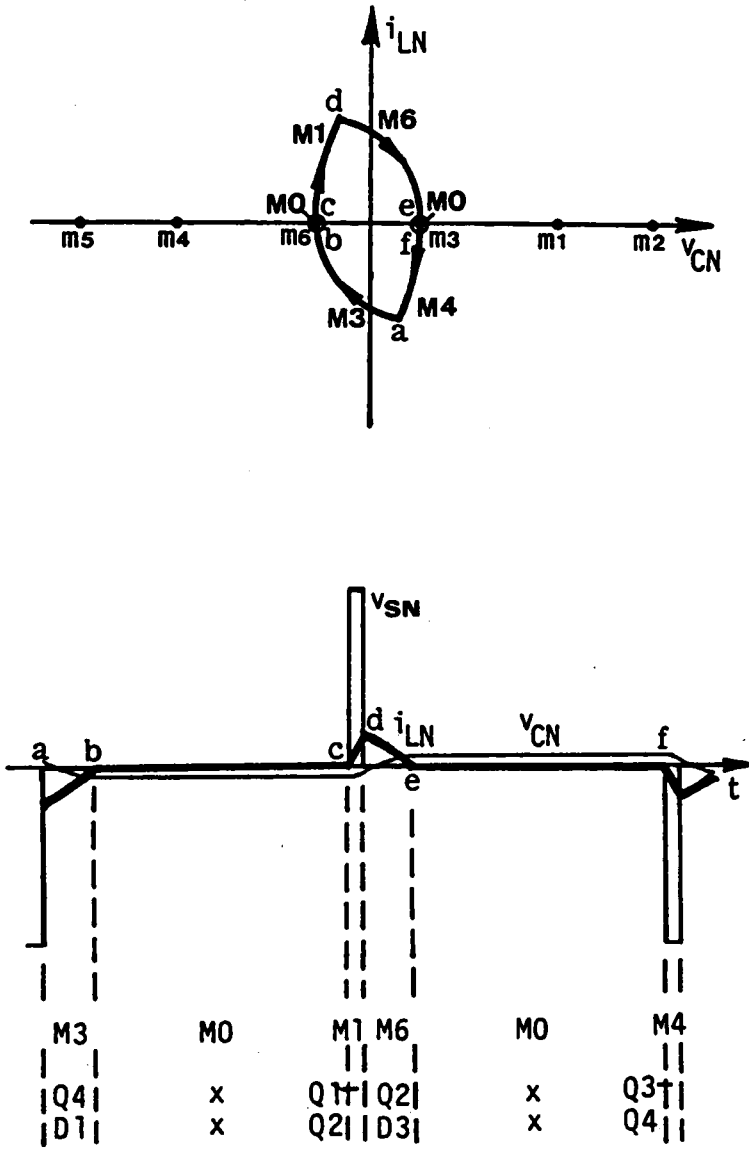
Figure 2.8 Continued

Trajectory 6: Further increasing the zero-voltage interval in v_s , Trajectory 3, 4 or 5 may degenerate into this trajectory. Consider Trajectory 5. If the magnitude of v_{CN} is less than V_{ON} when i_{LN} reverses polarity at $t = b$ (or f), transistor Q1 and diode D4 (or Q3 and D2) will be reverse-biased and none of the switching devices will conduct. The circuit will stay in a recess mode(M0) until transistor Q2 (or Q4) is triggered at $t = c$ (or f) to initiate another resonant mode. The circuit's operation for this trajectory is illustrated in Figure 2.8(h). The topological mode sequence is $M3-M0-M1-M6-M0-M4$, which is defined as "mode-VI operation".

Table 2.2 summarizes the topological mode sequences for the six operating modes. When the CM-SRC operates in mode I or mode II, all the transistors, Q1-Q4, are naturally commutated. When the CM-SRC operates in mode III or mode VI, transistors Q1 and Q3 are force-commutated while transistors Q2 and Q4 are naturally commutated. When the CM-SRC operates in mode IV, transistors Q1-Q4, are naturally commutated for their first conduction and force-commutated for their second conduction. When the CM-SRC operates in mode V, transistors Q1,Q3 are naturally commutated for their first conduction and force-commutated for their second conduction; transistors Q2 and Q4 are always naturally commutated. Table 2.3 summarizes the commutation features of all the transistors in various operating modes. It should be pointed out that force-commutated transistors usually turn on at zero voltage. As a result, lossless capacitor snubbers can be used to reduce their turn-off losses.

2.3.5.2 Operating modes above resonant frequency

Figure 2.9 shows a series of equilibrium state trajectories which illustrate all the possible operating modes of a CM-SRC operating above resonant frequency. The corresponding circuit waveforms for the trajectories are also included in the figure to help explain the converter's operation.



(h) Trajectory 6 and its corresponding circuit waveforms (Mode-VI operation)

Figure 2.8 Continued

**Table 2.2 Topological Mode Sequences for Circuit
Operating Modes Below Resonant Frequency**

Operating Modes	Topological Mode Sequences
I	M6-M1-M2-M3-M4-M5
II	M6-M1-M0-M3-M4-M0
III	M6-M1-M6-M3-M4-M3
IV	M3-M6-M3-M2-M1-M6-M3-M6-M5-M4
V	M3-M6-M0-M1-M6-M3-M0-M4
VI	M3-M0-M1-M6-M0-M4

**Table 2.3 Commutation Features for Transistors
in Various Circuit Operating Modes
Below Resonant Frequency**

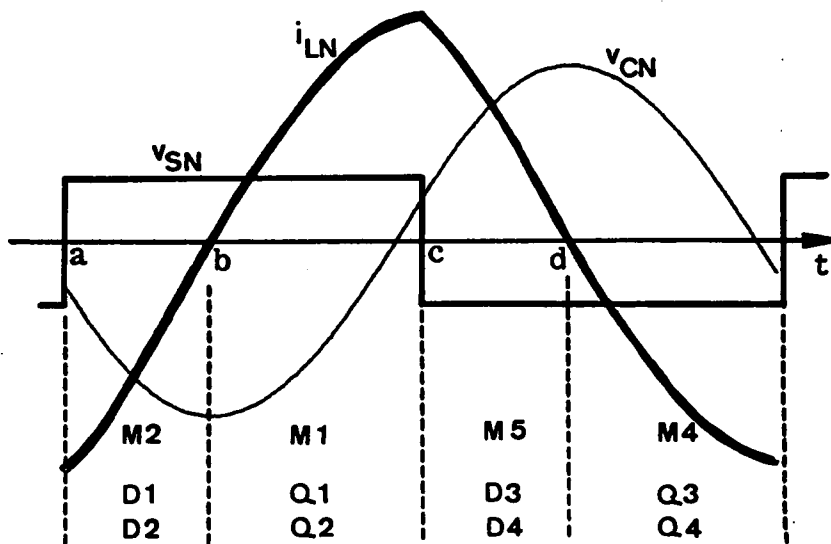
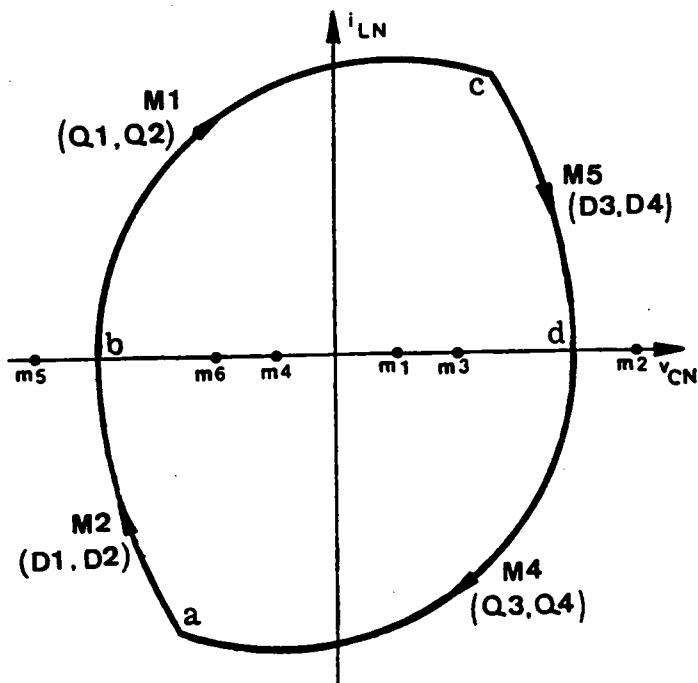
Mode	i_L	Turn-On		Turn-Off		Comments
		Q1,Q3	Q2,Q4	Q1,Q3	Q2,Q4	
I	cont.	n.z.v.	n.z.v.	z.c.	z.c.	*****
II	discont.	z.v.	n.z.v.	z.c.	z.c.	*****
III	cont.	z.v.	n.z.v.	n.z.c.	z.c.	*****
IV	cont.	z.v.	z.v.	z.c.	z.c.	Q1-Q4 turn on twice
		z.v.	z.v.	n.z.c.	n.z.c.	
V	discont.	z.v.	z.v.	z.c.	z.c.	Q1,Q3 turn on twice
		z.v.	*****	n.z.c.	*****	
VI	discont.	z.v.	z.v.	n.z.c.	z.c.	*****

n.z.c. - turn off at nonzero current
z.c. - turn off at zero current
n.z.v. - turn on at nonzero voltage
z.v. - turn on at zero voltage

Trajectory A_0 : This trajectory represents the case when the converter operates as a conventional SRC. As shown in Figure 2.9(a), at $t = a$, transistors Q3,Q4 are *forced off* and Q1,Q2 are triggered. Transistors Q1,Q2 cannot conduct since i_{LN} is negative. Instead, diodes D1,D2 conduct. The inductor current resonates through D1 and D2(M2). At $t = b$, i_{LN} reverses polarity due to resonance. Diodes D1,D2 *turn off naturally* and transistors Q1,Q2 conduct subsequently. The inductor current resonates through Q1 and Q2(M1). At $t = c$, transistors Q1,Q2 are *forced off* and Q3,Q4 are triggered. A similar process occurs with the roles of Q1,Q2,D1,D2 and Q3,Q4,D3,D4 interchanged, respectively. The topological mode sequence of this trajectory is M2-M1-M5-M4.

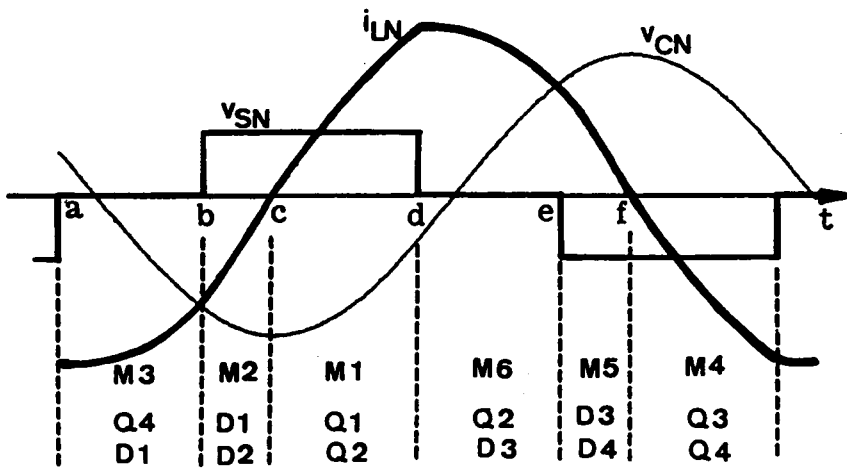
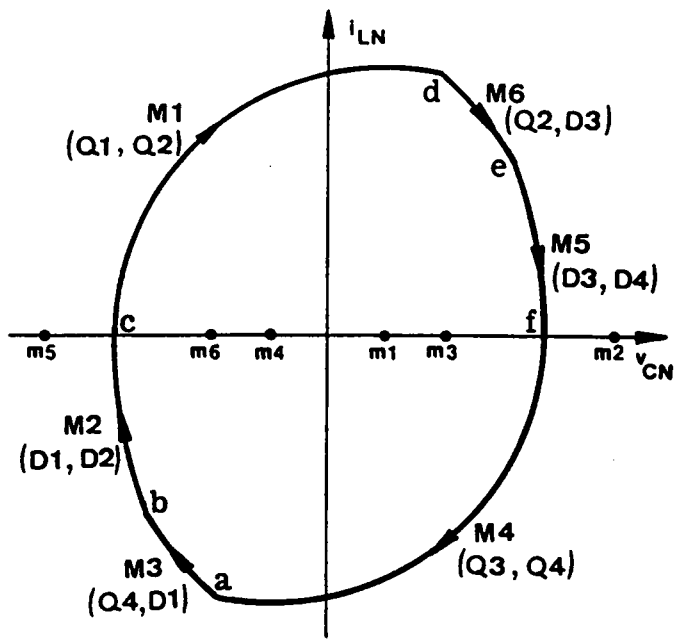
Trajectory A: When a zero-voltage interval is introduced into v_s , topological modes M3 and M6 will be present in the trajectory. As shown in Figure 2.9(b), at $t = a$, transistor Q3 is *forced off* and Q1 is triggered. Diode D1 conducts instead of Q1 since i_{LN} is negative. The inductor current resonates through Q4 and D1(M3). At $t = b$, transistor Q4 is *forced off* and Q2 is triggered. Diode D2 conducts instead of Q2 since i_{LN} is still negative. The inductor current resonates through D1 and D2(M1). At $t = c$, i_{LN} reverses polarity due to resonance. Diodes D1,D2 *turn off naturally* and transistors Q1,Q2 conduct subsequently. The inductor current resonates through Q1 and Q2(M1). At $t = d$, transistor Q1 is *forced off* and Q3 is triggered. A similar process occurs with the roles of Q1,Q2,D1,D2 and Q3,Q4,D3,D4 interchanged, respectively. The topological mode sequence of this trajectory is M6-M1-M2-M3-M4-M5, which is defined as “mode-A operation” of CM-SRC. Obviously, Trajectory A_0 is a special case of Trajectory A.

Trajectory A': As the zero-voltage interval in v_s increases, the force commutation boundary of Q2 and Q4 is reached. As shown in Figure 2.9(c), Q2 and Q4 are commutated at the instants when i_{LN} reverses polarity ($t = b$ and d). In other words, Q2 and Q4 no longer turn off with current. The topological mode sequence for this trajectory is M3-M1-M6-M4, also a special case of Trajectory A.



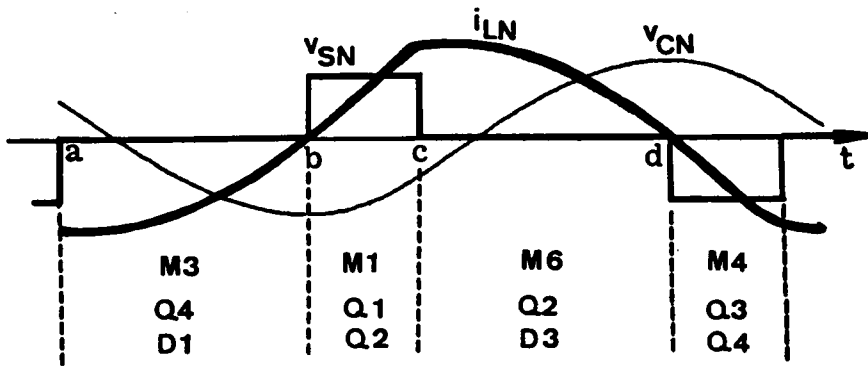
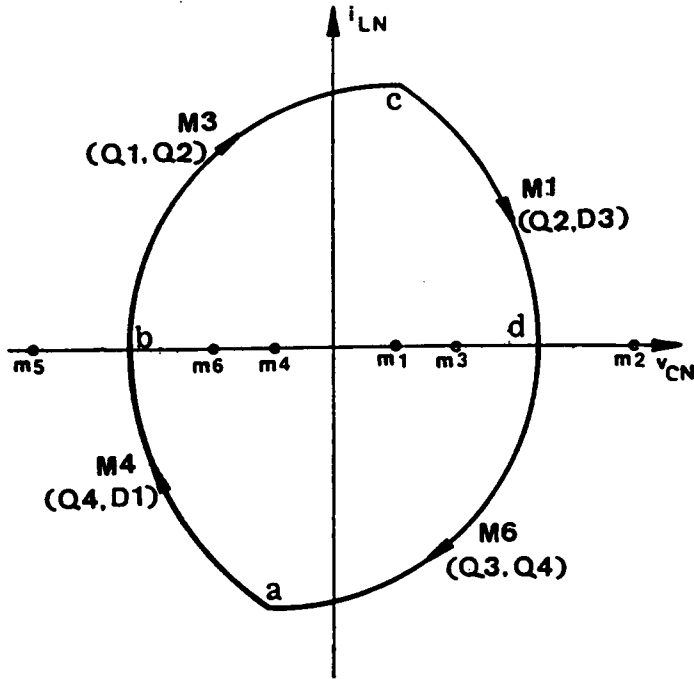
(a) Trajectory A_0 and its corresponding circuit waveforms (SRC operation)

Figure 2.9 Equilibrium Trajectories of a CM-SRC Operating Above Resonant Frequency



(b) Trajectory A and its corresponding circuit waveforms (Mode-A operation)

Figure 2.9 Continued



(c) Trajectory A' and its corresponding circuit waveforms (Mode-A operation)

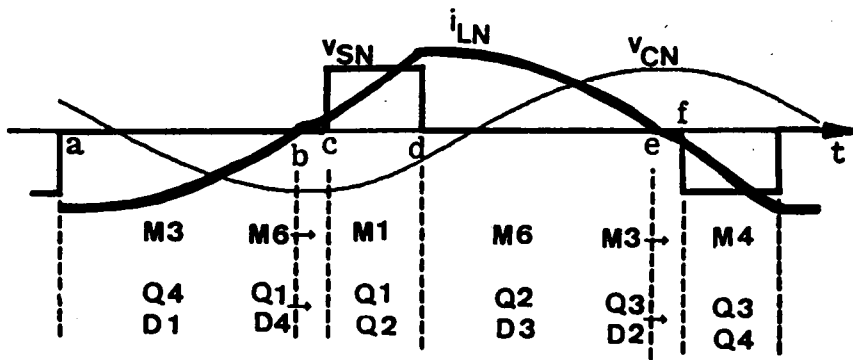
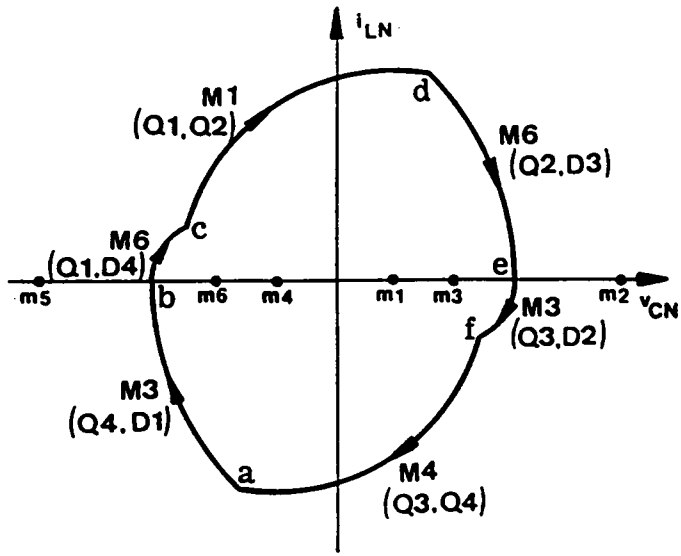
Figure 2.9 Continued

Trajectory B: When the zero-voltage interval in v_s is further increased, transistors Q2 and Q4 become naturally commutated. In this case, the converter's operation is the same as mode-III operation below resonant frequency, as illustrated in Figure 2.9(d). The topological mode sequence for this trajectory is $M3-M6-M1-M6-M3-M4$ and is defined as "mode-B operation".

Trajectory C: Further increasing the zero-voltage interval in v_s , Trajectory B will degenerate into this trajectory if the magnitude of v_{CN} is less than V_{ON} when i_{LN} reverses polarity at $t=b$ (or e). The converter's operation is the same as Mode-VI operation below resonant frequency, as illustrated in Figure 2.9(e). The topological mode sequence is $M3-M0-M1-M6-M0-M4$ and is defined as "mode-C operation".

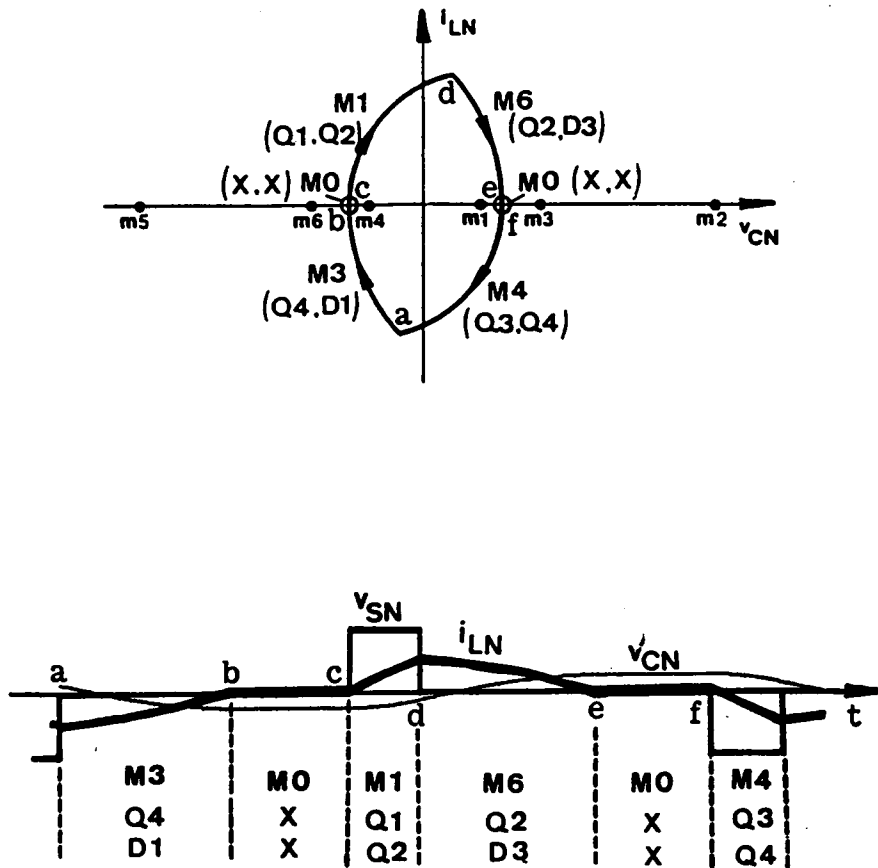
Table 2.4 summarizes the topological mode sequences for the three operating modes above resonant frequency. The commutation features for the transistors in each operating modes are summarized in Table 2.5.

Note that the trajectories discussed above are used only to qualitatively illustrate the existence of various operating modes and to demonstrate the transitions between different modes. The frequencies corresponding to the trajectories may not be the same. Some trajectories exist only for certain frequency and output-to-input voltage ratio range, as shall be seen in the following section.



(d) Trajectory B and its corresponding circuit waveforms (Mode-B operation)

Figure 2.9 Continued



(e) Trajectory C and its corresponding circuit waveforms (Mode-C operation)

Figure 2.9 Continued

**Table 2.4 Topological Mode Sequences for Circuit
Operating Modes Above Resonant Frequency**

Operating Modes	Topological Mode Sequences
A	M3-M2-M1-M6-M5-M4
B	M3-M6-M1-M6-M3-M4
C	M3-M0-M1-M6-M0-M4

**Table 2.5 Commutation Features for Transistors
in Various Circuit Operating Modes
Above Resonant Frequency**

Mode	i_L	Turn-On		Turn-Off	
		Q1,Q3	Q2,Q4	Q1,Q3	Q2,Q4
A	cont.	z.v.	z.v.	n.z.c.	n.z.c.
B	cont.	z.v.	n.z.v.	n.z.c.	z.c.
C	discont.	z.v.	z.v.	n.z.c.	z.c.

n.z.c. - turn off at nonzero current
z.c. - turn off at zero current
n.z.v. - turn on at nonzero voltage
z.v. - turn on at zero voltage

2.3.6 Regions of Operation

Since the commutation features of the power switches in each operating mode are different, it is important to determine the converter's modes of operation for a specific design. Knowing the converter's operating mode(s) enables one to choose proper devices for the converter to optimize circuit performance. For example, if a CM-SRC operates in Mode III or Mode VI below resonant frequency, a simple lossless capacitor snubber, C_S , as shown in Figure 2.10, can be used across transistor Q1 and Q3 to reduce their turn-off losses. This is feasible since Q1 and Q3 always turn on at zero voltage. Slower diodes can be used for D1 and D3 since D1 and D3 always turn off at zero current. The simple lossless capacitor snubbers, however, cannot be used when the converter operates in other operating modes below resonant frequency since Q1 and Q3 no longer turn on at zero voltage. Faster diodes are required for D1 and D3 since these diodes are no longer commutated at zero current.

To determine the converter's operating modes, regions of operation for a CM-SRC must be defined.

2.3.6.1 Operating regions below resonant frequency

Operating regions: Figure 2.11 shows the operating regions for a CM-SRC at frequencies below the resonant frequency. In the figure, the mode of operation is represented as a function of the pulse width, β_S , of the quasi-square-wave voltage v_S and the ratio of output to input voltage, V_{ON} . The frequencies are normalized to the resonant frequency, ω_{SN} , $\omega_{SN} = \omega_S / \omega_0$. Given a range of V_{ON} , β_S , and a specific operating frequency, the converter's modes of operation can be easily determined using these figures. For example, if ω_{SN} is equal to 0.7, V_{ON} is from 0.4 to 0.6, and β_S is from 25° to 75° , the converter will operate in either mode III or mode VI, as indicated by the shaded area in Figure 2.11(d).

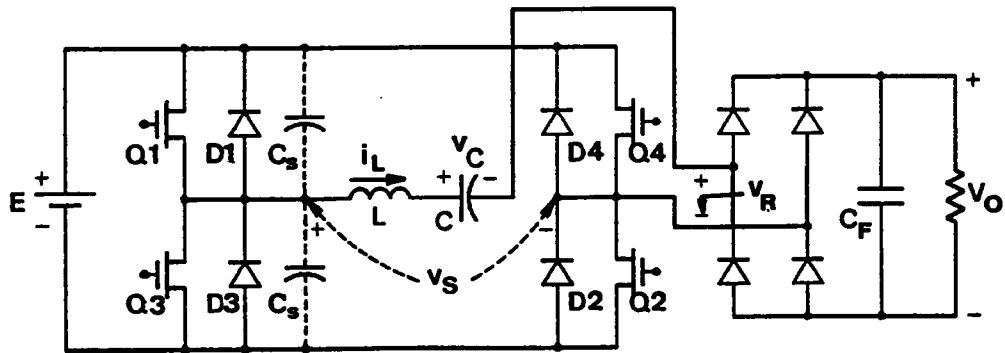
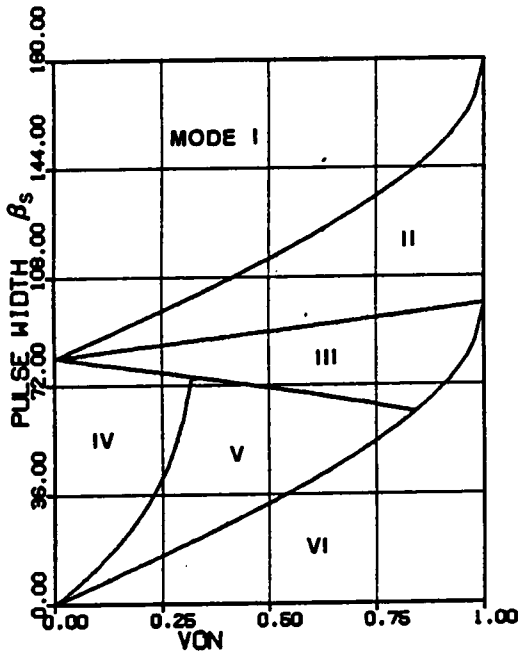
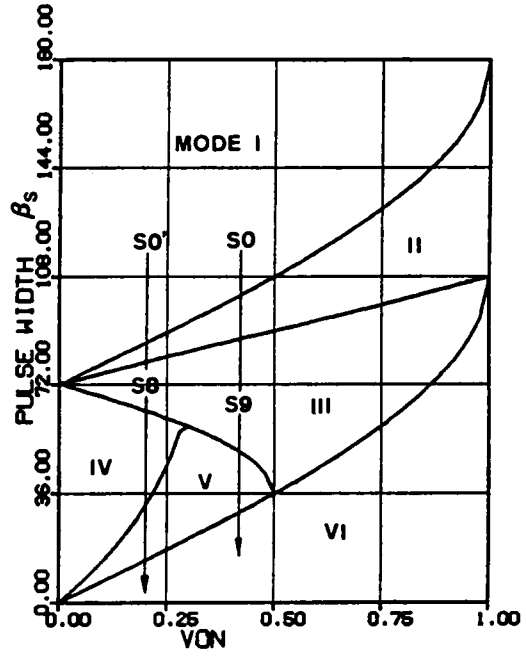


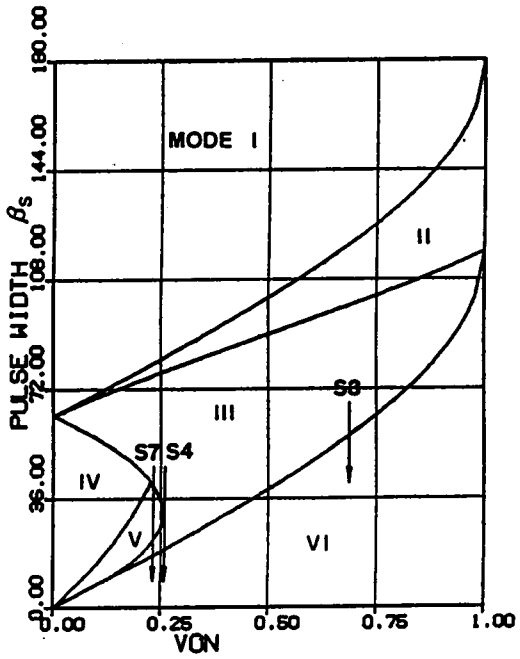
Figure 2.10 Lossless Snubbers Used Across Force-Commutated Transistors $Q1$ and $Q3$



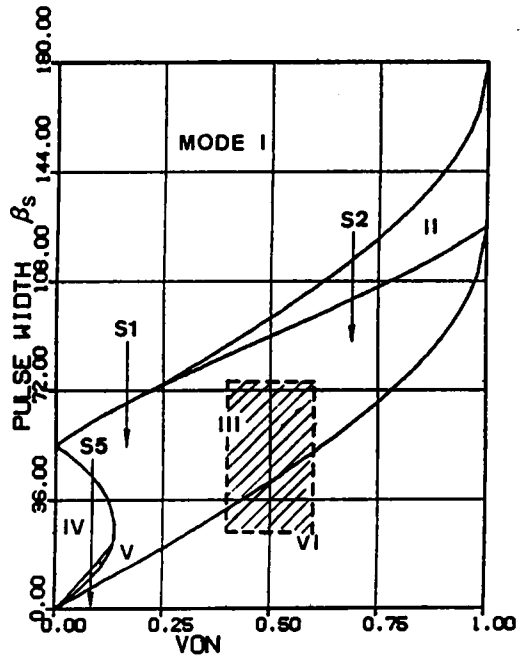
(a) $\omega_{SN} = 0.55$



(b) $\omega_{SN} = 0.6$

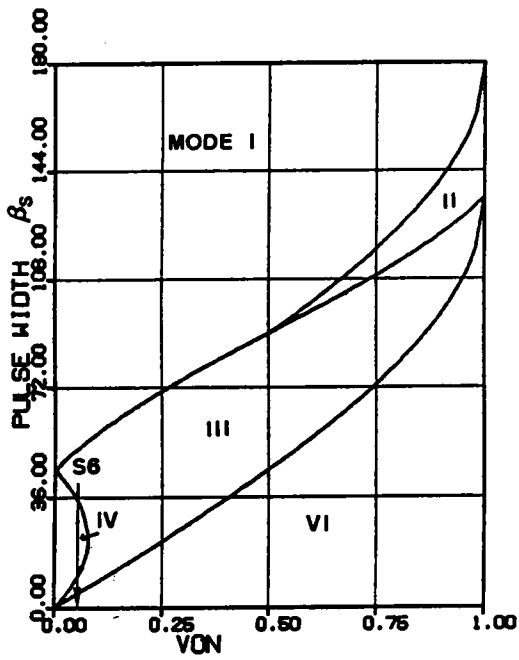


(c) $\omega_{SN} = 0.65$

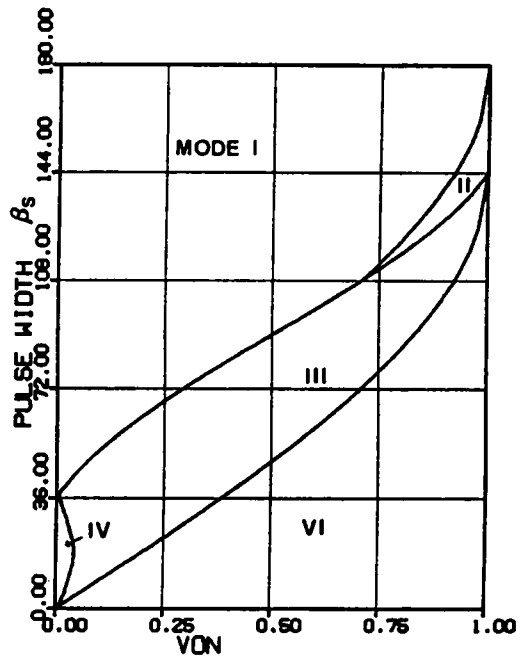


(d) $\omega_{SN} = 0.7$

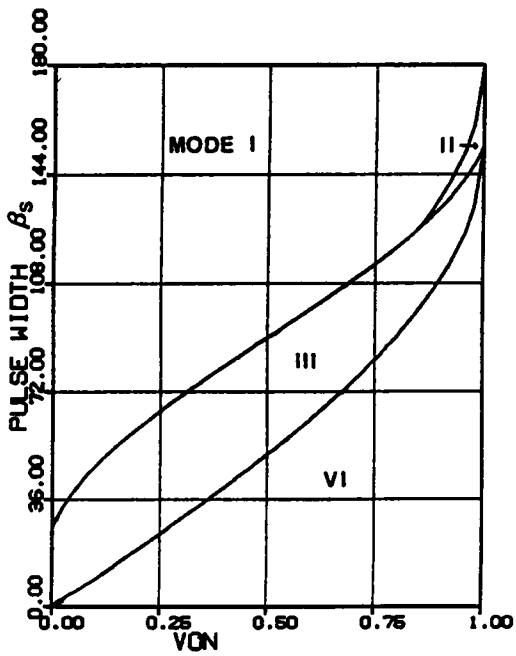
Figure 2.11 Regions of Operation Below Resonant Frequency



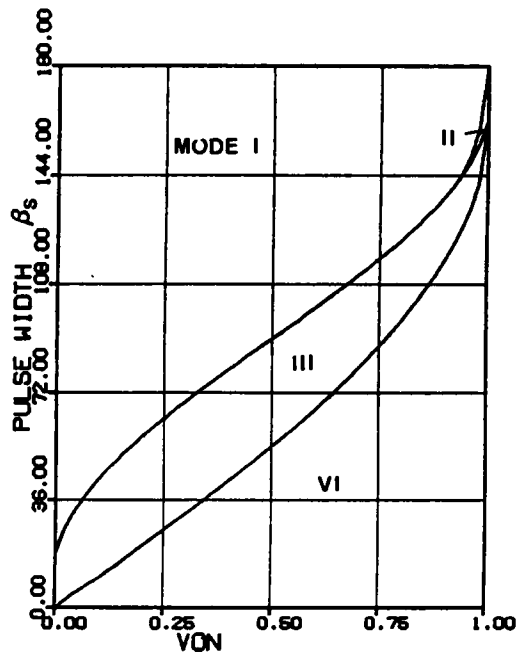
(e) $\omega_{SN} = 0.75$



(f) $\omega_{SN} = 0.8$



(g) $\omega_{SN} = 0.85$



(h) $\omega_{SN} = 0.9$

Figure 2.11 Continued

For other frequencies not shown in Figure 2.11, an algorithm is developed in the following which enables one to plot a similar graph to those in Figure 2.11.

Mode transitions: The first step in defining the operating regions of an CM-SRC is to determine the existing operating modes for a given ω_{SN} and V_{ON} . The corresponding β_S ranges to different operating modes can then be determined by solving the mode boundaries.

For a given V_{ON} and ω_{SN} possible operating modes can be found from the mode transition sequence when β_S angle is reduced from 180° to 0° . For example, as indicated by S0 in Figure 2.11(b), the mode transition sequence for $V_{ON} = 0.4$ and $\omega_{SN} = 0.6$ is Mode I - Mode II - Mode III - Mode V - Mode VI. This implies that all the operating modes except Mode IV exist for $V_{ON} = 0.4$ and $\omega_{SN} = 0.6$. The boundaries for the different operating modes are found to be $\beta_{S(I-II)} = 100^\circ$, $\beta_{S(II-III)} = 87^\circ$, $\beta_{S(III-V)} = 52^\circ$, and $\beta_{S(V-VI)} = 28^\circ$. The β_S ranges for the operating modes are thus $180^\circ \sim 100^\circ$ for Mode I, $100^\circ \sim 87^\circ$ for Mode II, $87^\circ \sim 52^\circ$ for Mode III, $52^\circ \sim 28^\circ$ for Mode V, and $28^\circ \sim 0^\circ$ for Mode VI. The transition in the circuit behavior as β_S varies was illustrated in Figure 2.8, Section 2.3.5.1.

It should be noticed that the mode transition sequence of a CM-SRC is not unique. A total of twelve mode transition sequences may exist below resonant frequency, as illustrate in Figure 2.12. The transition of the waveforms in Figure 2.8 corresponds to the case when $V_{ON} = 0.2$ and $\omega_{SN} = 0.6$, which sweeps through all the six operating modes and is indicated by S0' in Figure 2.11(b).

In the following, an algorithm is developed which predicts the mode transition sequence (as β_S decreases) and determines the mode boundaries for any arbitrary V_{ON} and ω_{SN} .

Mode boundaries: As shown in Figure 2.12, from Mode I the converter's operation may change to Mode II or Mode III when β_S is reduced. Consider the boundary trajectory,

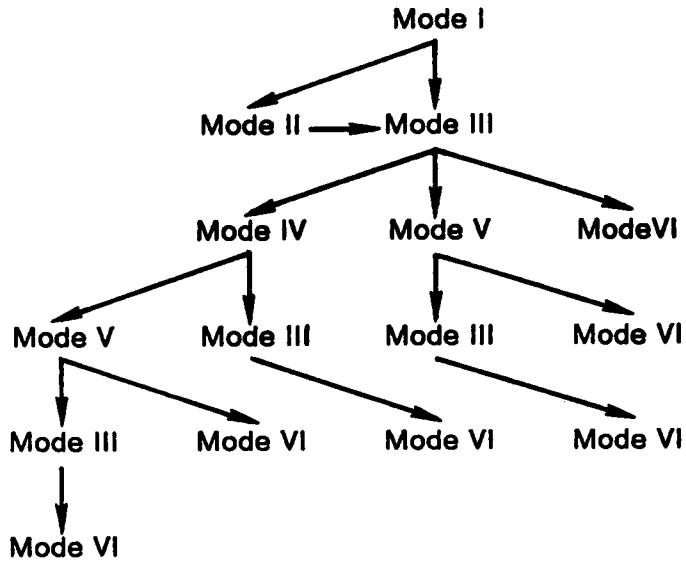


Figure 2.12 Mode Transition Sequences Below Resonant Frequency (β_S decreases from 180° to 0°)

T_{12} , between Mode I and Mode II, as shown in Figure 2.13. The frequency of T_{12} is calculated as

$$\omega_{12} = \frac{\pi}{\zeta + \delta + \theta}, \quad (2.5)$$

where $\zeta = \pi - \cos^{-1}(1 - 2V_{ON}^2)$, $\delta = \pi - \cos^{-1}(V_{ON})$, and $\theta \geq 0$ is the corresponding phase angle at stationary points a and b.

To construct this boundary trajectory, the maximum possible frequency is $\omega_{12\max} = \pi/(\zeta + \delta)$. Thus, when the converter operates at a frequency $\omega_{SN} > \omega_{12\max}$, trajectory T_{12} can not exist. This implies that mode-II operation does not exist and the converter's operation transits from Mode I to Mode III, as indicated by S1 in Figure 2.11(d).

The boundary β_S angle, β_{13} , separating Mode I and Mode III can be calculated from trajectory T_{13} , as shown in Figure 2.14, by solving equations

$$\begin{aligned} \cos(\pi - \zeta) &= \frac{1 + (1 + R - 2V_{ON})^2 - R^2}{2(1 + R - 2V_{ON})}, \\ \cos(\pi - \delta) &= \frac{1 + R_2 - (1 + R - 2V_{ON})^2}{2R}, \\ \omega_{SN} &= \frac{\pi}{\zeta + \delta}. \end{aligned} \quad (2.6)$$

Angle β_{13} is equal to $\omega_{SN} \times \delta$.

When $\omega_{SN} \leq \omega_{12\max}$, trajectory T_{12} exists. This implies that mode-II operation exists and the circuit's operation transits from Mode I to Mode II to Mode III, as indicated by S2 in Figure 2.11(d).

The boundary β_S angle, β_{12} , separating Mode I and Mode II is calculated from trajectory T_{12} ,

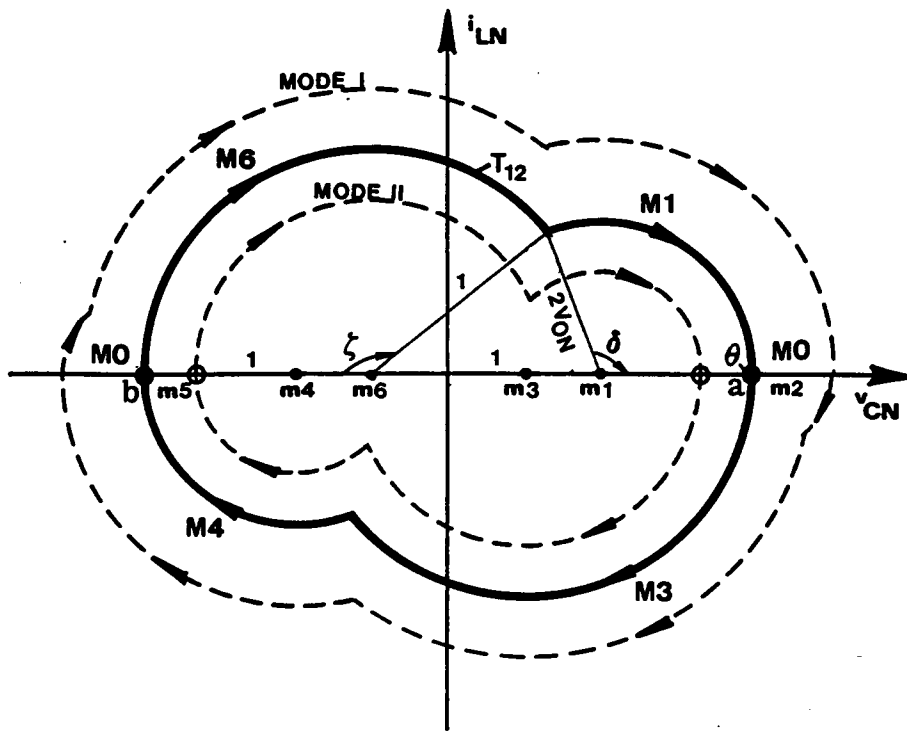


Figure 2.13 Boundary Trajectory Between Mode I and Mode II

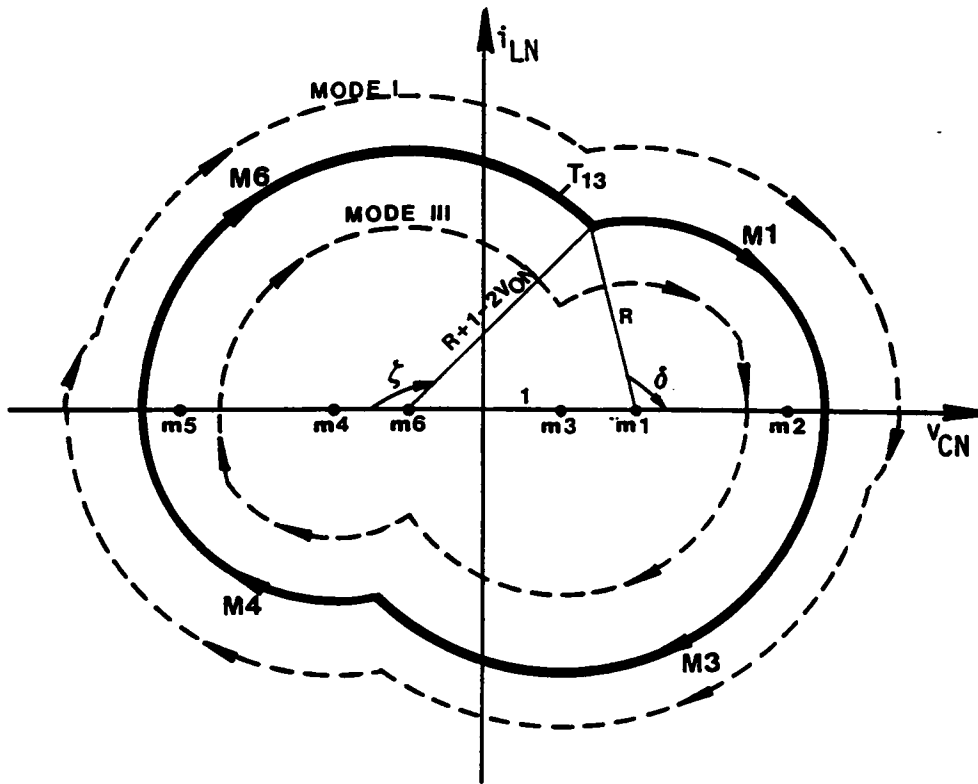


Figure 2.14 Boundary Trajectory Between Mode I and Mode III

$$\beta_{12} = (\delta + \theta) \times \omega_{SN}, \quad \theta = \left(\frac{\pi}{\omega_{SN}} - \zeta - \delta \right). \quad (2.7)$$

The boundary β_S angle, β_{23} , separating Mode II and Mode III can be calculated from trajectory T_{23} , as shown in Figure 2.15, by solving the same equations as in (2.2). Angle β_{23} is equal to $\omega_{SN} \times \delta$.

From mode-III operation, as β_S is reduced, the mode transitions and mode boundaries are discussed in Appendix B.2.

Using the algorithm described above, the mode transition sequence and the mode boundaries at various V_{ON} and ω_{SN} can be easily determined. The operating regions shown in Figure 2.11 were results obtained using the algorithm.

It can be seen from Figure 2.11 that the undesirable Mode IV and Mode V operations tend to occur at low V_{ON} and low ω_{SN} .

2.3.6.2 Operating regions above resonant frequency

Figure 2.16 shows several operating regions at frequencies above the resonant frequency. These regions are derived from a similar process as discussed previously in section 2.3.6.1. There are, however, only two possible mode transition sequences existing, as illustrated in Figure 2.17. An algorithm for predicting the mode transition sequence and determining the mode boundaries in this frequency range is developed in Appendix B.3.

2.3.7 DC Characteristics

Once the mode of operation is determined for a given V_{ON} , ω_{SN} , and β_S , the corresponding equilibrium state trajectory can be defined and employed to derive various circuit salient features such as average inductor current (load current), rms inductor

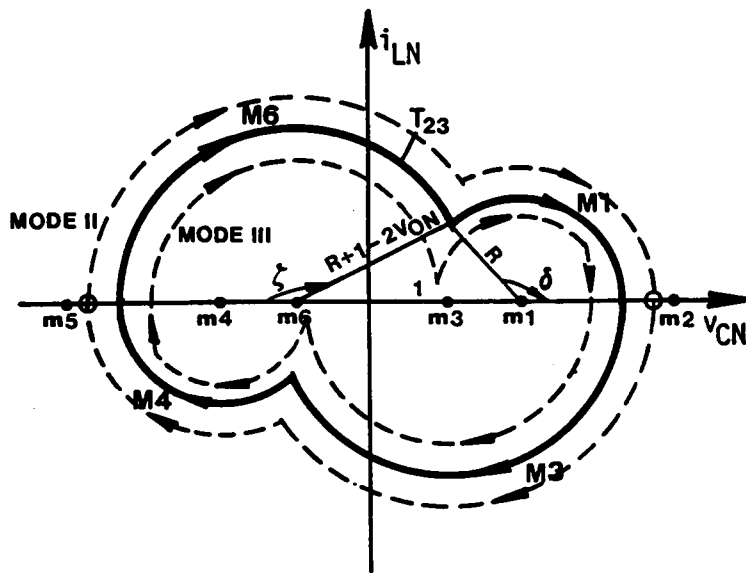
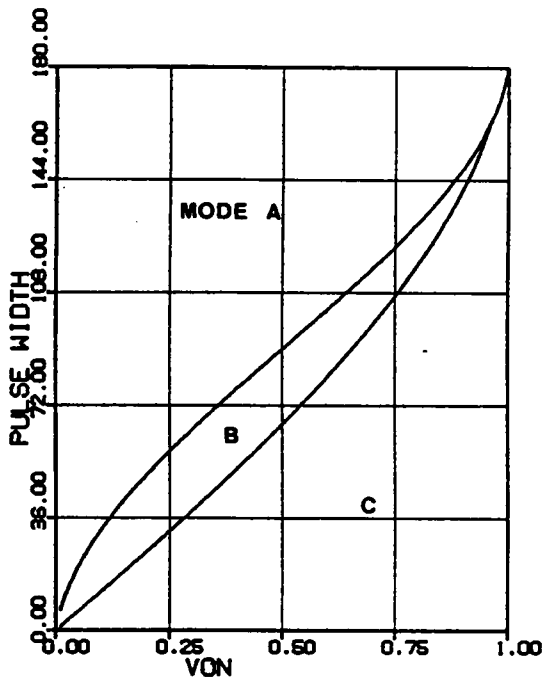
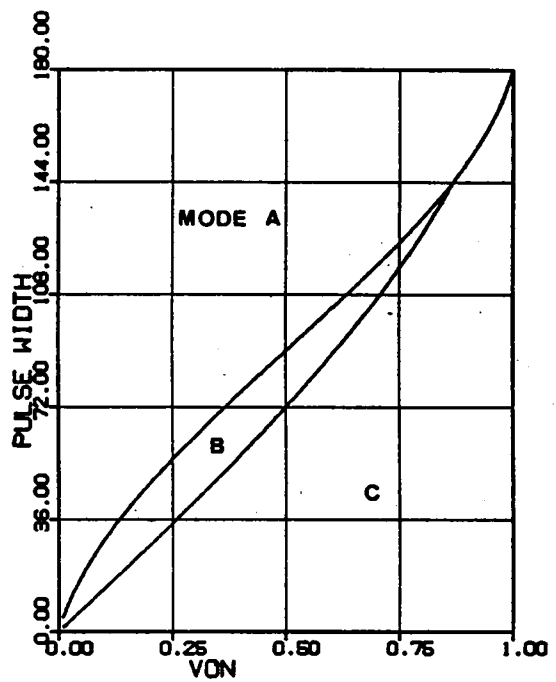


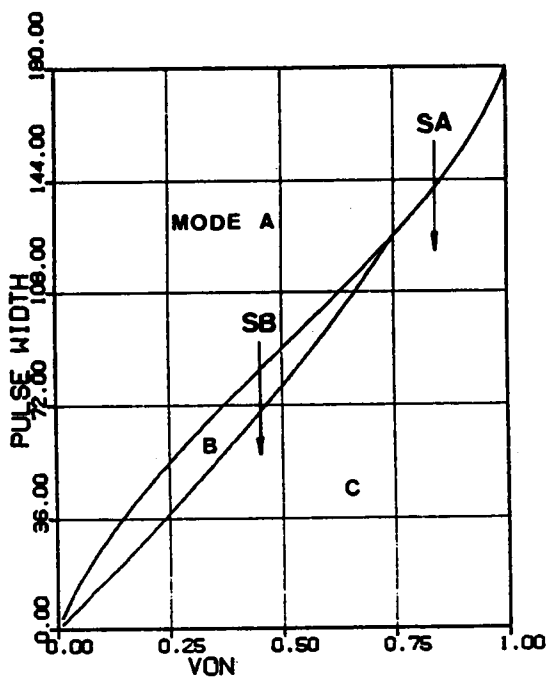
Figure 2.15 Boundary Trajectory Between Mode II and Mode III



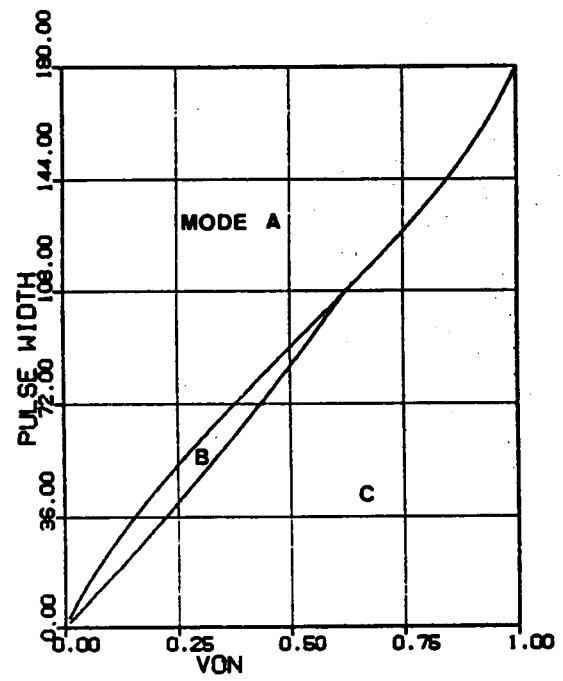
(a) $\omega_{SN} = 1.1$



(b) $\omega_{SN} = 1.2$



(c) $\omega_{SN} = 1.3$



(d) $\omega_{SN} = 1.4$

Figure 2.16 Regions of Operation Above Resonant Frequency

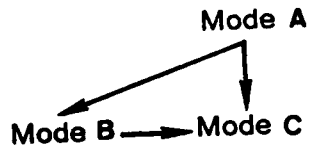


Figure 2.17 Mode Transition Sequences Above Resonant Frequency
(β_S decreases from 180° to 0°)

current, peak capacitor voltage, rms switch currents, average diode currents, switch turn-on currents, and switch turn-off currents. In this section, various important dc characteristics for the CM-SRC are derived.

2.3.7.1 DC characteristics below resonant frequency

Trajectory parameters: To employ an equilibrium state trajectory to calculate various circuit salient features, the parameters defining the trajectory must be obtained first. As illustrated in Figure 2.18, an equilibrium state trajectory is uniquely defined by a number of parameters including several radii, R_1 , R_2 , R_3 , and angles, η , ζ , δ , γ . These parameters can be obtained by solving a set of nonlinear equations derived from the state trajectory. For example, the parameters for the Mode-I trajectory in Figure 2.18 can be obtained by solving equations

$$\begin{aligned}
 \cos(\pi - \gamma) &= \frac{1 + R_1^2 - R_2^2}{2R_1}, \\
 \cos(\pi - \eta) &= \frac{1 + R_3^2 - R_2^2}{2R_3}, \\
 \cos \zeta &= \frac{1 + R_2^2 - R_3^2}{2R_2}, \\
 \cos \delta &= \frac{1 + R_2^2 - R_1^2}{2R_2}, \\
 R_3 &= R_1 - 2V_{ON}, \\
 \frac{\beta_S}{\omega_{SN}} &= \eta + \gamma, \\
 \frac{\pi}{\omega_{SN}} &= \eta + \gamma + \pi - (\zeta + \delta),
 \end{aligned} \tag{2.8}$$

where V_{ON} , ω_{SN} , and β_S are given values.

Since equation (2.8) have multiple solutions, constraints should be imposed on the parameters to obtain the correct one. These constraints can be directly derived from the state trajectory. For example, from Figure 2.18, the parameters for Mode-I trajectory should satisfy

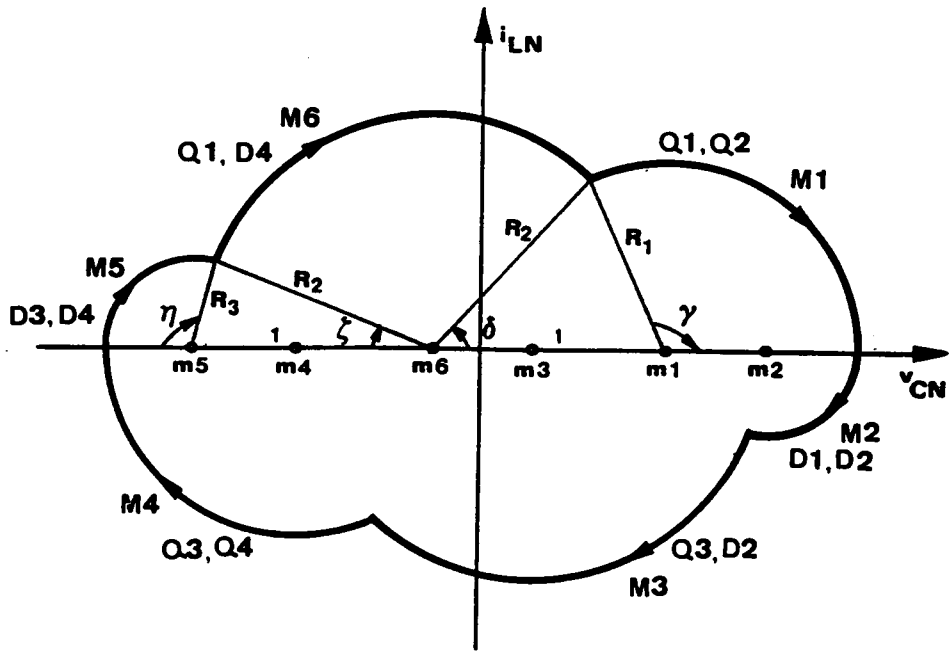


Figure 2.18 Mode-I Trajectory Below Resonant Frequency

$$0 \leq \eta, \zeta, \delta, \gamma \leq \pi, \quad 0 \leq R_2, R_3, \quad 2V_{ON} \leq R_1.$$

The equations and constraints for calculating trajectory parameters for other operating modes are summarized in Appendix B.4.

Circuit salient features: After the trajectory parameters are determined, various salient features of the circuit can be easily calculated. Consider the Mode-I trajectory in Figure 2.18, the following circuit features can be calculated:

- *peak capacitor voltage* $V_{CPK} = (1 - V_{ON}) + R_1;$

- *average inductor current* $I_{AV} = \frac{(DA + DB + DC)}{\omega_0 T_S},$

where,

$$DA = \int_0^\eta R_3 \sin \lambda d\lambda = R_3 \times (1 - \cos \eta),$$

$$DB = \int_\zeta^{\pi-\delta} R_2 \sin \lambda d\lambda = R_2 \times (\cos \zeta + \cos \delta),$$

$$DC = \int_{\pi-\gamma}^\pi R_1 \sin \lambda d\lambda = R_1 \times (1 - \cos \gamma);$$

- *rms inductor current* $I_{LRMS} = \left(\frac{RA + RB + RC}{\omega_0 T_S} \right)^{\frac{1}{2}},$

where,

$$RA = \int_0^\eta (R_3 \sin \lambda)^2 d\lambda = \frac{R_3^2}{2} \times \left(\eta - \frac{\sin 2\eta}{2} \right),$$

$$RB = \int_\zeta^{\pi-\delta} (R_2 \sin \lambda)^2 d\lambda = \frac{R_2^2}{2} \times \left(\pi - \zeta - \delta + \frac{\sin 2\zeta}{2} + \frac{\sin 2\delta}{2} \right),$$

$$RC = \int_{\pi-\gamma}^\pi (R_1 \sin \lambda)^2 d\lambda = \frac{R_1^2}{2} \times \left(\gamma - \frac{\sin 2\gamma}{2} \right);$$

- *rms switch (Q1,Q3) current* $I_{Q1RMS} = \left(\frac{RB + RC}{\omega_0 T_S} \right)^{\frac{1}{2}};$

- *rms switch (Q2,Q4) current* $I_{Q2RMS} = \left(\frac{RC}{\omega_0 T_S} \right)^{\frac{1}{2}};$

- average diode (D1,D3) current $I_{D1AV} = \frac{DA}{\omega_0 T_S}$;
- average diode (D2,D4) current $I_{D2AV} = \frac{DA + DB}{\omega_0 T_S}$;
- switch (Q1,Q3) turn-off current $I_{Q1off} = 0$;
- switch (Q2,Q4) turn-off current $I_{Q2off} = 0$;
- switch (Q1,Q3) turn-on current $I_{Q1on} = R_2 \sin \zeta$;
- switch (Q2,Q4) turn-on current $I_{Q2on} = R_2 \sin \delta$.

The expressions for calculating salient features under other operating modes are tabulated in Appendix B.5.

Output characteristics: Employing the above-derived expressions, various circuit characteristics can be generated using the flowchart shown in Figure 2.19. Figure 2.20 shows the dc control-to-output characteristics for the CM-SRC at several frequencies below the resonant frequency. In the figure, the average inductor current (output current) is plotted as a function of the pulse-width, β_S , of v_S , and the output-to-input voltage ratio, V_{ON} . A β_S angle of 180° corresponds to a full pulse width of v_S (duty ratio = 1). A dotted line is used in each graph to indicate the boundary of natural commutation. Above the dotted line, all the transistors are naturally commutated. Below the dotted line, at least two of the transistors, Q1 and Q3, are force-commutated. It can be seen that the converter is able to regulate the output from no load to a full load. A minimum load, however, has to be maintained to achieve natural commutation of all the transistors. The converter usually operates in the mixed-commutation region under light load where Q2,Q4 are naturally commutated and Q1,Q3 are force-commutated.

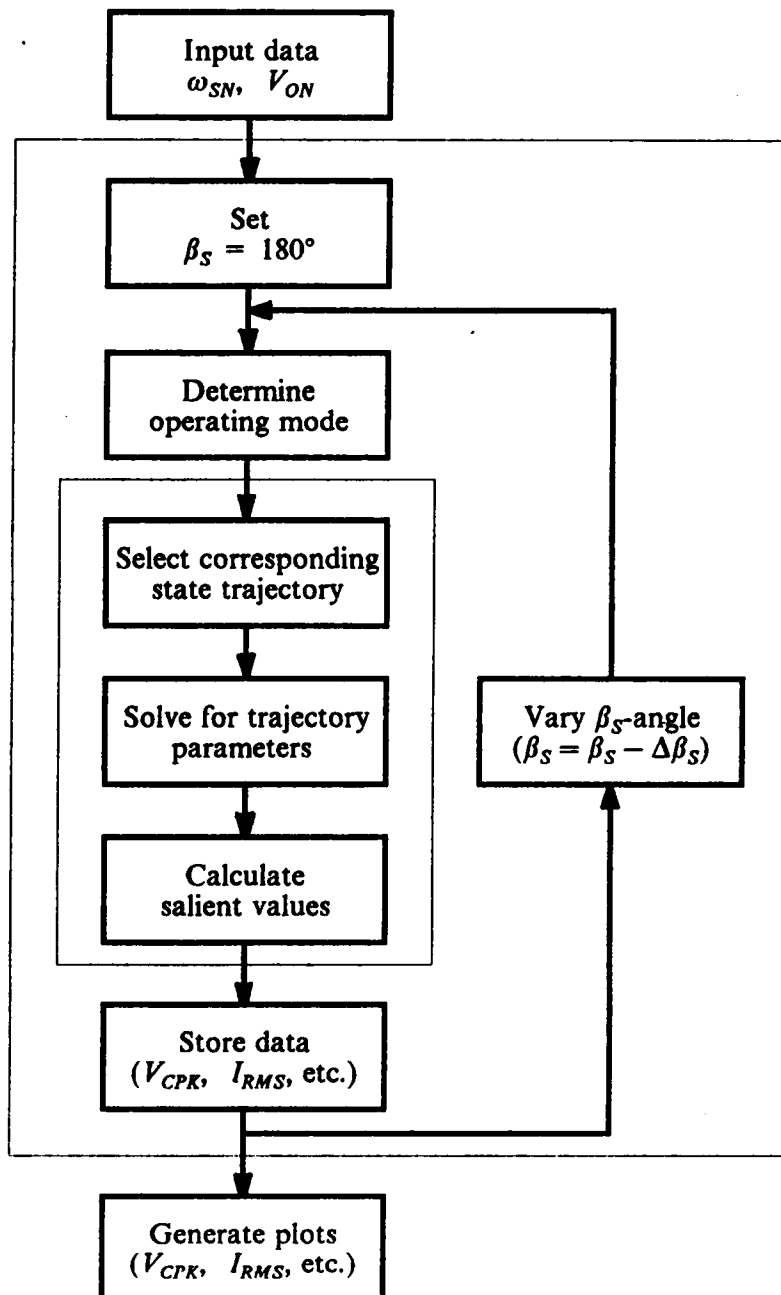
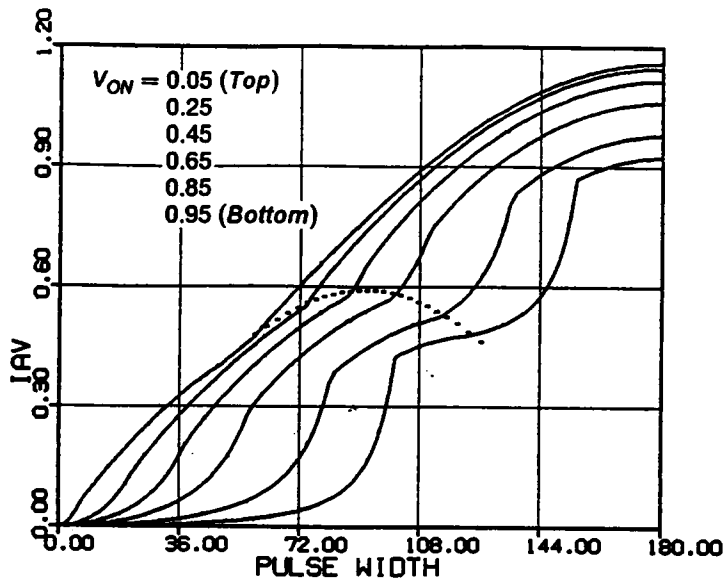
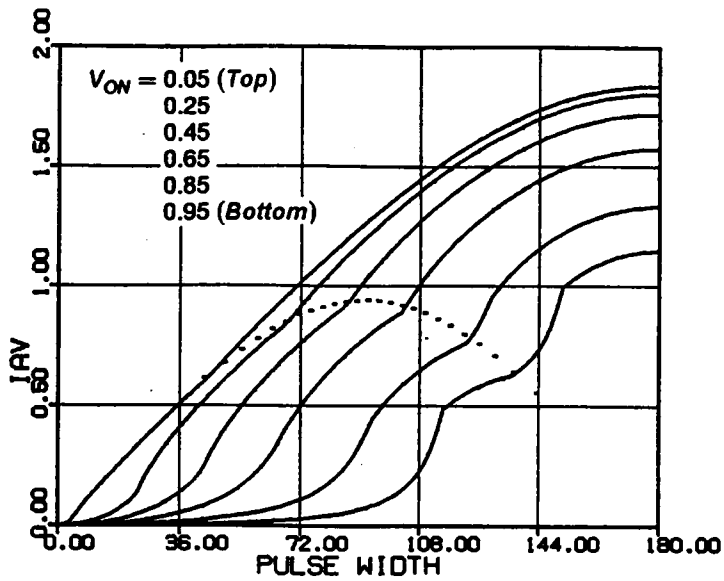


Figure 2.19 A Flowchart Used to Generate Plots of DC Characteristics

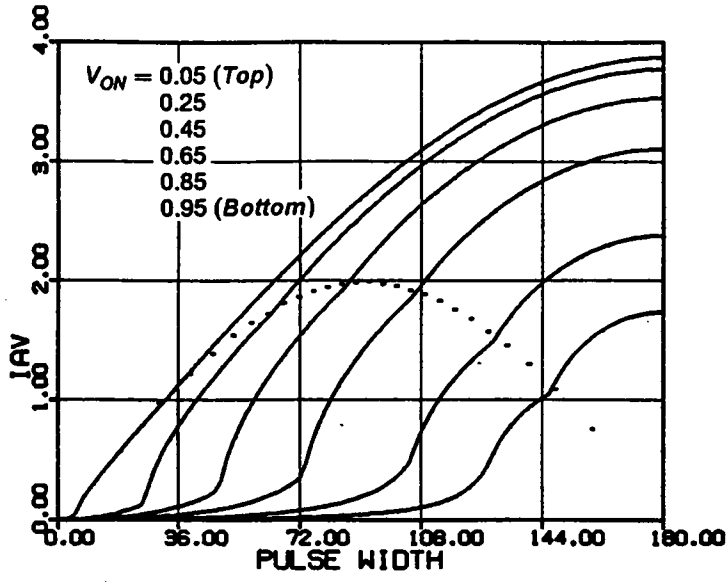


(a) $\omega_{SN} = 0.7$



(b) $\omega_{SN} = 0.8$

Figure 2.20 DC Control-to-Output Characteristics Below Resonant Frequency

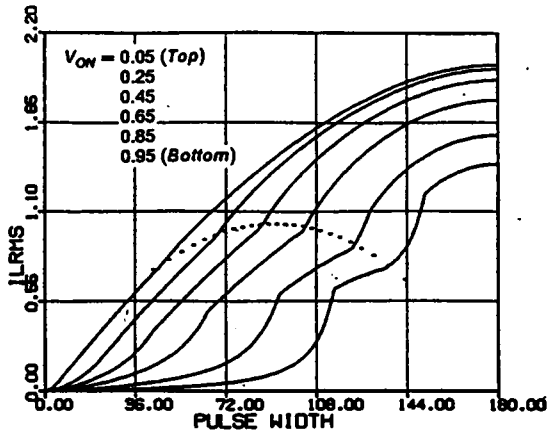


(c) $\omega_{SN} = 0.9$

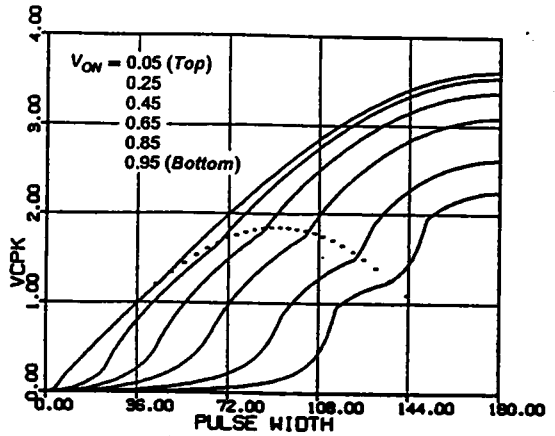
Figure 2.20 Continued

Figure 2.21 shows other important dc characteristics for the CM-SRC at frequency $\omega_{SN} = 0.8$. Notice that the currents of Q1,Q3 and the currents of Q2,Q4 are not balanced, as can be seen from Figures 2.21(c) and 2.21(d). Same phenomenon also exists between the currents of D1,D3 and D2,D4. This is due to the phase displacement in the triggering of the transistors. In general, transistors Q1,Q3 and diodes D2,D4 carry higher currents when the converter operates below the resonant frequency.

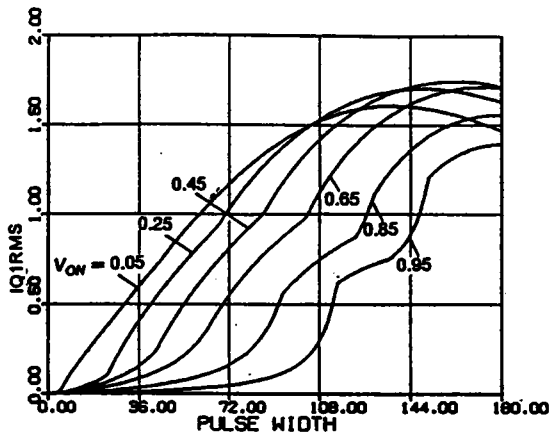
Similar dc characteristics for other frequencies can be found in Appendix B.6.



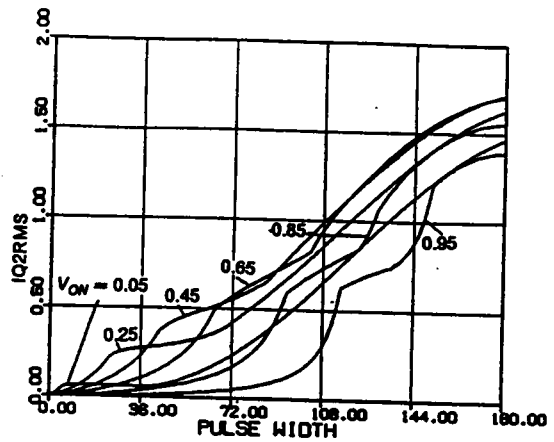
(a) RMS inductor current



(b) Peak capacitor voltage

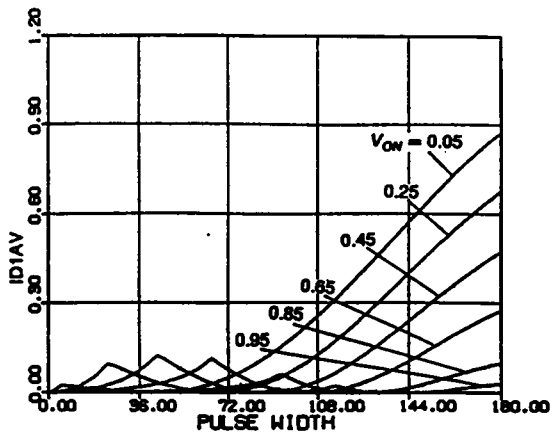


(c) RMS switch current ($Q1, Q3$)

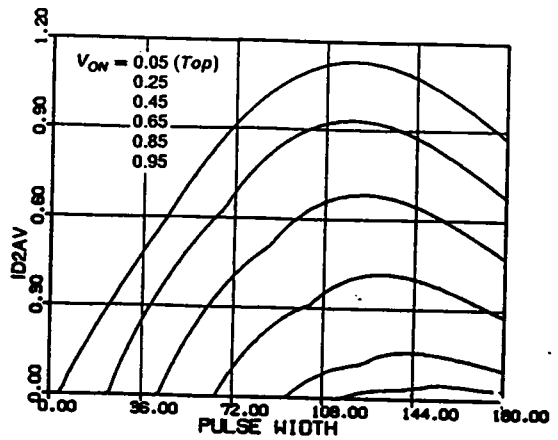


(d) RMS switch current ($Q2, Q4$)

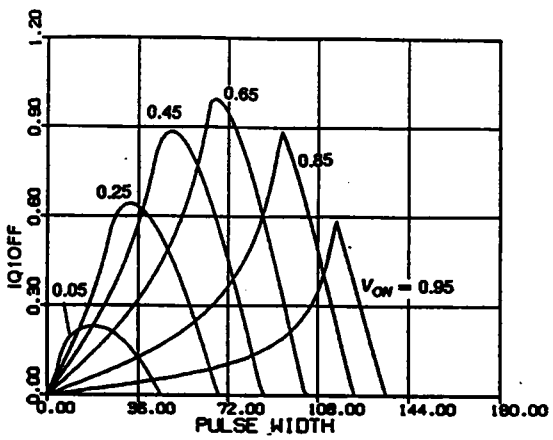
Figure 2.21 Characteristics for Various Circuit Salient Features at $\omega_{SN} = 0.8$



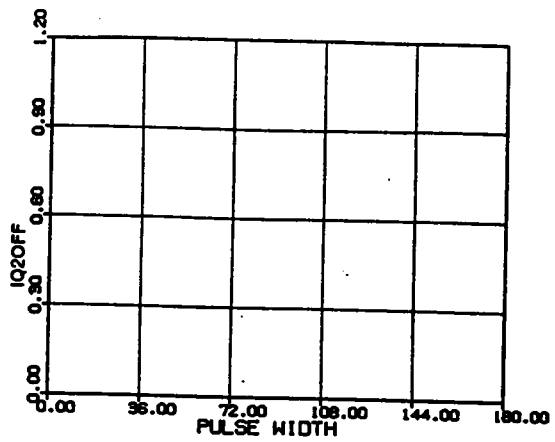
(e) Average diode current (D1,D3)



(f) Average diode current (D2,D4)

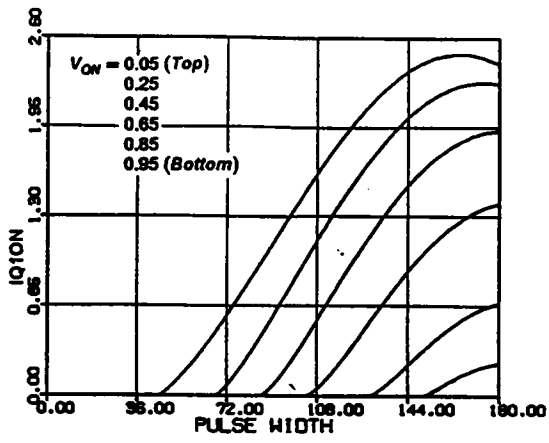


(g) Switch turn-off current (Q1,Q3)

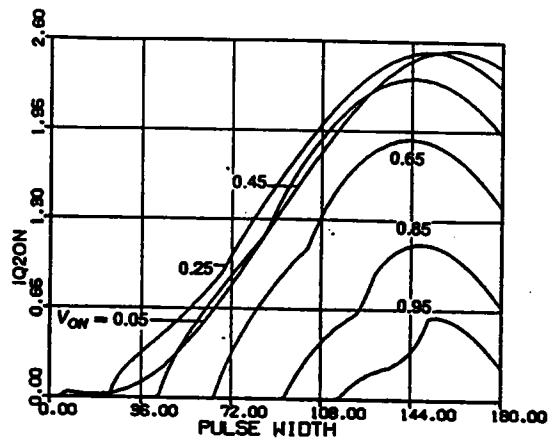


(h) Switch turn-off current (Q2,Q4)

Figure 2.21 Continued



(i) Switch turn-on current ($Q1, Q3$)



(j) Switch turn-on current ($Q2, Q4$)

Figure 2.21 Continued

2.3.7.2 DC characteristics above resonant frequency

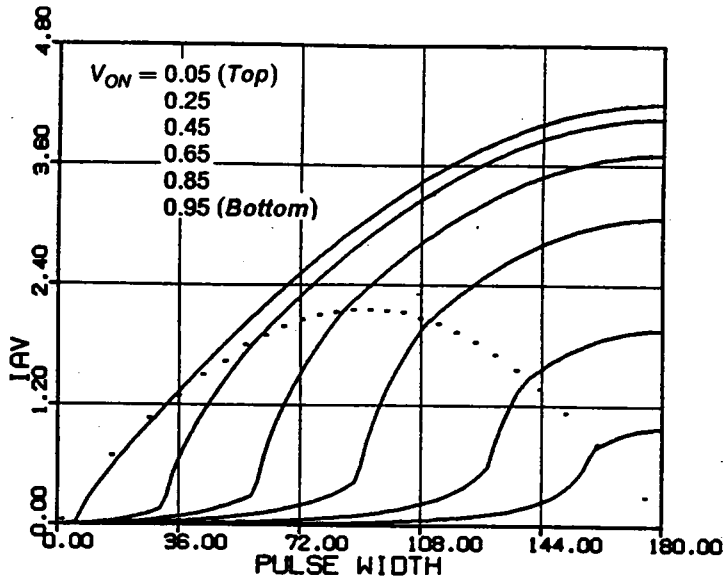
Trajectory parameters: The parameters for the equilibrium trajectories above resonant frequency are defined in Appendix B.7. The equations and the constraints for calculating these parameters are also included in the same Appendix.

Circuit salient features: The expressions for calculating various circuit salient features under different operating modes above resonant frequency are tabulated in Appendix B.8.

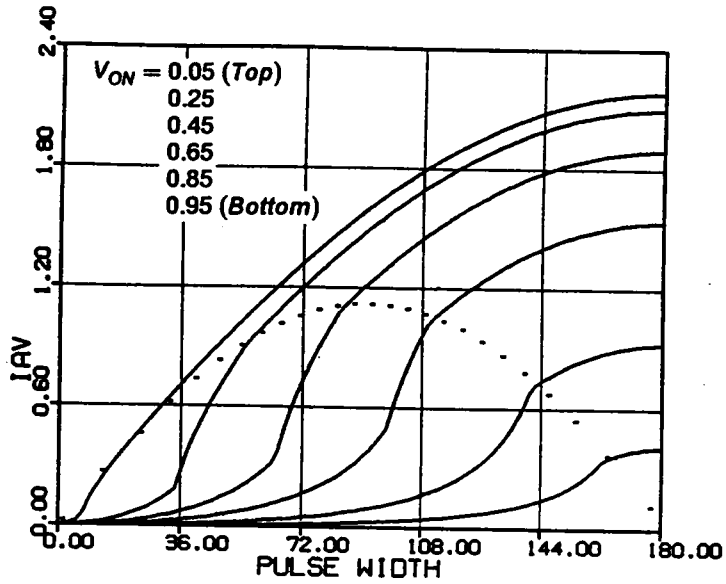
Output characteristics: Figure 2.22 shows the dc control-to-output characteristics at frequencies $\omega_{SN} = 1.1, 1.2, 1.3,$ and 1.4 . The characteristics are similar to those obtained below resonant frequency. A dotted line is used in each figure to indicate the force-commutation boundary. Above the dotted line, all the transistors are force-commutated. Below the dotted line, transistors Q1 and Q3 are force-commutated while transistors Q2 and Q4 are naturally commutated. Again, the converter is able to regulate its output from no load to a full load. A minimum load, however, has to be maintained to achieve zero-voltage turn-on (force commutation) of all the transistors. The converter usually operate in the mixed-commutation region under light load.

Figure 2.23 shows other important dc characteristics at frequency $\omega_{SN} = 1.2$. Again, the currents in the transistors and the currents in the diodes are unbalanced, as shown in Figures 2.23(c) and 2.23(d) and Figures 2.23(e) and 2.23(f), respectively. However, in this frequency range, transistors Q2,Q4 and diodes D1,D3 carry higher currents.

Similar dc characteristics for other frequencies can be found in Appendix B.9.

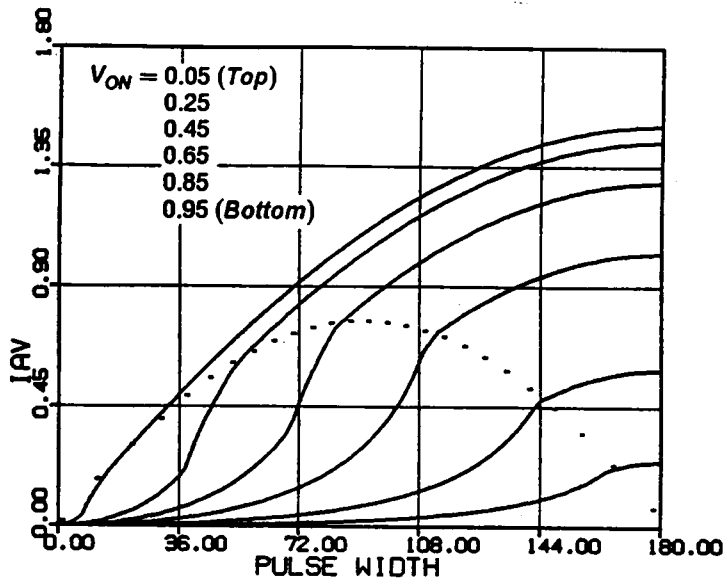


(a) $\omega_{SN} = 1.1$

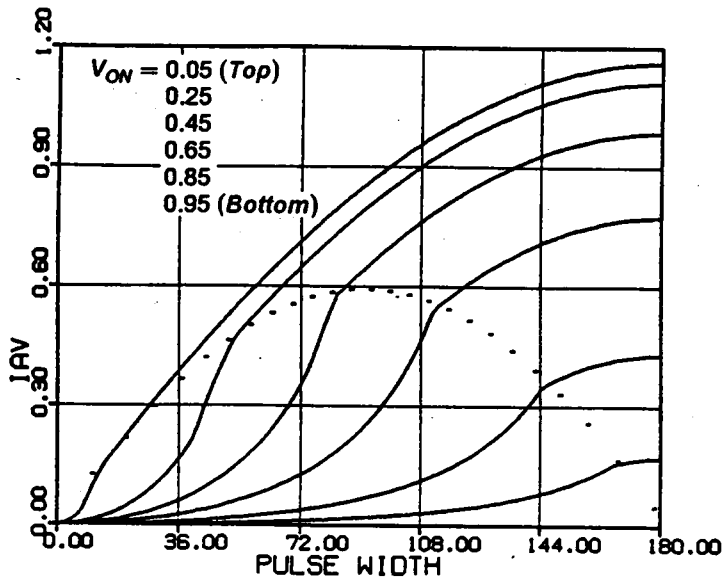


(b) $\omega_{SN} = 1.2$

Figure 2.22 DC Control-to-Output Characteristics Above Resonant Frequency

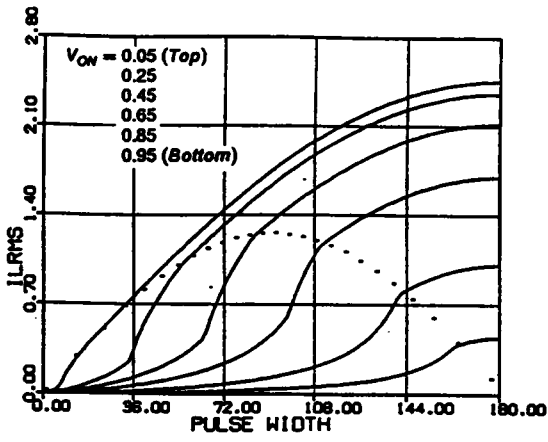


(c) $\omega_{SN} = 1.3$

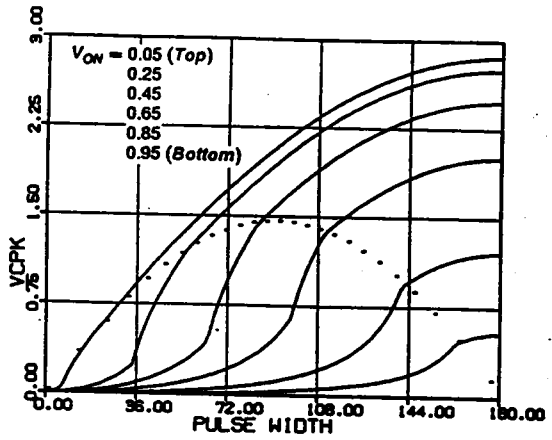


(d) $\omega_{SN} = 1.4$

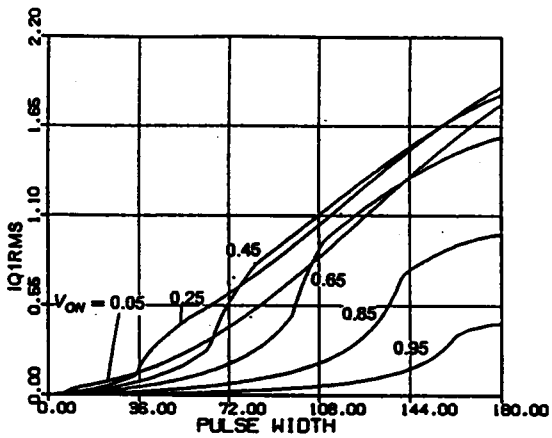
Figure 2.22 Continued



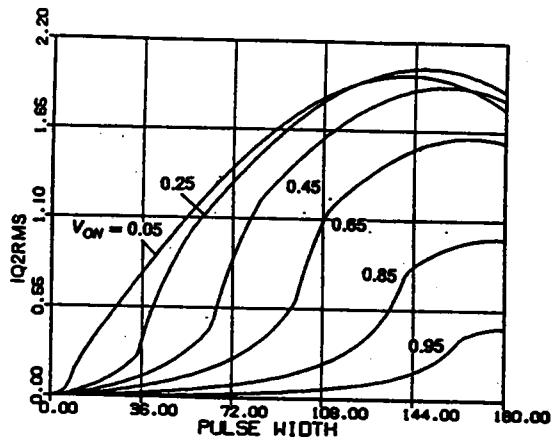
(a) RMS inductor current



(b) Peak capacitor voltage

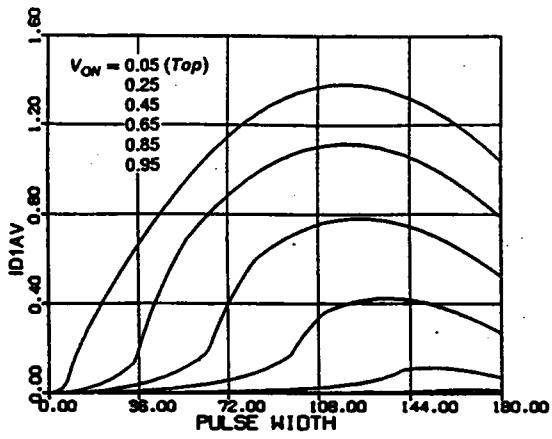


(c) RMS switch current ($Q1, Q3$)

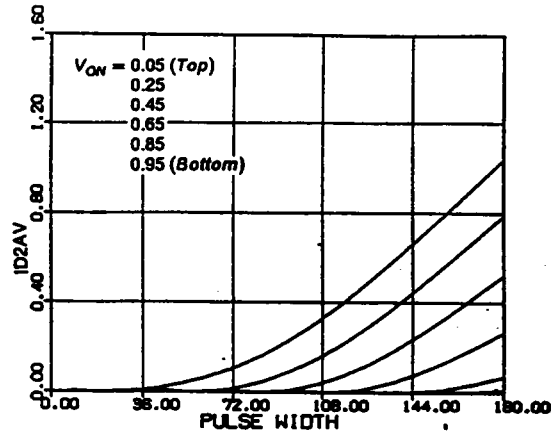


(d) RMS switch current ($Q2, Q4$)

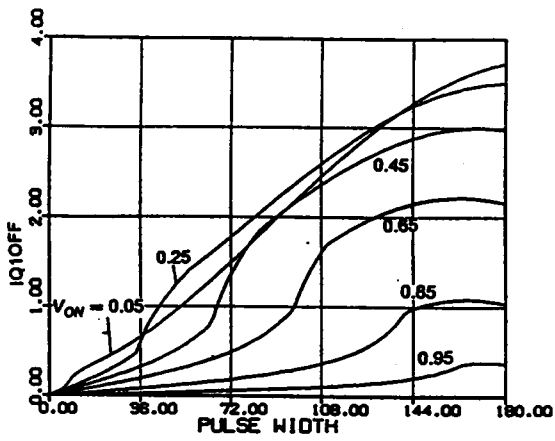
Figure 2.23 Characteristics for Various Circuit Salient Features at $\omega_{SN} = 1.2$



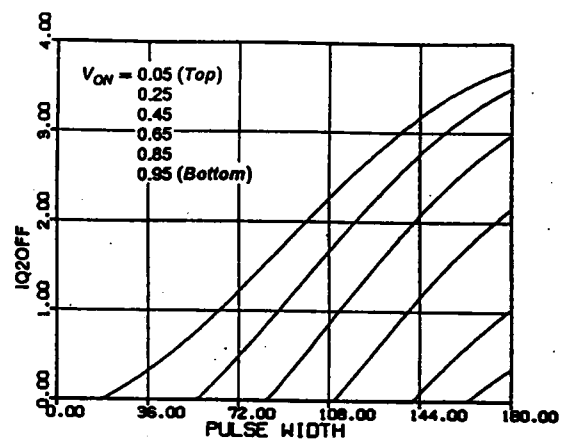
(e) Average diode current ($D1, D3$)



(f) Average diode current ($D2, D4$)



(g) Switch turn-off current ($Q1, Q3$)



(h) Switch turn-off current ($Q2, Q4$)

Figure 2.23 Continued

2.4 DESIGN EXAMPLES

The dc characteristics derived in the previous section are employed to facilitate design of a CM-SRC in this section. Three design examples are given. The first example designs the converter to operate in a natural-commutation region ($\omega_{SN} < 1$) such that all the transistors' turn-off losses are eliminated. The second example designs the converter to operate in a mixed-commutation region ($\omega_{SN} < 1$) such that the turn-on losses of Q1,Q3 and the turn-off losses of Q2,Q4 are eliminated. Lossless capacitor snubbers can be used across Q1 and Q3 to reduce their turn-off losses. The third example designs the converter to operate in a force-commutation region ($\omega_{SN} > 1$) such that all the transistors turn-on losses are eliminated. Lossless capacitor snubbers can be used across all the transistors to reduce their turn-off losses.

The converter is designed to satisfy the following requirements.

$$\text{Input voltage} = 40\text{V} \sim 60\text{V}.$$

$$\text{Output voltage} = 5\text{V}.$$

$$\text{Output power} = 40\text{W} \sim 50\text{W}.$$

Assume an output transformer with turn ratio $n : 1$ is used between the resonant tank and the load circuit. Then,

$$V_{ONmax} = \frac{5n}{40}, \quad V_{ONmin} = \frac{5n}{60},$$
$$I_{AVmax} = \frac{10}{n \times 40/Z_0}, \quad I_{AVmin} = \frac{8}{n \times 60/Z_0}.$$

(The load current range is from 8A to 10A)

2.4.1 Example 1 - Design in Natural Commutation Region

To achieve natural commutation of all the transistors, an operating frequency below resonant frequency must be chosen. Choose $\omega_{SN} = 0.8$. From Figure 2.24(a), to ensure output regulation, choose

$$I_{AVmax} = \frac{10}{n \times 40/Z_0} = 1.7.$$

The minimum I_{AV} is then

$$I_{AVmin} = \frac{8}{n \times 60/Z_0} = 0.9.$$

In order to maintain natural commutation of transistors at I_{AVmin} , V_{ONmin} should be chosen less than or equal to 0.28. Choose $V_{ONmin} = 0.25$. This leads to

$$n = V_{ONmin} \times \frac{60}{5} = 3,$$

and

$$V_{ONmax} = \frac{5n}{40} = 0.375.$$

The characteristic impedance, Z_0 , is calculated as

$$Z_0 = I_{AVmax} \times n \times 40 \times \frac{1}{10} = 18\Omega.$$

This value together with the resonant frequency, $\omega_0 = 1/\sqrt{LC}$, can be used to determine the values of resonant capacitance C and resonant inductance L.

The normalized load range, as can be seen from Figure 2.24(a), is from $8/(n \times 40/Z_0) = 1.36$ to $I_{AVmax} = 1.7$ at $V_{ONmax} = 0.375$ and from $I_{AVmin} = 0.9$ to $10/(n \times 60/Z_0) = 1.125$ at $V_{ONmin} = 0.25$.

The normalization factor for current, $I_{P.U.}$, is equal to $40/Z_0 = 2.22A$ at $V_{ONmax} = 0.375$, and equal to $60/Z_0 = 3.33A$ at $V_{ONmin} = 0.25$.

The ranges of β_S in this design are

$$\beta_S = 113^\circ \sim 152^\circ \quad \text{at } V_{ONmax}$$

$$\beta_S = 71^\circ \sim 85^\circ \quad \text{at } V_{ONmin}$$

The converter operates in Mode I, as can be seen from Figure 2.10(f).

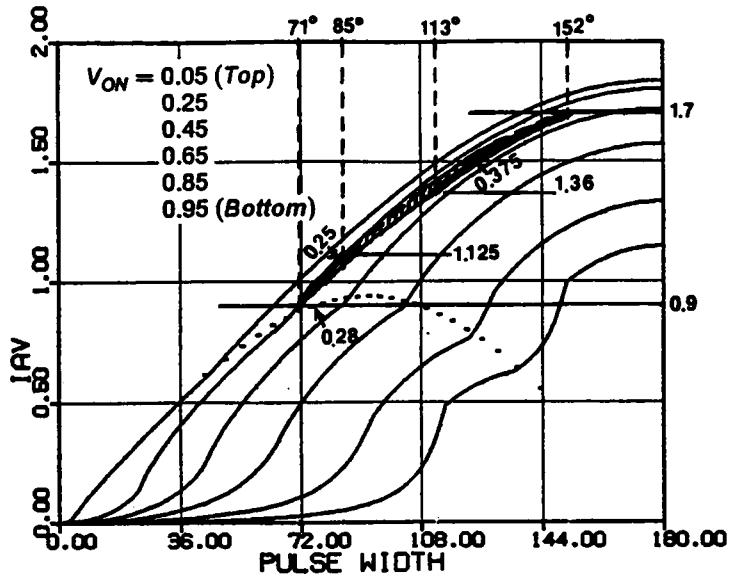
Using the above β_S ranges, various important circuit features can be derived from Figure 2.24. In Figure 2.24, the ranges of various circuit features at V_{ONmax} and V_{ONmin} are highlighted with dotted line segments. An 'X' is used to indicate the particular operating point where the maximum circuit feature occurs.

Since the characteristics are normalized, the obtained data should be denormalized to reflect the real values. For example, the maximum normalized rms switch current, $I_{Q1RMSmax}$, is 1.27, as can be seen from Figure 2.24(d). This value should be multiplied by the current normalization factor $I_{P.U.} = 3.33A$ at $V_{ON} = 0.25$. Thus, the real maximum rms switch currents of Q1 and Q3 are

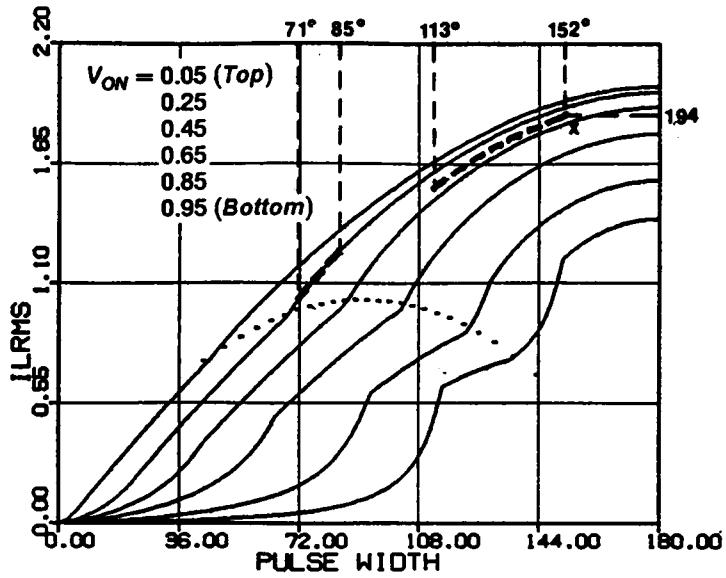
$$I_{Q1RMSmax} = 1.27 \times 3.33 = 4.23A.$$

The various circuit salient features for this design are summarized in the following:

$$V_{CPKmax} = 132V, \quad I_{LRMSmax} = 4.3A,$$

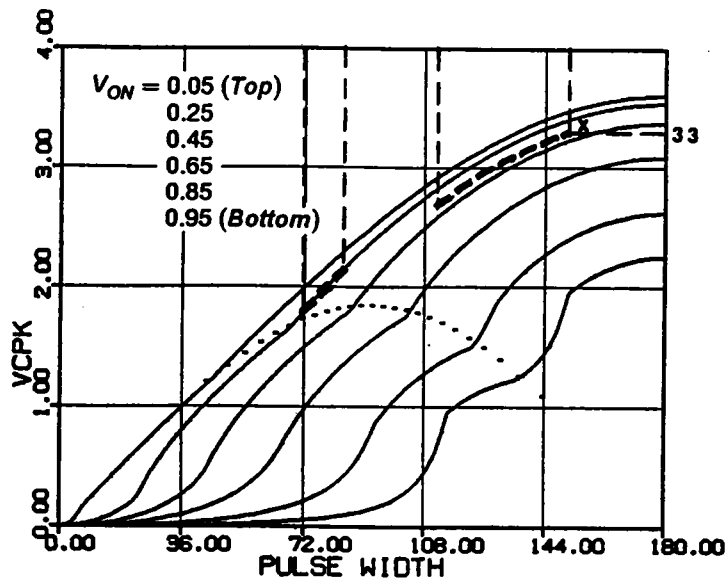


(a) Average inductor current (Load current)



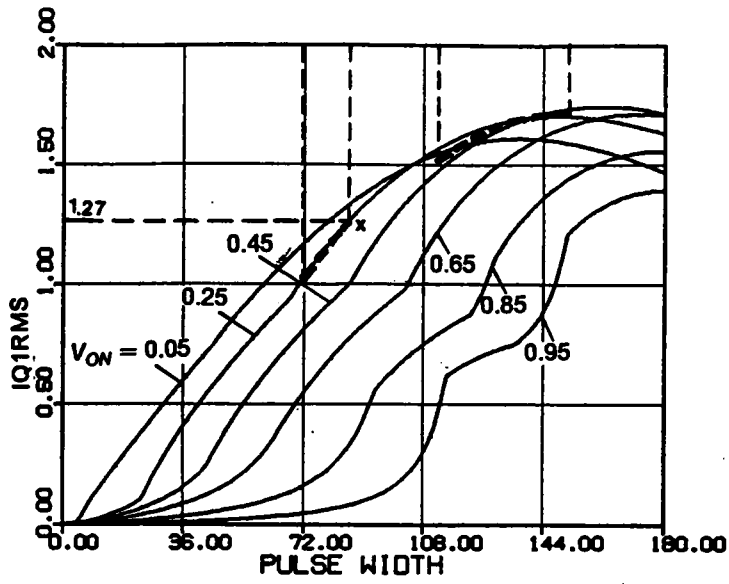
(b) RMS inductor current

Figure 2.24 Design Example in Natural Commutation Region

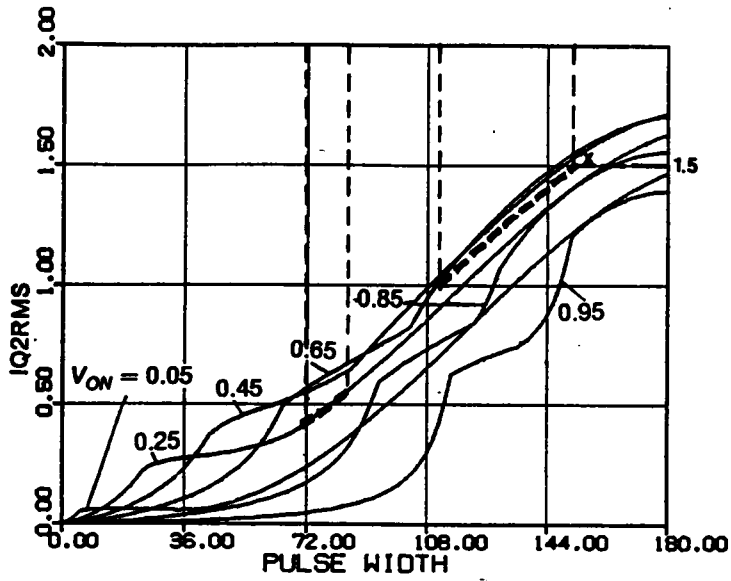


(c) Peak capacitor voltage

Figure 2.24 Continued

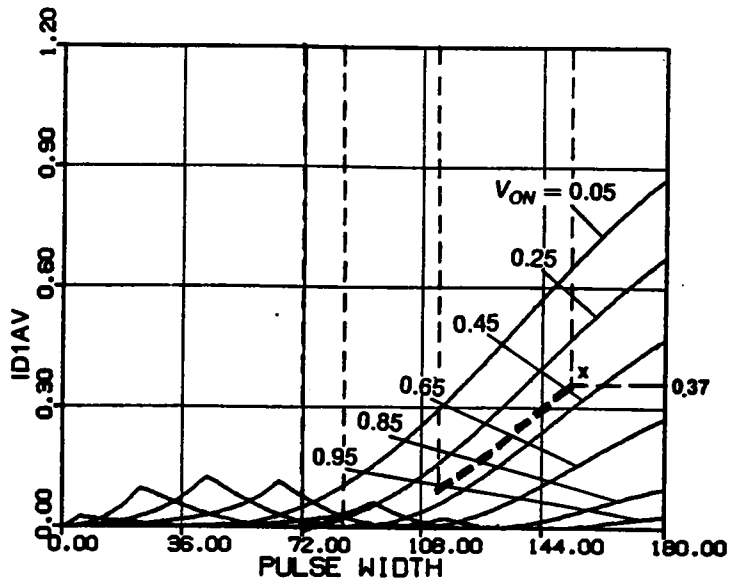


(d) RMS switch current ($Q1, Q3$)

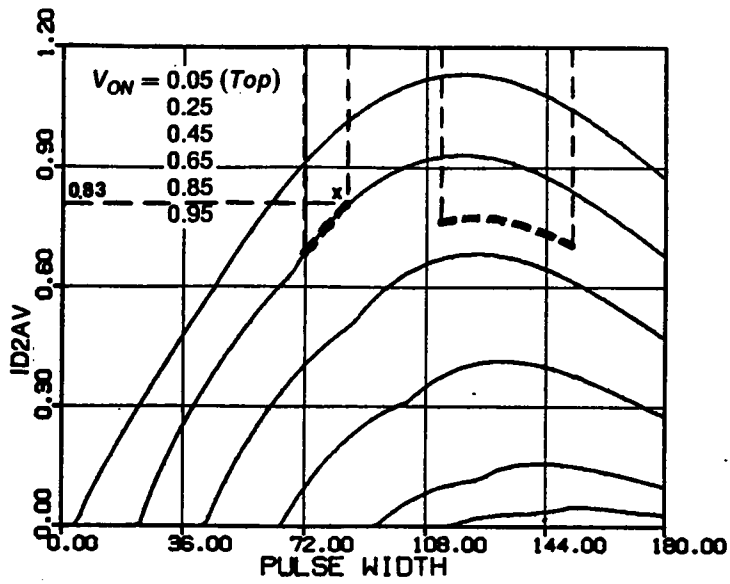


(e) RMS switch current ($Q2, Q4$)

Figure 2.24 Continued

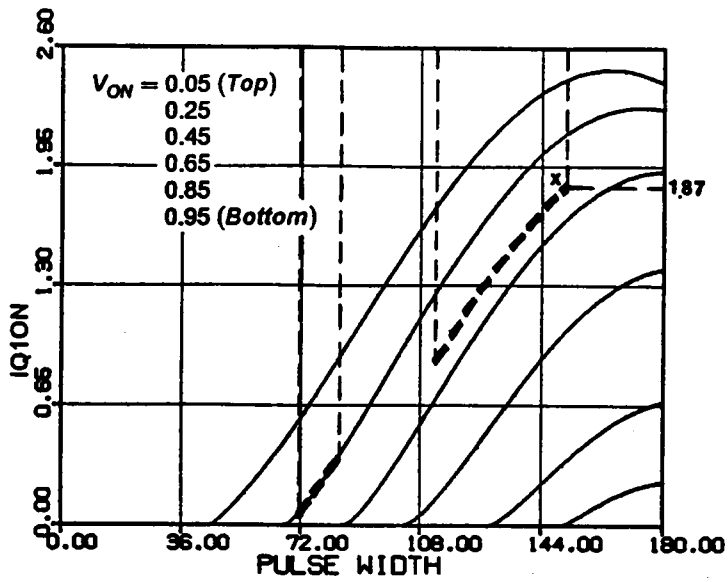


(f) Average diode current (D1,D3)

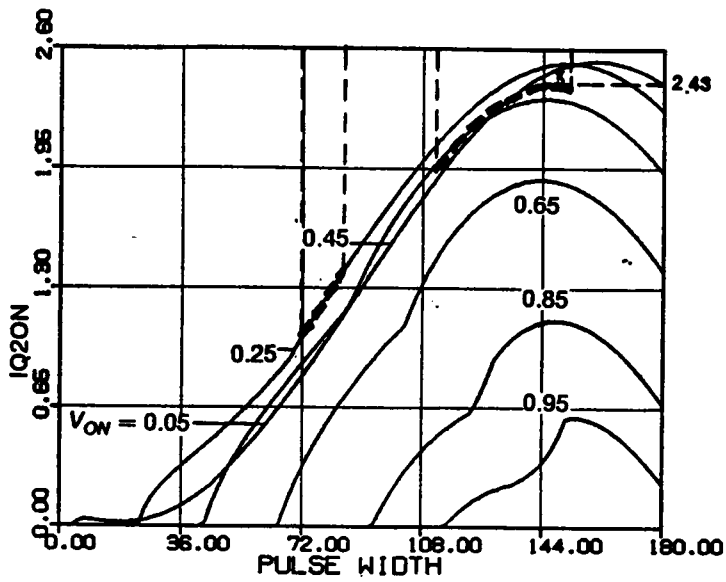


(g) Average diode current (D2,D4)

Figure 2.24 Continued



(h) Transistor turn-on Current ($Q1, Q3$)



(i) Transistor turn-on Current ($Q2, Q4$)

Figure 2.24 Continued

$$\begin{aligned}
I_{Q1RMSmax} &= 4.23A, & I_{Q2RMSmax} &= 3.3A, \\
I_{D1AVmax} &= 0.83A, & I_{D2AVmax} &= 2.75A, \\
I_{Q1offmax} &= 0.A & I_{Q2offmax} &= 0.A, \\
I_{Q1onmax} &= 4.16A, & I_{Q2onmax} &= 5.39A .
\end{aligned}$$

2.4.2 Example 2 - Design in Mixed-Commutation Region

To achieve zero-voltage turn-on (force commutation) of Q1,Q3 and zero-current turn-off (natural commutation) of Q2,Q4, the operating frequency can be chosen either below or above resonant frequency. Choose $\omega_{SN} = 0.8$. From Figure 2.25(a), to ensure force-commutation of Q1 and Q3, choose $I_{AVmax} = 10/(n \times 40/Z_0) = 0.75$. This leads to

$$I_{AVmin} = \frac{8}{n \times 60/Z_0} = 0.4.$$

Although V_{ONmax} can be chosen anywhere between 0.15 and 0.85, as shown in Figure 2.25(a), choose $V_{ONmax} = 0.65$ to avoid possible Mode-IV operation (refer to Figure 2.11(f)). This leads to

$$n = V_{ONmax} \times \frac{40}{5} = 5.2,$$

and

$$V_{ONmin} = \frac{5n}{60} = 0.43.$$

The characteristic impedance, Z_0 , is calculated as

$$Z_0 = I_{AVmax} \times n \times 40 \times \frac{1}{10} = 15.6\Omega.$$

The normalized load range, as can be seen from Figure 2.25(a), is from $8/(n \times 40/Z_0) = 0.6$ to $I_{AVmax} = 0.75$ at $V_{ONmax} = 0.65$ and from $I_{AVmin} = 0.4$ to $10/(n \times 60/Z_0) = 0.5$ at $V_{ONmin} = 0.43$.

The current normalization factor, $I_{P.U.}$, is equal to $40/Z_0 = 2.56A$ at $V_{ONmax} = 0.65$, and equal to $60/Z_0 = 3.85A$ at $V_{ONmin} = 0.43$.

The ranges of β_S in this design are

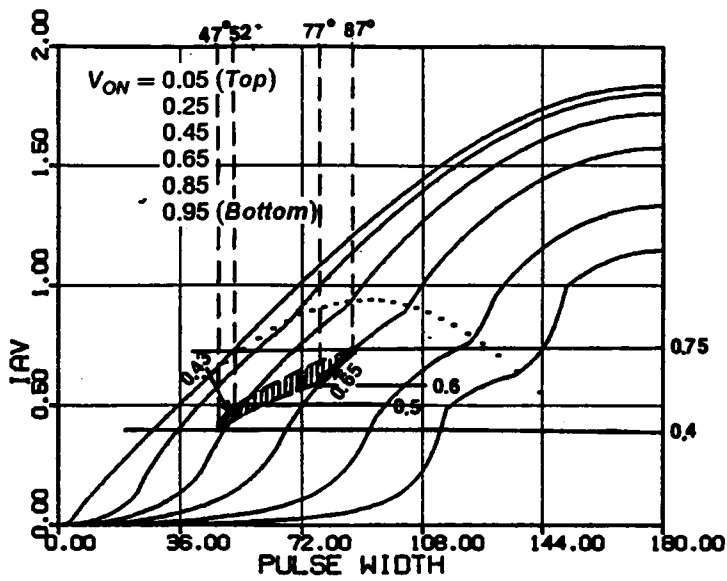
$$\begin{aligned} \beta_S &= 77^\circ \sim 87^\circ && \text{at } V_{ONmax}, \\ \beta_S &= 47^\circ \sim 52^\circ && \text{at } V_{ONmin}. \end{aligned}$$

The converter operates in Mode III, as can be seen from Figure 2.11(f).

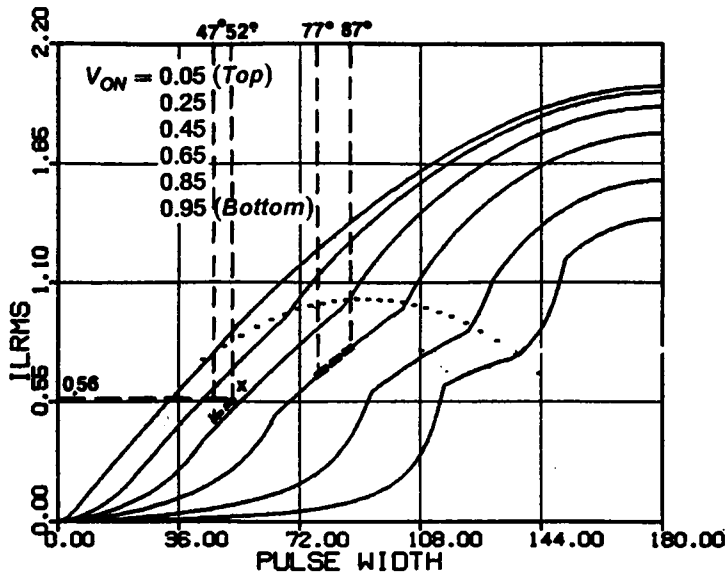
Again, using the above β_S ranges, the following salient features are obtained for this design,

$$\begin{aligned} V_{CPKmax} &= 57.2V, & I_{LRMSmax} &= 2.14A, \\ I_{Q1RMSmax} &= 2.0A, & I_{Q2RMSmax} &= 1.76A, \\ I_{D1AVmax} &= 0.3A, & I_{D2AVmax} &= 0.8A, \\ I_{Q1offmax} &= 3.3A & I_{Q2offmax} &= 0A, \\ I_{Q1onmax} &= 0A, & I_{Q2onmax} &= 1.95A. \end{aligned}$$

The ranges of various salient features at V_{ONmax} and V_{ONmin} are highlighted with dotted line segments in Figure 2.25.

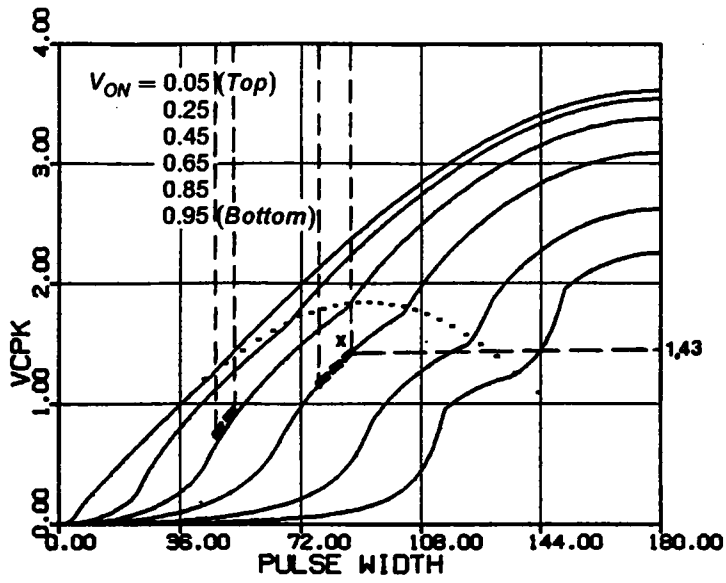


(a) Average inductor current (Load current)



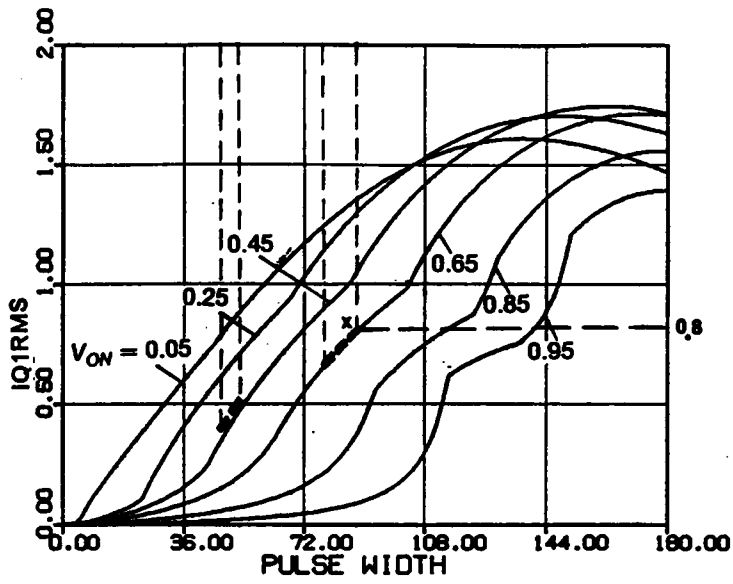
(b) RMS inductor current

Figure 2.25 Design Example in Mixed-Commutation Region

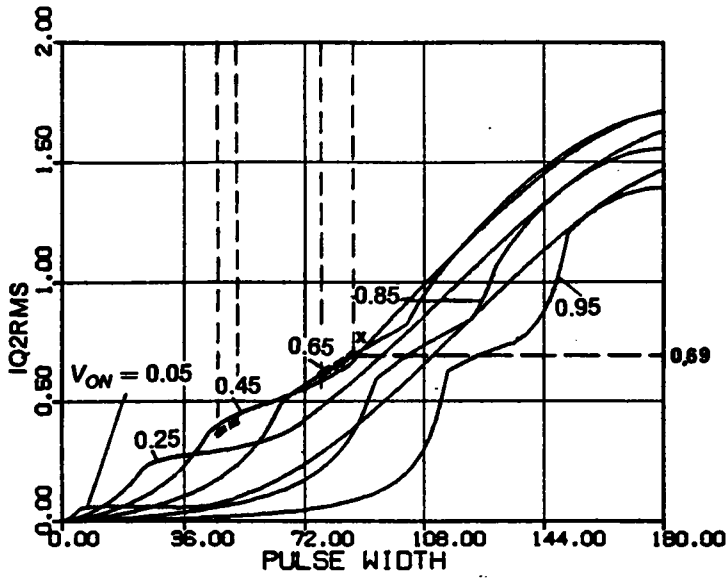


(c) Peak capacitor voltage

Figure 2.25 Continued

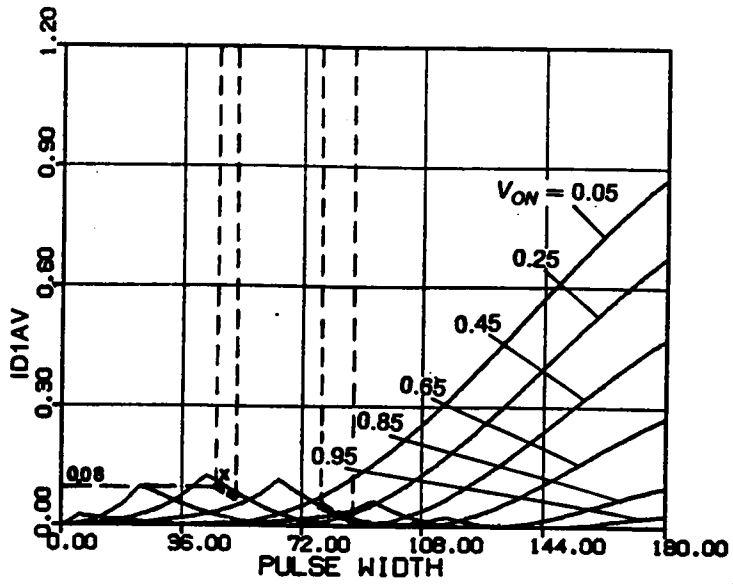


(d) RMS switch current (Q1,Q3)

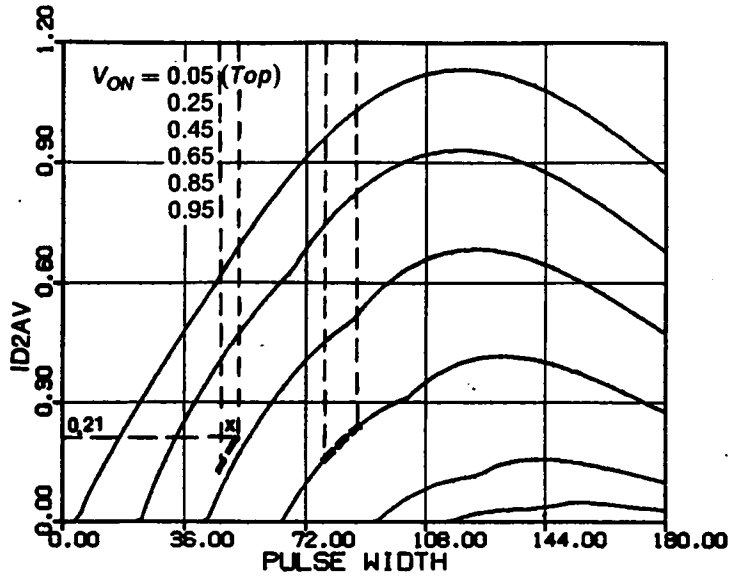


(e) RMS switch current (Q2,Q4)

Figure 2.25 Continued

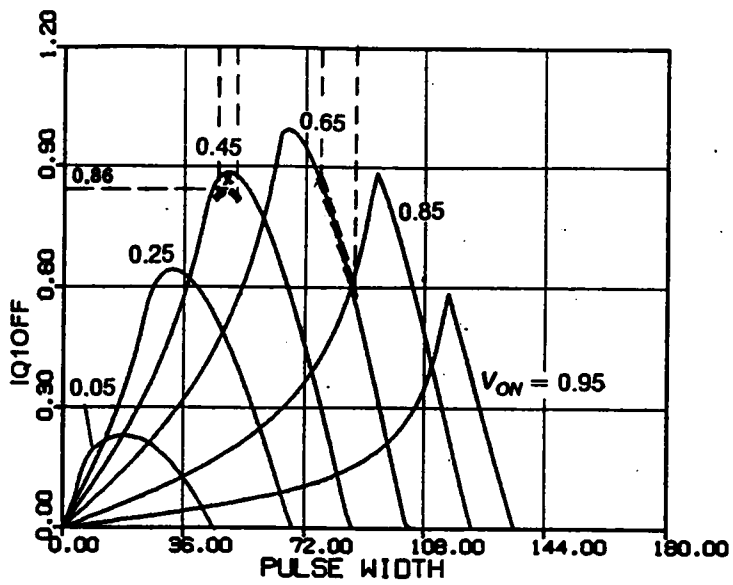


(f) Average diode current (D1,D3)

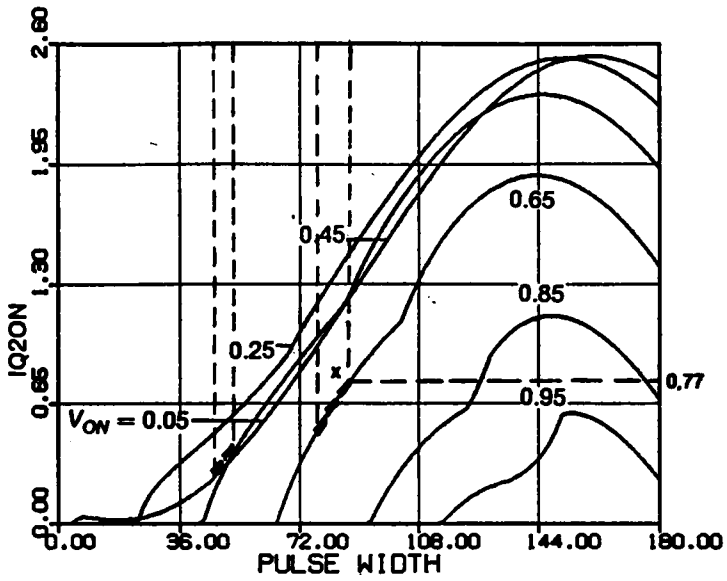


(g) Average diode current (D2,D4)

Figure 2.25 Continued



(h) Transistor turn-off Current ($Q1, Q3$)



(i) Transistor turn-on Current ($Q2, Q4$)

Figure 2.25 Continued

2.4.3 Example 3 - Design in Force-Commutation Region

To achieve zero-voltage turn-on (force commutation) of all the transistors, the operating frequency must be chosen above resonant frequency. Choose $\omega_{SN} = 1.2$. From Figure 2.26(a), to ensure output regulation, choose

$$I_{AVmax} = \frac{10}{n \times 40/Z_0} = 1.8.$$

The minimum I_{AV} can then be determined as

$$I_{AVmin} = \frac{8}{n \times 60/Z_0} = 0.96.$$

In order to maintain force commutation of transistors at I_{AVmin} , V_{ONmin} should be chosen less than or equal to 0.28, as can be seen from Figure 2.26(a). Choose $V_{ONmin} = 0.25$. This leads to

$$n = V_{ONmin} \times \frac{60}{5} = 3,$$

and

$$V_{ONmax} = \frac{5n}{40} = 0.375.$$

The characteristic impedance, Z_0 , is calculated as

$$Z_0 = I_{AVmax} \times n \times 40 \times \frac{1}{10} = 21.6\Omega.$$

The normalized load range, as can be seen from Figure 2.26(a), is from $8/(n \times 40/Z_0) = 1.44$ to $I_{AVmax} = 1.8$ at $V_{ONmax} = 0.375$ and from $I_{AVmin} = 0.96$ to $10/(n \times 60/Z_0) = 1.2$ at $V_{ONmin} = 0.25$.

The normalization factor for current, $I_{P.U.}$, is equal to $40/Z_0 = 1.85A$ at $V_{ONmax} = 0.375$, and equal to $60/Z_0 = 2.78A$ at $V_{ONmin} = 0.25$.

The ranges of β_S in this design are

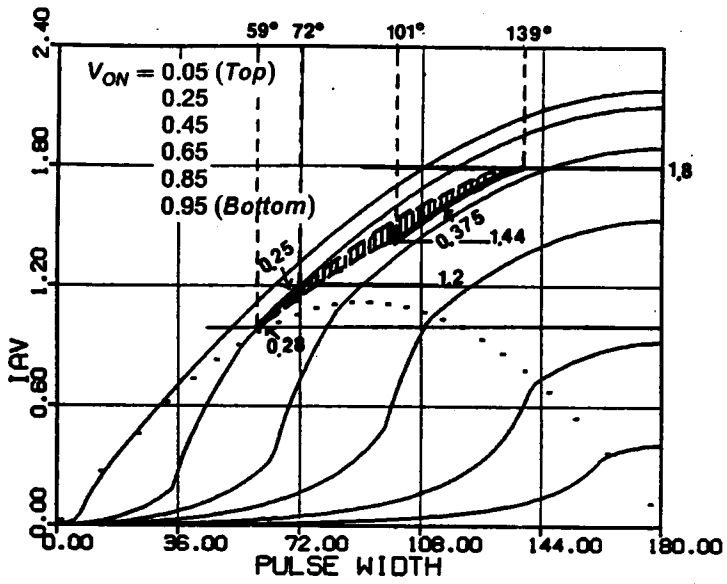
$$\begin{aligned} \beta_S &= 101^\circ \sim 139^\circ && \text{at } V_{ONmax}, \\ \beta_S &= 59^\circ \sim 72^\circ && \text{at } V_{ONmin}. \end{aligned}$$

The converter operates in Mode A, as can be seen from Figure 2.16(b).

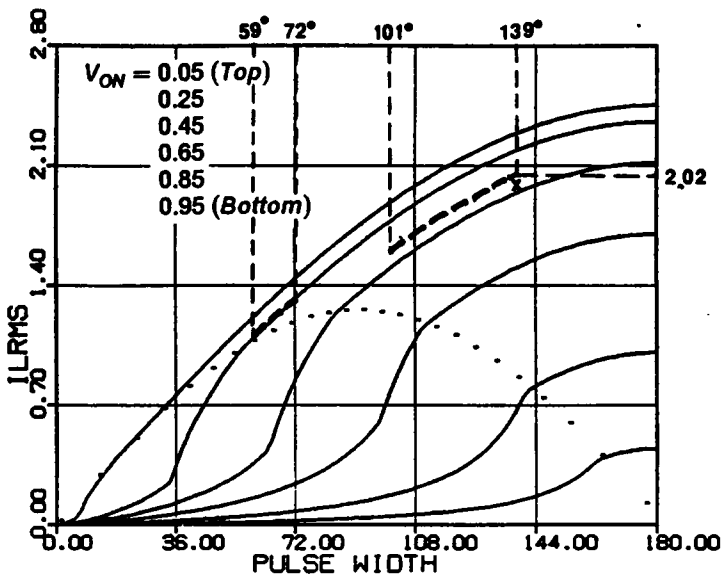
Using the above β_S ranges, the following salient features are obtained,

$$\begin{aligned} V_{CPKmax} &= 96V, & I_{LRMSmax} &= 3.74A, \\ I_{Q1RMSmax} &= 2.7A, & I_{Q2RMSmax} &= 3.64A, \\ I_{D1AVmax} &= 2.45A, & I_{D2AVmax} &= 0.52A, \\ I_{Q1offmax} &= 5.46A & I_{Q2offmax} &= 4.1A, \\ I_{Q1onmax} &= 0A, & I_{Q2onmax} &= 0A. \end{aligned}$$

The ranges of various salient features at V_{ONmax} and V_{ONmin} are highlighted with dotted line segments in Figure 2.26.

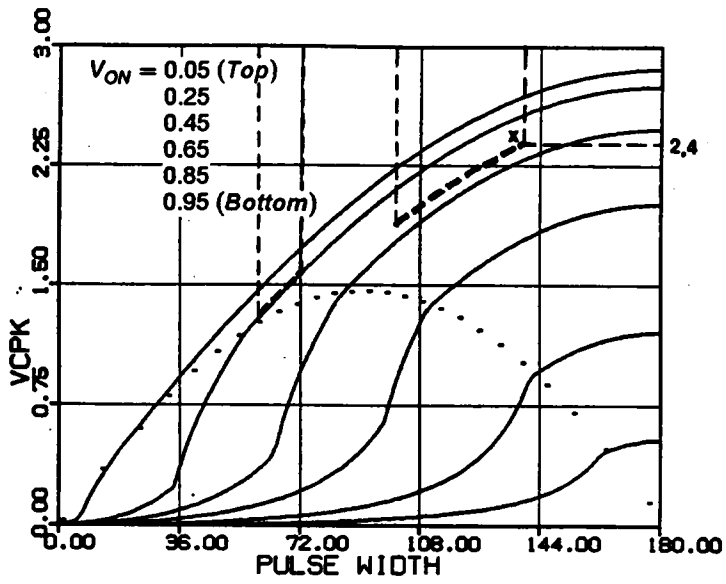


(a) Average inductor current (Load current)



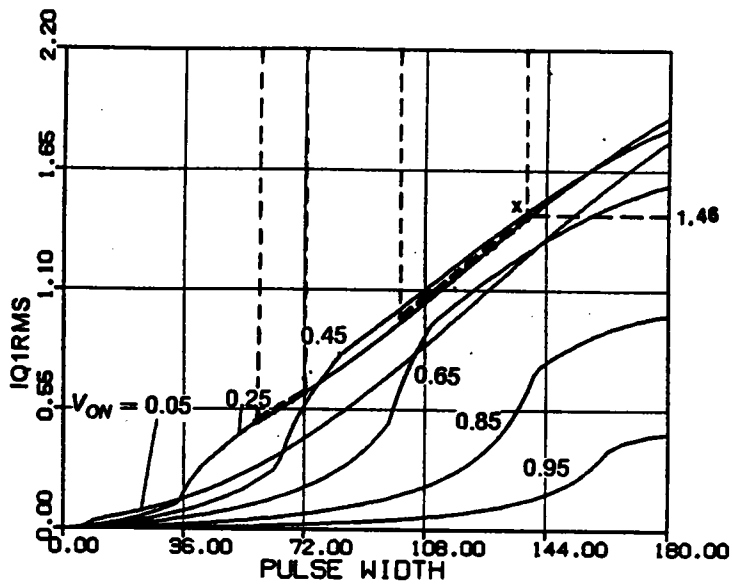
(b) RMS inductor current

Figure 2.26 Design Example in Force-Commutation Region

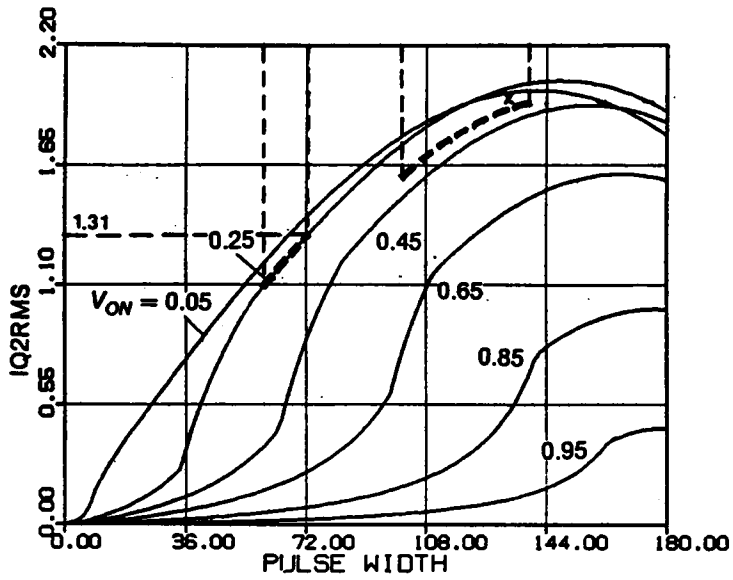


(c) Peak capacitor voltage

Figure 2.26 Continued

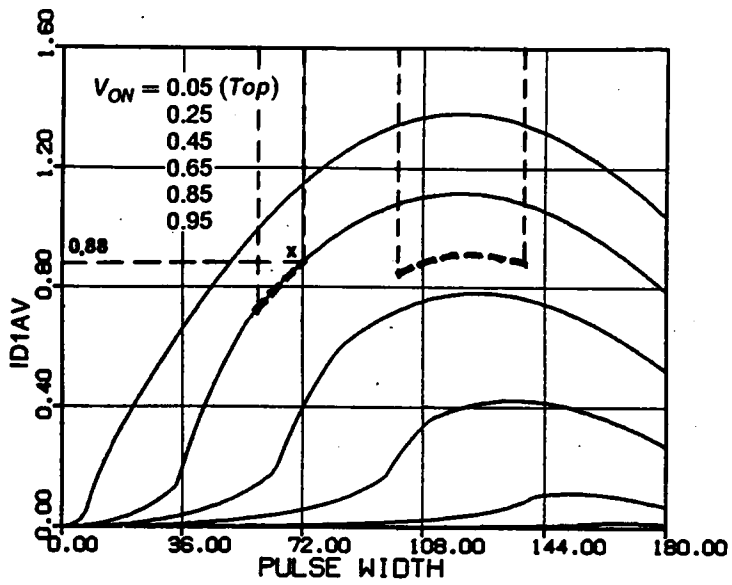


(d) RMS switch current ($Q1, Q3$)

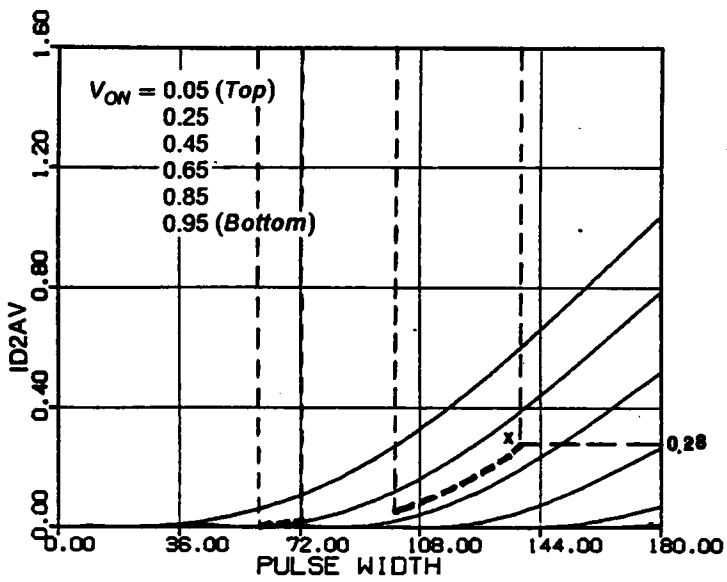


(e) RMS switch current ($Q2, Q4$)

Figure 2.26 Continued

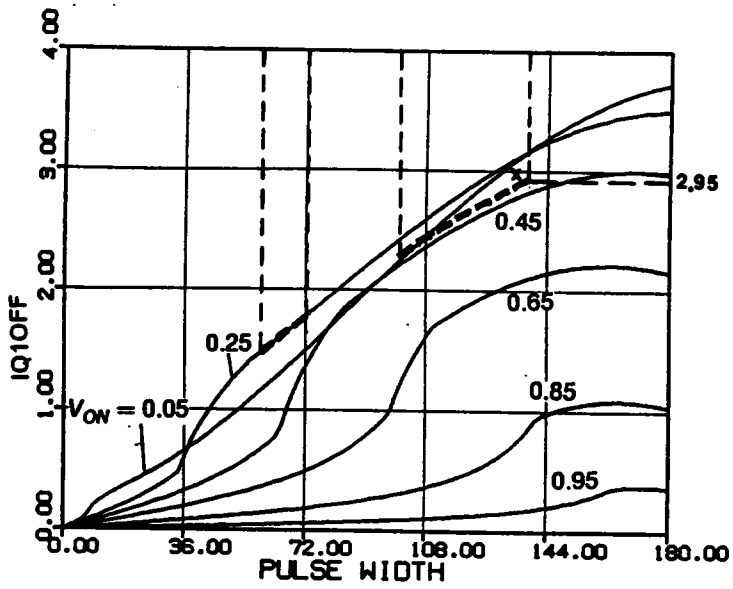


(f) Average diode current ($D1, D3$)

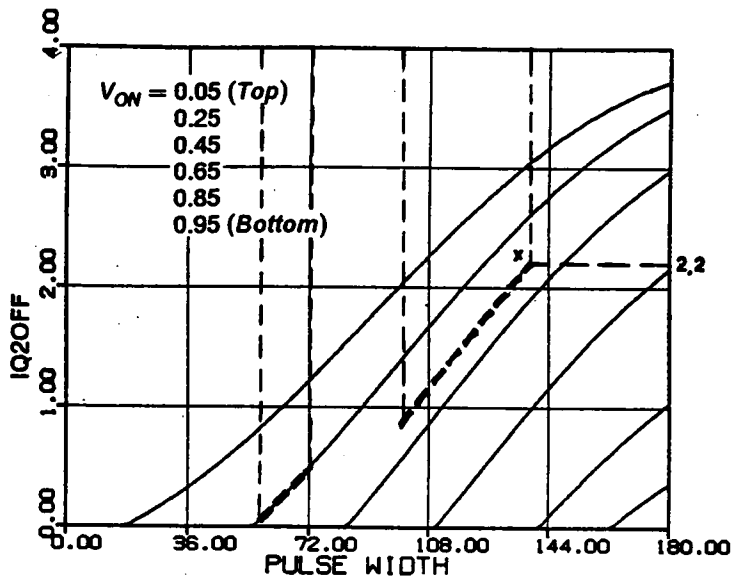


(g) Average diode current ($D2, D4$)

Figure 2.26 Continued



(h) Transistor turn-off Current ($Q1, Q3$)



(i) Transistor turn-off Current ($Q2, Q4$)

Figure 2.26 Continued

From the above examples, it can be seen that wider β_S range and higher component ratings are usually required to design a CM-SRC in the natural- or in the force-commutation region.

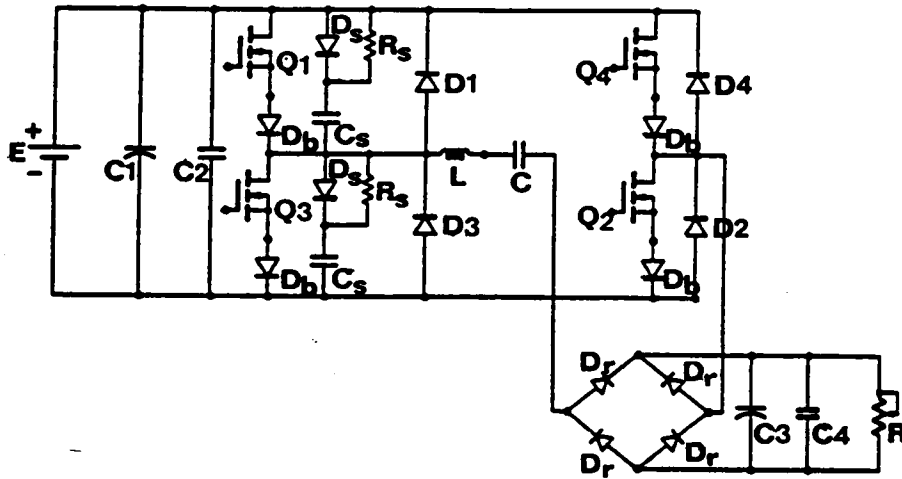
2.5 HARDWARE VERIFICATIONS

Two prototype circuits have been built to verify the circuit operation of a CM-SRC. The first circuit is designed at 24kHz with a resonant frequency of 42kHz ($\omega_{SN} = 0.57 \approx 0.6$) to verify the operating modes below resonant frequency. The second circuit is designed at 100kHz with a resonant frequency of 83.3kHz ($\omega_{SN} = 1.2$) to verify the operating modes above resonant frequency. The experimented circuits are shown in Figure 2.27 and Figure 2.28, respectively.

2.5.1 Circuit Operation Below Resonant Frequency

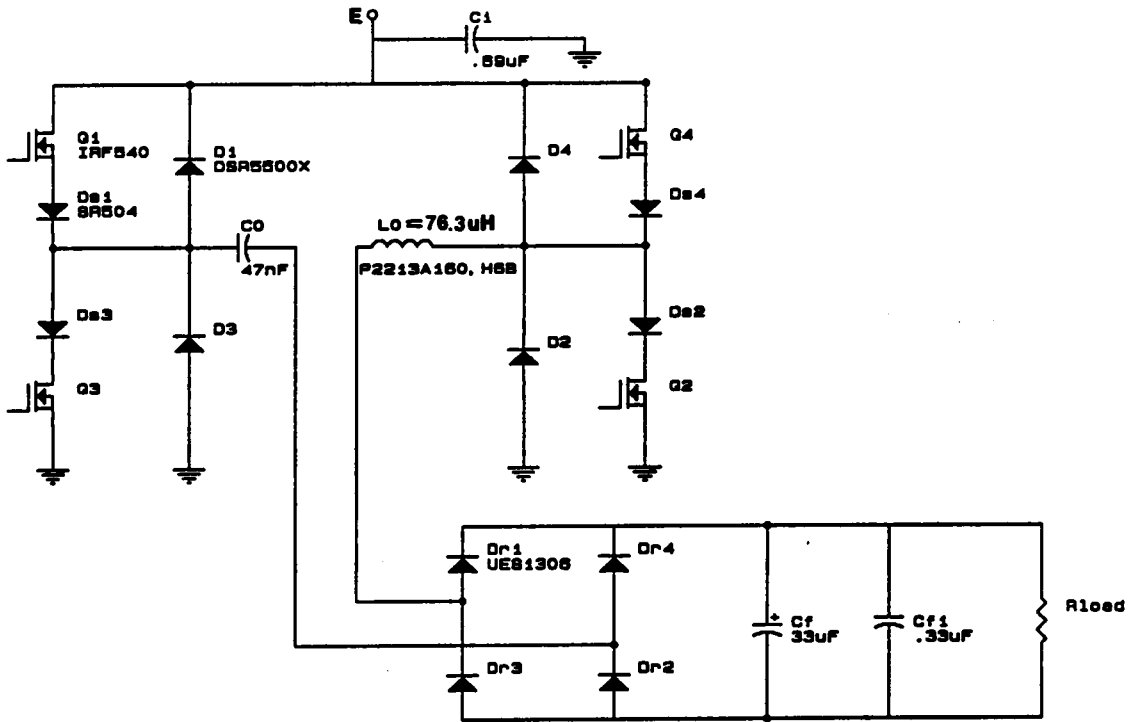
A series of experimental waveforms obtained from the circuit in Figure 2.27 are shown in Figure 2.29. These waveforms are obtained by fixing V_{ON} at 0.2 while reducing angle β_S from 180° to 10° . The operating points are indicated by x's in Figure 2.30. It can be seen that the converter sweeps through all the six operating modes. The tank energy decreases as β_S is decreased. Circulating current in the resonant tank is small under light load since the pulse-width of the exciting voltage v_S is reduced. The circuit is able to provide a load range from no load to full load which is not feasible for a conventional SRC. Figure 2.29(h) shows an operating condition clearly illustrating Mode-IV operation. The waveforms are obtained at the same β_S as in Figure 2.29(e) but with a $V_{ON} = 0.1$.

Another series of waveforms obtained analytically at the same operating points indicated in Figure 2.30 is shown in Figure 2.31. A close resemblance can be observed between the waveforms in Figure 2.29 and Figure 2.31. The slight difference is caused by the fact that the normalized frequency of the experimented circuit is not exactly equal to 0.6. The losses in the converter have negligible effects on the waveforms at the chosen switching frequency.



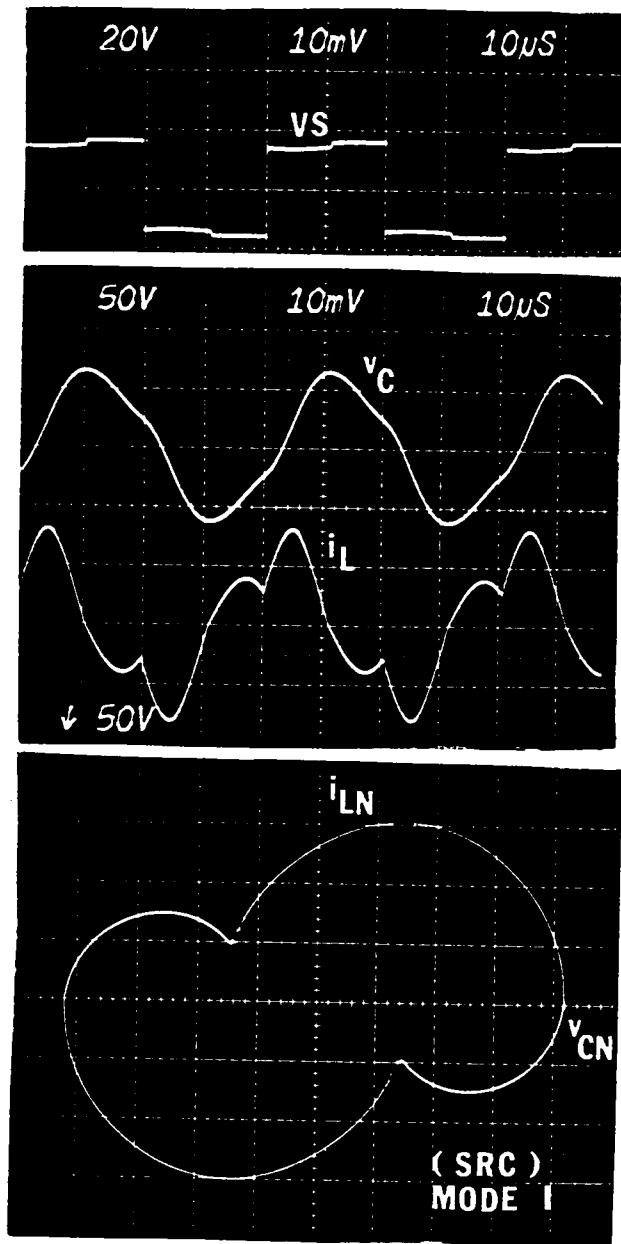
Q1,Q2,Q3,Q4: IRF520; D1,D2,D3,D4,Dr,Db: UES1303;
 C1,C3 = $2200\mu F$, C2 = $100nF$, C4 = $56nF$, $R_s = 56\Omega$,
 $C_s = 18nF$, $L = 105.2\mu H$, $C = 136.3nF$, $E = 30V$.

Figure 2.27 A Breadboard Circuit Used to Verify Circuit Operations Below Resonant Frequency



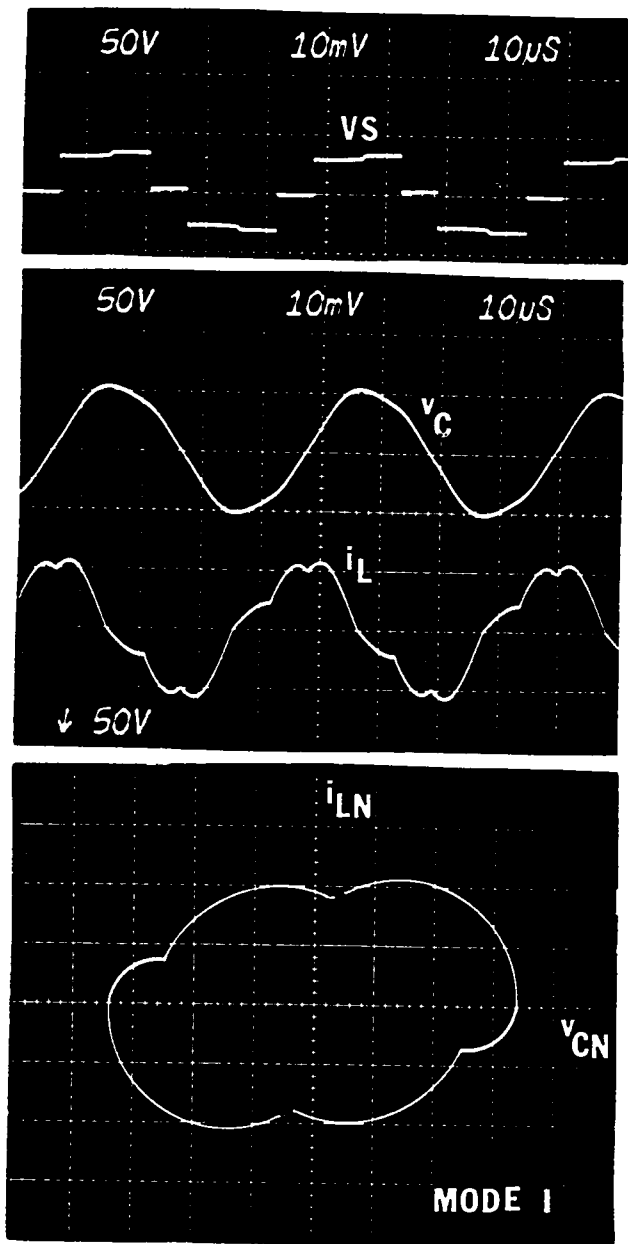
Q1,Q2,Q3,Q4: IRF540; D1,D2,D3,D4: DSR5500X;
 Ds1,Ds2,Ds3,Ds4: SR504; Dr1,Dr2,Dr3,Dr4: UES1306;
 E = 50V, $V_o = 12.5V$.

Figure 2.28 A Breadboard Circuit Used to Verify Circuit Operations Above Resonant Frequency



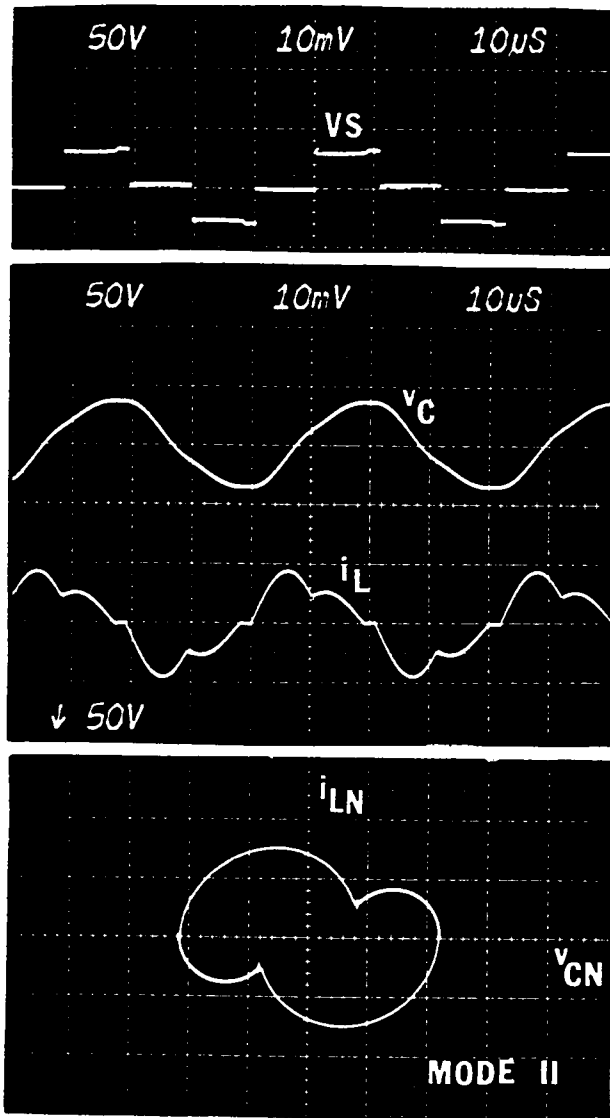
(a) SRC operation (operating point A)

Figure 2.29 Experimental Results from the Circuit in Figure 2.27



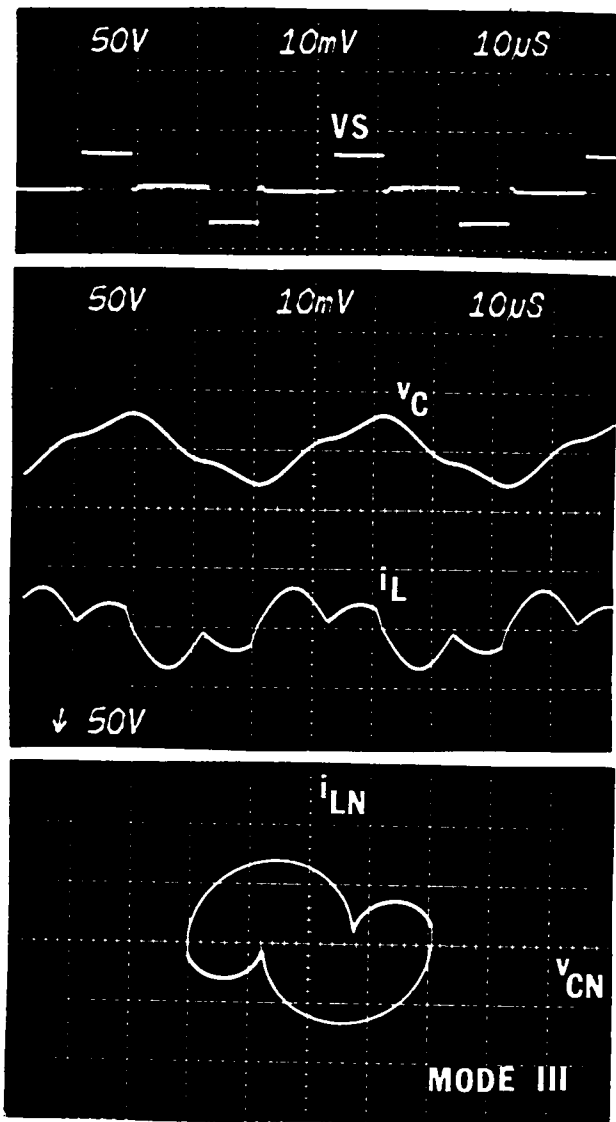
(b) Mode-I operation (operating point B)

Figure 2.29 Continued



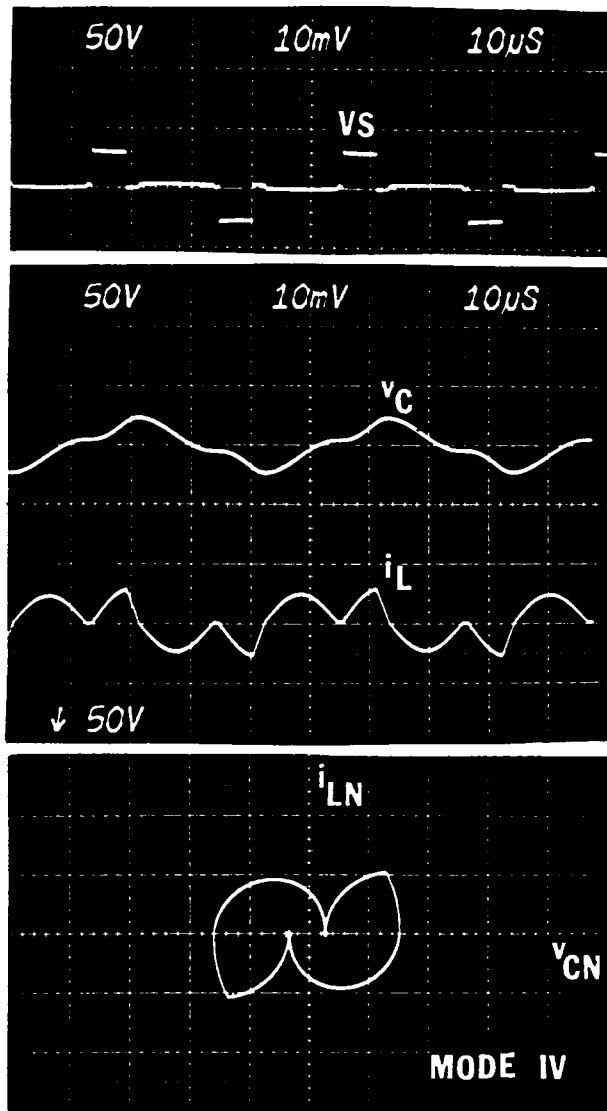
(c) Mode-II operation (operating point C)

Figure 2.29 Continued



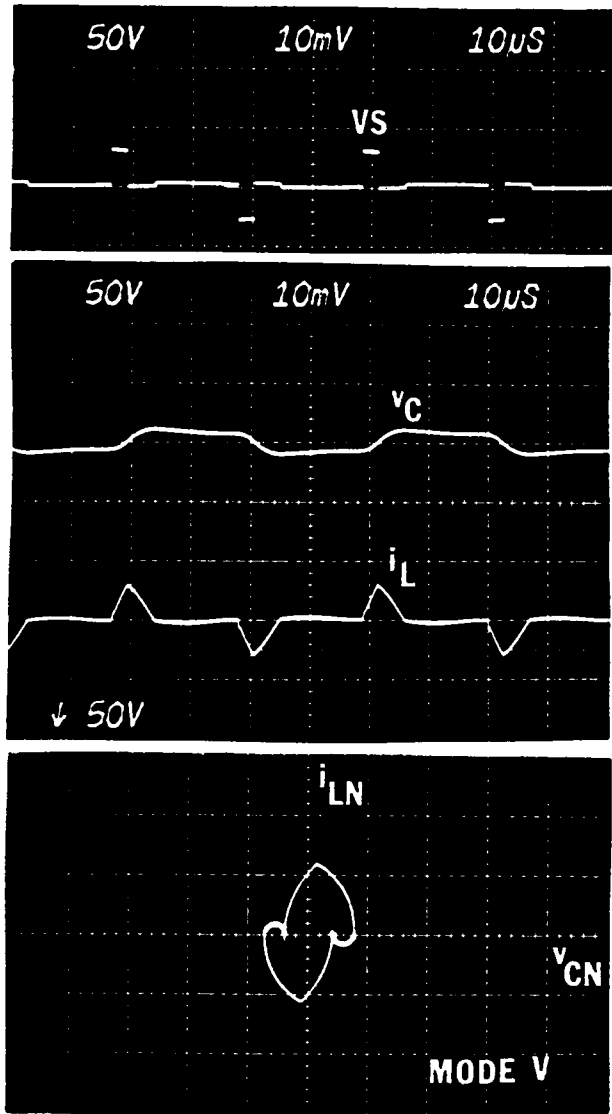
(d) Mode-III operation (operating point D)

Figure 2.29 Continued



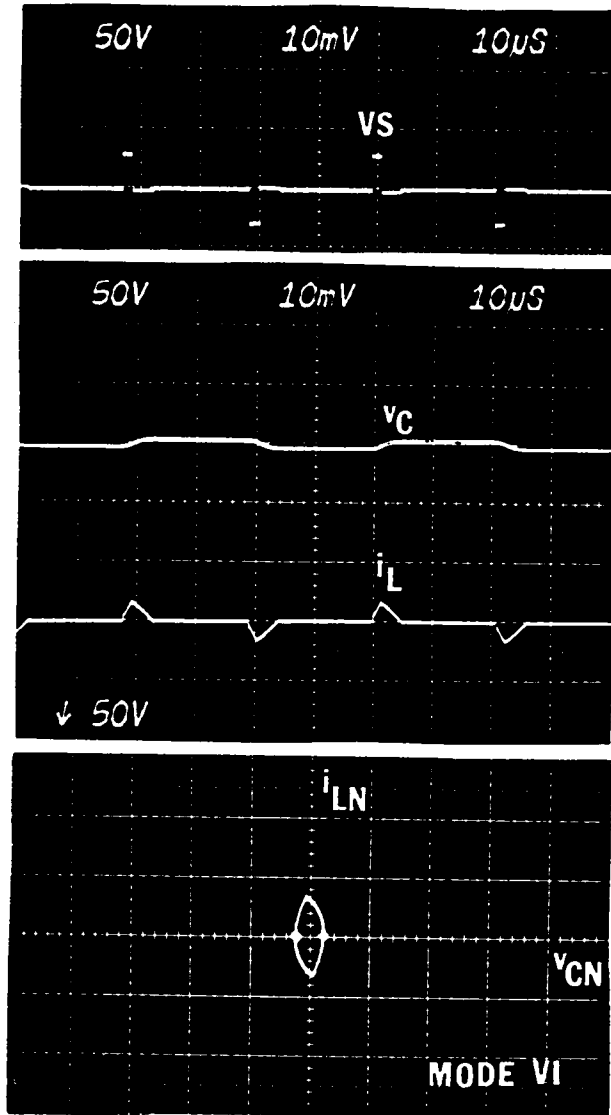
(e) Mode-IV operation (operating point E)

Figure 2.29 Continued



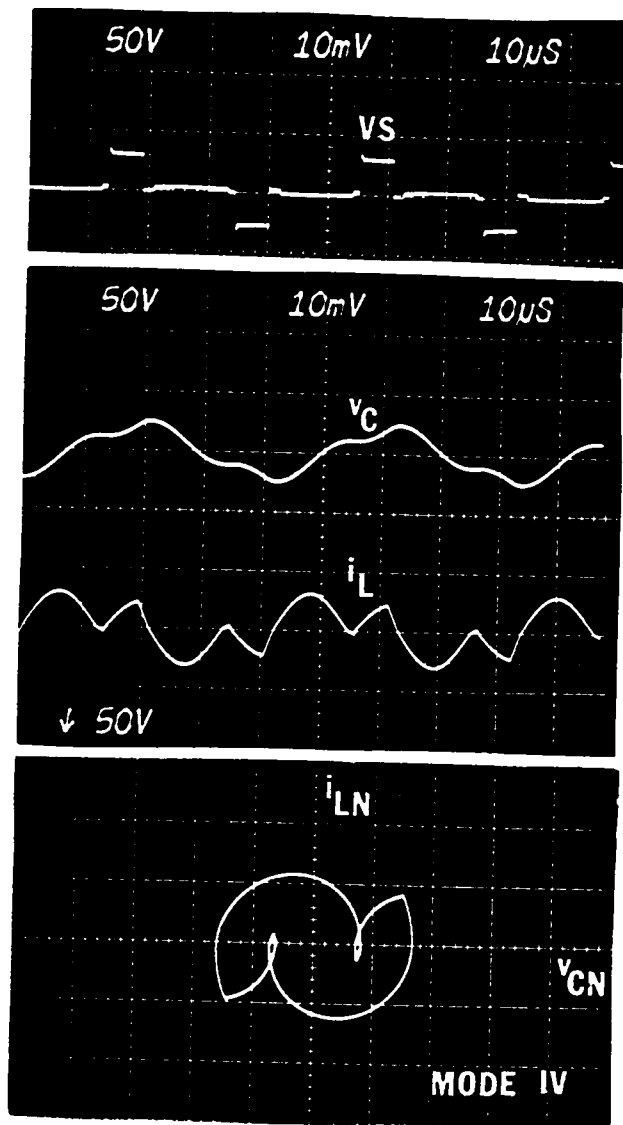
(f) Mode-V operation (operating point F)

Figure 2.29 Continued



(g) Mode-VI operation (operating point G)

Figure 2.29 Continued



(h) Mode-IV Operation ($\beta_S = 52^\circ$, $V_{ON} = 0.1$)

Figure 2.29 Continued

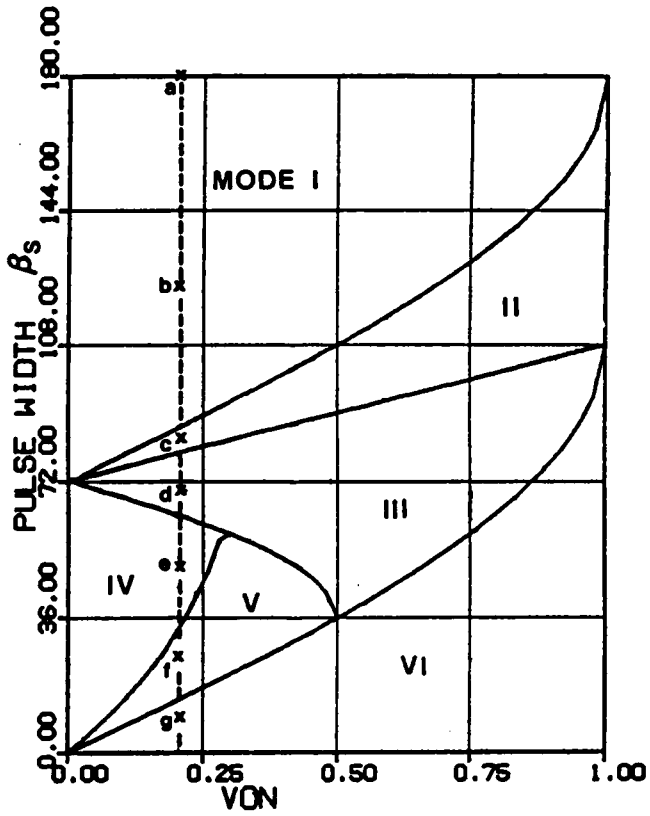
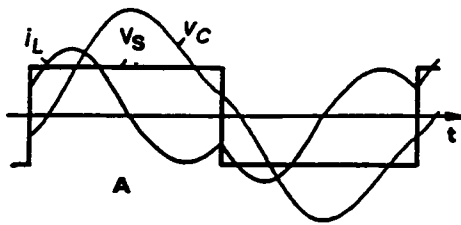
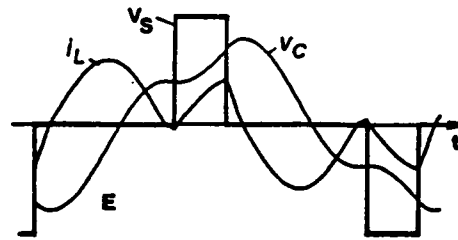


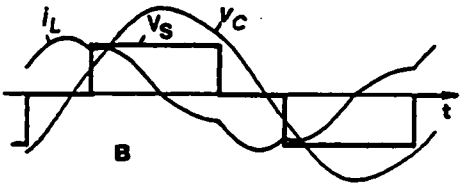
Figure 2.30 Operating Points for the Waveforms in Figure 2.29 ($\omega_{SN} = 0.6$)



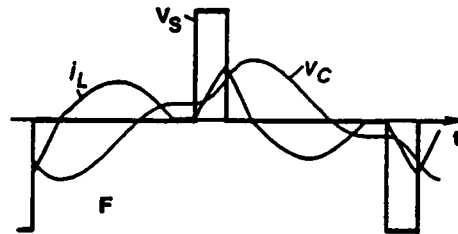
(a) SRC operation (operating point A)



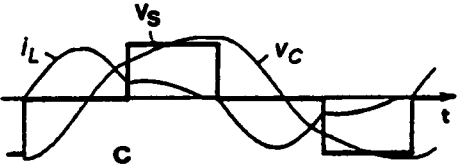
(e) Mode-IV operation (operating point E)



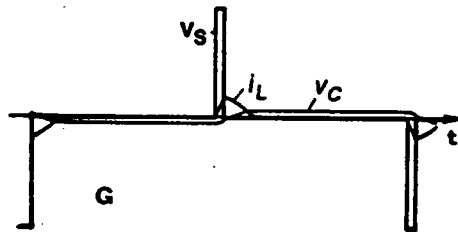
(b) Mode-I operation (operating point B)



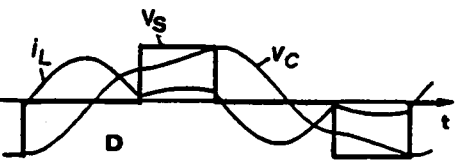
(f) Mode-V operation (operating point F)



(c) Mode-II operation (operating point C)

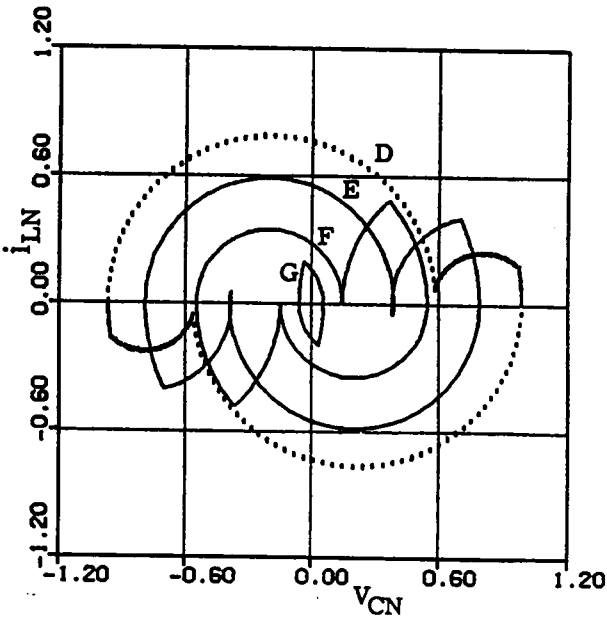
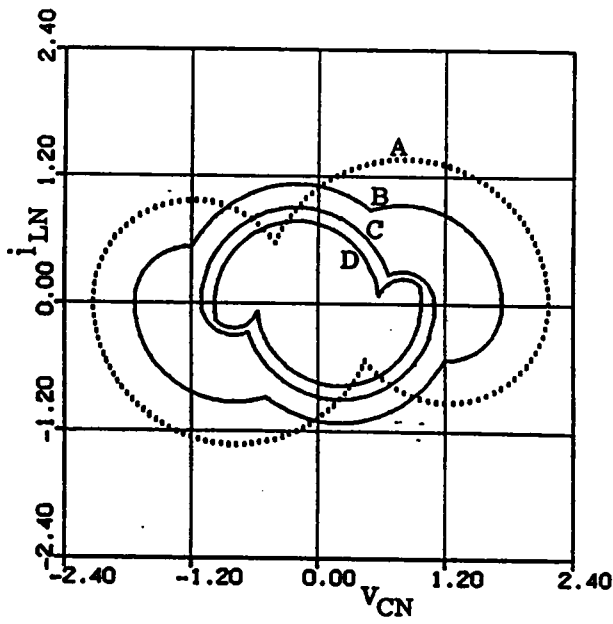


(g) Mode-VI operation (operating point G)



(d) Mode-III operation (operating point D)

Figure 2.31 Analytically Predicted Waveforms at the Operating Points Indicated in Figure 2.30



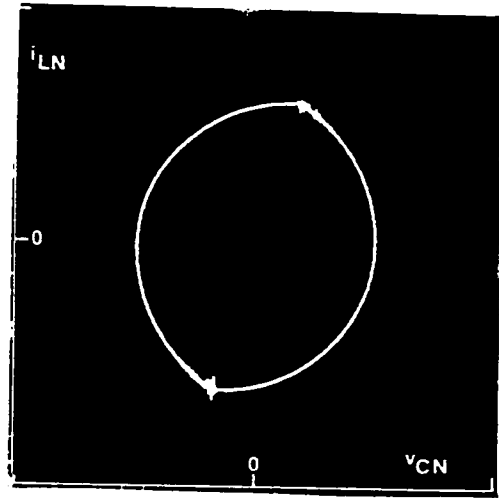
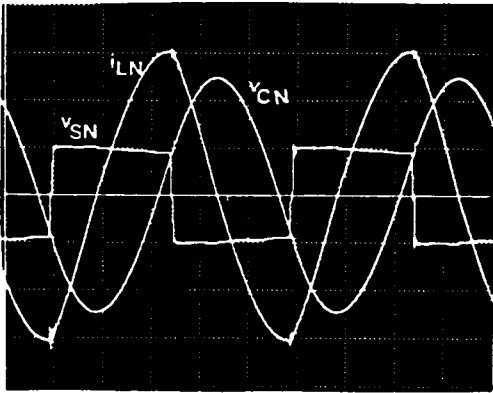
(h) Corresponding state trajectories

Figure 2.31 Continued

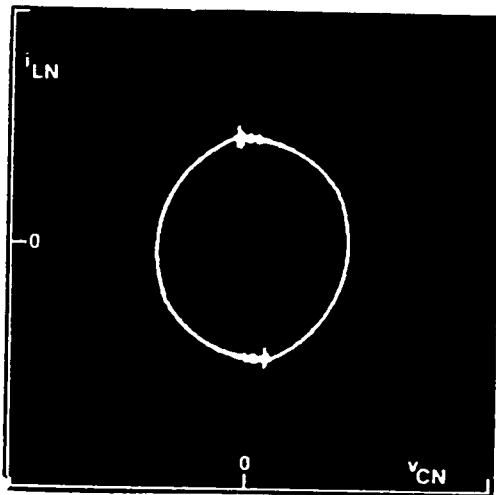
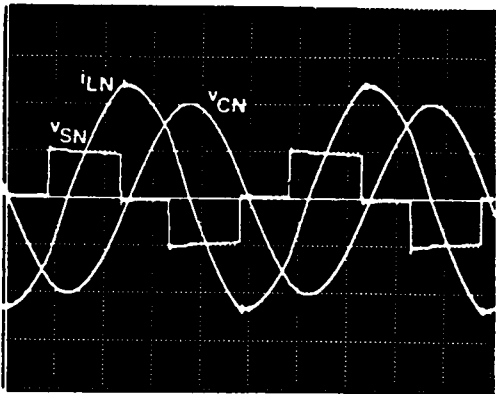
2.5.2 Circuit Operation Above Resonant Frequency

Figure 2.32 shows a series of experimental waveforms obtained from the circuit in Figure 2.28. The waveforms are obtained by fixing V_{ON} at 0.2 while reducing angle β_S from 180° to 29° . The operating points are indicated by asterisks in Figure 2.33. It can be seen that the converter sweeps through all the three operating modes above resonant frequency.

Another series of waveforms obtained analytically at the operating points **A,B,C,D** in Figure 2.33 is shown in Figure 2.34. The waveforms resemble those shown in Figure 2.32 and little difference can be observed. Again, the tank energy decreases as β_S is decreased. Circulating current in the resonant tank is small under light load. The converter is able to provide a load range from no load to a full load.

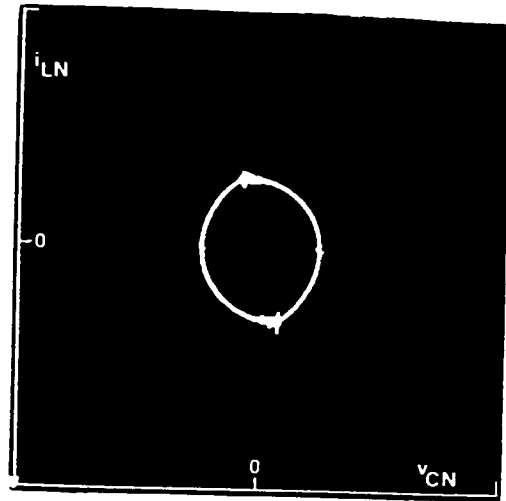
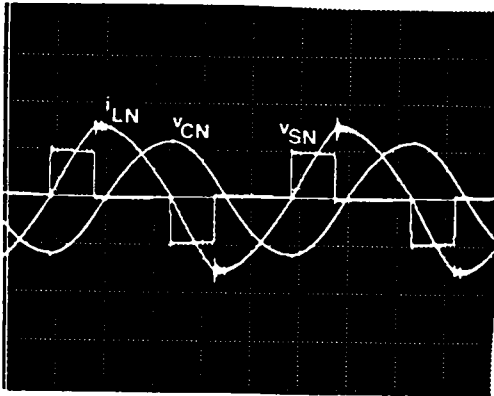


(a) SRC operation (operating point A)

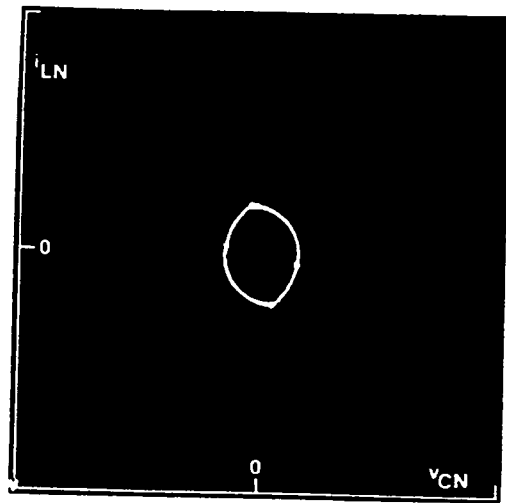
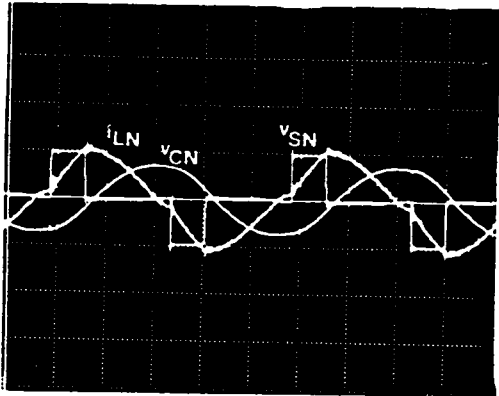


(b) Mode-A operation (operating point B)

Figure 2.32 Experimental Results from the Circuit in Figure 2.28

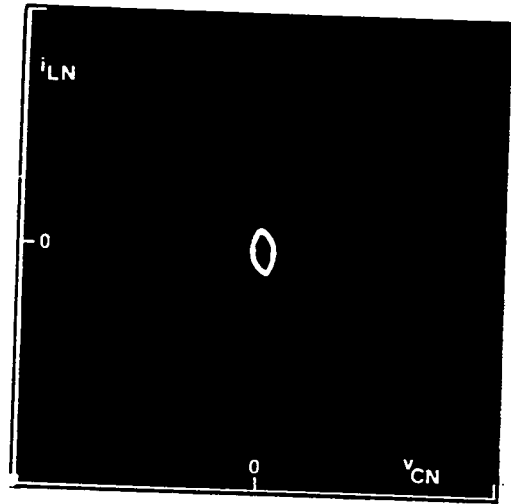
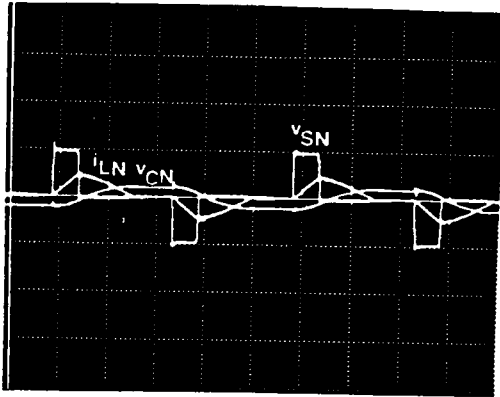


(c) Boundary Between Mode A and Mode B (operating point B')

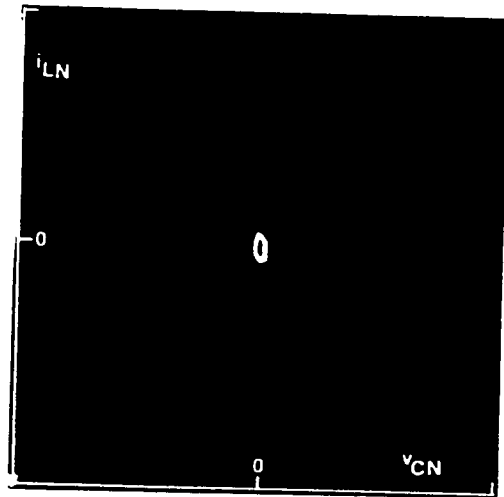
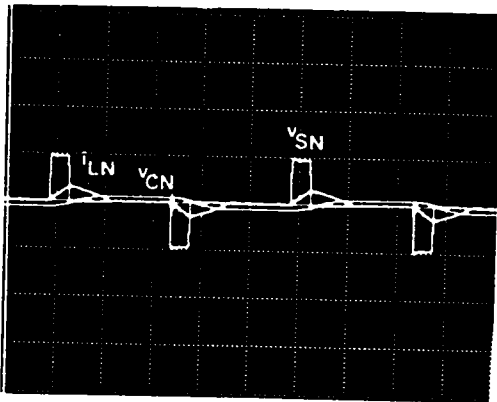


(d) Mode-B operation (operating point C)

Figure 2.32 Continued



(e) Boundary Between Mode B and Mode C (operating point C')



(f) Mode-C operation (operating point D)

Figure 2.32 Continued

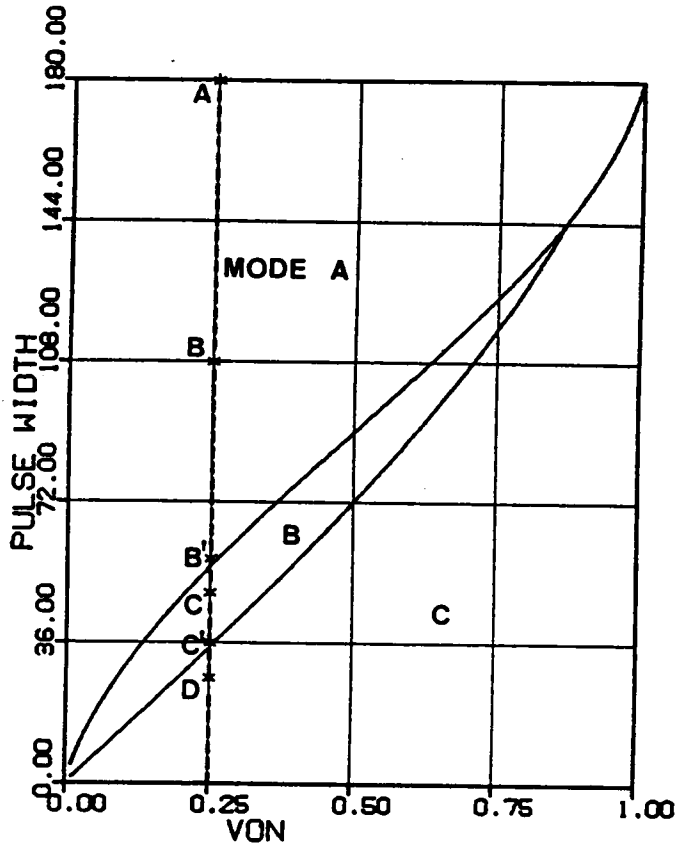
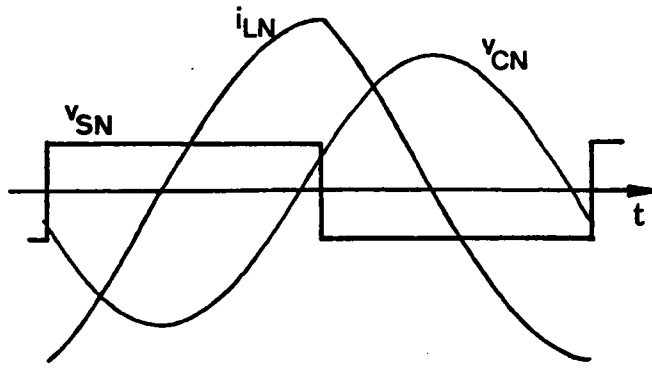
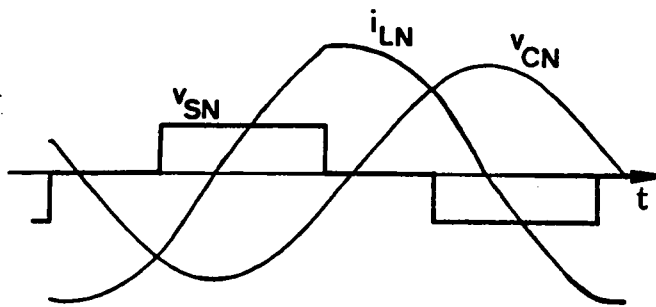


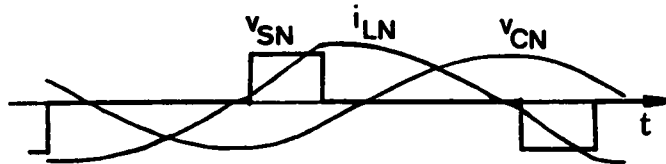
Figure 2.33 Operating Points for the Waveforms in Figure 2.31 ($\omega_{SN} = 1.2$)



(a) SRC operation (operating point A)



(b) Mode-A operation (operating point B)

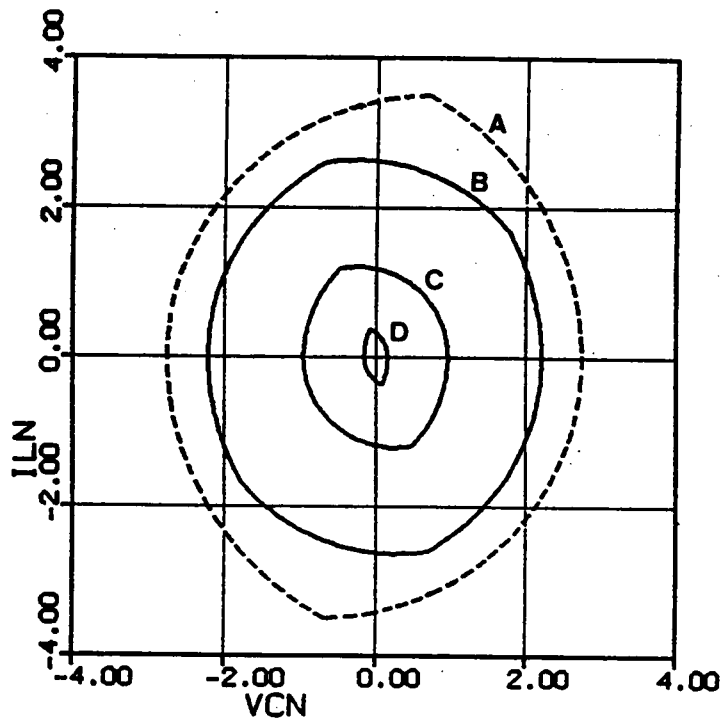


(c) Mode-B operation (operating point C)



(d) Mode-C operation (operating point D)

Figure 2.34 Analytically Predicted Waveforms at Operating Points A,B,C,D in Figure 2.33



(h) Corresponding state trajectories

Figure 2.34 Continued

2.6 CONCLUSIONS

A comprehensive analysis of the constant-frequency, clamped-mode, series-resonant converter has been performed in this chapter. Employing state-plane techniques, six operating modes below resonant frequency and three operating modes above resonant frequency are identified for the first time. These operating modes represent different device conduction sequences, resulting in different device commutation requirements.

To predict the converter's operating mode at a given condition, an algorithm is developed to define the regions of operation of the converter. The regions of operation can be used to determine the operating modes of the converter for a specific design.

There are mainly three different commutation regions for the converter. Each region has its advantages. In the natural commutation region, the turn-off losses of all the transistors are eliminated. In the mixed-commutation region, the turn-on losses of transistors Q1, Q3 and the turn-off losses of transistors Q2, Q4 are eliminated. Lossless capacitor snubbers can be used across Q1 and Q3. In the force-commutation region, the turn-on losses of all the transistors are eliminated. Lossless snubbers can be used across all the transistors.

State trajectories are conveniently used to calculate various circuit salient features. The parameters defining the trajectories are solved using sets of nonlinear equations. Expressions for the output current, rms inductor current, peak capacitor voltage, switch currents and diode currents are then derived from these parameters.

Various dc characteristics have been derived. The characteristics are then employed to facilitate the converter design. Three design examples are given. The examples illustrate the procedures to design a CM-SRC operating in different commutation regions.

Finally, two breadboard circuits are used to verify the converter's operation. The presences of all the circuit operating modes, both below and above the resonant fre-

quency, are verified. The experimental results are in good agreement with the analytical predictions.

CHAPTER 3.

ANALYSIS OF CLAMPED-MODE PARALLEL RESONANT CONVERTER

3.1 INTRODUCTION

As discussed in Chapter 2, a clamped-mode series-resonant converter (CM-SRC) can be designed in three different regions to obtain certain desirable commutation features of the power switches. When a CM-SRC is designed to operate in the natural-commutation region (below resonant frequency) or in the force-commutation region (above resonant frequency), a minimum load current has to be maintained. To achieve output regulation from no load to full load, the converter must be designed in the mixed commutation region where two of the power switches are naturally commutated while the other two are force-commutated.

Similar to a CM-SRC, a clamped-mode parallel-resonant converter (CM-PRC) can also be designed in three different regions to obtain either natural commutation or mixed commutation or force commutation of its power switches. However, unlike the CM-SRC, it is possible to design a CM-PRC to regulate its output from no load to full load entirely in the natural or the force commutation regions. A minimum load current

has to be maintained if a CM-PRC is designed to operate in the mixed commutation region.

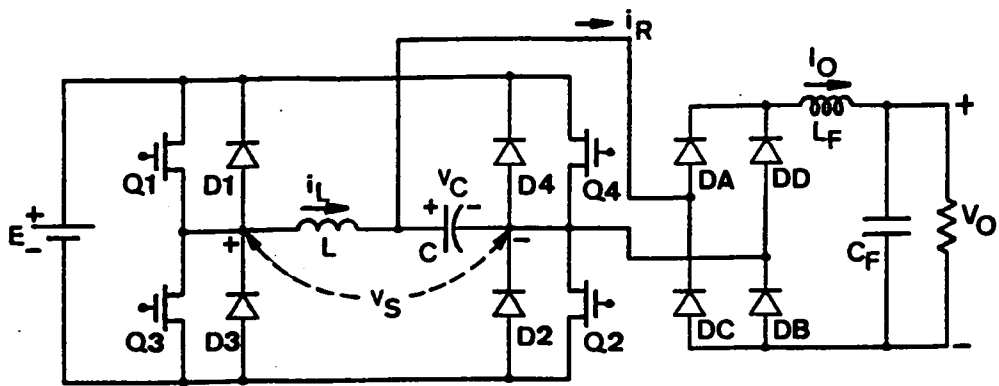
In this chapter, a complete dc characterization of the CM-PRC is presented. The analysis provides insights to the converter's operation and derives guidelines for the converter design. Again, graphical state-plane techniques are employed to identify all the possible circuit operating modes. The topological sequence and the device commutation requirements under each operating mode are detailed. The mode boundaries are determined and the regions for different commutations are defined. The dc control-to-output characteristics are derived. Finally, three design examples are illustrated and the predicted operating modes are verified experimentally.

3.2 CIRCUIT OPERATION

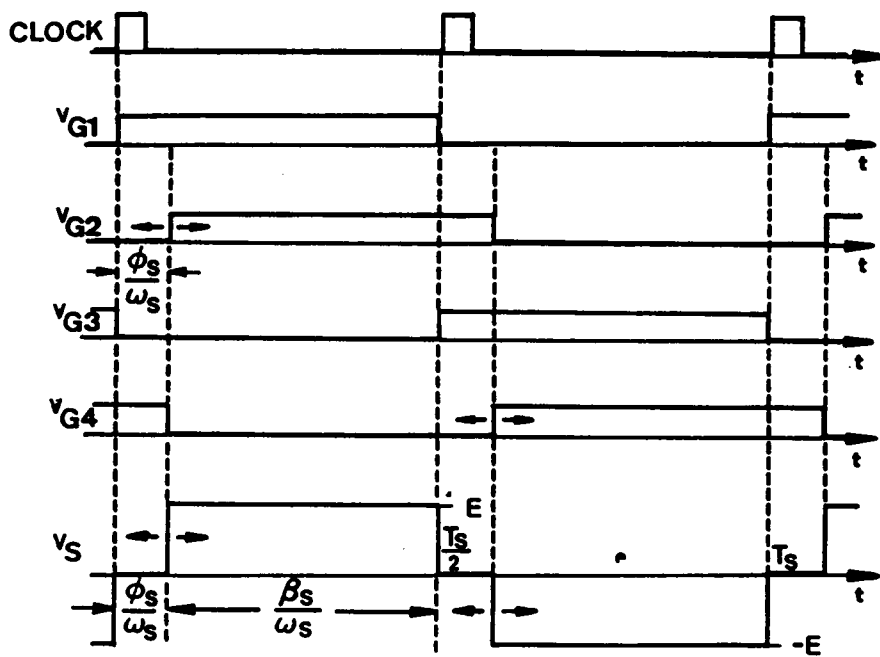
Figure 3.1(a) shows a clamped-mode, parallel-resonant converter with the controlled switches S1,S2,S3,S4 in Figure A.1(d) implemented by transistors Q1,Q2,Q3,Q4 and their antiparallel diodes D1,D2,D3,D4, respectively. The transistors are triggered in a timing sequence as illustrated in Figure 3.1(b). All the transistors are driven with 50% duty-cycle gating signals. Transistors Q1,Q3 are triggered according to a clock signal whose frequency determines the operating frequency of the converter. Transistors Q2,Q4 are triggered with a controllable time delay, $\frac{\phi_S}{\omega_S}$, with respect to the triggering of Q1,Q3, respectively. The time delay is the interval during which the resonant tank is clamped as a short circuit. By controlling the time delay, the pulse-width, β_S , of the quasi-square-wave voltage, v_S , is controlled and the converter's output voltage, V_O , is regulated.

Depending upon the operating conditions, a CM-PRC may result in different modes of operation. Each mode of operation represents a unique conduction sequence of the switching devices.

A typical circuit operation of a CM-PRC operating below resonant frequency is illustrated in Figure 3.2. At $t=0$, transistor Q1 turns on while diodes D3,D4 are conducting. Diode D3 is commutated due to the conduction of Q1 and the inductor current, i_L , resonates through Q1 and D4. At $t=t_1$, transistor Q2 is triggered and diode D4 is commutated. The inductor current resonates through Q1 and Q2. At $t=t_2$, inductor current i_L decreases to zero due to resonance. Transistors Q1,Q2 are **naturally** commutated and diodes D1,D2 conduct, subsequently. The inductor current resonates through D1 and D2. At the end of the first half switching cycle, $t = \frac{T_S}{2}$, transistor Q3 turns on, commutating diode D1. A similar process takes place in the second half switching cycle with the roles of Q1,Q2,D1,D2 and Q3,Q4,D3,D4 interchanged, respectively. The reflected load current, i_R , changes polarity whenever capacitor voltage v_C crosses the



(a) Circuit diagram



(b) Gating Signals

Figure 3.1 A Clamped-Mode Parallel-Resonant Converter

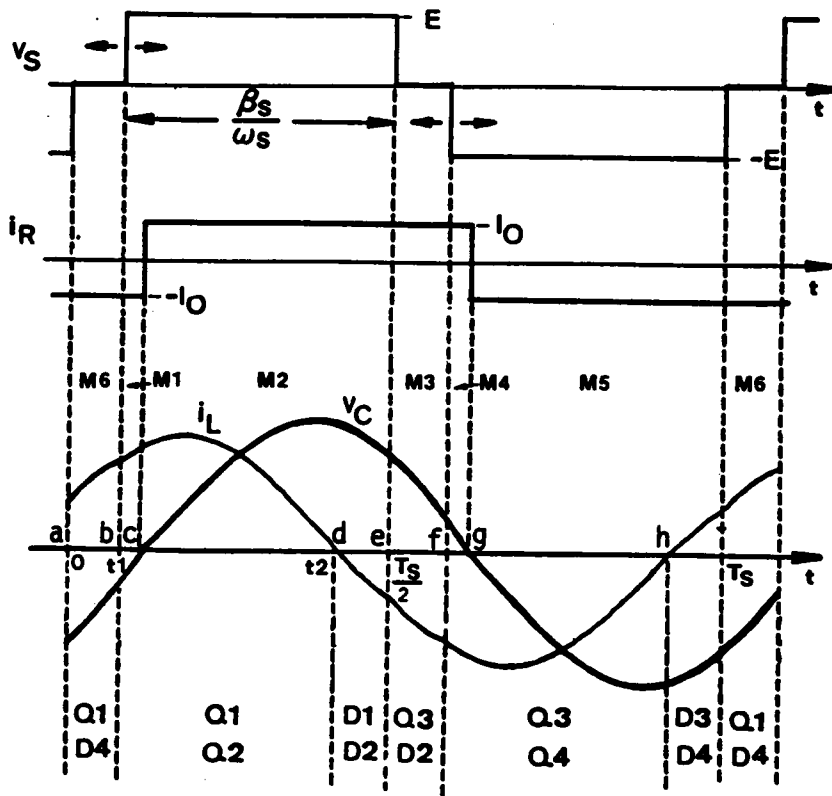


Figure 3.2 A Typical Circuit Operation Below Resonant Frequency

zero-axis. In other words, the output bridge diodes switch from DA,DB to DC,DD or vice versa.

A typical circuit operation of a CM-PRC operating above resonant frequency is illustrated in Figure 3.3. At $t=0$, transistor Q3 is forced off and Q1 is triggered with a gate voltage. Since the inductor current i_L is negative, Q1 can not conduct. Instead, diode D1 conducts. The inductor current resonates through Q4 and D1. At $t=t_1$, transistor Q4 is forced off, and Q2 is triggered. Transistor Q2 can not conduct since i_L is still negative. Instead, diode D2 conducts. The inductor current resonates through D1 and D2. At $t=t_2$, inductor current i_L increases to zero. Diodes D1,D2 turn off naturally and transistors Q1,Q2 conduct, subsequently. The inductor current resonates through Q1 and Q2. At the end of the first half switching cycle, $t=\frac{T_S}{2}$, transistor Q1 is forced off and Q3 is triggered. A similar process occurs with the roles of Q1,Q2,D1,D2 and Q3,Q4,D3,D4 interchanged, respectively. The reflected load current, i_R , changes polarity whenever capacitor voltage v_C crosses the zero-axis.

In the examples discussed above, the commutation features of the transistors, Q1,Q2,Q3,Q4, and the diodes, D1,D2,D3,D4, are the same as those in a conventional PRC. The commutation features for these devices, however, may change when the converter's operating conditions (such as frequency, load current, or pulse width of v_S) vary, as shall be seen in later sections.

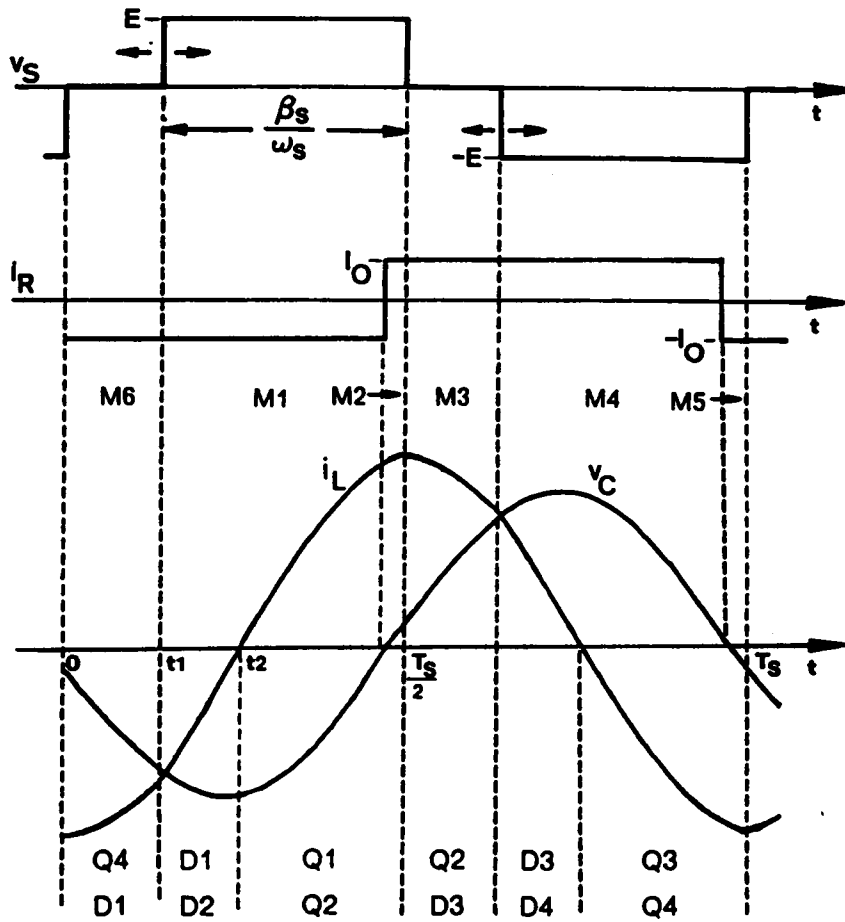


Figure 3.3 A Typical Circuit Operation Above Resonant Frequency

3.3 STATE-PLANE ANALYSIS

In this section, graphical state-plane techniques are employed to analyze the CM-PRC. Various circuit operating modes are identified and regions of operation are defined. Important dc characteristics such as control-to-output transfer ratio, rms inductor current, peak capacitor voltage, rms switch currents, etc. are also derived.

3.3.1 Assumptions

The following assumptions are made during the analysis:

1. all the transistors are ideal, with zero switching time and no conduction drop;
2. the quality factor of the resonant tank is infinite; in other words, there is no loss in the tank circuit;
3. the output filter is large enough such that the output current, I_o , can be assumed constant during several switching cycles;
4. the transistors are driven with ideal 50%-duty-cycle gating signals;
5. the switching frequency of the converter is greater than 50% of the resonant frequency.

3.3.2 Circuit Topological Modes

As illustrated in Figures 3.2 and 3.3, the one-cycle operation of a CM-PRC is composed of a sequence of linear circuits, each corresponding to a particular switching in-

terval. There are eight linear circuit topologies for a CM-PRC, as shown in Figure 3.4. These circuit topologies are referred to as **circuit topological modes** of a CM-PRC. Modes M1,M2,M3,M4,M5, and M6 are called "resonant modes". LC resonant actions occur in these modes. Mode M1 is called "linear-charging mode". The resonant inductor is linearly charged or discharged by the source voltage in this mode. Mode M0 is called "free-wheeling mode". The current in the resonant inductor freewheels through a transistor-diode pair of the input bridge in this mode. The circuit behavior of a CM-PRC under each topological mode can be described using the following equations.

For resonant modes M1,M2,M3,M4,M5, and M6,

$$\begin{aligned} L \frac{di_L}{dt} + v_C &= v_E, \\ C \frac{dv_C}{dt} - i_L &= i_E, \end{aligned} \tag{3.1}$$

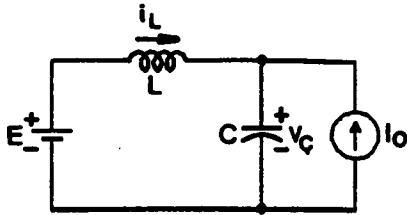
where,

$$v_E = \begin{cases} E - V_O & \text{for M1,} \\ E + V_O & \text{for M2,} \\ V_O & \text{for M3,} \\ -E + V_O & \text{for M4,} \\ -E - V_O & \text{for M5,} \\ -V_O & \text{for M6,} \end{cases} \quad i_E = \begin{cases} I_O & \text{for M1,} \\ -I_O & \text{for M2,} \\ -I_O & \text{for M3,} \\ -I_O & \text{for M4,} \\ I_O & \text{for M5,} \\ I_O & \text{for M6.} \end{cases}$$

For linear-charging mode M1,

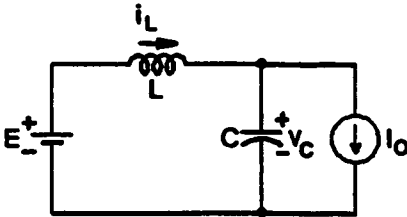
$$\begin{aligned} L \frac{di_L}{dt} &= \pm E \\ v_C &= 0. \end{aligned} \tag{3.2}$$

For free-wheeling mode M0,



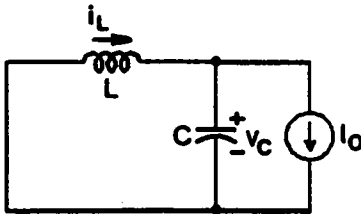
$$\begin{aligned} & \bullet (I_{LN} + I_{ON})^2 + (V_{CN} - 1)^2 = R^2 \\ & \bullet R^2 = (1 - V_{CON})^2 + (I_{LON} + I_{ON})^2 \end{aligned}$$

(a) M1 : $v_C < 0$, Q1,Q2 or D1,D2 on



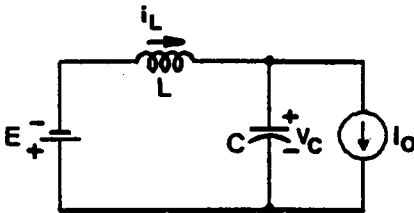
$$\begin{aligned} & \bullet (I_{LN} - I_{ON})^2 + (V_{CN} - 1)^2 = R^2 \\ & \bullet R^2 = (1 - V_{CON})^2 + (I_{LON} - I_{ON})^2 \end{aligned}$$

(b) M2 : $v_C > 0$, Q1,Q2 or D1,D2 on



$$\begin{aligned} & \bullet (I_{LN} - I_{ON})^2 + V_{CN}^2 = R^2 \\ & \bullet R^2 = V_{CON}^2 + (I_{LON} - I_{ON})^2 \end{aligned}$$

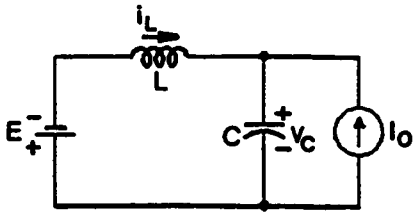
(c) M3 : $v_C > 0$, Q1,D4 or Q4,D1 or Q2,D3 or Q3,D2 on



$$\begin{aligned} & \bullet (I_{LN} - I_{ON})^2 + (V_{CN} + 1)^2 = R^2 \\ & \bullet R^2 = (1 + V_{CON})^2 + (I_{LON} - I_{ON})^2 \end{aligned}$$

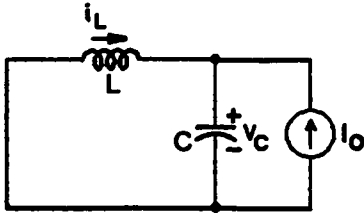
(d) M4 : $v_C > 0$, Q3,Q4 or D3,D4 on

Figure 3.4 Circuit Topological Modes of a CM-PRC



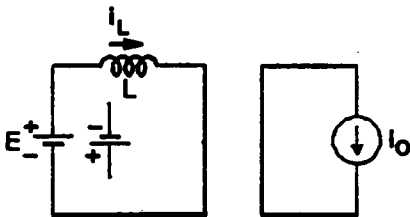
- $(i_{LN} + I_{ON})^2 + (v_{CN} + 1)^2 = R^2$
- $R^2 = (1 + V_{CON})^2 + (I_{LON} + I_{ON})^2$

(e) M5 : $v_C < 0$, Q3,Q4 or D3,D4 on



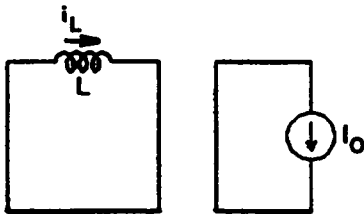
- $(i_{LN} + I_{ON})^2 + v_{CN}^2 = R^2$
- $R^2 = V_{CON}^2 + (I_{LON} + I_{ON})^2$

(f) M6 : $v_C < 0$, Q1,D4 or Q4,D1 or Q2,D3 or Q3,D2 on



- $i_{LN} = I_{LON} \pm \omega_0 t, v_{CN} = 0$
- (Linear-Charging Mode)

(g) M7 : $v_C = 0$, Q1,Q2 or D1,D2 or Q3,Q4 or D3,D4 on



- $i_{LN} = I_{LON}, v_{CN} = 0$
- (Free-Wheeling Mode)

(h) M8 : $v_C = 0$, Q1,D4 or Q4,D1 or Q2,D3 or Q3,D2 on

Figure 3.4 Continued

$$L \frac{di_L}{dt} = 0, \quad (3.3)$$

$$v_C = 0.$$

By solving these equations, the expressions for the inductor current, i_L , and the capacitor voltage, v_C , in each topological mode can be derived. These expressions are normalized and shown in the following.

For resonant modes M1,M2,M3,M4,M5, and M6,

$$i_{LN} = -(V_{CON} - v_{EN}) \sin \omega_0(t - t_0) + (I_{LON} + i_{EN}) \cos \omega_0(t - t_0) - i_{EN} \quad (3.4)$$

$$v_{CN} = (V_{CON} - v_{EN}) \cos \omega_0(t - t_0) + (I_{LON} + i_{EN}) \sin \omega_0(t - t_0) + v_{EN}$$

where, t_0 is the initial time and

$$\omega_0 = \frac{1}{\sqrt{LC}} \quad \text{is the angular resonant frequency,}$$

$$Z_0 = \sqrt{\frac{L}{C}} \quad \text{is the characteristic impedance,}$$

$$v_{CN} = \frac{v_C}{E} \quad \text{is the normalized capacitor voltage,}$$

$$i_{LN} = \frac{i_L}{E/Z_0} \quad \text{is the normalized inductor current,}$$

$$V_{CON} = \frac{V_{CO}}{E} \quad \text{is the normalized initial capacitor voltage,}$$

$$I_{LON} = \frac{I_{LO}}{E/Z_0} \quad \text{is the normalized initial inductor current,}$$

$$v_{EN} = \frac{v_E}{E},$$

$$i_{EN} = \frac{i_E}{E}.$$

For linear-charging mode ML,

$$\begin{aligned}i_{LN} &= I_{L0N} \pm \omega_0(t - t_0), \\v_{CN} &= 0.\end{aligned}\tag{3.5}$$

For free-wheeling mode M0,

$$\begin{aligned}i_{LN} &= I_{L0N}, \\v_{CN} &= 0.\end{aligned}\tag{3.6}$$

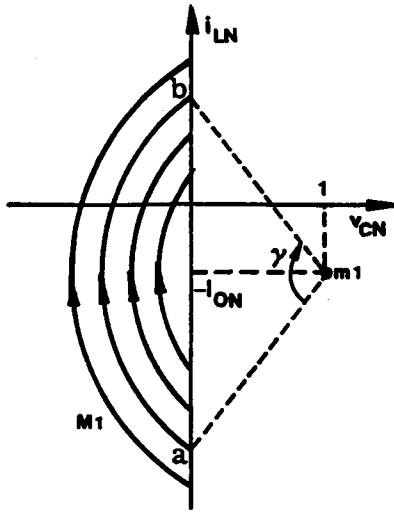
The normalizing factors for the voltages and currents are E and E/Z_0 , respectively.

3.3.3 State Trajectories for Circuit Topological Modes

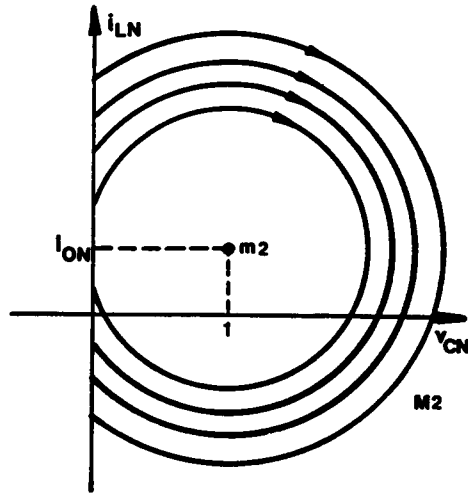
From the expressions for i_{LN} and v_{CN} (eq. 3.4), state representation for the resonant modes M1, M2, M3, M4, M5, and M6 can be portrayed on the state plane. It can be seen that the trajectories for these topological modes are circular arcs with centers located at $(-v_{EN}, i_{EN})$ and radii $R = \sqrt{(v_{EN} - V_{CON})^2 + (i_{EN} + I_{LON})^2}$. A family of the trajectories for each resonant mode is plotted in Figure 3.5, where the centers of M1-M6 are indicated by m1-m6, respectively. The trajectories only exist in either the right-half or the left-half plane depending on the polarity of v_C . The solution trajectory corresponding to a specific switching interval is determined by the topological mode, the initial condition of resonant inductor current and resonant capacitor voltage, and the duration of the interval. Time is implicit in these trajectories. The elapsed time in a trajectory segment is measured by the angle subtended by the segment with respect to its center. For example, the amount of time elapsed from point a to point b in topological mode M1 in Figure 3.5(a) is $\Delta t = \gamma/\omega_0$. As time advances, the trajectories travel clockwise as indicated by the arrows.

The state trajectory for the linear-charging mode ML is a line segment along the i_{LN} -axis, as illustrated in Figure 3.5(g). The amount of time elapsed in this mode is proportional to the link, ℓ , of the line segment, $\Delta t = \frac{\ell}{\omega_0}$. This mode occurs when voltage v_S is equal to E or -E and the magnitude current of i_{LN} is less than I_{ON} when voltage v_{CN} crosses the zero-axis. In this mode, the resonant capacitor C is shorted through the output bridge diodes.

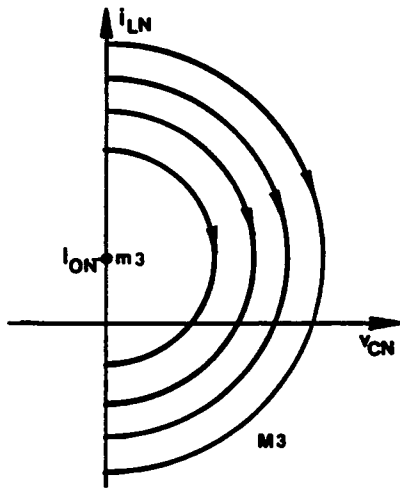
The state trajectory for the free-wheeling mode M0 is a stationary point on the i_{LN} -axis with coordinate $(0, I_{LON})$ or $(0, -I_{LON})$, as indicated by a circle in Figure 3.5(h). A finite amount of time elapses at such a stationary point since both i_{LN} and v_{CN} are independent of time. This mode occurs at a similar condition as ML except that when v_{CN} crosses the zero-axis, the voltage across the resonant tank is clamped at zero volt.



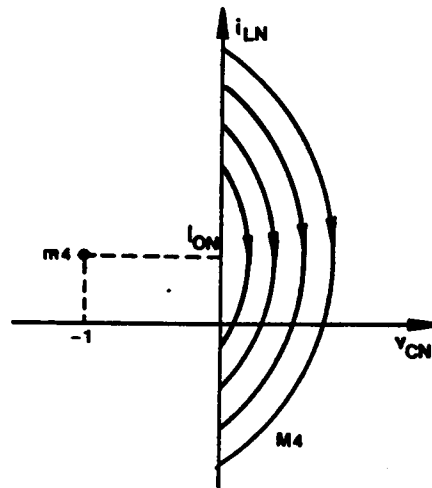
(a) Topological mode M1



(b) Topological mode M2

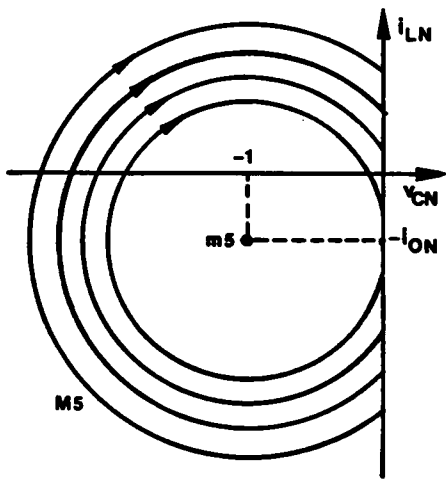


(c) Topological mode M3

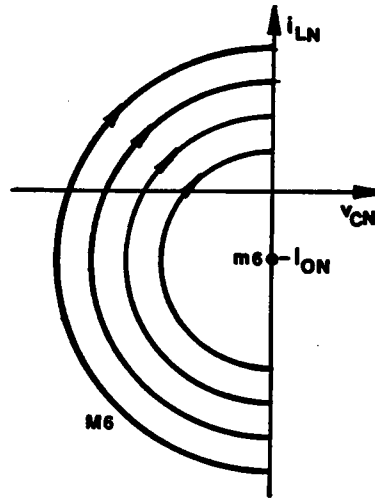


(d) Topological mode M4

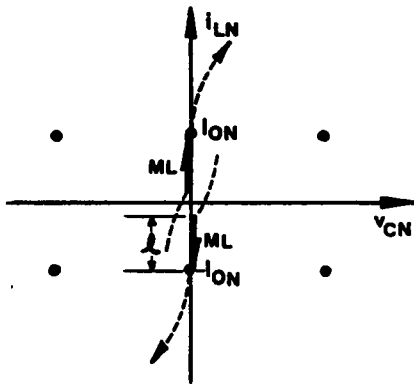
Figure 3.5 Families of State Trajectory for Various Circuit Topological Modes



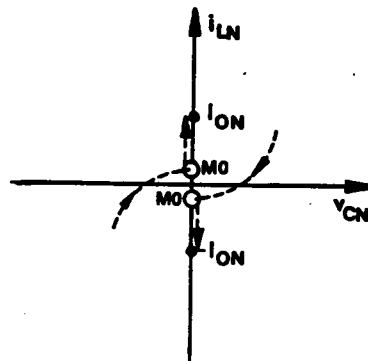
(e) Topological mode M5



(f) Topological mode M6



(g) Topological mode ML



(h) Topological mode M0

Figure 3.5 Continued

3.3.4 Equilibrium Trajectory

A steady-state operation of a CM-PRC can be represented by an equilibrium trajectory in the state plane [31]. An equilibrium trajectory is a closed contour composed of several trajectory segments. The solution trajectory is constructed via a particular sequence of circuit topological modes determined by the circuit operation.

An equilibrium state trajectory of a CM-PRC can be constructed using a composite diagram, as shown in Figure 3.6, which is generated by overlapping on the same i_{LN} , v_{CN} - axes the trajectories corresponding to each topological mode shown in Figure 3.5. The rules for constructing an equilibrium trajectory on the composite diagram are summarized in Appendix C.1. Figure 3.7 shows an example illustrating the construction of an equilibrium trajectory on the composite diagram. The constructed trajectory corresponds to the circuit operation described in Figure 3.2. In the trajectory, M6(M3) is initiated when Q1(Q3) is triggered at point a(e), M1(M4) is initiated when Q2(Q4) is triggered at point b(f), and M2(M5) is initiated when v_C reverses polarity at point c(g).

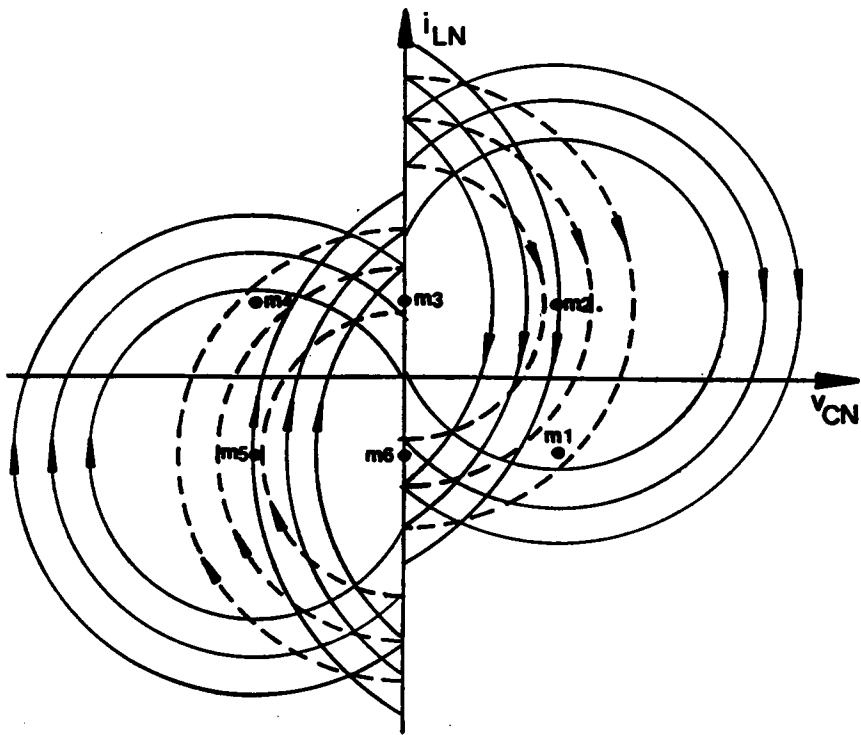


Figure 3.6 A Composite State Diagram for Constructing Equilibrium State Trajectories

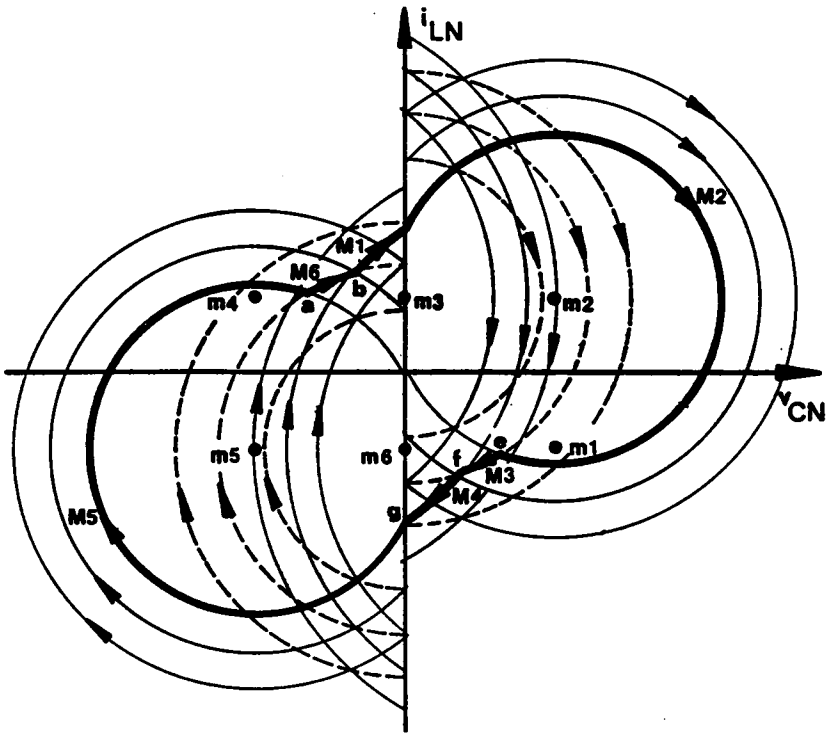


Figure 3.7 An Example Illustrating Construction of an Equilibrium State Trajectory on the Composite Diagram

3.3.5 Circuit Operating Modes

Equilibrium trajectories representing various circuit operating modes of a CM-PRC have been constructed. These trajectories are discussed in the following under two categories : below resonant frequency and above resonant frequency.

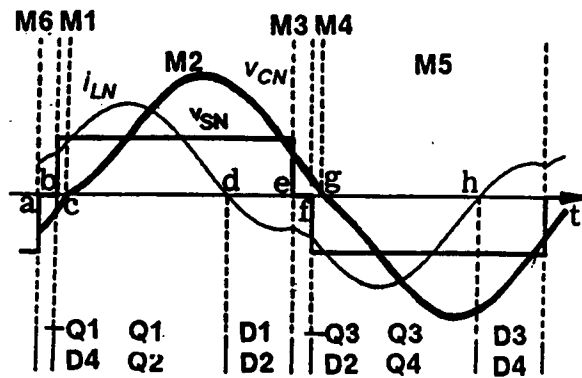
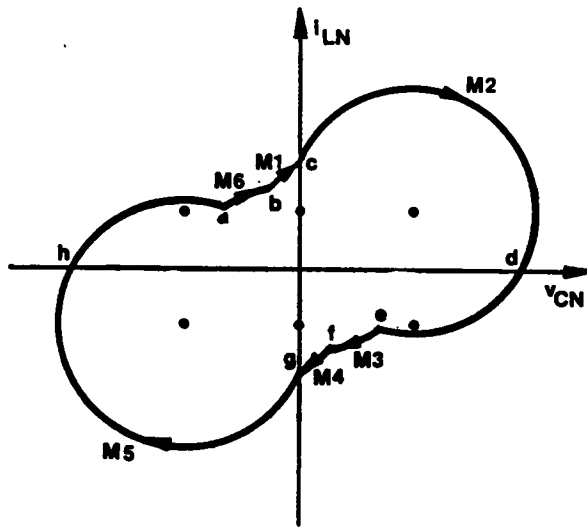
3.3.5.1 Operating modes below resonant frequency

Figure 3.8 shows a series of equilibrium state trajectories together with their corresponding circuit waveforms which illustrate all the possible operating modes of a CM-PRC operating below resonant frequency.

(a) *Natural-commutation modes*

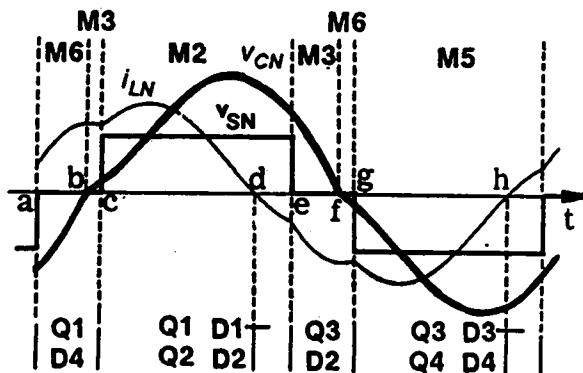
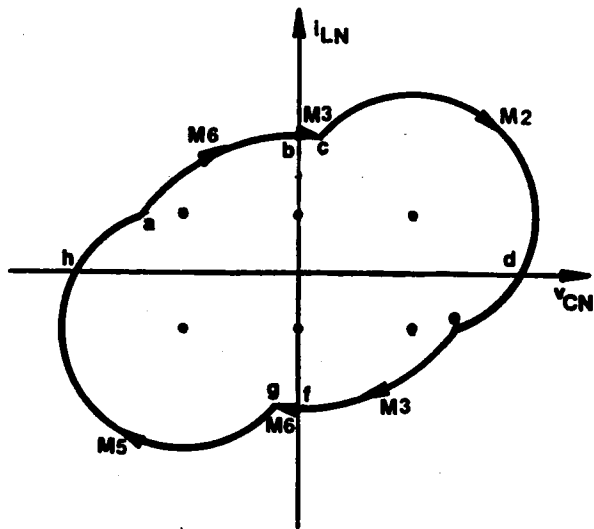
Trajectory 1_N: As shown in Figure 3.8(a), at $t = a$, transistor Q1 turns on commutating diode D3. The inductor current, i_{LN} , resonates through Q1 and D4 (M6). At $t = b$, transistor Q2 turns on commutating diode D4. The inductor current resonates through Q1 and Q2 (M1). At $t = c$, capacitor voltage v_{CN} reverses polarity. The inductor current continues to resonate through Q1 and Q2 (M2). At $t = d$, inductor current i_{LN} decreases to zero. Transistors Q1, Q2 *turn off naturally* and diodes D1, D2 conducts subsequently. The inductor current resonant through D1 and D2 (M2). At $t = e$, transistor Q3 turns on commutating diode D1 and a similar process occurs with the roles of Q1, Q2, D1, D2 and Q3, Q4, D3, D4 interchanged, respectively. The topological mode sequence of this trajectory is $M6-M1-M2-M3-M4-M5$, which is defined as "mode-I operation" of CM-PRC. Since the transistors are all naturally commutated, the circuit operation for this trajectory is referred to as "mode- I_N operation".

Trajectory 2_N: As shown in Figure 3.8(b), the circuit operation for this trajectory is similar to that for Trajectory 1_N except that v_{CN} changes polarity before Q2(Q4) is triggered at $t = c(g)$. The topological mode sequence of this trajectory is



(a) Trajectory I_N and its corresponding circuit waveforms (Mode- I_N operation)

Figure 3.8 Equilibrium Trajectories of a CM-PRC Operating Below Resonant Frequency



(b) Trajectory 2_N and its corresponding circuit waveforms (Mode-II_N operation)

Figure 3.8 Continued

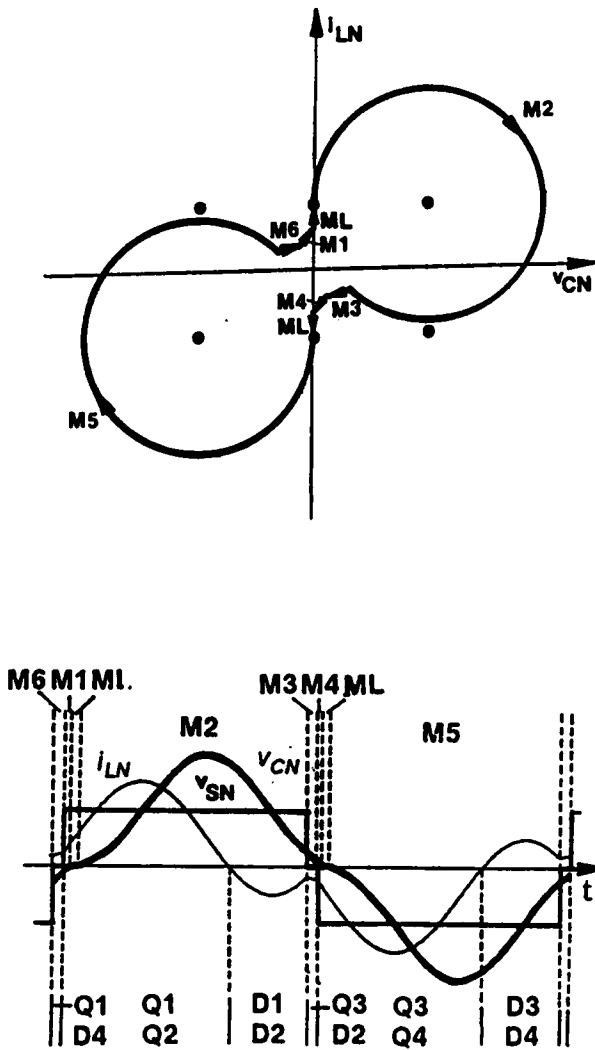
$M6-M3-M2-M3-M6-M5$, which is defined as “mode-II operation” of CM-PRC. The circuit operation for this trajectory is referred to as “mode-II_N operation”.

Trajectory 3_N: As shown in Figure 3.8(c), the circuit operation for this trajectory is similar to that for Trajectory 1_N except that when v_{CN} crosses the zero-axis, the magnitude of i_{LN} is less than I_{ON} . As a result, an inductor linear-charging interval (ML) exists. The linear-charging interval ends when the magnitude of i_{LN} increases beyond I_{ON} . The topological mode sequence of this trajectory is $M6-M1-ML-M2-M3-M4-ML-M5$, which is defined as “mode-III operation” of CM-PRC. The circuit operation for this trajectory is referred to as “mode-III_N operation”.

Trajectory 4_N: As shown in Figure 3.8(d), the circuit operation for this trajectory is similar to that for Trajectory 3_N except that v_{CN} crosses the zero-axis before Q2 or Q4 is triggered. Thus, in addition to the linear-charging interval, a free-wheeling interval (M0) also exists. The free-wheeling interval ends when Q2(Q4) is triggered. The topological mode sequence of this trajectory is $M6-M0-ML-M2-M3-M0-ML-M5$, which is defined as “mode-IV operation” of CM-PRC. The circuit operation for this trajectory is referred to as “mode-IV_N operation”.

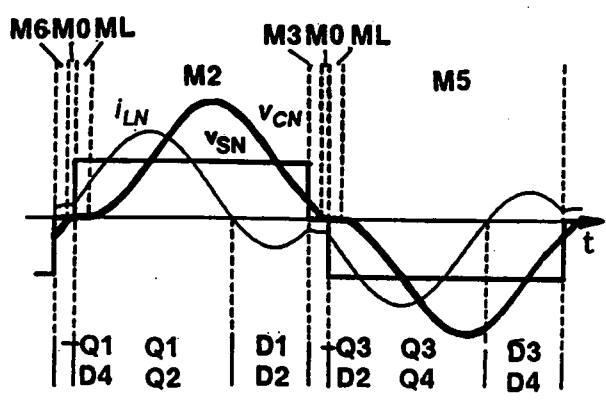
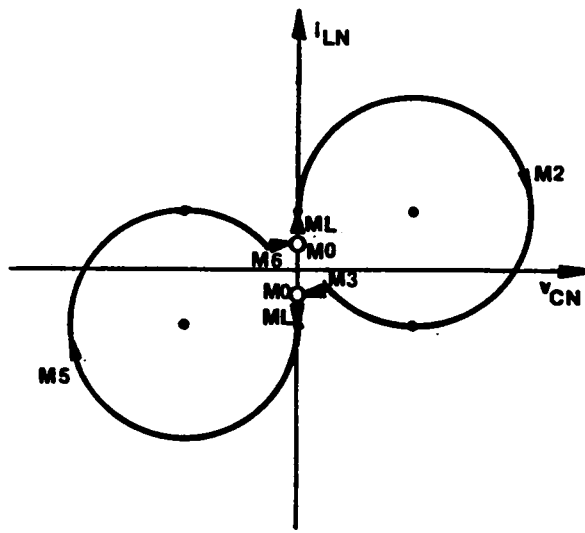
(b) Mixed-commutation modes

Trajectory 1_M: As shown in Figure 3.8(e), at $t = a$, transistor Q3 is *forced off* and Q1 is triggered. Transistor Q1 cannot conduct since i_{LN} is negative. Instead, diode D1 conducts. The inductor current resonates through Q4 and D1 (M6). At $t = b$, inductor current i_{LN} increases to zero. Transistor Q4 and diode D1 *turn off naturally* and transistor Q1 and diode D4 conduct subsequently. The inductor current resonates through Q1 and D4 (M6). At $t = c$, transistor Q2 turns on commutating diode D4. The inductor current resonates through Q1 and Q2 (M1). At $t = d$, capacitor voltage v_{CN} changes polarity. The inductor current continues to resonate through Q1 and Q2 (M2). At $t = e$, transistor Q1 is *forced off* and Q3 is triggered. A similar process occurs with the roles



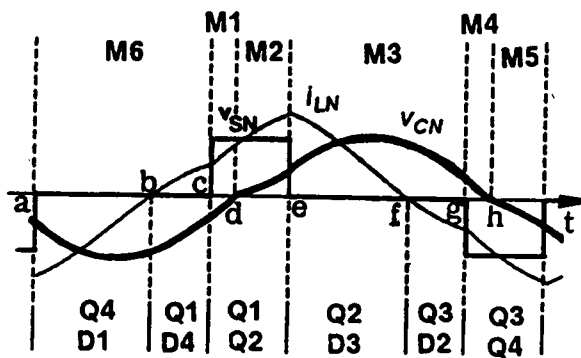
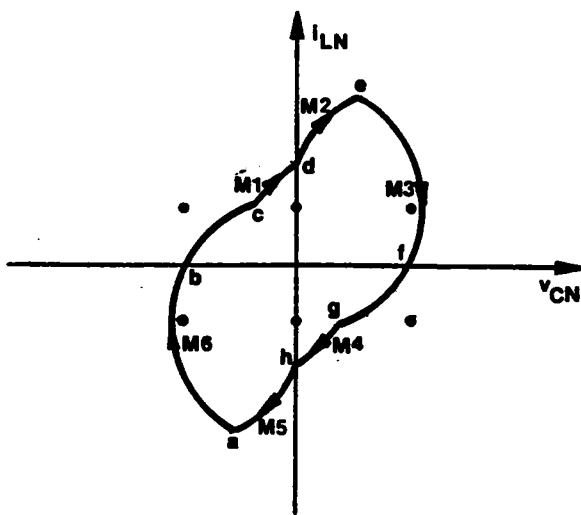
(c) Trajectory 3_N and its corresponding circuit waveforms (Mode-III_N operation)

Figure 3.8 Continued



(d) Trajectory 4_N and its corresponding circuit waveforms (Mode- IV_N operation)

Figure 3.8 Continued



(e) Trajectory I_M and its corresponding circuit waveforms (Mode- I_M operation)

Figure 3.8 Continued

of Q1,Q2,D1,Q2 and Q3,Q4,D3,D4 interchanged, respectively. The topological mode sequence of this trajectory is the same as that of Trajectory 1_N . However, since transistors Q1,Q3 are force-commutated while transistors Q2,Q4 are naturally commutated, the circuit operation for this trajectory is referred to as "mode- I_M operation".

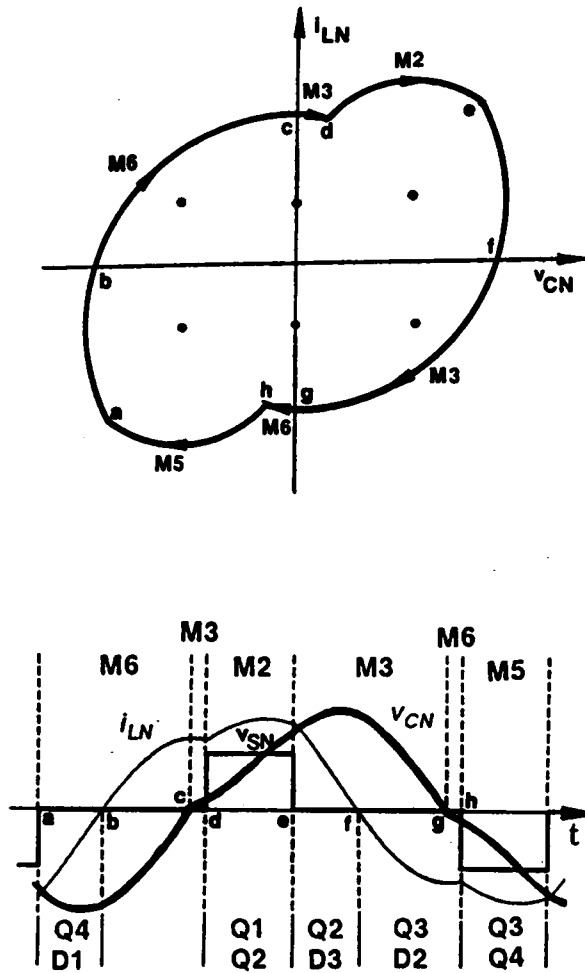
Trajectory 2_M : As shown in Figure 3.8(f), the circuit operation for this trajectory is similar to that for Trajectory 1_M except that v_{CN} changes polarity before Q2(Q4) is triggered at $t = d(h)$. The topological mode sequence of this trajectory is the same as that of Trajectory 2_N . The circuit operation for this trajectory is referred to as "mode- II_M operation".

Trajectory 3_M : As shown in Figure 3.8(g), the circuit operation for this trajectory is similar to that for Trajectory 1_M except that when v_{CN} crosses the zero-axis, the magnitude of i_{LN} is less than I_{ON} . As a result, an inductor linear-charging interval (ML) exists. The linear-charging interval ends when the magnitude of i_{LN} increases beyond I_{ON} . The topological mode sequence of this trajectory is the same as that of Trajectory 3_N . The circuit operation for this trajectory is referred to as "mode- III_M operation".

Trajectory 4_M : As shown in Figure 3.8(h), the circuit operation for this trajectory is similar to that for Trajectory 3_M except that v_{CN} crosses the zero-axis before Q2 or Q4 is triggered. Thus, in addition to the linear-charging interval, a free-wheeling interval (M0) also exists. The free-wheeling interval ends when Q2(Q4) is triggered. The topological mode sequence of this trajectory is the same as that of Trajectory 4_N . The circuit operation for this trajectory is referred to as "mode- IV_M operation".

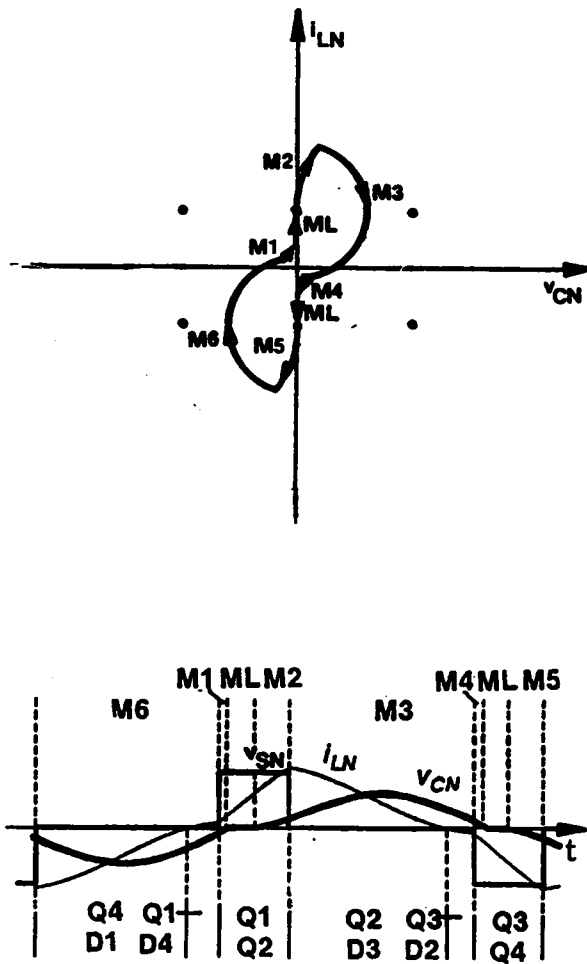
(c) Force-commutation modes

Trajectory 1_F : As shown in Figure 3.8(i), at $t = a$, transistor Q3 is *forced off* and Q1 is triggered. Transistor Q1 cannot conduct since i_{LN} is negative. Instead, diode D1 conducts. The inductor current resonates through Q4 and D1 (M6). At $t = b$, transistor Q4 is *forced off* and Q2 is triggered. Transistor Q2 cannot conduct since i_{LN} is still neg-



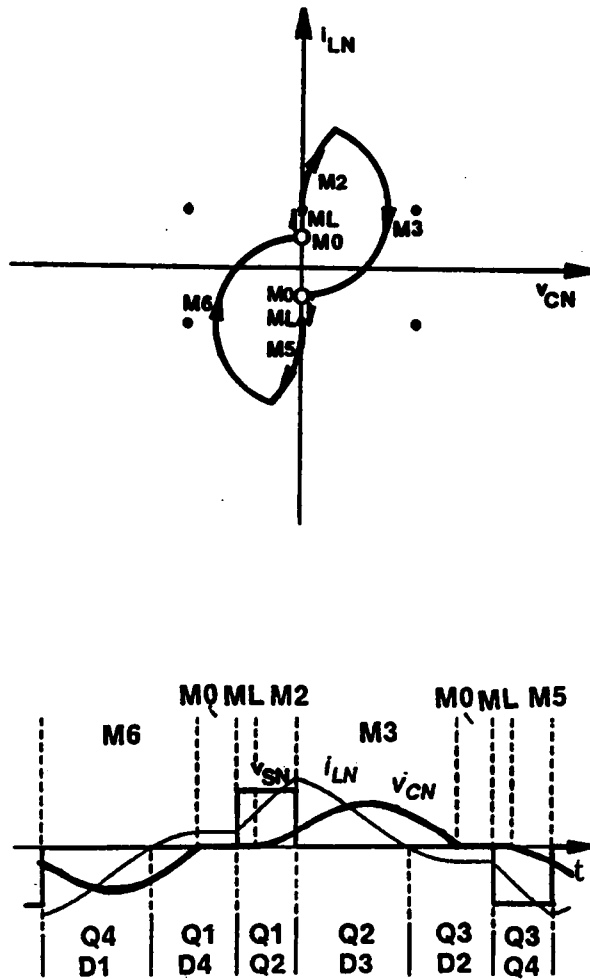
(f) Trajectory 2_M and its corresponding circuit waveforms (Mode-II_M operation)

Figure 3.8 Continued



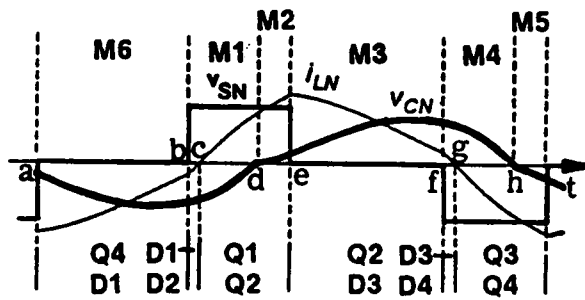
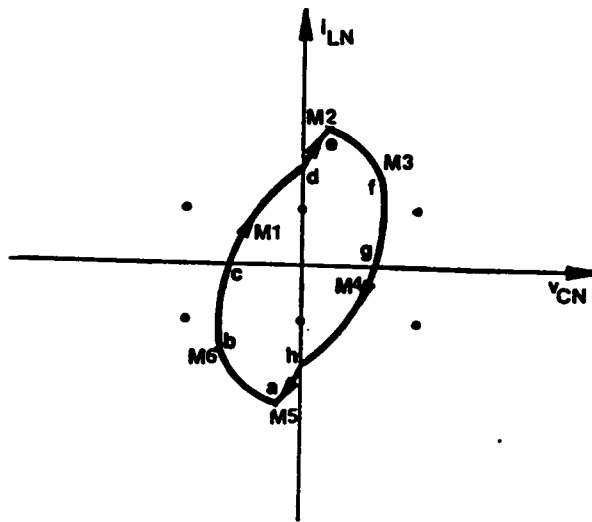
(g) Trajectory 3_M and its corresponding circuit waveforms (Mode-III_M operation)

Figure 3.8 Continued



(h) Trajectory 4_M and its corresponding circuit waveforms (Mode- IV_M operation)

Figure 3.8 Continued

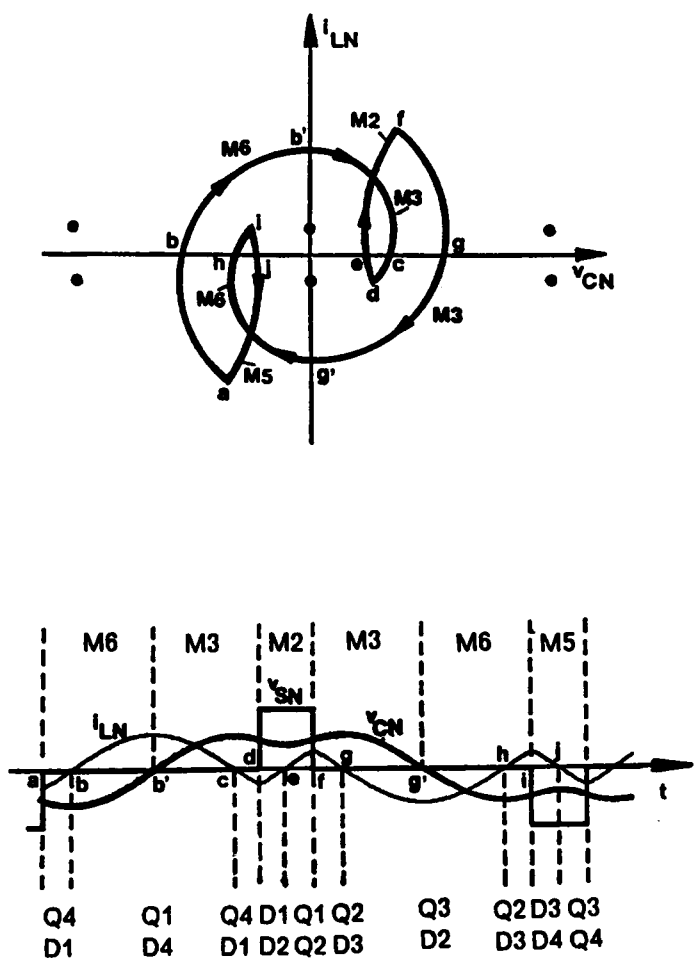


(i) Trajectory I_F and its corresponding circuit waveforms (Mode- I_F operation)

Figure 3.8 Continued

ative. Instead, diode D2 conducts. The inductor current resonates through D1 and D2 (M1). At $t=c$, i_{LN} increases to zero. Diodes D1,D2 turn off naturally and transistors Q1,Q2 conduct subsequently. The inductor current resonates through Q1 and Q2 (M1). At $t=d$, capacitor voltage v_{CN} changes polarity. The inductor current continues to resonates through Q1 and Q2 (M2). At $t=e$, transistor Q1 is *forced off* and Q3 is triggered. A similar process occurs with the roles of Q1,Q2,D1,Q2 and Q3,Q4,D3,D4 interchanged, respectively. The topological mode sequence of this trajectory is the same as that of Trajectory 1_N. However, since all the transistors are force-commutated, the circuit operation for this trajectory is referred to as "mode- I_F operation".

Trajectory 2_{ML}: This trajectory is a special case of "mode-II operation". The transistors conduct twice during a switching period. As shown in Figure 3.8(j), at $t=a$, transistor Q3 is *forced off* and Q1 is triggered. Transistor Q1 cannot conduct since i_{LN} is negative. Instead, diode D1 conducts. The inductor current resonates through Q4 and D1 (M6). At $t=b$, inductor current i_{LN} increases to zero. Transistor Q4, diode D1 *turn off naturally* and transistor Q1, diode D4 conduct subsequently. The inductor current resonates through Q1 and D4 (M6). At $t=b'$, capacitor voltage v_{CN} changes polarity. The inductor current continues to resonates through Q1 and D4 (M3). At $t=c$, i_{LN} changes polarity for the second time. Transistor Q1, diode D4 *turn off naturally* and transistor Q4, diode D1 conduct again. The inductor current resonates through Q4 and D1 (M3). At $t=d$, transistor Q4 is *forced off* and Q2 is triggered. Transistor Q2 cannot conduct since i_{LN} is negative. Instead, diode D2 conducts. The inductor current resonates through D1 and D2 (M2). At $t=e$, i_{LN} changes polarity for the third time. Diodes D1,D2 turn off naturally and transistors Q1,Q2 conduct subsequently. The inductor current resonates through Q1 and Q2 (M2). At $t=f$, transistor Q1 is *forced off* and Q3 is triggered. A similar process occurs with the roles of Q1,Q2,D1,D2 and Q3,Q4,D3,D4 interchanged, respectively. The topological mode sequence of this trajec-



(j) Trajectory 2_{ML} and its corresponding circuit waveforms (Mode-II $_{ML}$ operation)

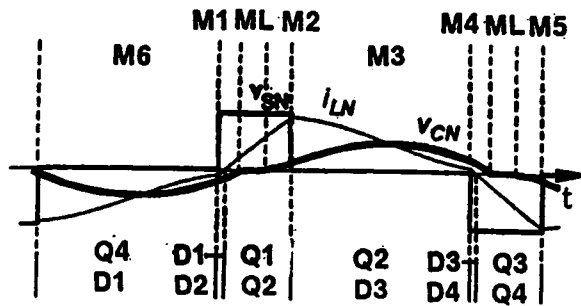
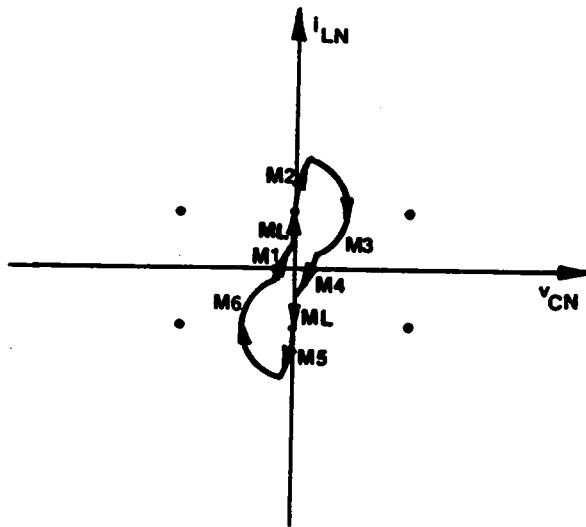
Figure 3.8 Continued

tory is the same as that of Trajectory 2_N . However, due to the multiple-conduction feature, the circuit operation for this trajectory is referred to as "mode-II_{ML} operation".

Trajectory 3_F: As shown in Figure 3.8(k), the circuit operation for this trajectory is similar to that for Trajectory 1_F except that when v_{CN} crosses the zero-axis, the magnitude of i_{LN} is less than I_{ON} . As a result, an inductor linear-charging interval (ML) exists. The linear-charging interval ends when the magnitude of i_{LN} increases beyond I_{ON} . The topological mode sequence of this trajectory is the same as that of Trajectory 3_N. The circuit operation for this trajectory is referred to as "mode-III_F operation".

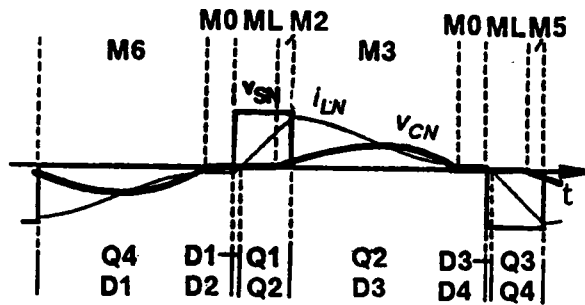
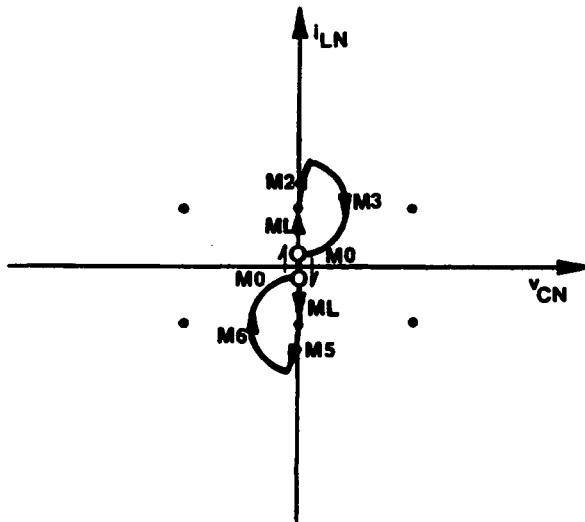
Trajectory 4_F: As shown in Figure 3.8(l), the circuit operation for this trajectory is similar to that for Trajectory 3_F except that v_{CN} crosses the zero-axis before Q2 or Q4 is triggered. Thus, in addition to the linear-charging interval, a free-wheeling interval (M0) also exists. The free-wheeling interval ends when Q2(Q4) is triggered. The topological mode sequence of this trajectory is the same as that of Trajectory 4_N. The circuit operation for this trajectory is referred to as "mode-IV_F operation".

Trajectory 5_F: As shown in Figure 3.8(m), this trajectory is degenerated either from Trajectory 3_F or from Trajectory 4_F. The capacitor voltage, v_{CN} , is always zero. In other words, the resonant capacitor, C, is always shorted through the output bridge diodes. The resonant inductor, L, is either linearly charged or discharged by the source voltage or shorted through two parallel switch branches in the input bridge. No resonant action occurs and no output voltage is generated. The topological mode sequence of this trajectory is *M0-ML-M0-ML*, which is defined as "mode-V operation" of CM-PRC. Since all the transistors are force-commutated, the circuit operation for this trajectory is referred to as "mode-V_F operation". This operating mode can only exist momentarily when the energy in the output (filter) inductor is discharging into the load through the rectifier diodes. It cannot exist under steady state.



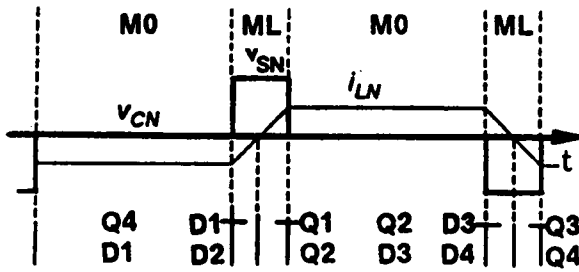
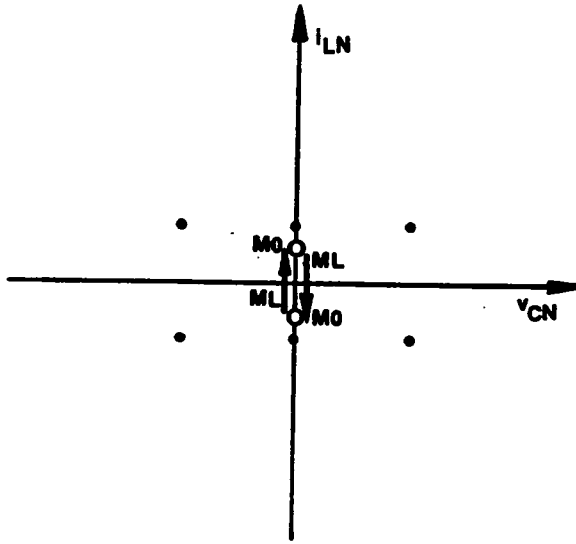
(k) Trajectory 3_F and its corresponding circuit waveforms (Mode-III_F operation)

Figure 3.8 Continued



(l) Trajectory 4_F and its corresponding circuit waveforms (Mode- IV_F operation)

Figure 3.8 Continued



(m) Trajectory S_F and its corresponding circuit waveforms (Mode- V_F operation)

Figure 3.8 Continued

Table 3.1 summarizes the operating modes below resonant frequency and their corresponding topological mode sequences. The subscript in each operating mode indicates the commutation features for the transistors, where "N" stands for natural commutation, "M" stands for mixed commutation, "ML" stands for multiple conduction, and "F" stands for force commutation.

3.3.5.2 Operating modes above the resonant frequency

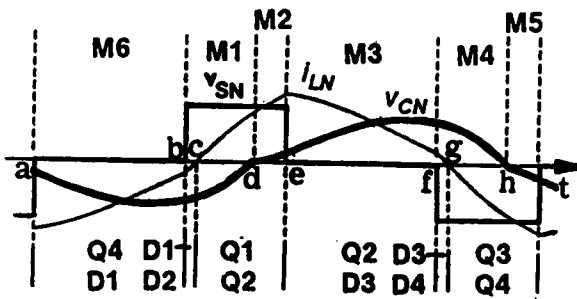
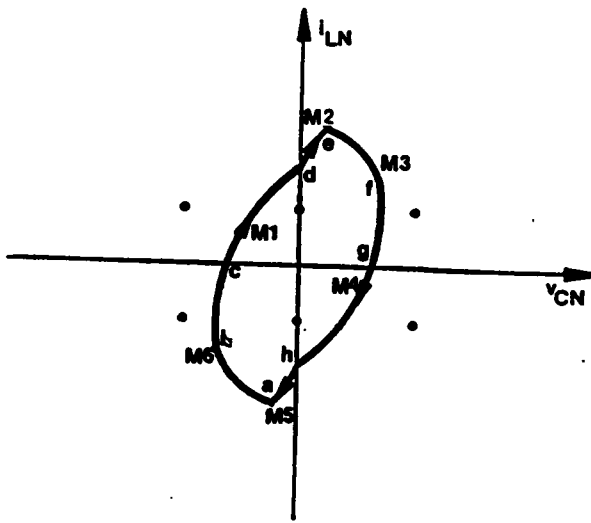
Figure 3.9 shows a series of equilibrium state trajectories which illustrate all possible operating modes of a CM-PRC operating above resonant frequency. The trajectories shown in Figs. 3.9(a), (c), (d), (e) have already been discussed in the previous section. The trajectories shown in Figs. 3.9(b) and 3.9(f) are discussed in the following.

(a) Force-commutation modes

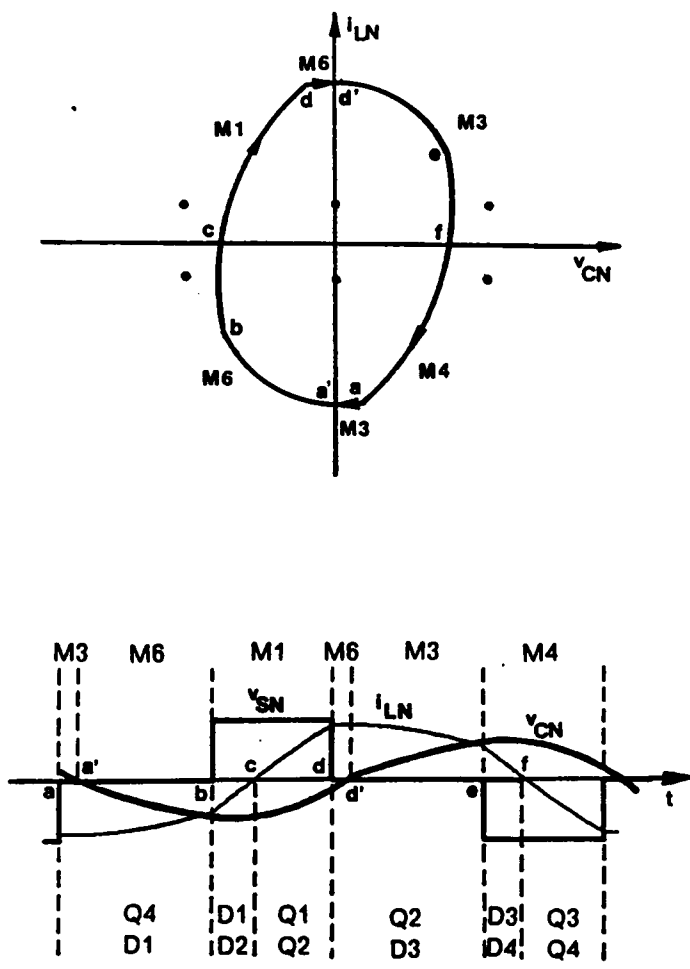
Trajectory 2A_F: As shown in Figure 3.9(b), at $t = a$, transistor Q3 is *forced off* and Q1 is triggered. Transistor Q1 cannot conduct since i_{LN} is negative. Instead, diode D1 conducts. The inductor current resonates through Q4 and D1 (M3). At $t = a'$, capacitor voltage v_{CN} changes polarity. The inductor current continues to resonate through Q4 and D1 (M6). At $t = b$, transistor Q4 is *forced off* and Q2 is triggered. Transistor Q2 cannot conduct since i_{LN} is still negative. Instead, diode D2 conducts. The inductor current resonates through D1 and D2 (M1). At $t = c$, inductor current i_{LN} increases to zero. Diodes D1, D2 turn off naturally and transistors Q1, Q2 conduct subsequently. The inductor current resonates through Q1 and Q2 (M1). At $t = d$, transistor Q1 is *forced off* and Q3 is triggered. A similar process occurs with the roles of Q1, Q2, D1, Q2 and Q3, Q4, D3, D4 interchanged, respectively. The topological mode sequence of this trajectory is $M3-M6-M1-M6-M3-M4$, which is defined as "mode-IIA operation" of CM-PRC. Since all the transistors are force-commutated, the circuit operation for this trajectory is referred to as "mode-IIA_F operation".

Table 3.1 Topological Mode Sequences for Circuit Operating Modes Below Resonant Frequency

Operating Modes	Topological Mode Sequences
I_N, I_M, I_F	M6-M1-M2-M3-M4-M5
II_N, II_M, II_{ML}	M6-M3-M2-M3-M6-M5
III_N, III_M, III_F	M6-M1-ML-M2-M3-M4-ML-M5
IV_N, IV_M, IV_F	M6-M0-ML-M2-M3-M0-ML-M5
V_F	M0-ML-M0-ML

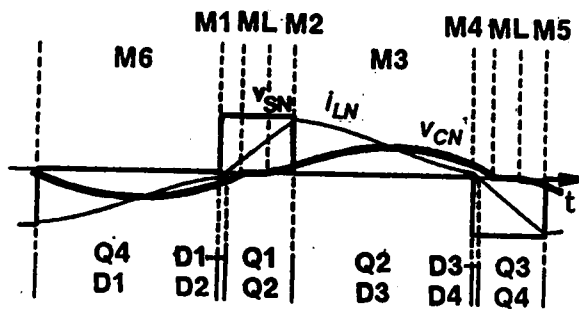
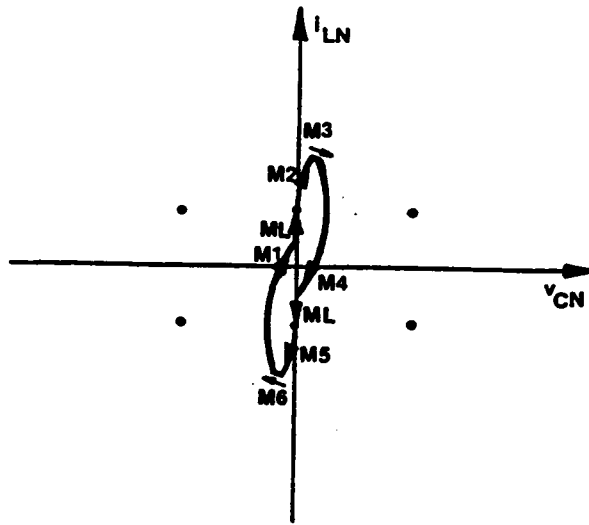


(a) Trajectory 1_F and its corresponding circuit waveforms (Mode- I_F operation)



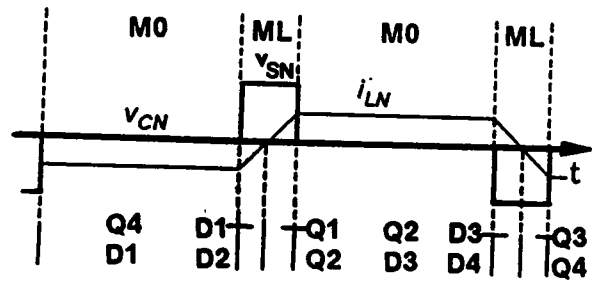
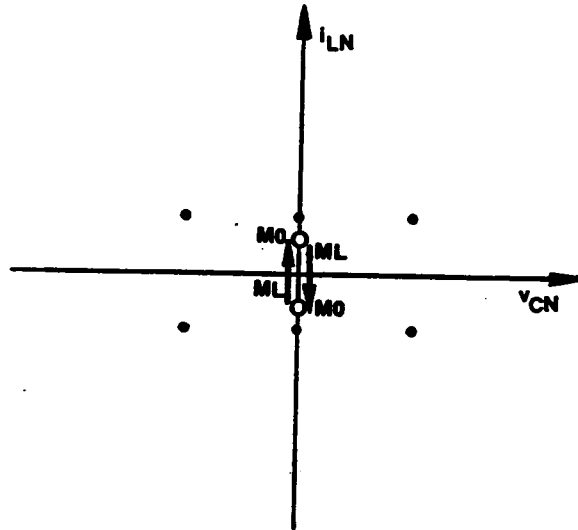
(b) Trajectory $2A_F$ and its corresponding circuit waveforms (Mode-II A_F operation)

Figure 3.9 Continued



(c) Trajectory 3_F and its corresponding circuit waveforms (Mode-III_F operation)

Figure 3.9 Continued



(d) Trajectory S_F and its corresponding circuit waveforms (Mode- V_F operation)

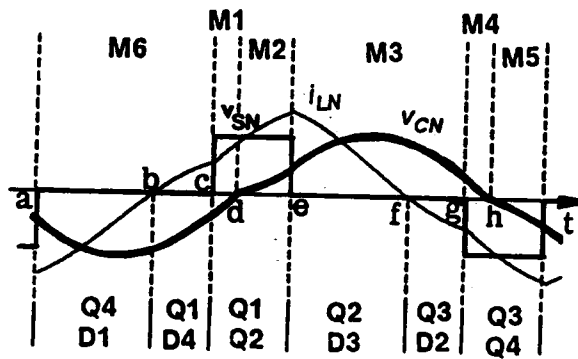
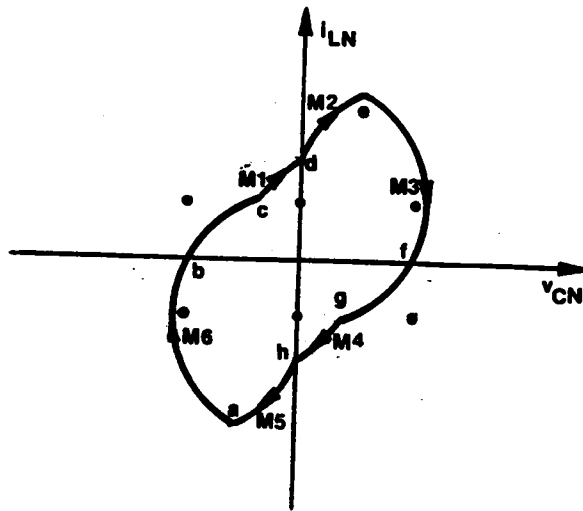
Figure 3.9 Continued

(b) Mixed-commutation modes

Trajectory $2A_M$: As shown in Figure 3.9(f), at $t=a$, transistor Q3 is *forced off* and Q1 is triggered. Transistor Q1 cannot conduct since i_{LN} is negative. Instead, diode D1 conducts. The inductor current resonates through Q4 and D1 (M3). At $t=a'$, capacitor voltage v_{CN} changes polarity. The inductor current continues to resonate through Q4 and D1 (M6). At $t=b$, inductor current i_{LN} increases to zero. Transistor Q4, diode D1 *turn off naturally* and transistors Q1, diode D4 conduct subsequently. The inductor current resonates through Q1 and D4 (M6). At $t=c$, transistor Q2 is triggered commutating diode D4. The inductor current resonates through Q1 and Q2 (M1). At $t=d$, transistor Q1 is *forced off* and Q3 is triggered. A similar process occurs with the roles of Q1,Q2,D1,Q2 and Q3,Q4,D3,D4 interchanged, respectively. The topological mode sequence of this trajectory is the same as that of Trajectory $2A_F$. However, since transistors Q1,Q3 are force-commutated while Q2,Q4 are naturally commutated, the circuit operation for this trajectory is referred to as "mode- IIA_M operation".

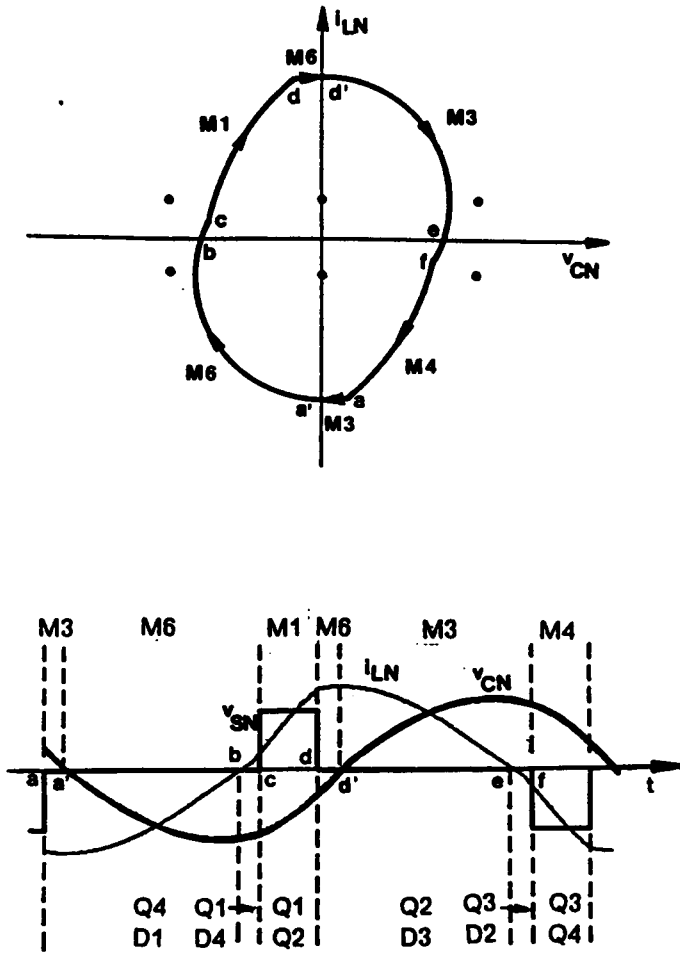
Table 3.2 summarizes the operating modes above resonant frequency and their corresponding topological mode sequences.

It should be noted that the trajectories discussed above are used only to qualitatively illustrate the existence of various operating modes of a CM-PRC. The frequencies corresponding to the trajectories may not be the same. Some trajectories exist only for a certain range of frequency and load current, as shall be seen in the following section.



(e) Trajectory I_M and its corresponding circuit waveforms (Mode- I_M operation)

Figure 3.9 Continued



(f) Trajectory $2A_M$ and its corresponding circuit waveforms (Mode-II A_M operation)

Figure 3.9 Continued

**Table 3.2 Topological Mode Sequences for Circuit
Operating Modes Above Resonant Frequency**

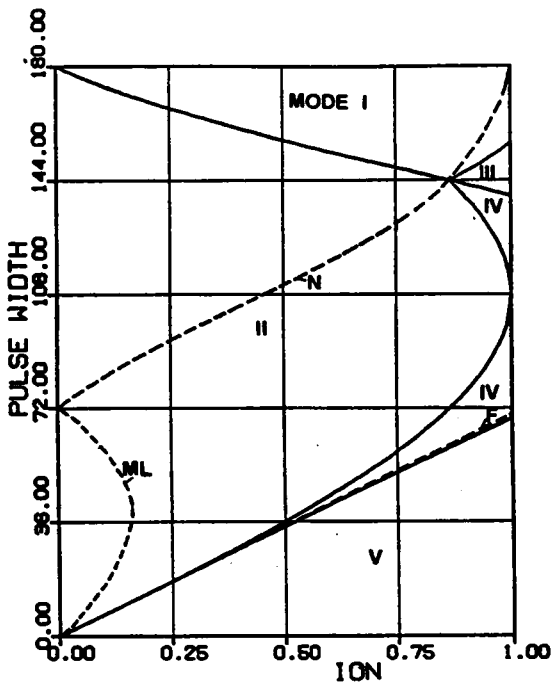
Operating Modes	Topological Mode Sequences
I_M, I_F	M6-M1-M2-M3-M4-M5
IIA_M, IIA_F	M3-M6-M1-M6-M3-M4
III_F	M6-M1-ML-M2-M3-M4-ML-M5
V_F	M0-ML-M0-ML

3.3.6 Regions of Operation

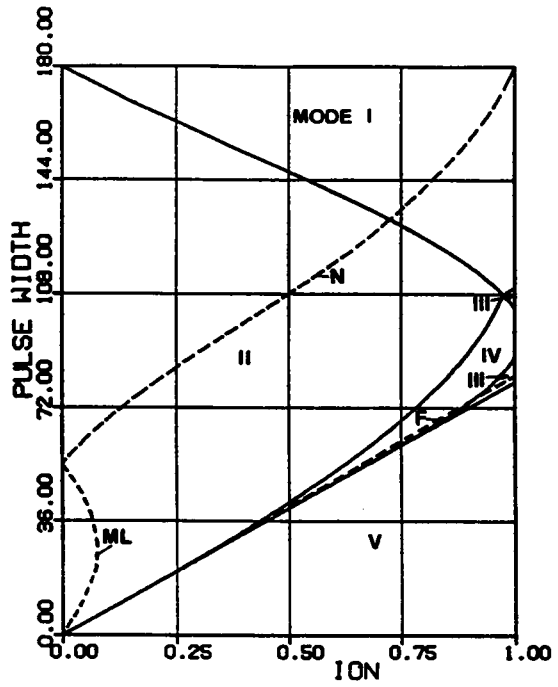
As mentioned in Chapter 2, it is important to know the converter's mode of operation for a specific design such that circuit devices such as diodes and snubbers can be optimally selected for the converter. In this section, regions of operation for a CM-PRC are defined to determine the converter's mode of operation for given normalized switching frequency, $\omega_{SN} = \frac{\omega_S}{\omega_0}$, pulse width, β_S , of the quasi-square-wave voltage v_S , and the normalized load current, $I_{ON} = \frac{Z_0 \times I_O}{E}$.

3.3.6.1 Operating regions below resonant frequency

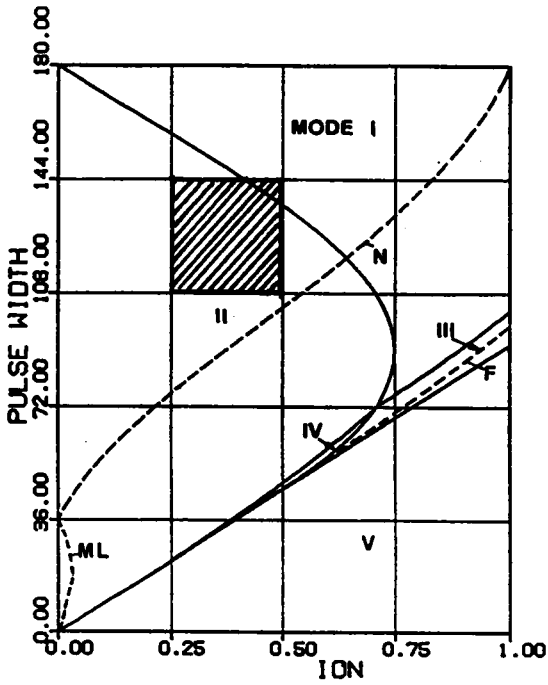
Figure 3.10 shows the operating regions of a CM-PRC operating below resonant frequency. In the figure, the mode of operation is represented as a function of the pulse width, β_S , of the quasi-square-wave voltage, v_S , and the load current, I_{ON} , at several frequencies $\omega_{SN} = 0.6, 0.7, 0.8, \text{ and } 0.9$. A β_S angle of 180° is equivalent to a full pulse-width of v_S (duty ratio = 1). Three dotted lines are shown in each figure to indicate boundaries for different device commutation conditions. Above the dotted line "N" is the natural-commutation region in which all the transistors are naturally commutated. Between the dotted lines "N" and "F" is the mixed-commutation region in which transistors Q1,Q3 are force-commutated and Q2,Q4 are naturally commutated. Below the dotted line "F" is the force-commutation region in which all the transistors are force-commutated. The dotted line "MI." defines a region corresponding to mode-II_{ML} operation, where the transistors conduct twice during a switching period. This multiple-conduction region is undesirable and should be avoided. Given the range of I_{ON} , β_S , and a specific operating frequency, the converter's modes of operation can be easily determined. For example, if ω_{SN} equals 0.8, I_{ON} ranges from 0.25 to 0.5, and β_S ranges from 144° to 108° , the converter will operate either in mode I_N or in mode II_N , as indicated by the shaded area in Figure 3.10(c).



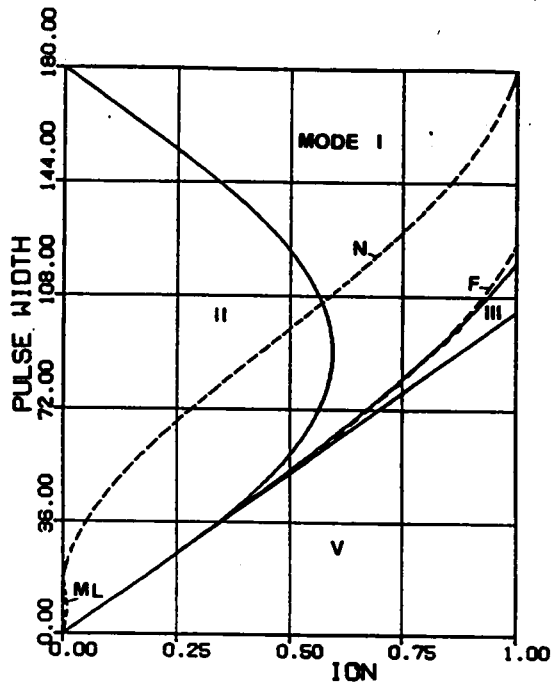
(a) $\omega_{SN} = 0.6$



(b) $\omega_{SN} = 0.7$



(c) $\omega_{SN} = 0.8$



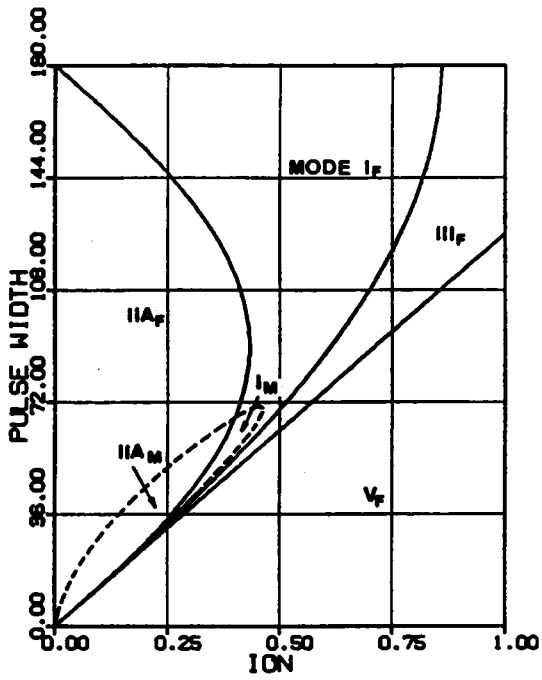
(d) $\omega_{SN} = 0.9$

Figure 3.10 Regions of Operation Below Resonant Frequency

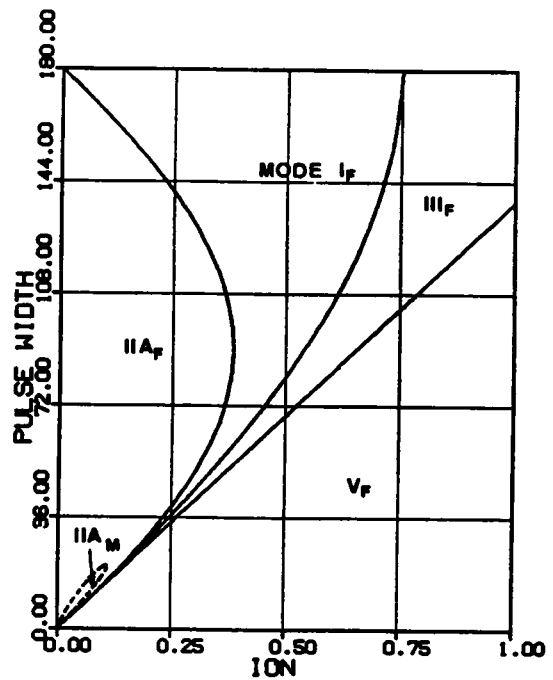
For other frequencies not shown in Figure 3.10, an algorithm is developed in Appendix C.2 which can be used to plot similar graphs to those in Figure 3.10.

3.3.6.2 Operating regions above resonant frequency

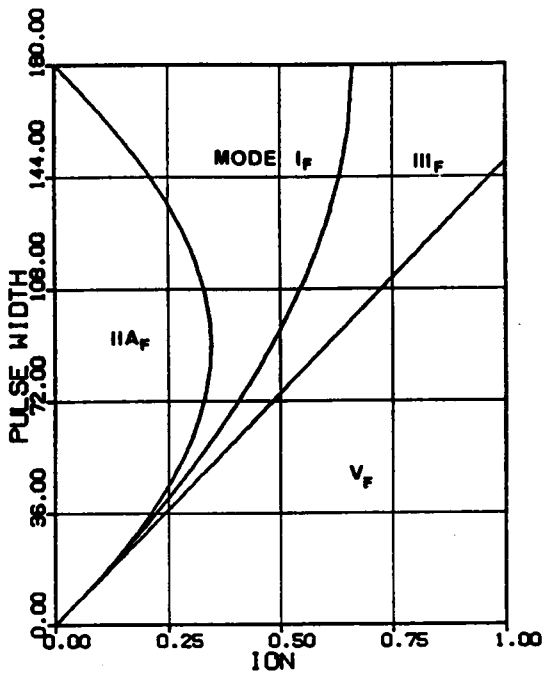
Figure 3.11 shows several operating regions above resonant frequency. These regions are derived from the algorithm developed in Appendix C.3. A dotted line is used in the figures for $\omega_{SN} = 1.1$ and 1.2 to define the mixed-commutation region. Inside the dotted line, transistors Q1,Q3 are force-commutated and Q2,Q4 are naturally commutated. Outside the dotted line, all the transistors are force-commutated. The mixed-commutation region disappears when the normalized switching frequency increases beyond 1.2, as can be seen from the figure.



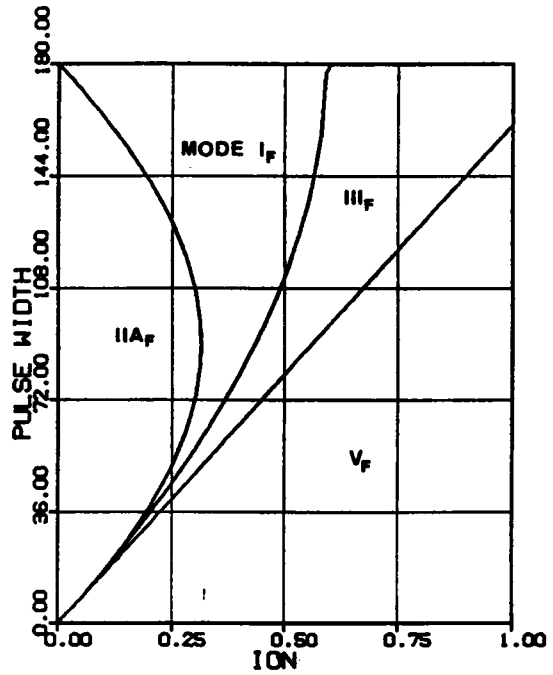
(a) $\omega_{SN} = 1.1$



(b) $\omega_{SN} = 1.2$



(c) $\omega_{SN} = 1.3$



(d) $\omega_{SN} = 1.4$

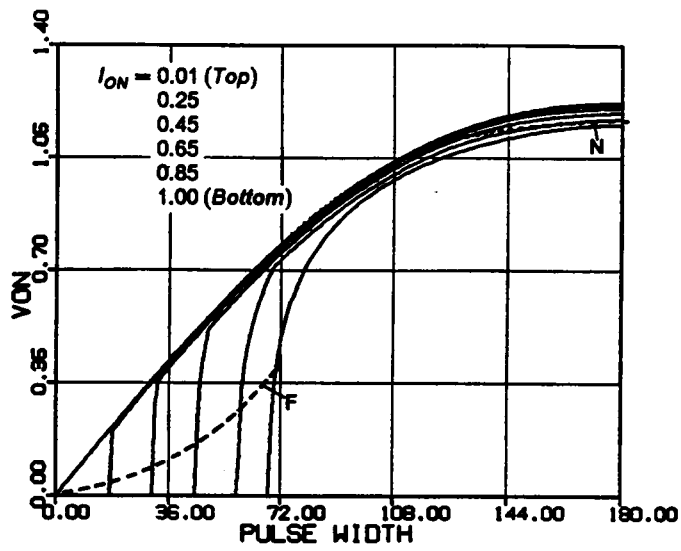
Figure 3.11 Regions of Operation Above Resonant Frequency

3.3.7 DC Characteristics

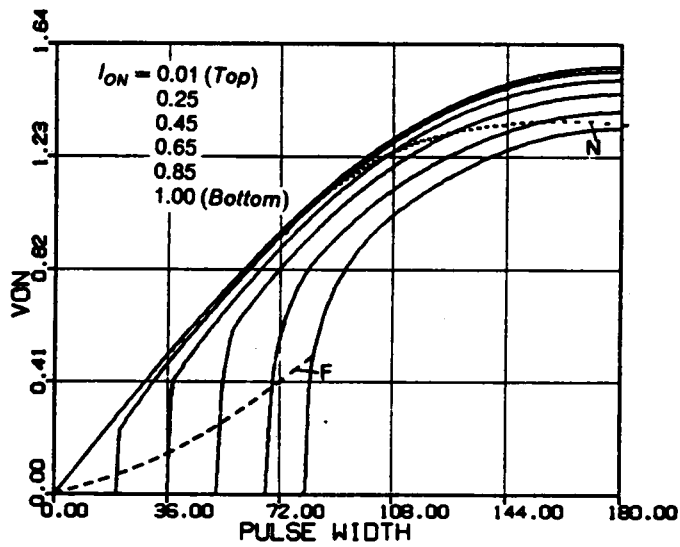
Once the regions of operation is defined, the dc characteristics for a CM-PRC can be derived following a similar approach as in Section 2.3.7. The equations for solving trajectory parameters for various operating modes below and above resonant frequency are summarized in Appendix C.4. A Fortran program for calculating salient circuit features such as control-to-output transfer ratio, rms inductor current, peak capacitor voltage, rms switch currents, etc. is included in Appendix C.5.

3.3.7.1 DC characteristics below resonant frequency

Figure 3.12 shows the dc control-to-output characteristics for several frequencies below the resonant frequency. In these figures, the output voltage (average capacitor voltage), V_{ON} , is plotted as a function of the pulse-width, β_S , of v_S , and the output current, I_{ON} . Two dotted lines are used in each graph to indicate the boundaries of natural commutation and force commutation. Above the dotted line "N", all the transistors are naturally commutated. Between the dotted lines "N" and "F", transistors Q1,Q3 are force-commutated and Q2,Q4 are naturally commutated. Below the dotted line "F", all the transistors are force-commutated. It can be seen that the converter is able to regulate the output from no load to a full load in the natural-commutation region. The region, however, is limited, especially when the switching frequency is below 80% of the resonant frequency. It is thus difficult to design a CM-PRC in the natural-commutation region when the output-to-input voltage ratio, V_{ON} , varies over a wide range. For example, if $\omega_{SN} = 0.8$ and V_{ON} ranges from 1.2 to 1.8, I_{ON} has to be limited less than 0.15, as can be seen from Figure 3.12(c). This can only be achieved either by using a small characteristic impedance or by limiting the load current to a small value. In either case, the circulating current in the tank circuit is high and the components are subjected to excessive stresses.

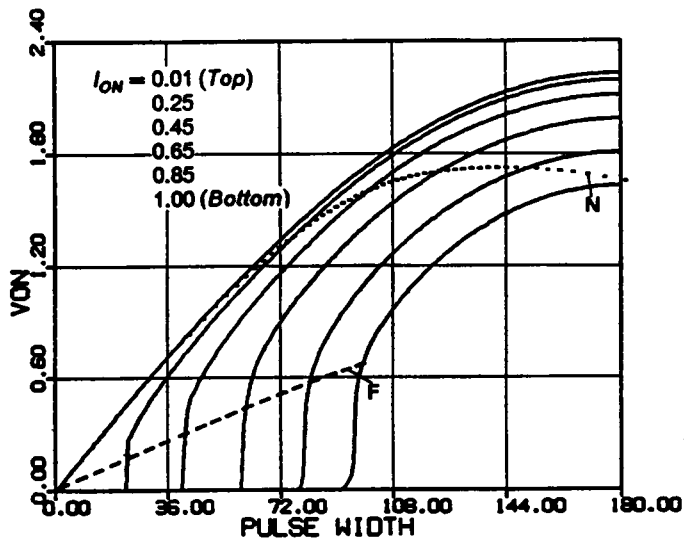


(a) $\omega_{SN} = 0.6$

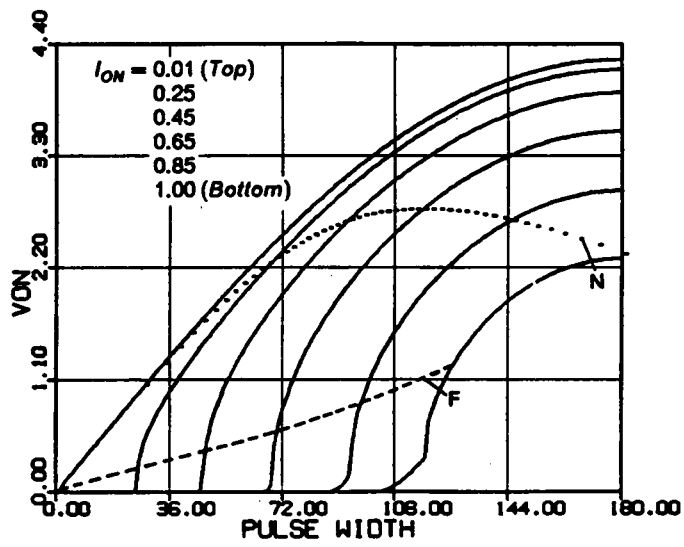


(b) $\omega_{SN} = 0.7$

Figure 3.12 DC Control-to-Output Characteristics Below Resonant Frequency

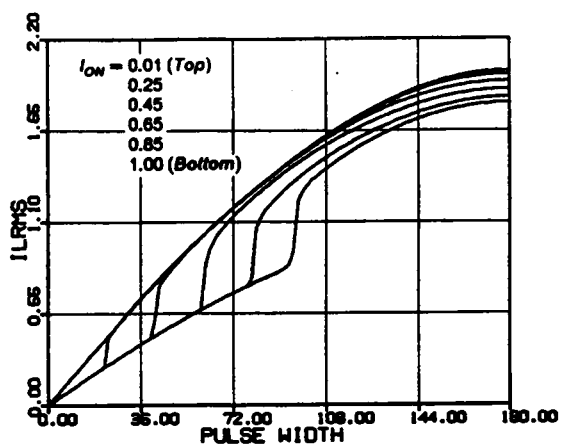


(c) $\omega_{SN} = 0.8$

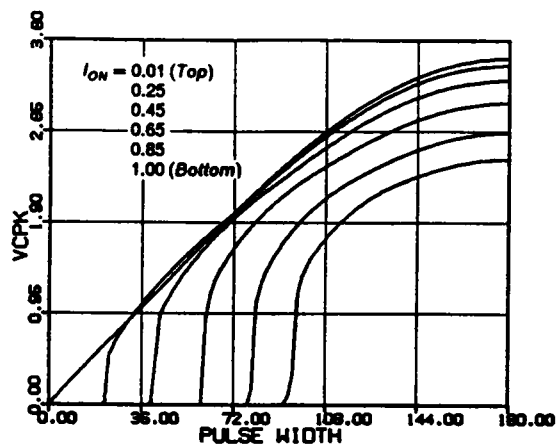


(d) $\omega_{SN} = 0.9$

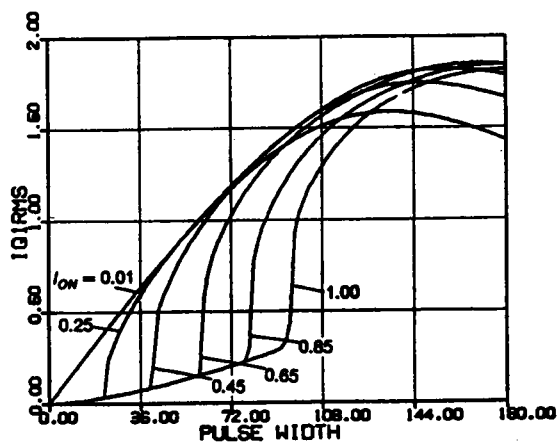
Figure 3.12 Continued



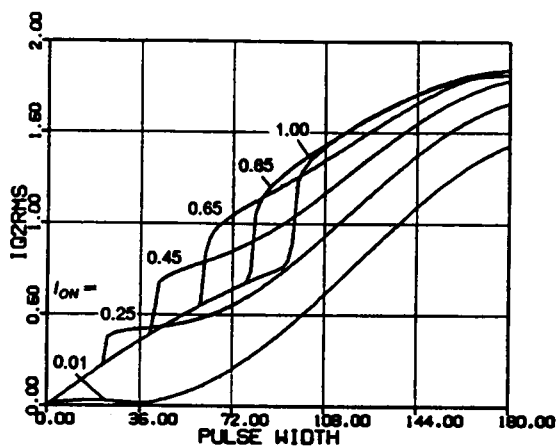
(a) RMS inductor current



(b) Peak capacitor voltage

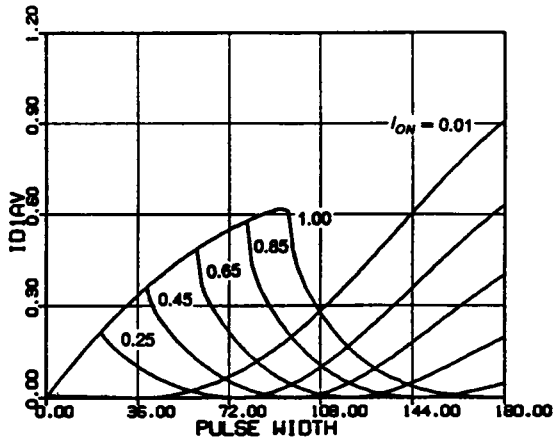


(c) RMS switch current (Q1,Q3)

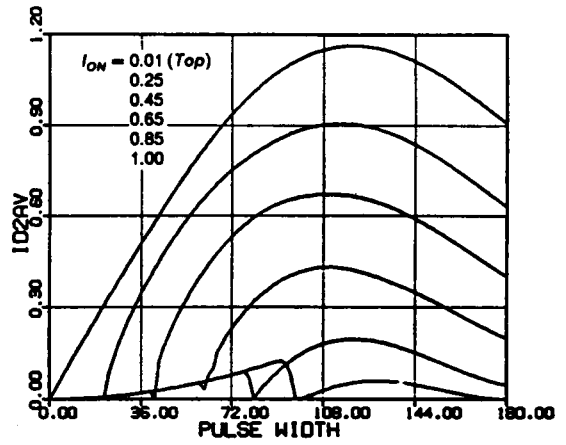


(d) RMS switch current (Q2,Q4)

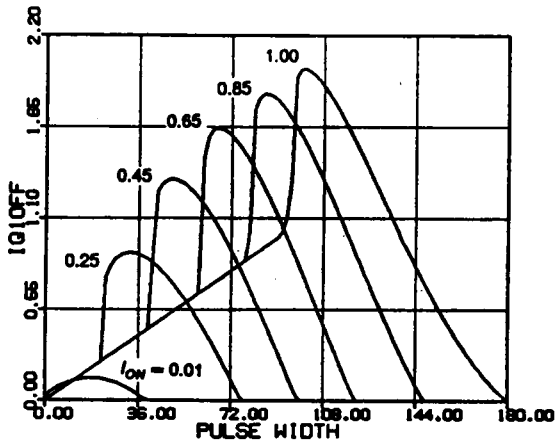
Figure 3.13 Characteristics for Various Circuit Salient Features at $\omega_{SN} = 0.8$



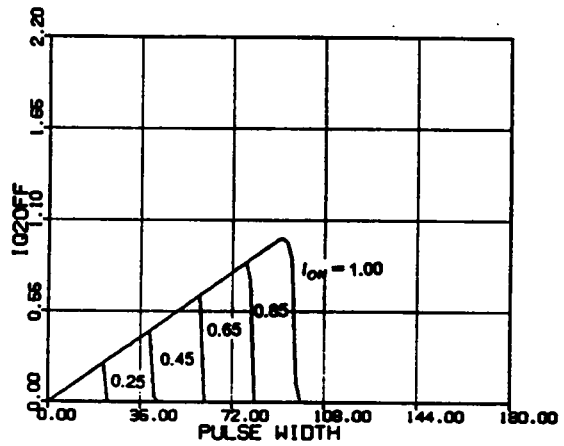
(e) Average diode current (D1,D3)



(f) Average diode current (D2,D4)

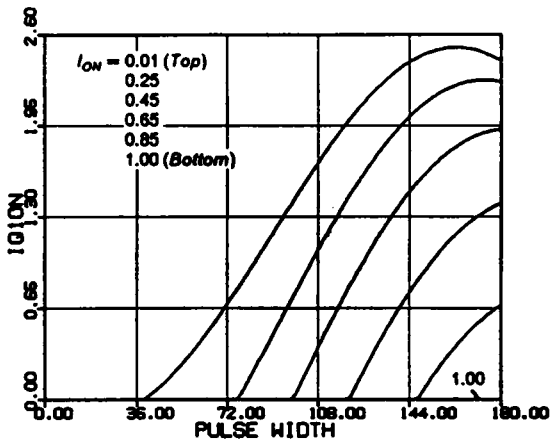


(g) Switch turn-off current (Q1,Q3)

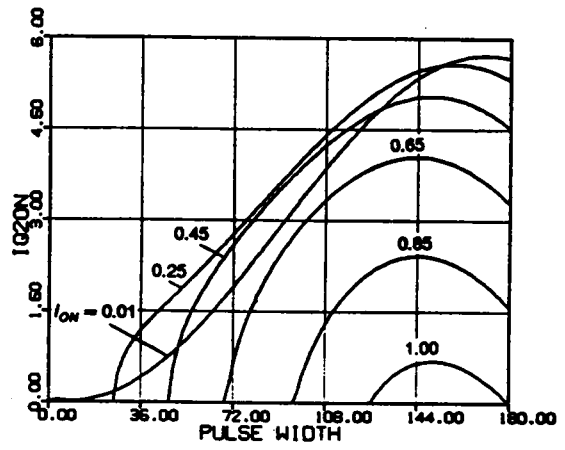


(h) Switch turn-off current (Q2,Q4)

Figure 3.13 Continued



(i) Switch turn-on current (Q1,Q3)



(j) Switch turn-on current (Q2,Q4)

Figure 3.13 Continued

An alternative is to design the converter in the mixed-commutation region. From Figure 3.12, it can be seen that the mixed-commutation mode can be operated over a wide range of load current and output-to-input voltage ratio. However, a minimum load has to be maintained if the converter is to be designed in this region.

The force-commutation region in this frequency range is very limited and is impractical to use. essentially useless. It allows only a small variation in the output-to-input voltage ratio. It requires a minimum load current. Most of all, since the slopes of the characteristics in this region are very steep, the converter is very difficult to control.

Figure 3.13 shows other important dc characteristics at frequency $\omega_{SN} = 0.8$. Notice that the currents of Q1,Q3 and the currents of Q2,Q4 are not balanced, as can be seen from Figures 3.13(c) and (d). Same phenomenon exists between the currents of D1,D3 and D2,D4. This is due to the phase displacement in the triggering of the transistors. In general, transistors Q1,Q3 and diodes D2,D4 carry higher currents when CM-PRC operates below the resonant frequency.

Similar dc characteristics for the frequency, $\omega_{SN} = 0.9$, can be found in Appendix C.6.

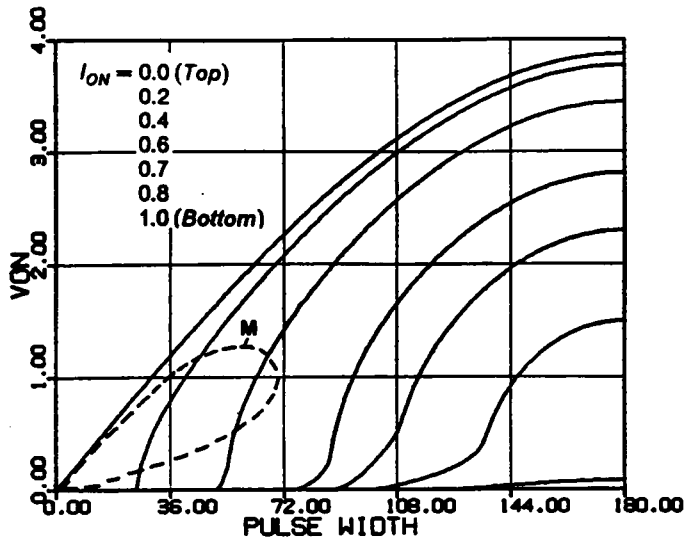
3.3.7.2 DC characteristics above resonant frequency

Figure 3.14(a)~(d) shows the dc control-to-output characteristics for $\omega_{SN} = 1.1, 1.2, 1.3,$ and 1.4 , respectively. A dotted line is used in the figures for $\omega_{SN} = 1.1$ and 1.2 to indicate the mixed-commutation boundary. Inside the dotted line, transistors Q1,Q3 are force-commutated and Q2,Q4 are naturally commutated. Outside the dotted line, all the transistors are force-commutated. It can be seen that in this frequency range, the converter is able to regulate its output from no load to full load over a wide range of output-to-input voltage ratio.

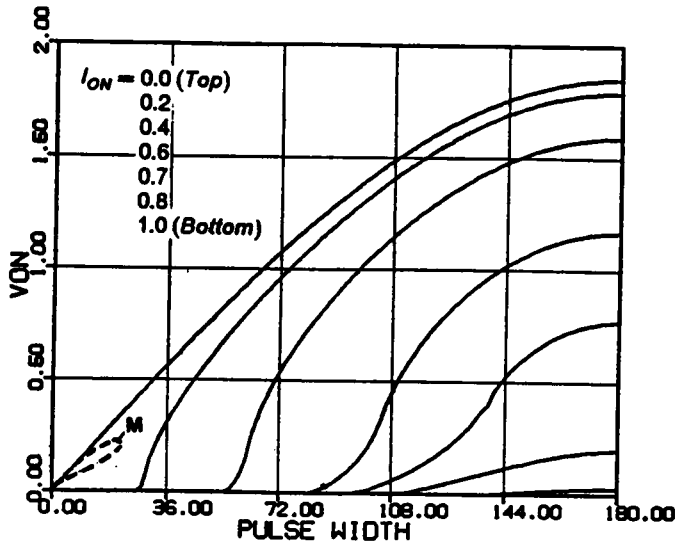
Figure 3.15 shows other important dc characteristics at frequency $\omega_{SN} = 1.2$. Again, the currents in the transistors and the currents in the diodes are unbalanced, as shown

in Figures 3.15(c) and (d) and Figures 3.15(e) and (f), respectively. However, in this frequency range, transistors Q2,Q4 and diodes D1,D3 carry higher currents.

Similar dc characteristics for other frequencies can be found in Appendix C.7.

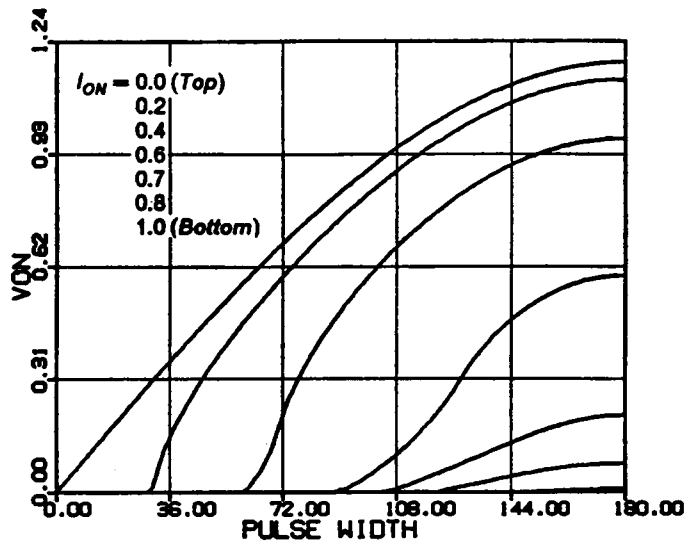


(a) $\omega_{SN} = 1.1$

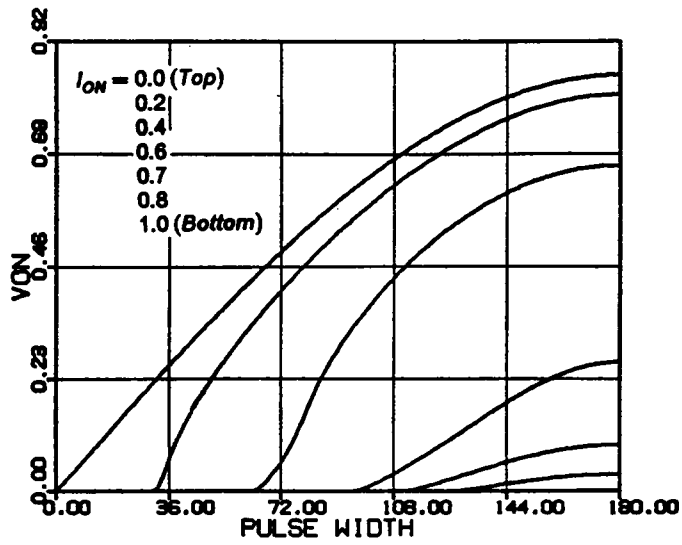


(b) $\omega_{SN} = 1.2$

Figure 3.14 DC Control-to-Output Characteristics Above Resonant Frequency

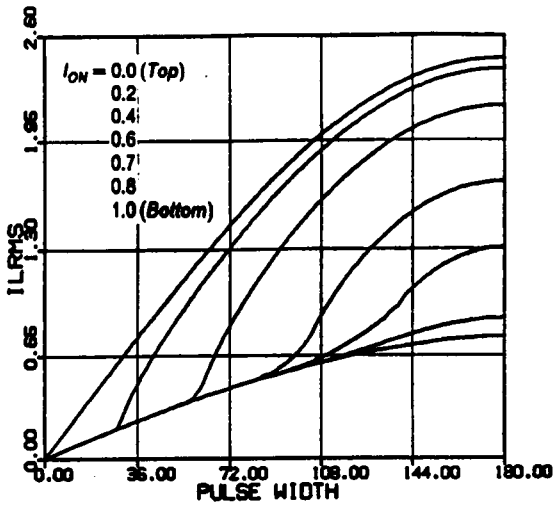


(c) $\omega_{SN} = 1.3$

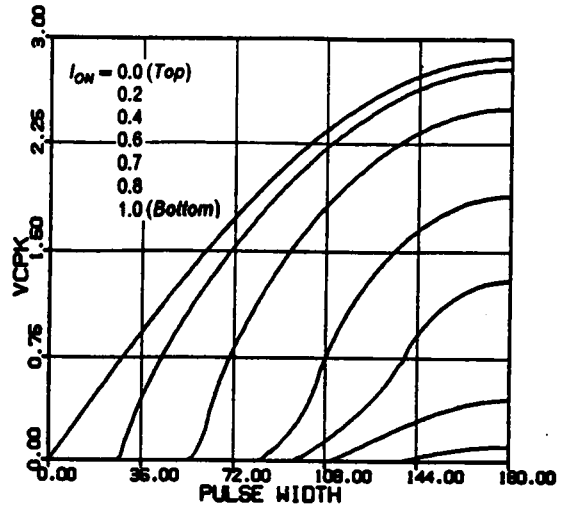


(d) $\omega_{SN} = 1.4$

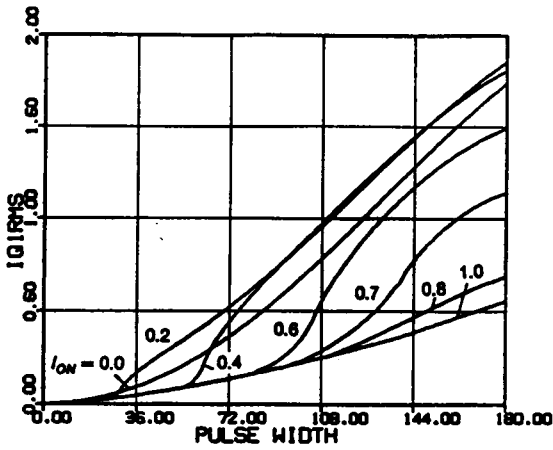
Figure 3.14 Continued



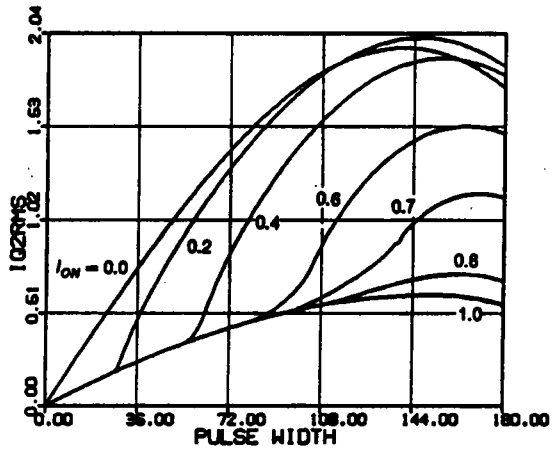
(a) RMS inductor current



(b) Peak capacitor voltage

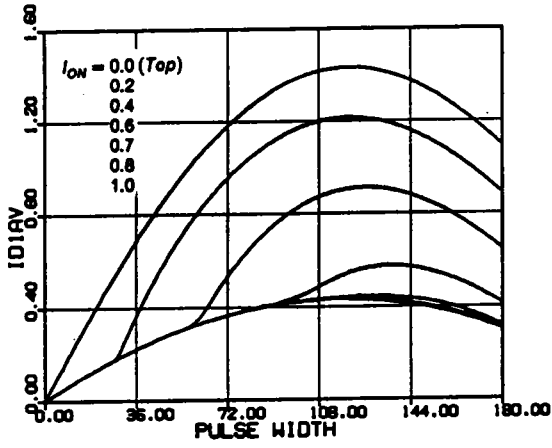


(c) RMS switch current ($Q1, Q3$)

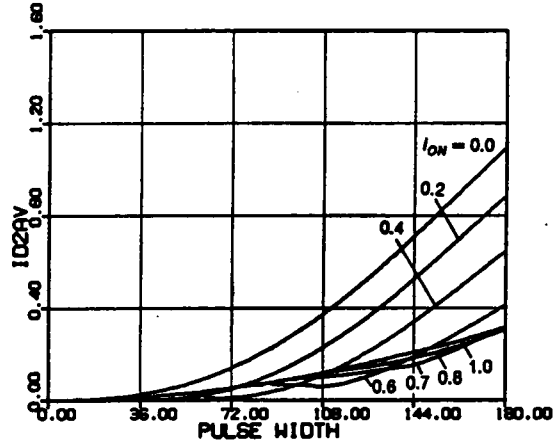


(d) RMS switch current ($Q2, Q4$)

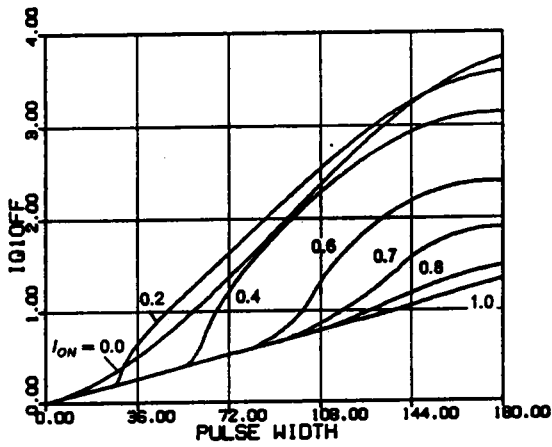
Figure 3.15 Characteristics for Various Circuit Salient Features at $\omega_{SN} = 1.2$



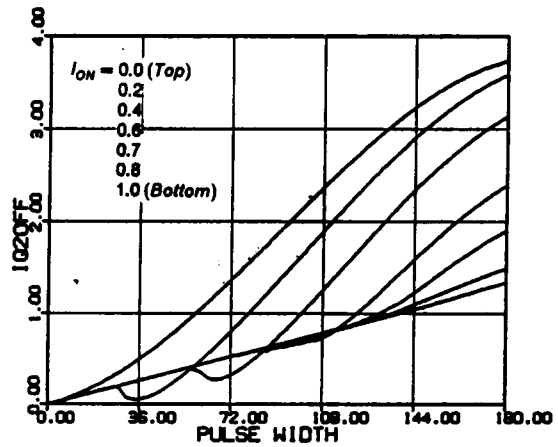
(e) Average diode current (D1,D3)



(f) Average diode current (D2,D4)



(g) Switch turn-off current (Q1,Q3)



(h) Switch turn-off current (Q2,Q4)

Figure 3.15 Continued

3.4 DESIGN EXAMPLES

The dc characteristics derived in the previous section are employed to facilitate design of a CM-PRC in this section. Three design examples are given. The first example designs the converter to operate in a natural commutation region ($\omega_{SN} < 1$) such that all the transistors' turn-off losses are eliminated. The second example designs the converter to operate in a mixed-commutation region ($\omega_{SN} < 1$) such that the turn-on losses of Q1, Q3 and the turn-off losses of Q2, Q4 are eliminated. Lossless snubbers can be used across Q1 and Q3 to reduce their turn-off losses. The third example designs the converter to operate in a force-commutation region ($\omega_{SN} > 1$) such that all the transistors' turn-on losses are eliminated. Lossless snubbers can be used across all the transistors to reduce their turn-off losses.

The converter is designed to satisfy the following requirements.

$$\text{Input voltage} = 40\text{V} \sim 60\text{V}.$$

$$\text{Output voltage} = 5\text{V}.$$

$$\text{Output power} = 40\text{W} \sim 50\text{W}.$$

Assume an output transformer with turn ratio $n:1$ is used between the resonant tank and the load circuit. Then,

$$V_{ONmax} = \frac{5n}{40}, \quad V_{ONmin} = \frac{5n}{60},$$
$$I_{ONmax} = \frac{10}{n \times 40/Z_0}, \quad I_{ONmin} = \frac{8}{n \times 60/Z_0}.$$

(The load current range is from 8A to 10A.)

3.4.1 Example 1 - Design in Natural-Commutation Region

To achieve natural commutation of all the transistors, an operating frequency below the resonant frequency must be chosen. Choose $\omega_{SN} = 0.8$.

Case I. From Figure 3.16, to obtain maximum achievable load current magnitude, choose

$$V_{ONmin} = \frac{5 \times n}{60} = 1.7.$$

The transformer turn ratio n can then be calculated as

$$n = \frac{60 \times 1.7}{5} = 21,$$

and the maximum V_{ON} is

$$V_{ONmax} = \frac{5 \times 21}{40} = 2.62.$$

From Figure 3.16, this voltage level can not be achieved. Thus, the design is impossible.

Case II. From Figure 3.16, to ensure output regulation for the entire input voltage range, choose

$$V_{ONmax} = \frac{5 \times n}{40} = 2.13.$$

The transformer turn ratio n is calculated as

$$n = \frac{40 \times 2.13}{5} = 17,$$

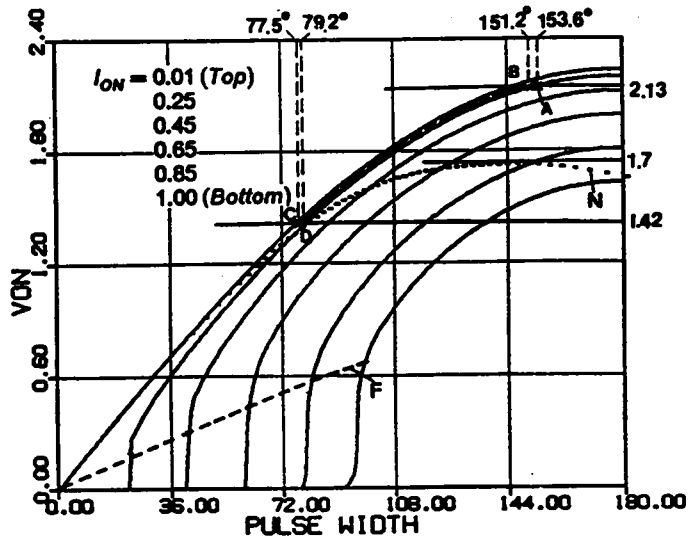


Figure 3.16 Design Example in Natural Commutation Region

and the minimum V_{ON} is

$$V_{ONmin} = \frac{5 \times 17}{60} = 1.42.$$

From Figure 3.16, it can be seen that the load current at V_{ONmin} can not exceed 0.26 if natural commutation is to be maintained. To ensure this, choose

$$I_{ONmax} = \frac{10}{n \times 40/Z_0} = 0.25.$$

The characteristic impedance is calculated as

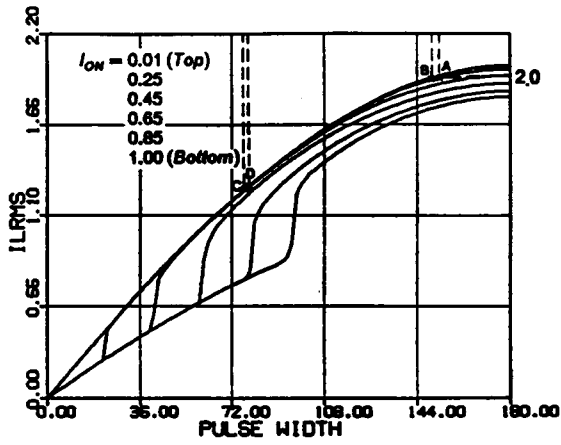
$$Z_0 = I_{ONmax} \times n \times 40 \times \frac{1}{10} = 17\Omega.$$

The normalized load range at V_{ONmax} is from $8/(n \times 40/Z_0) = 0.2$ to $I_{ONmax} = 0.25$, which are indicated by points **B** and **A** in Figure 3.16, respectively. The normalized load range at V_{ONmin} is from $8/(n \times 60/Z_0) = 0.13$ to $10/(n \times 60/Z_0) = 0.17$, which are indicated by points **C** and **D** in Figure 3.16, respectively.

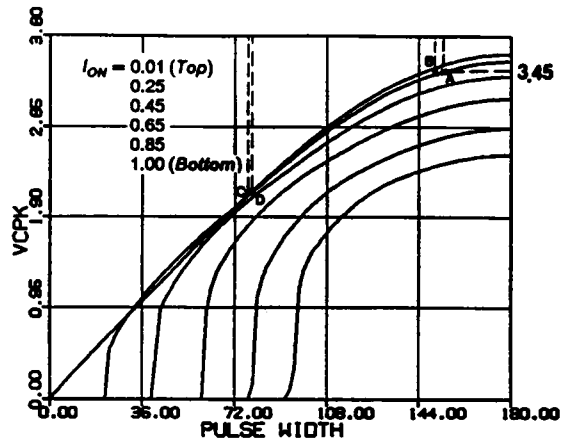
The normalization factor for the current, $I_{P.U.}$, is equal to $40/Z_0 = 2.35A$ at V_{ONmax} (points **A,B**) and equal to $60/Z_0 = 3.53A$ at V_{ONmin} (points **D**).

The four boundary points, **A,B,C,D**, define the operating region for the converter in this design, which is indicated by the shaded area in Figure 3.16. The β_S angles corresponding to these points are **A**: 153.6° , **B**: 151.2° , **C**: 77.5° , **D**: 79.2° . By mapping these boundary points (using their corresponding β_{ON} and I_{ON}) into other characteristics as illustrated in Figure 3.17, various important circuit features can be obtained. The circuit's salient feature usually occurs at one of the four boundary points.

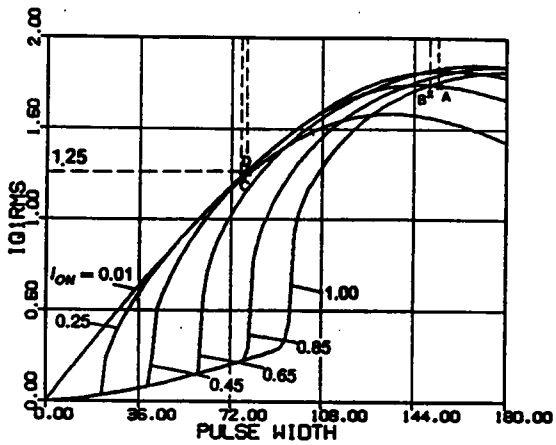
The following salient features are obtained for this design,



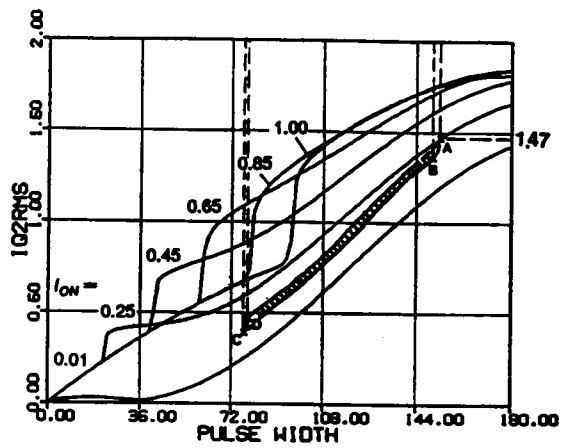
(a) RMS inductor current



(b) Peak capacitor voltage

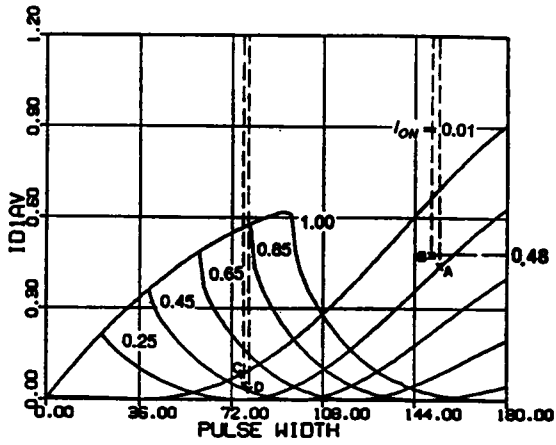


(c) RMS switch current ($Q1, Q3$)

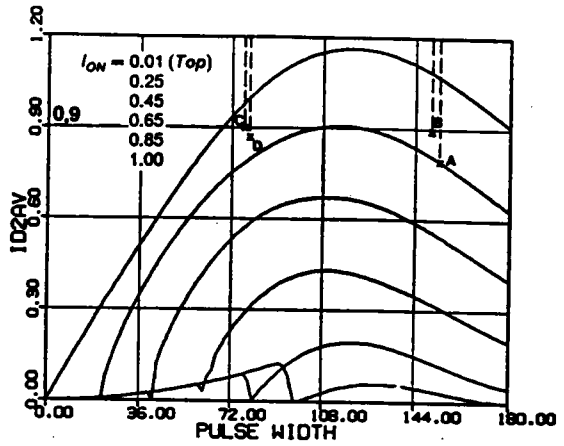


(d) RMS switch current ($Q2, Q4$)

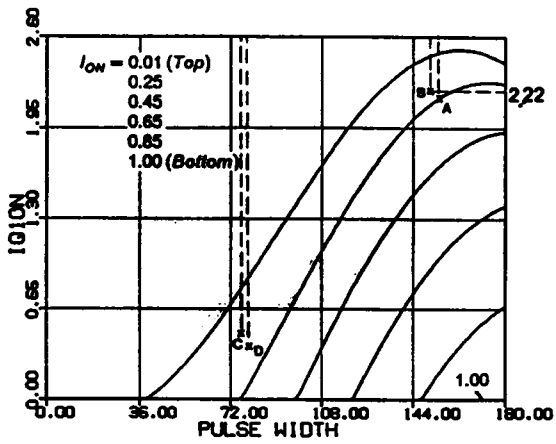
Figure 3.17 Circuit Salient Features for the Design in Figure 3.16



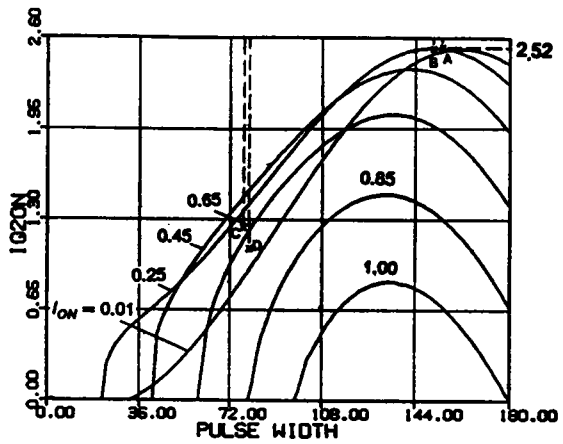
(e) Average diode current (D1,D3)



(f) Average diode current (D2,D4)



(g) Switch turn-on current (Q1,Q3)



(h) Switch turn-on current (Q2,Q4)

Figure 3.17 Continued

$$\begin{aligned}
V_{CPKmax} &= 138.V, & I_{LRMSmax} &= 4.7A, \\
I_{Q1RMSmax} &= 4.4A, & I_{Q2RMSmax} &= 3.45A, \\
I_{D1AVmax} &= 1.13A, & I_{D2AVmax} &= 3.18A, \\
I_{Q1offmax} &= 0.A, & I_{Q2offmax} &= 0.A, \\
I_{Q1onmax} &= 5.23A, & I_{Q2onmax} &= 6.39A .
\end{aligned}$$

3.4.2 Example 2 - Design in Mixed-Commutation Region

To achieve zero-voltage turn-on (force commutation) of Q1,Q3 and zero-current turn-off (natural commutation) of Q2,Q4, the operating frequency should be chosen below the resonant frequency. Choose $\omega_{SN} = 0.8$. From Figure 3.18, to ensure Q1 and Q3 are force-commutated, choose

$$V_{ONmax} = \frac{5 \times n}{40} = 1.5.$$

The transformer turn ratio n is calculated as

$$n = \frac{40 \times 1.5}{5} = 12.$$

The minimum V_{ON} is

$$V_{ONmin} = \frac{5 \times 12}{60} = 1.0.$$

To obtain a high characteristic impedance, I_{ON} should be chosen as high as possible.

Choose

$$I_{ONmax} = \frac{10}{n \times 40/Z_0} = 1.0.$$

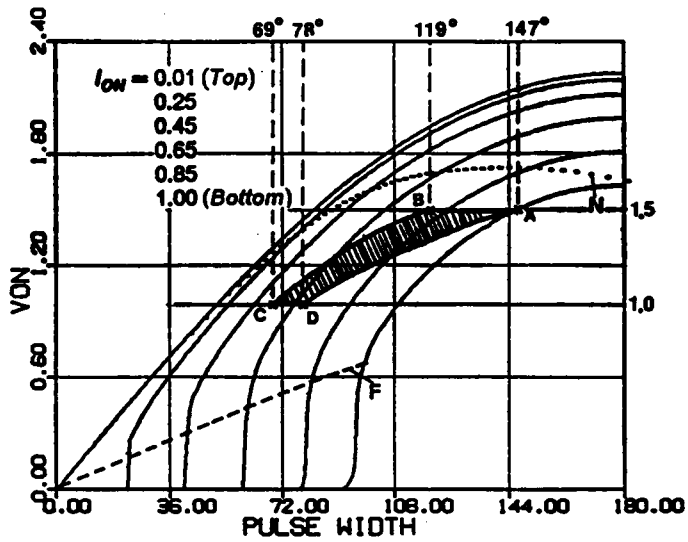


Figure 3.18 Design Example in Mixed-Commutation Region

The characteristic impedance is calculated as

$$Z_0 = I_{ONmax} \times n \times 40 \times \frac{1}{10} = 48\Omega.$$

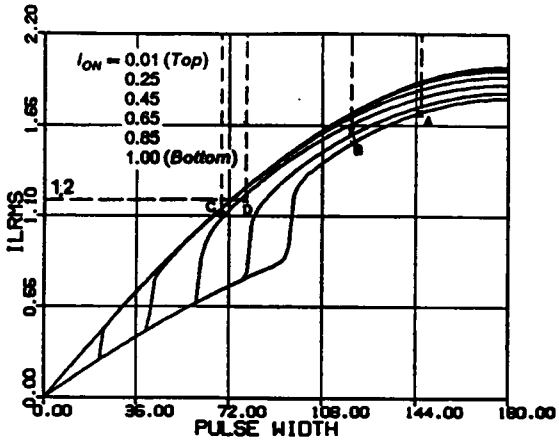
The normalized load range at V_{ONmax} is from $8/(n \times 40/Z_0) = 0.8$ to $I_{ONmax} = 1.0$, which are indicated by points **B** and **A** in Figure 3.18, respectively. The normalized load range at V_{ONmin} is from $8/(n \times 60/Z_0) = 0.53$ to $10/(n \times 60/Z_0) = 0.67$, which are indicated by points **C** and **D** in Figure 3.18, respectively.

The normalization factor for current, $I_{P.U.}$, is equal to $40/Z_0 = 0.833A$ at V_{ONmax} (points **A,B**) and equal to $60/Z_0 = 1.25A$ at V_{ONmin} (points **C,D**).

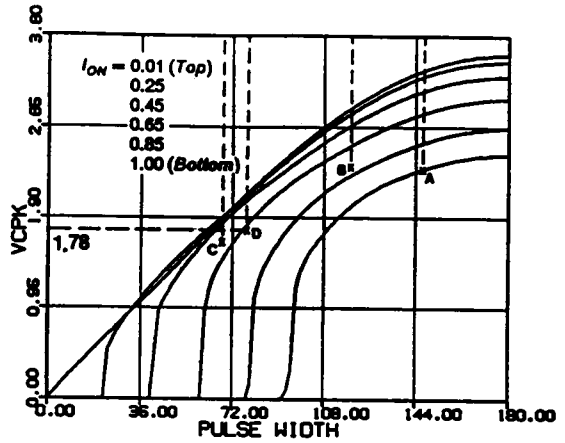
The four boundary points, **A,B,C,D**, define the operating region for the converter in this design, which is indicated by the shaded area in Figure 3.18. The β_S angles corresponding to these points are **A**: 147° , **B**: 119° , **C**: 69° , **D**: 78° . By mapping these boundary points (using their corresponding β_{ON} and I_{ON}) into other characteristics as illustrated in Figure 3.19, various important circuit features are obtained and shown in the following:

$$\begin{array}{ll} V_{CPKmax} = 107.V, & I_{LRMSmax} = 1.5A, \\ I_{Q1RMSmax} = 1.44A, & I_{Q2RMSmax} = 1.43A, \\ I_{D1AVmax} = 0.25A, & I_{D2AVmax} = 0.5A, \\ I_{Q1offmax} = 1.92A & I_{Q2offmax} = 0.A, \\ I_{Q1onmax} = 0.A, & I_{Q2onmax} = 1.4A. \end{array}$$

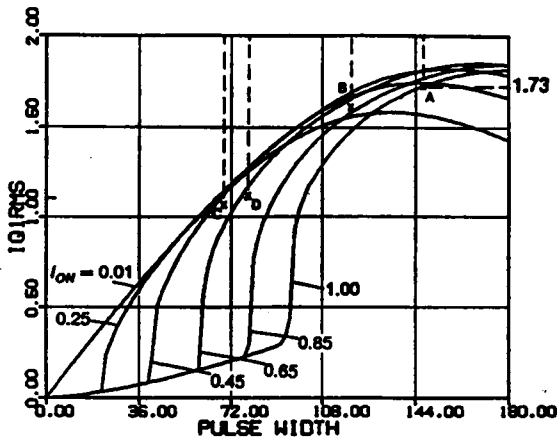
3.4.3 Example 3 - Design in Force-Commutation Region



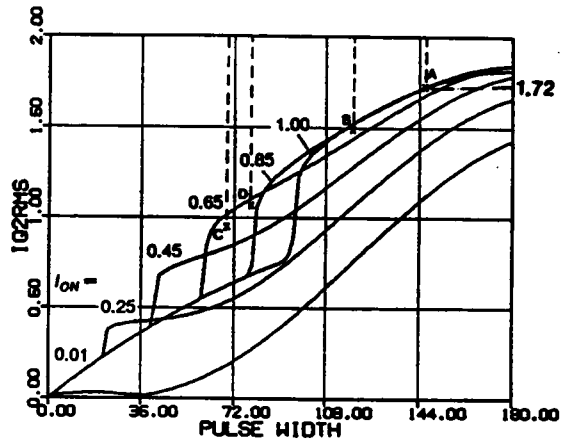
(a) RMS inductor current



(b) Peak capacitor voltage

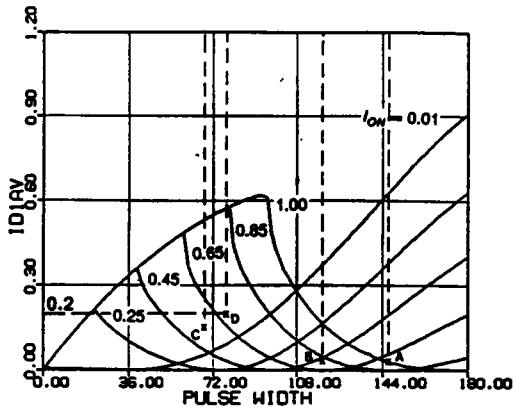


(c) RMS switch current ($Q1, Q3$)

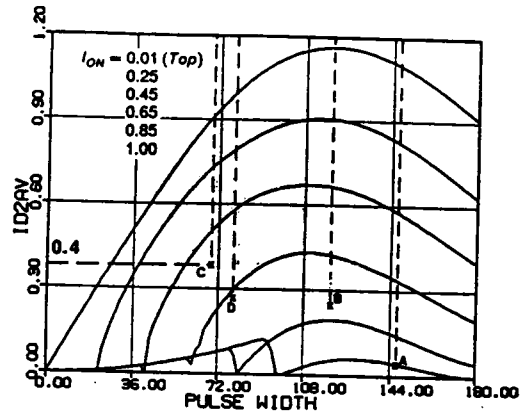


(d) RMS switch current ($Q2, Q4$)

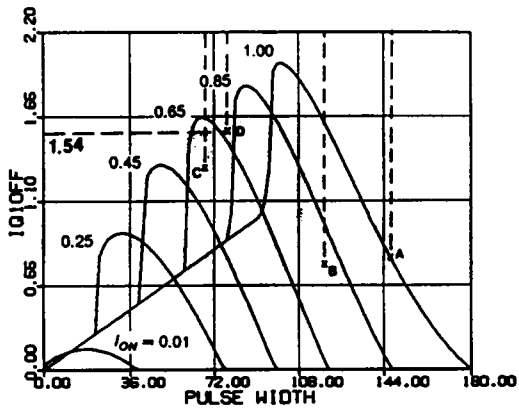
Figure 3.19 Circuit Salient Features for the Design in Figure 3.18



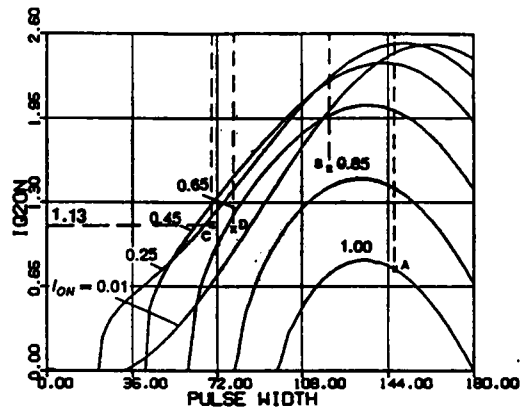
(e) Average diode current (D1,D3)



(f) Average diode current (D2,D4)



(g) Switch turn-off current (Q1,Q3)



(h) Switch turn-on current (Q2,Q4)

Figure 3.19 Continued

To achieve zero-voltage turn-on (force commutation) of all the transistors, the operating frequency must be chosen above the resonant frequency. Choose $\omega_{SN} = 1.2$. From Figure 3.20, to ensure force commutation of all the transistors (avoiding the mixed-commutation region), choose

$$V_{ONmin} = \frac{5 \times n}{60} = 0.4.$$

The transformer turn ratio n is calculated as

$$n = \frac{60 \times 0.4}{5} = 4.8.$$

The maximum V_{ON} is

$$V_{ONmax} = \frac{5 \times 4.8}{40} = 0.6.$$

From Figure 3.20, I_{ONmax} must not exceed 0.72. Choose

$$I_{ONmax} = \frac{10}{n \times 40/Z_0} = 0.7.$$

The characteristic impedance is calculated as

$$Z_0 = I_{ONmax} \times n \times 40 \times \frac{1}{10} = 13.44\Omega.$$

The normalized load range at V_{ONmax} is from $8/(n \times 40/Z_0) = 0.56$ to $I_{ONmax} = 0.7$, which are indicated by points B and A in Figure 3.20, respectively. The normalized load range at V_{ONmin} is from $8/(n \times 60/Z_0) = 0.37$ to $10/(n \times 60/Z_0) = 0.47$, which are indicated by points C and D in Figure 3.20, respectively.

The normalization factor for current, $I_{p.u.}$, is equal to $40/Z_0 = 2.98A$ at V_{ONmax} (points A,B) and equal to $60/Z_0 = 4.46A$ at V_{ONmin} (points C,D).

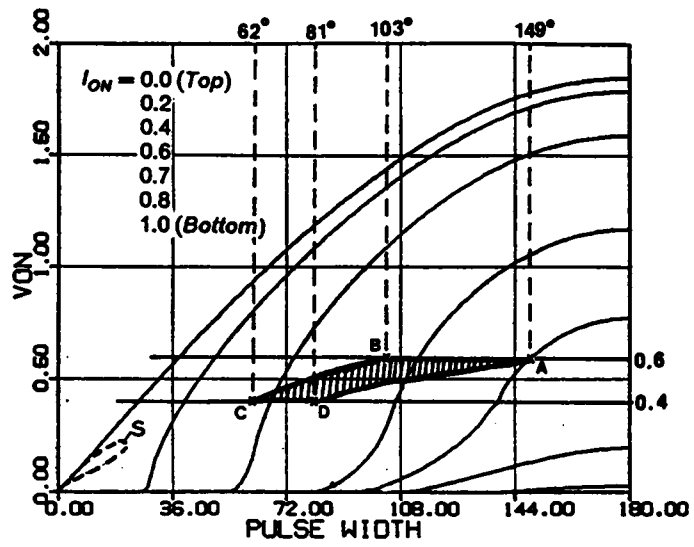
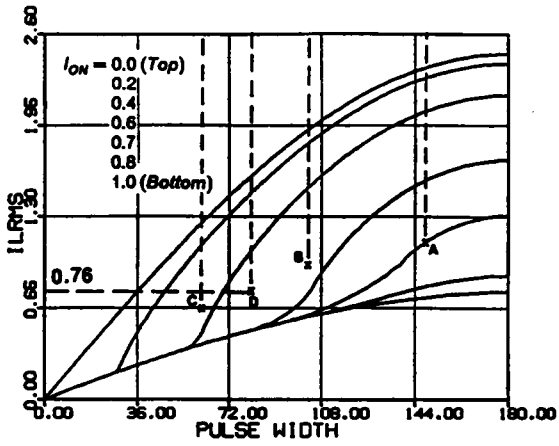
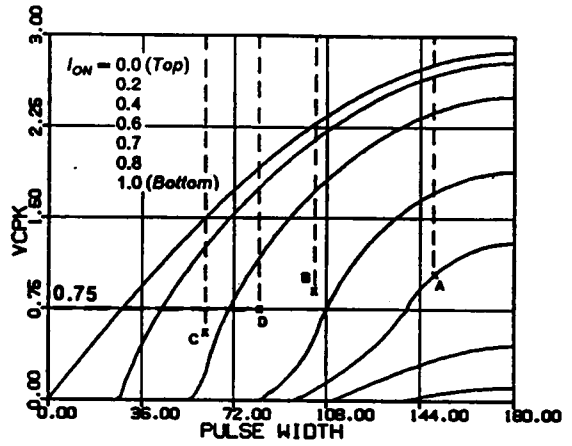


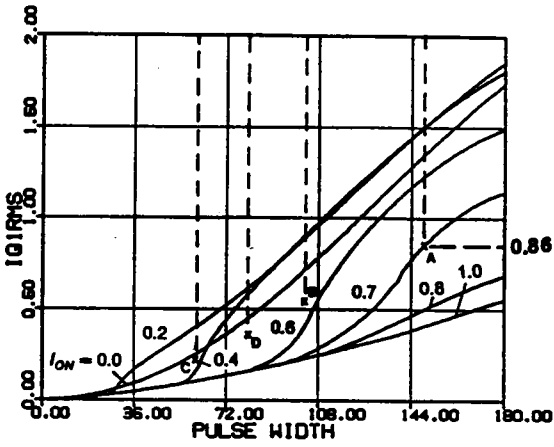
Figure 3.20 Design Example in Force-Commutation Region



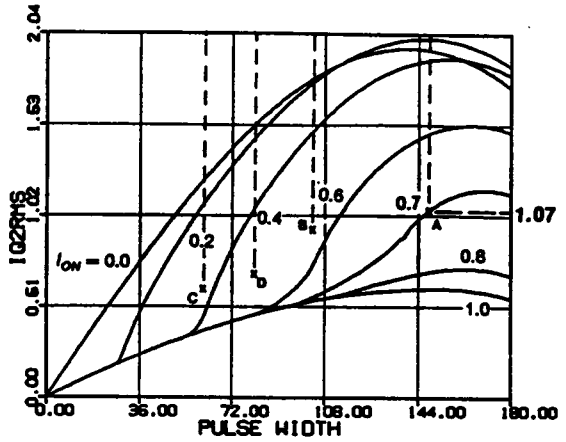
(a) RMS inductor current



(b) Peak capacitor voltage

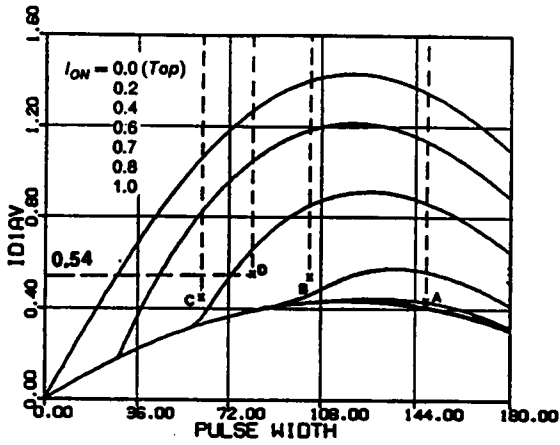


(c) RMS switch current ($Q1, Q3$)

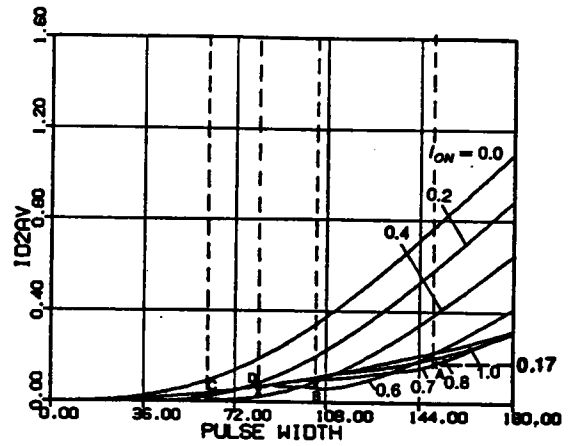


(d) RMS switch current ($Q2, Q4$)

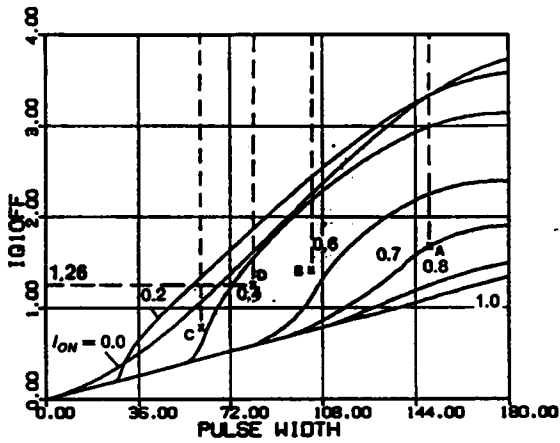
Figure 3.21 Circuit Salient Features for the Design in Figure 3.20



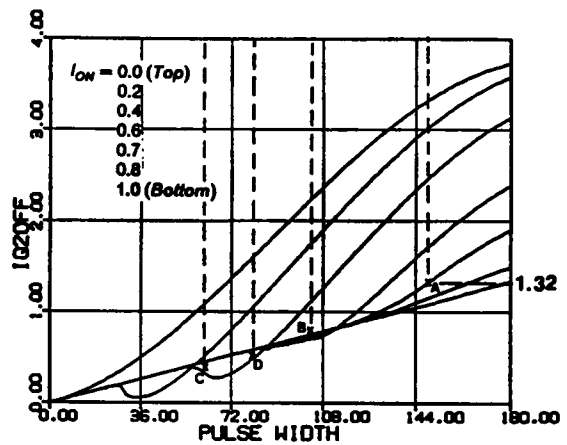
(e) Average diode current (D1,D3)



(f) Average diode current (D2,D4)



(g) Switch turn-off current (Q1,Q3)



(h) Switch turn-off current (Q2,Q4)

Figure 3.21 Continued

The four boundary points, **A,B,C,D**, define the operating region for the converter in this design, which is indicated by the shaded area in Figure 3.20. The β_S angles corresponding to these points are **A: 149°, B: 103°, C: 62°, D: 81°**. By mapping these boundary points (using their corresponding β_{ON} and I_{ON}) into other characteristics as illustrated in Figure 3.21, various important circuit features are obtained and shown in the following:

$$\begin{array}{ll}
 V_{CPKmax} = 45.V & I_{LRMSmax} = 3.37A, \\
 I_{Q1RMSmax} = 2.35A, & I_{Q2RMSmax} = 3.2A, \\
 I_{D1AVmax} = 2.4A, & I_{D2AVmax} = 0.51A, \\
 I_{Q1offmax} = 5.61A & I_{Q2offmax} = 3.94A, \\
 I_{Q1onmax} = 0.A, & I_{Q2onmax} = 0.A.
 \end{array}$$

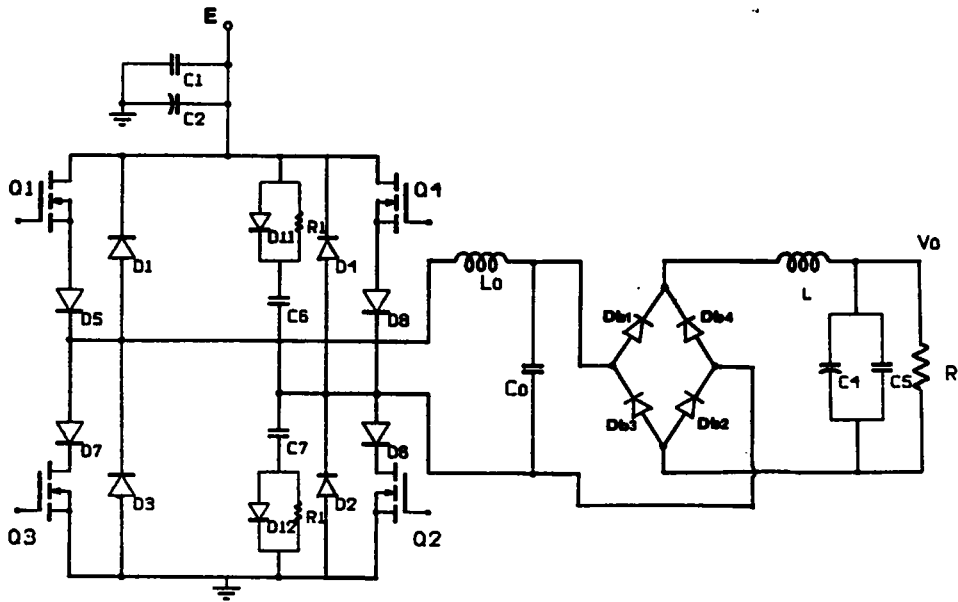
From the above examples, it can be seen that higher component ratings are usually required when a CM-PRC is to be designed either in the natural- or in the force commutation region.

3.5 HARDWARE EXPERIMENTS

A prototype circuit, as shown in Figure 3.22, was built to verify the circuit operation of a CM-PRC. The circuit was designed at 105.4kHz with a resonant frequency of 145kHz ($\omega_{SN} = 0.72$).

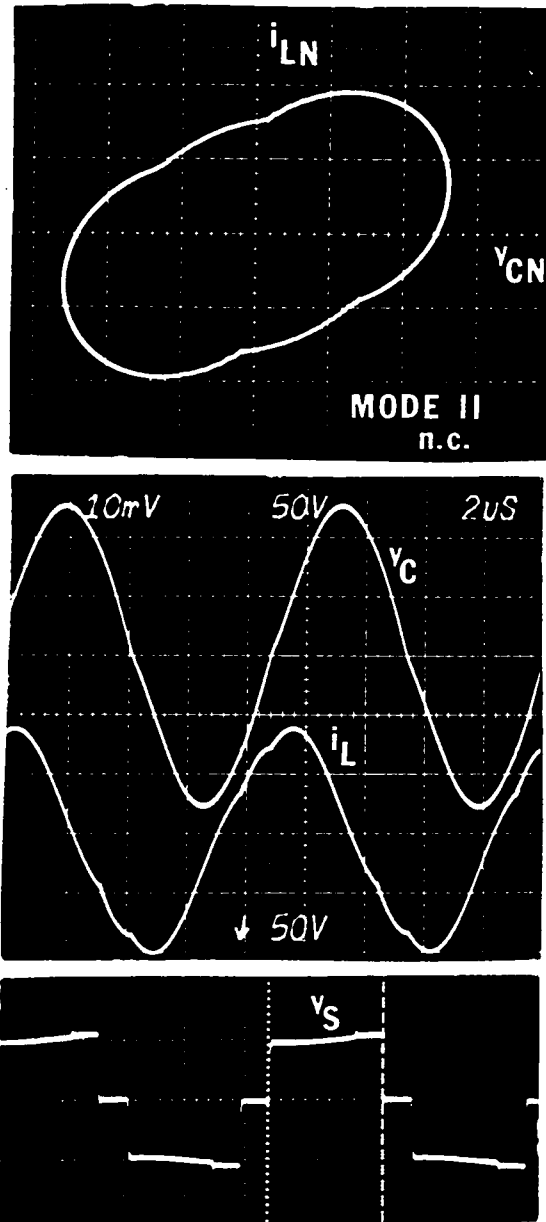
Figure 3.23 shows the experimental results. All the predicted operating modes below resonant frequency have been illustrated except Mode V operation. (Mode V operation does not exist under steady state.) The state trajectories are obtained by externally calibrating the inductor current so that the ratio of the y-axis scale to the x-axis scale is the same as the ratio of i_{LN} to v_{CN} .

Figure 3.23(g) shows a trajectory close to Mode V operation. This trajectory is obtained by shorting the output resistor ($R = 0. \Omega$). Slight asymmetry in the trajectories exists due to the imbalance in the gating signals.



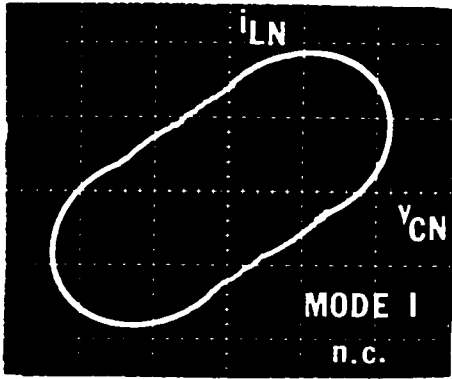
Q1,Q2,Q3,Q4: IRF450; D1,D2,D3,D4,Db1,Db2,Db3,Db4: UES1403;
D11,D12,D5,D6,D7,D8: IR31DQ06; C2 = 40 μ F, C1,C5 = 0.01 μ F;
C4 = 10 μ F, C6,C7 = 1000pF, R1 = 150 Ω , L = 15.6mH;
L0 = 55.32 μ H, C = 21.87nF, E = 50V.

Figure 3.22 A Breadboard Circuit Used to Verify Circuit Operations Below Resonant Frequency

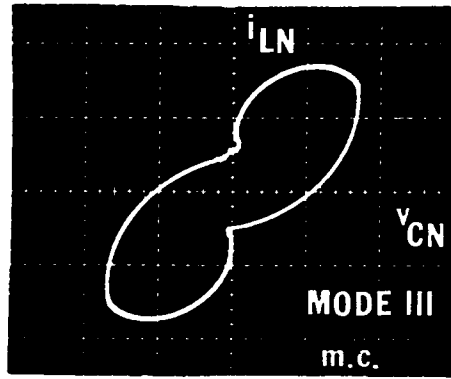


(a) Mode-II_N operation

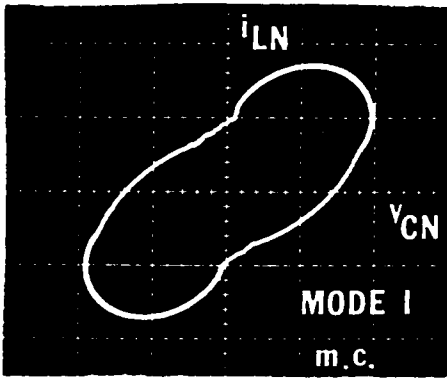
Figure 3.23 Experimental Results from the Circuit in Figure 3.22



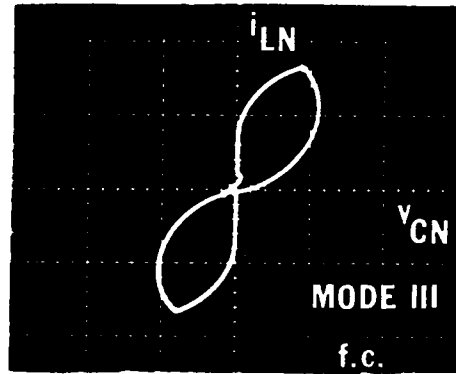
(b) Mode- I_N operation



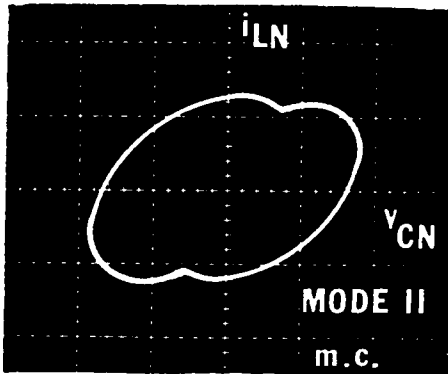
(e) Mode- III_M operation



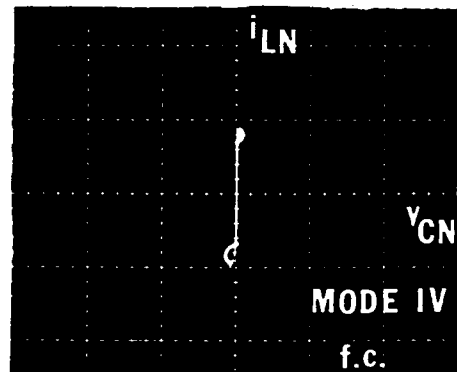
(c) Mode- I_M operation



(f) Mode- III_F operation



(d) Mode- II_M operation



(g) Mode- IV_F operation

Figure 3.23 Continued

3.6 CONCLUSIONS

A complete analysis of the constant-frequency, clamped-mode, parallel-resonant converter has been performed in this chapter. Employing state-plane analysis techniques, all the circuit operating modes are identified for the frequency range above 50% of the resonant frequency. The operating modes are categorized into six different circuit topological mode sequences, each representing a unique device conduction sequence.

Three different commutation modes for the transistors exist: natural commutation, mixed commutation, and force commutation. To predict the converter's mode of operation and determine the transistors' commutation conditions, an algorithm is developed to define the regions of operation.

Unlike the CM-SRC, a CM-PRC can be designed to operate in the natural or the force commutation region from no load to full load. Design in natural commutation region, however, is difficult when the output-to-input voltage ratio varies over a wide range since the natural commutation region is very limited, especially at frequencies below 80% of the resonant frequency. High circulating current usually exists in the converter since a small characteristic impedance must be used.

The converter can be easily designed in the force-commutation region for a wide range of input voltage and output current since a very large force commutation region exists for the converter when the operating frequency is above the resonant frequency.

The converter can also be designed in the mixed-commutation region at frequencies below the resonant frequency. A minimum load current, however, has to be maintained.

Three design examples are given. The examples illustrate how to employ the dc characteristics to design a CM-PRC in different commutation regions. The results show that higher component ratings are usually required to design the converter in either the natural or the force commutation region.

Finally, a 105kHz prototype circuit is breadboarded to verify the operation of a CM-PRC. All the predicted operating modes below resonant frequency are experimentally substantiated.

CHAPTER 4.

CONCLUSIONS

The distinct advantages of resonant converters, such as zero-current turn-off, zero-voltage turn-on, low EMI, and fast responses, have attracted much attention in power electronics industry. Numerous efforts have been made to extend the soft switching resonant techniques into other types of converters such that the performances of these converters can be improved. For example, recently a new family of quasi-resonant converters and multi-resonant converters were developed which can be operated above one megahertz and can achieve very high power density [47-56]. These converters are obtained by properly adding LC resonant components into conventional PWM converters such that zero-current and/or zero-voltage switching features can be obtained. These converters are, however, controlled via frequency modulation, as in the conventional resonant converters.

Variable-frequency operation often results in poor utilization of magnetic components and capacitor filters since these components has to be designed according to the lowest operating frequency. The bandwidth of the control loop is also limited by the lowest operating frequency. Variable-frequency operation can also results in undesirable low beat frequencies which are difficult to filter.

In view of this, efforts have been made to search for circuit topologies and control techniques which enable resonant converters to operate at a constant frequency.

Recently, two fixed frequency clamped-mode resonant (series and parallel) converters were proposed which show very promising features, such as simple control (similar to PWM), no load to full load operation, low circulating current under light load, and zero-current or zero-voltage switching.

In the dissertation, the behaviors of both the clamped-mode series-resonant converter and the clamped-mode parallel-resonant converter were completely characterized to provide insights to the complex circuit operations and to derive design guidelines. State-plane analysis techniques were employed to identify for the first time various circuit operating modes and to define mode boundaries and operating regions. Based on the state plane analysis, important dc characteristics, such as control-to-output transfer ratio, inductor rms current, peak capacitor voltage, switch rms currents, average diode currents, turn-on current and turn-off current of the switches were derived to facilitate design of the converters.

Three different regions, natural commutation region, forced commutation region, and mixed mode of natural and forced commutation region, exist for both the CM-SRC and the CM-PRC. In the natural commutation region, all the controlled switches turn off at zero current. Fast antiparallel diodes are required for all the switches. In the mixed commutation region, two of the switches turn off at zero current while the other two turn on at zero voltage. Fast antiparallel diodes are required for the two switches which are naturally commutated, while slow antiparallel diodes and simple lossless capacitor snubbers can be used for the other two switches which are turned on at zero voltage. In the force commutation region, all the switches turn on at zero voltage. In this case, slow antiparallel diodes and simple lossless capacitor snubbers can be used for all the switches. To optimize the design and the utilization of available components, it is sug-

gested that the converter be designed to operate strictly within a specific commutation region, although it is not necessary.

For a CM-SRC, design in both natural and force commutation requires a minimum load to be maintained. To achieve output regulation from no load to full load, the converter has to be designed in the mixed commutation region.

For a CM-PRC, design in the mixed-commutation mode requires a minimum load. The converter can be designed to regulate the output from no load to full load in both the natural and force commutation regions. However, design in the natural commutation region is not practical since the region for natural commutation is very limited.

In applications where MOSFETS are used as switching devices, it is most desirable to design the converters in the force commutation regions where all the switches are turned on at zero voltage. The slow recovery internal diodes can be used and the output capacitors of the MOSFETS can be utilized as the lossless snubbers. The CM-PRC operating above resonant frequency is found to be most attractive since zero-voltage turn-on can be implemented for all the switches in an operation from no load to full load.

The clamped-mode SRC and PRC are emerging as the mainstay in high performance and high power conversion applications. The clamped-mode concept can be further extended to applications in dc-ac power inversions, where a high frequency ac output or an ac distributed bus is required.

REFERENCES

1. N. Marpham, "An SCR Inverter with Good Regulation and Sinewave Output", IEEE Transactions on Industrial and General Applications, IGA-3, No.2, Mar/Apr 1967, pp. 176~187.
2. V.T. Ranganathan, P.D. Ziogas, and V.R. Stefanovic, "A Regulated DC-DC Voltage Source Converter Using a High-Frequency Link", IEEE Transactions on Industrial Applications, Vol. IA-18, No.3, pp. 279~287, May/June 1982.
3. R.L. Steigerwald, "High-Frequency Resonant Transistor DC-DC Converters", IEEE Transactions on Industrial Electronics, Vol. IE-31, No.2, pp. 181~191, May 1984.
4. F.C. Schwarz, "A Method of Resonant Current Pulse Modulation for Power Converters", IEEE Transactions of Industrial Electronics and Control Instrumentation, IECI-17, No.3, May 1970, pp. 209~221.
5. F.C. Schwarz, "An Improved Method of Resonant Current Pulse Modulation for Power Converters", IEEE Power Electronics Specialists Conference, Record, 1975, pp. 194~204.
6. J.G. Kassakian, "A new Current Mode Sine Wave Inverter", IEEE Transactions on Industrial Applications, IA-18, No.3, May/June 1982, pp. 273~278.
7. J.G. Kassakian, A.F. Goldberg, and D.R. Moretti, "A Comparative Evaluation of Series and Parallel Structure for High Frequency Transistor Inverters", IEEE Power Electronics Specialists Conference, Record, 1982, pp. 20~26. pp. 273~278.
8. J.B. Klassens, "DC to AC Series Resonant Converter System with High Internal Frequency Generating Synthesized Waveforms for Multikilowatt Power Levels", IEEE Power Electronics Specialists Conference, Record. 1984, pp. 99~110.

9. S. Muroyama and K. Sakakibara, "Characteristics of a New Series Resonant Converter", IEEE INTELEC Conference Record, 1982, pp. 111~116.
10. R.J. King and T.A. Stuart, "A Normalized Model for the Half-Bridge Series Resonant Converter", IEEE Transactions on Aerospace and Electronics Systems, AES-17, No.2, Mar 1981, pp 190~198.
11. R.J. King and T.A. Stuart, "Modeling the Full Bridge Series Resonant Converter", IEEE Transactions on Aerospace and Electronics Systems, AES-18, No.4, Mar 1982, pp 449~459.
12. V. Vorperian and S. Cuk, "A Complete DC Analysis of the Series Resonant Converter", IEEE Power Electronics Specialists Conference, Record, 1982, pp. 85~100.
13. V. Vorperian and S. Cuk, "Small Signal Analysis of Resonant Converters", IEEE Power Electronics Specialists Conference, Record, 1983, pp. 269~282.
14. A. F. Witulski and R.W. Erickson, "Steady State Analysis of the Series Resonant Converter", IEEE Transactions on Aerospace and Electronic Systems, AES-21, No.6, November 1985.
15. S.D. Johnson and R.W. Erickson, "Steady State Analysis and Design of the Parallel Resonant Converter", IEEE Power Electronics Specialists Conference, Record 1986.
16. R.J. King and T.A. Stuart, "Inherent Overload Protection for the Series Resonant Converters", IEEE Transactions on Aerospace and Electronic Systems, AES-19, No. 6, November 1983, pp. 829~830.
17. R.R. Robson and D.J. Hancock, "A 10KW Series Resonant Converter Design, Transistor Characterization, and Base Drive Optimization", IEEE Power Electronics Specialists Conference, Record, 1982, pp. 33~44.
18. R. Oruganti and F.C. Lee, "Resonant Power Processors: Part I - State Plane Analysis", IEEE IAS Annual Meeting, Conference Record, 1984, pp. 860~867.
19. R. Oruganti and F.C. Lee, "Resonant Power Processors: Part II - Methods of Control", IEEE IAS Annual Meeting, Conference Record, 1984, pp. 868~878.
20. V.T. Ranganathan, P.D. Ziogas, and V.R. Stefanovic, "A DC-AC Power Conversion Technique using Twin Resonant High Frequency Links", IEEE Transactions on Industrial Applications, IA-19, No. 3, May/June 1983, pp. 393~400.
21. V. Vorperian, "High-Q Approximations in the Small-Signal Analysis of Resonant Converters", IEEE PESC Record, 1985, pp. 707~715.
22. R.J. King and T.A. Stuart, "A Large Signal Dynamic Simulation for the Series Resonant Converter," IEEE Transactions on Aerospace and Electronic Systems, AES-19, No.6, November 1983, pp. 859~870.

23. R.J. King and T.A. Stuart, "Transformer Induced Instability of the Series Resonant Converter," IEEE Transactions on Aerospace and Electronic Systems, AES-19, No.3, May 1983, pp. 474~482.
24. D.L. Cronin, "2800 Watt Series Inverter DC Power Supply", IEEE PESC Conference Record, 1971, pp. 117~123.
25. J. Biess, L. Inouye, and J.H. Shank, "High Voltage Series Resonant Inverter Ion Engine Screen Supply", IEEE PESC Conference Record, 1974, pp. 97~105.
26. D. Champers, "Designing High Power SCR Resonant Converters for Very High Frequency Operation", Proceedings of Powercon-9, 1982, Session F, Paper 2.
27. R.R. Robson, "Designing a 25 Kilowatt High Frequency Series Resonant DC/DC Converter", Proceedings of Powercon-11, 1984, Session H1, Paper 3.
28. E.E. Buchanan, Jr. and E.J. Miller, "Resonant Switching Power Conversion Technique", IEEE PESC Conference Record, 1975, pp. 183~193.
29. E.J. Miller, "Resonant Switching Power Conversions", IEEE PESC Conference Record, 1976, pp. 206~211.
30. R. Redl, B. Molnar, and N.O. Sokal, "Class-E Resonant Regulated DC/DC Power Converters: Analysis of Operation, and Experimental Results at 1.5MHz", IEEE PESC Conference Record, 1983, pp. 50~60.
31. R. Oruganti and F.C. Lee, "State-Plane Analysis of Parallel Resonant Converters", IEEE PESC Conference Record, 1985, pp. 56~73.
32. K. Karube, T. Nomura, and T. Nakano, "High-Frequency Resonant MOS-FET DC-DC Converter", IEEE PESC Conference Record, 1988, pp. 26~34.
33. V.T. Ranganathan, P.D. Ziogas, V. Stefanovic, "Performance Characteristics of High Frequency Links under Forward and Regenerative Power Flow Conditions", IEEE IAS Annual Meeting, Conference Record, 1983, pp. 831~839.
34. F.S. Tsai, R. Oruganti, and F.C. Lee, "A Novel Control for Bidirectional Power Flow of a Parallel Resonant Converter", IEEE IAS Annual Meeting, Conference Record, 1985, pp. 1124~1129.
35. I.J. Pitel, "Phase-Modulated, Resonant Power Conversion Techniques for High Frequency Link Inverters", IEEE IAS Annual Meeting, Conference Record, 1985, pp. 1163~1172.
36. F.S. Tsai and F.C. Lee, "Constant-Frequency, Phase-Controlled Resonant Power Processor", IEEE IAS Annual Meeting, Conference Record, 1986, pp. 617~622.
37. F.S. Tsai, "Constant-Frequency Resonant Power Processors", MS Thesis, Electrical Engineering Department, Virginia Polytechnic Institute & State University, June, 1985.

38. O.D. Patterson, D.M. Divan, "Pseudo-Resonant Full Bridge DC-DC Converter", IEEE PESC Conference Record, 1987, pp. 424~430.
39. K. Harada and W. Gu, "Controlled Resonant -Converters with Switching Frequency Fixed", IEEE PESC Conference Record, 1987, pp. 431~438.
40. K.D.T. Ngo, "Analysis of a Series Resonant Converter Pulse-Width-Modulated or Current Controlled for Low Switching Losses", IEEE PESC Conference Record, 1987, pp. 527~536.
41. S.G. Trabert and R.W. Erickson, "Steady State Analysis of the Duty-Cycle Controlled Series Resonant Converter", IEEE PESC Conference Record, 1987, pp. 545~556.
42. F.S. Tsai, P. Materu, and F.C. Lee, "Constant-Frequency, Clamped-Mode Resonant Converters", IEEE PESC Conference Record, 1987, pp. 557~566.
43. F.S. Tsai, Y. Chin, and F.C. Lee, "State-Plane Analysis of Clamped-Mode Parallel Resonant Converter", IEEE INTELEC Conference Record, 1987, pp. 220~227.
44. J. Sabate, "Clamped-Mode Fixed-Frequency Series-Resonant Converter: Off-Line Applications, Analysis, and Implementation", MS Thesis, Electrical Engineering Department, Virginia Polytechnic Institute & State University, November, 1988.
45. K. Kuwabara, J. Chida, and E. Miyachika, "A Constant-Frequency, Series-Resonant DC-DC Converter with PWM Controlled Output", IEEE PESC Conference Record, 1988, pp. 563~566.
46. B. Ray and T.A. Stuart, "A Cascaded Schwarz Converter for High Frequency Power Converter", IEEE PESC Conference Record, 1988, pp. 1199~1206.
47. K.H. Liu and F.C. Lee, "Resonant Switches - A Unified Approach to Improve Performances of Switching Converters", IEEE INTELEC Conference Record, 1984, pp. 344~351.
48. K.H. Liu, R. Oruganti, and F.C. Lee, "Resonant Switches - Topologies and Characteristics", IEEE PESC Conference Record, 1985, pp. 860~867.
49. K.H. Liu and F.C. Lee, "Zero-Voltage Switching Techniques in DC/DC Converters", IEEE PESC Conference Record, 1986, pp. 58~70.
50. R. Oruganti and F.C. Lee, "Effects of Parasitic Losses on the Performance of Series Resonant Converters", IEEE IAS Annual Meeting, Conference Record, 1985, pp. 1233~1243.
51. M.M. Jovanovic, K.H. Liu, and F.C. Lee, "State-Plane Analysis of Quasi-Resonant Converters", IEEE Transactions on Power Electronics, PE-2, No. 5, January 1987.

52. V. Vorperian, R. Tymerski, K.H. Liu, and F.C. Lee, "Generalized Resonant Switches Part 1: Topologies", Proceedings, Power Electronics Seminar, Virginia Power Electronics Center, Virginia Polytechnic Institute & State University, November 1986.
53. V. Vorperian, R. Tymerski, K.H. Liu, and F.C. Lee, "Generalized Resonant Switches Part 2: Analysis and Circuit Models", Proceedings, Power Electronics Seminar, Virginia Power Electronics Center, Virginia Polytechnic Institute & State University, November 1986.
54. W. Tabisz, P. Gradzki, and F.C. Lee, "Zero-Voltage-Switched Quasi-Resonant Buck and Flyback Converters - Experimental Results at 10 MHz", IEEE PESC Conference Record, 1987, pp. 404~413.
55. A.W. Lotfi, V. Vorperian, and F.C. Lee, "Comparison of Stresses in Quasi-Resonant and Pulse-Width-Modulated Converters", IEEE PESC Conference Record, 1988, pp. 591~598.
56. W. Tabisz and F.C. Lee, "Zero-Voltage-Switching Multi-Resonant Technique - A Novel Approach to Improve Performance of High-Frequency Quasi-Resonant Converters", IEEE PESC Conference Record, 1988, pp. 9~17.

APPENDIX A.1

DERIVATION OF CLAMPED-MODE, PARALLEL- RESONANT CONVERTER

Figure A.1 illustrates the combination of the two resonant inverters in a phase-controlled, parallel-resonant converter(PC-PRC). The outputs of the inverters are connected in series. Viewing tank voltages v_1 and v_2 as new voltage sources, a simplified circuit for the PC-PRC is shown in Figure A.1(b). The circuit equations for the PC-PRC are

$$v_1 = v_{C1} + L \frac{di_{L1}}{dt}, \quad (A.1)$$

$$i_{L1} = C \frac{dv_{C1}}{dt} + i_O, \quad (A.2)$$

$$v_2 = v_{C2} + L \frac{di_{L2}}{dt}, \quad (A.3)$$

$$i_{L2} = C \frac{dv_{C2}}{dt} + i_O, \quad (A.4)$$

and

$$v_O = (v_{C1} + v_{C2}). \quad (A.5)$$

By adding Equ. (A.1) to (A.3), and (A.2) and (A.4), we obtain

$$(v_1 + v_2) = (v_{C1} + v_{C2}) + L\left(\frac{di_{L1}}{dt} + \frac{di_{L2}}{dt}\right), \quad (A.6)$$

$$(i_{L1} + i_{L2}) = C\left(\frac{dv_{C1}}{dt} + \frac{dv_{C2}}{dt}\right) + 2i_O. \quad (A.7)$$

Rewriting Eqs. (A.6) and (A.7),

$$(v_1 + v_2) = v_O + (2L) \frac{d}{dt} \left(\frac{i_{L1} + i_{L2}}{2} \right), \quad (A.8)$$

$$\frac{(i_{L1} + i_{L2})}{2} = i_O + \left(\frac{C}{2} \right) \frac{d}{dt} v_O. \quad (A.9)$$

From Eqs. (A.8) and (A.9), viewing v_O and $(i_{L1} + i_{L2})/2$ as new state variables, an equivalent circuit for the PC-PRC can be derived, as shown in Figure A.1(c), where

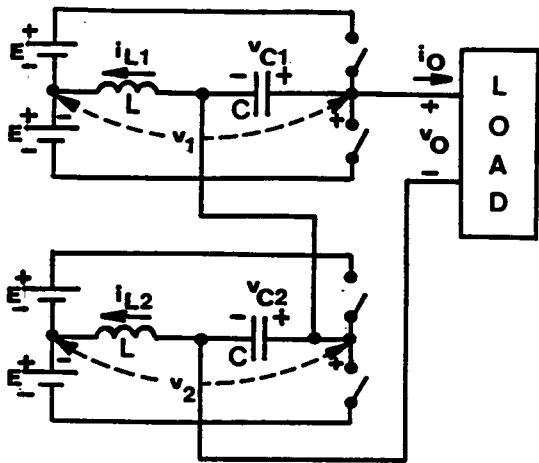
$$v_C = v_O, \quad (A.10)$$

$$i_L = \frac{(i_{L1} + i_{L2})}{2}, \quad (A.11)$$

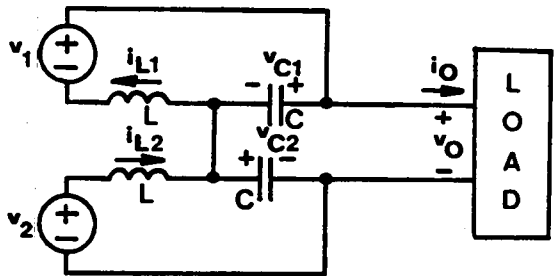
and

$$v_S = v_1 + v_2. \quad (A.12)$$

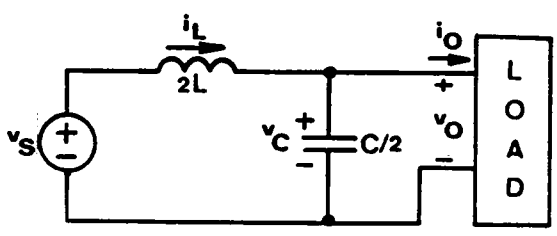
The quasi-square-wave voltage v_S , as shown in Figure A.1(e), can be realized using the full-bridge circuit shown in Figure A.1(d), which is a clamped-mode, parallel-resonant converter(PC-PRC).



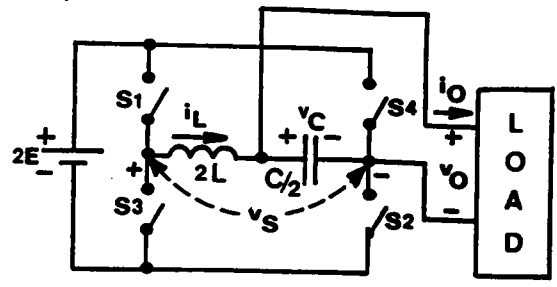
(a) A PC-PRC



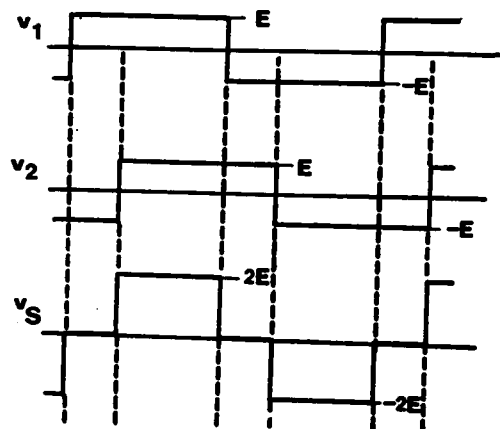
(b) Simplified circuit



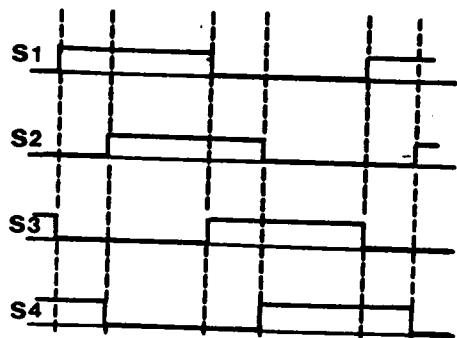
(c) Equivalent circuit



(d) A CM-PRC



(e) Equivalent source voltage



(f) Switch conduction sequence

Figure A.1 Derivation of Clamped-Mode Parallel-Resonant Converter

APPENDIX B.1

RULES FOR CONSTRUCTING EQUILIBRIUM STATE TRAJECTORIES OF A CM-SRC

An equilibrium state trajectory constructed in the composite diagram discussed in Section 2.3.4 must satisfy the following rules. These rules are obtained from the converter's operation.

- On the upper half plane ($i_{L,N} > 0$)
 - Triggering Q1 or forcing Q1 off initiates M6.
 - Triggering Q2 initiates M1.
 - Forcing Q2 off initiates M5.
- On the lower half plane ($i_{L,N} < 0$)
 - Triggering Q3 or forcing Q3 off initiates M3.
 - Triggering Q4 initiates M4.
 - Forcing Q4 off initiates M2.
- On the v_{CN} -axis ($i_{L,N} = 0$)
 - If the previous topological mode is M2,

- ▲ M1 is initiated if $v_{CN} < 1 - V_{ON}$ (trajectory crosses v_{CN} -axis on the left-hand side of m1);
 - ▲ M6 is initiated if $v_{CN} < -V_{ON}$ (trajectory crosses v_{CN} -axis on the left-hand side of m6) and Q1 is forced off the instant of crossing.

- If the previous topological mode is M3,
 - ▲ M6 is initiated if $v_{CN} < -V_{ON}$ (trajectory crosses v_{CN} -axis on the left-hand side of m6);
 - ▲ M1 is initiated if $v_{CN} < 1 - V_{ON}$ (trajectory crosses v_{CN} -axis on the left-hand side of m1) and Q2 is triggered at the instant of crossing;
 - ▲ M5 is initiated if $v_{CN} < -1 - V_{ON}$ (trajectory crosses v_{CN} -axis on the left-hand side of m5) and Q2 is forced off at the instant of crossing;
 - ▲ M0 is initiated if $v_{CN} > -V_{ON}$ (trajectory crosses v_{CN} -axis on the right-hand side of m6). If the crossing point of the trajectory is to the left of m1 ($v_{CN} < 1 - V_{ON}$), M0 will be terminated when Q2 is triggered which initiates M1.

- If the previous topological mode is M4,
 - ▲ M5 is initiated if $v_{CN} < -1 - V_{ON}$ (trajectory crosses v_{CN} -axis on the left-hand side of m5);
 - ▲ M6 is initiated if $v_{CN} < -V_{ON}$ (trajectory crosses v_{CN} -axis on the left-hand side of m6) and Q1 is triggered at the instant of crossing;
 - ▲ M0 is initiated if $v_{CN} > -1 - V_{ON}$ (trajectory crosses v_{CN} -axis on the right-hand side of m5). If the crossing point of the trajectory is to the left of m6 ($v_{CN} < -V_{ON}$), M0 will be terminated when Q1 is triggered which initiates M6.

- If the previous topological mode is M5,
 - ▲ M1 is initiated if $v_{CN} > -1 + V_{ON}$ (trajectory crosses v_{CN} -axis on the right-hand side of m4);
 - ▲ M3 is initiated if $v_{CN} > V_{ON}$ (trajectory crosses v_{CN} -axis on the right-hand side of m3) and Q3 is forced off the instant of crossing.

- If the previous topological mode is M6,
 - ▲ M3 is initiated if $v_{CN} > V_{ON}$ (trajectory crosses v_{CN} -axis on the right-hand side of m3);
 - ▲ M4 is initiated if $v_{CN} > -1 + V_{ON}$ (trajectory crosses v_{CN} -axis on the right-hand side of m4) and Q4 is triggered at the instant of crossing;
 - ▲ M2 is initiated if $v_{CN} > 1 + V_{ON}$ (trajectory crosses v_{CN} -axis on the right-hand side of m2) and Q4 is forced off at the instant of crossing;
 - ▲ M0 is initiated if $v_{CN} < V_{ON}$ (trajectory crosses v_{CN} -axis on the left-hand side of m3). If the crossing point of the trajectory is to the right of m4 ($v_{CN} > -1 + V_{ON}$), M0 will be terminated when Q4 is triggered which initiates M4.

- If the previous topological mode is M1,
 - ▲ M2 is initiated if $v_{CN} > 1 + V_{ON}$ (trajectory crosses v_{CN} -axis on the right-hand side of m2);
 - ▲ M3 is initiated if $v_{CN} > V_{ON}$ (trajectory crosses v_{CN} -axis on the right-hand side of m3) and Q4 is triggered at the instant of crossing;

- ▲ M0 is initiated if $v_{CN} < 1 + V_{ON}$ (trajectory crosses v_{CN} -axis on the left-hand side of m2). If the crossing point of the trajectory is to the right of m3 ($v_{CN} > V_{ON}$), M0 will be terminated when Q4 is triggered which initiates M3.

APPENDIX B.2

PREDICTION OF MODE TRANSITIONS OF A CM-SRC OPERATING BELOW RESONANT FREQUENCY

Consider the boundary trajectories, T_{34} , between Mode III and Mode IV, and T_{35} , between Mode III and Mode V, as shown in Figure B.2.1 and Figure B.2.2, respectively. These two trajectories are constructed via same topological mode sequence and can be represented by the same equations,

$$\begin{aligned}\cos \zeta &= \frac{1 + (1 - R + 2V_{ON})^2 - R^2}{2(1 - R + 2V_{ON})}, \\ \cos \delta &= \frac{1 + R^2 - (1 - R + 2V_{ON})^2}{2R}, \\ \omega_{SN} &= \frac{\pi}{\pi + \delta + \zeta}.\end{aligned}\tag{B.2.1}$$

The parameter R can be used to determine whether a trajectory defined by equations (B.2.1) is a T_{34} , or T_{45} . When $R \leq 1 - 2V_{ON}$, equations (B.2.1) represent a T_{34} . When $R > 1 - 2V_{ON}$, equations (B.2.1) represent a T_{35} .

Such a boundary trajectory can only be constructed with R in between V_{ON} and 1, as illustrated in Figure B.2.3. The frequency, ω_{TN} , of the trajectory is related to R in a way as shown in Figure B.2.4, where

$$\begin{aligned}\omega_{3N} &= \frac{\pi}{\pi + 2\cos^{-1}\left(\frac{1}{1 + 2V_{ON}}\right)}, \\ \omega_{4N} &= \frac{\pi}{\pi + \cos^{-1}V_{ON} + \cos^{-1}(1 - 2V_{ON}^2)}.\end{aligned}\tag{B.2.2}$$

This relationship can be used to determine the transitions of operating modes as follows.

(a). $V_{ON} \leq 0.5$

(a.1) If $\omega_{SN} > \omega_{3N}$, such a boundary trajectory does not exist, implying both mode-IV and mode-V operations do not exist. The converter's operation transits from Mode III directly to Mode VI, as indicated by S3 in Figure 2.10(c).

The boundary β_S angle, β_{36} , separating mode III and Mode VI, can be calculated from trajectory T_{36} , as shown in Figure B.2.5,

$$\beta_{36} = \omega_{SN} \times \delta, \quad \delta = \cos^{-1}(1 - 2V_{ON}^2).$$

(a.2) If $\omega_{SN} = \omega_{3N}$, one such boundary trajectory exists. The converter's operation transits from mode III to the boundary trajectory back to Mode III then to Mode VI, as indicated by S4 in Figure 2.10(c). If the boundary trajectory is viewed as a special case of Mode-III operation, the converter's mode transition sequence is the same as **(a.1)**.

(a.3) If $\omega_{4N} \leq \omega_{SN} < \omega_{3N}$, two such boundary trajectories exist. Equations (B.2.1) have two sets of solutions, (R_1, ζ_1, δ_1) and (R_2, ζ_2, δ_2) .

- **(a.3.1)** If $R_1 \leq 1 - 2V_{ON}$ and $R_2 > 1 - 2V_{ON}$, a boundary trajectory, T_{34} , between Mode III and Mode IV and another boundary trajectory, T_{35} , between Mode III and Mode V exist, implying both Mode-IV and Mode-V operations exist. The converter's operation transits from Mode III to Mode IV to Mode V back to Mode III to Mode VI, as indicated by S5 in Figure 2.10(d).

The boundary β_S angle, β_{34} , between Mode III and Mode IV is equal to $\omega_{SN} \times \delta_1$.

The boundary β_S angle, β_{45} , between Mode IV and Mode V can be calculated from trajectory T_{45} , as shown in Figure B.2.6,

$$\beta_{45} = \omega_{SN} \times \delta, \quad \delta = \cos^{-1}\left(1 - \frac{6V_{ON}^2}{1 - 2V_{ON}}\right).$$

The boundary β_S angle, β_{53} , between Mode V and Mode III is equal to $\omega_{SN} \times \delta_2$.

The boundary β_S angle, β_{36} , between Mode III and Mode VI is calculated as in (a.1).

- (a.3.2) If $R_1 \leq 1 - 2V_{ON}$ and $R_2 \leq 1 - 2V_{ON}$, two boundary trajectories exist between Mode III and Mode IV, implying Mode-V operation does not exist. The converter's operation transits from Mode III to Mode IV back to Mode III to Mode VI, as indicated by S6 in Figure 2.10(e).

The boundary β_S angle, β_{34} , between Mode III and Mode IV is equal to $\omega_{SN} \times \delta_1$.

The boundary β_S angle, β_{43} , between Mode IV and Mode III is equal to $\omega_{SN} \times \delta_2$.

The boundary β_S angle, β_{36} , between Mode III and Mode VI is calculated as in (a.1).

- (a.3.3) If $R_1 > 1 - 2V_{ON}$ and $R_2 > 1 - 2V_{ON}$, two boundary trajectories exist between Mode III and Mode V, implying Mode-IV operation does not exist. The converter's operation transits from Mode III to Mode V back to Mode III to Mode VI, as indicated by S7 in Figure 2.10(c).

The boundary β_S angle, β_{35} , between Mode III and Mode V is equal to $\omega_{SN} \times \delta_1$.

The boundary β_S angle, β_{53} , between Mode V and Mode III is equal to $\omega_{SN} \times \delta_2$.

The boundary β_S angle, β_{36} , between Mode III and Mode VI is calculated as in (a.1).

(a.4) If $0.5 \leq \omega_{SN} < \omega_{4N}$, one such boundary trajectory exists. Equations (B.2.1) have one solution, (R_1, ζ_1, δ_1) .

- (a.4.1) If $R_1 \leq 1 - 2V_{ON}$, a boundary trajectory exists between Mode III and Mode IV. Since a Mode-IV trajectory can not transit directly into a Mode-VI trajectory, Mode-V operation must also exist. The converter's operation transits from Mode III to Mode IV to Mode V to Mode VI, as indicated by S8 in Figure 2.10(b).

The boundary β_S angle, β_{34} , between Mode III and Mode IV is equal to $\omega_{SN} \times \delta_1$.

The boundary β_S angle, β_{45} , between Mode IV and Mode V is calculated as in (a.3.1).

The boundary β_S angle, β_{56} , between Mode V and Mode VI can be calculated from trajectory T_{56} , as shown in Figure B.2.7,

$$\beta_{56} = \omega_{SN} \times \delta, \quad \delta = \cos^{-1}(1 - 2V_{ON}^2).$$

- (a.4.2) If $R_1 > 1 - 2V_{ON}$, a boundary trajectory exists between Mode III and Mode V, implying Mode-IV operation does not exist. The converter's operation transits from Mode III to Mode V to Mode VI, as indicated by S9 in Figure 2.10(d).

The boundary β_S angle, β_{35} , between Mode III and Mode V is equal to $\omega_{SN} \times \delta_1$.

The boundary β_S angle, β_{56} , between Mode V and Mode VI is calculated as in (a.4.1).

(b). $V_{ON} > 0.5$

(b.1) If $\omega_{SN} > \omega_{4N}$, such a boundary trajectory does not exist, implying both Mode-IV and Mode-V operations do not exist. The converter's operation transits from Mode III directly to Mode VI, as in **(a.1)**.

(b.2) If $\omega_{SN} \leq \omega_{4N}$, one such boundary trajectory exists. Since $R > V_{ON} > 1 - 2V_{ON}$, the trajectory is between Mode III and Mode V, implying Mode-IV operation does not exist. The converter's operation transits from Mode III to Mode V to Mode VI, as in **(a.4.2)**.

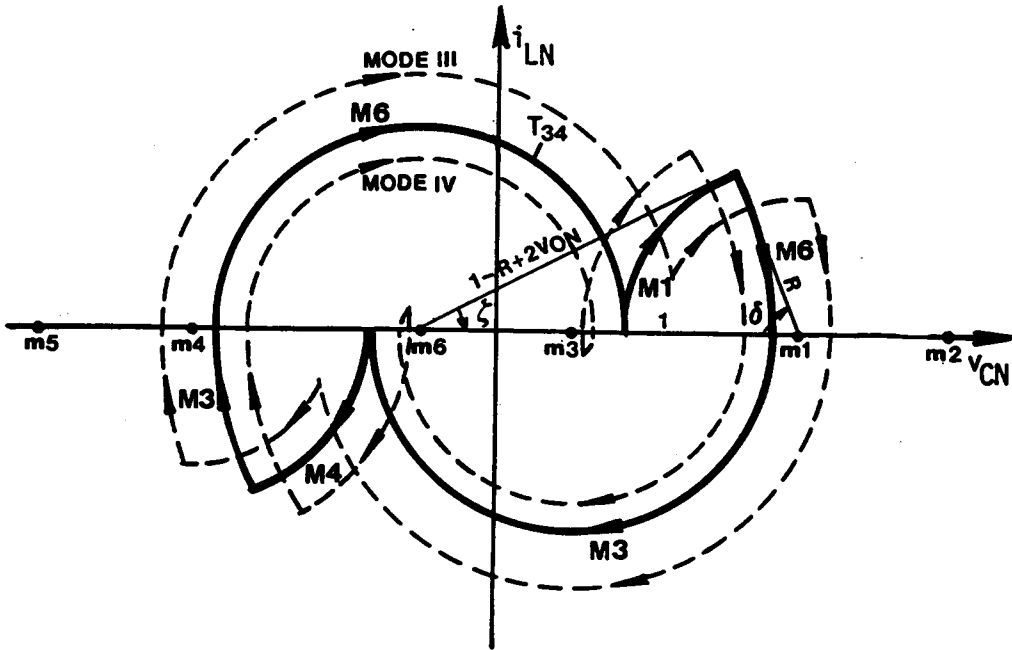


Figure B.2.1 Boundary Trajectory Between Mode III and Mode IV

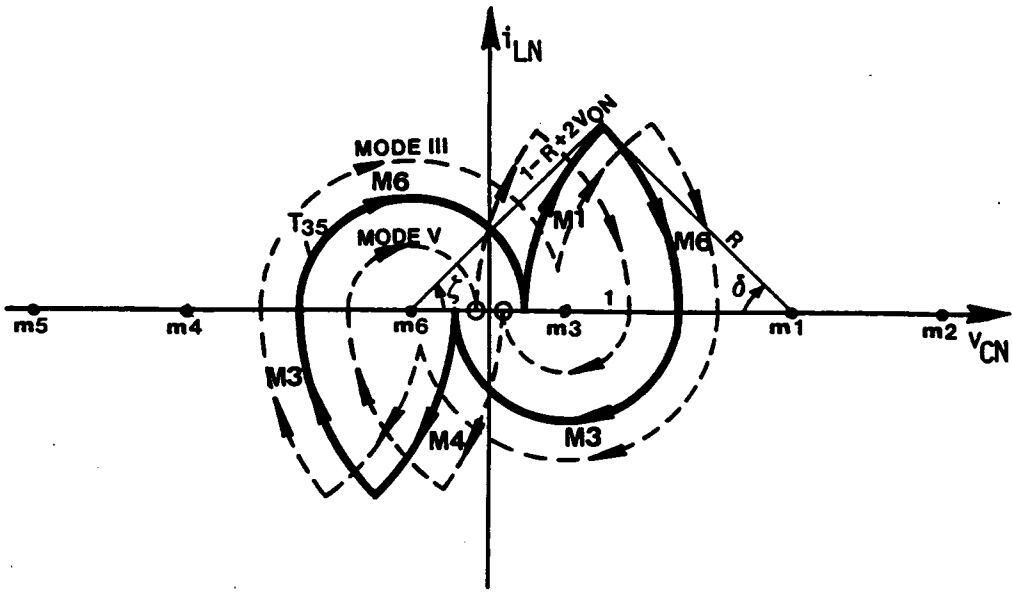


Figure B.2.2 Boundary Trajectory Between Mode III and Mode V

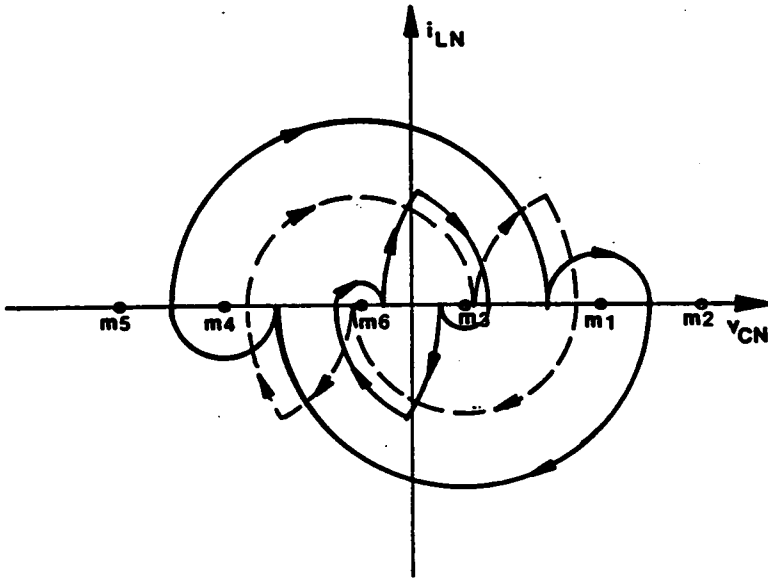


Figure B.2.3 Extreme Trajectory Described by Equation (B.2.1)

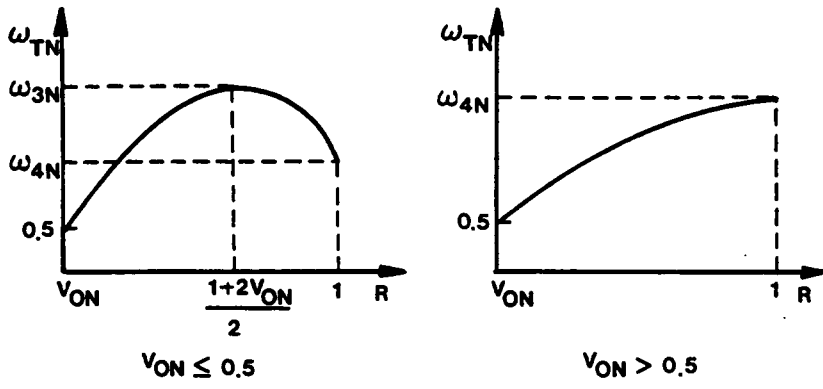


Figure B.2.4 Relationship Between Frequency of the Trajectory Described by Equation (B.2.1) and Radius R

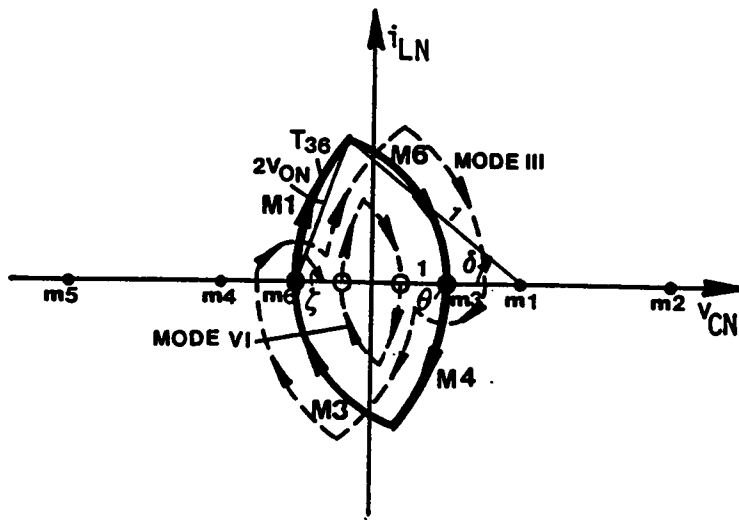


Figure B.2.5 Boundary Trajectory Between Mode III and Mode VI

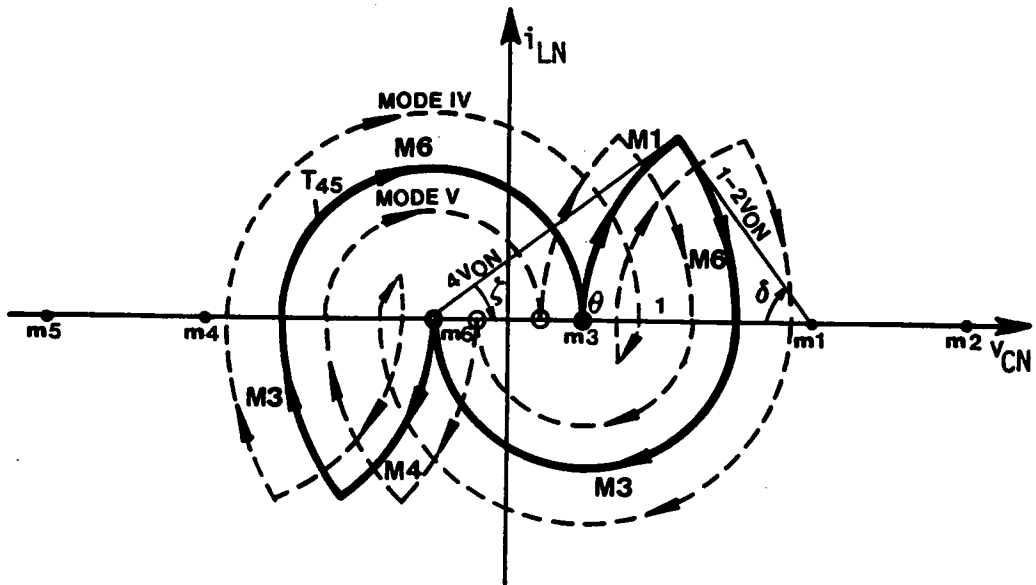


Figure B.2.6 Boundary Trajectory Between Mode IV and Mode V

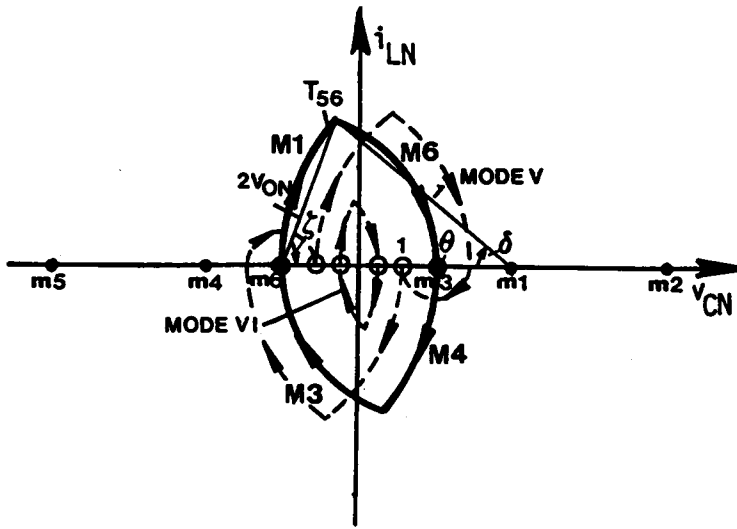


Figure B.2.7 Boundary Trajectory Between Mode V and Mode VI

FORTRAN Program for Determining Mode Transitions and Mode Boundaries Below Resonant Frequency

```

C *****
C *****
C ***** PROGRAM NAME : SCBD.FOR
C ***** FUNCTION : CALCULATE BOUNDARY B ANGLES AND PREDICT
C ***** MODE TRANSITIONS OF A CM-SRC OPERATING
C ***** BELOW RESONANT FREQUENCY.
C *****
C *****
C *****
C *****
C ***** FOR B > BETA(1) ---> MODE I OPERATION
C ***** FOR BETA(1) > B > BETA(2) ---> MODE II OPERATION
C ***** FOR BETA(2) > B > BETA(3) ---> MODE III OPERATION
C ***** FOR BETA(3) > B > BETA(4) ---> MODE IV OPERATION
C ***** FOR BETA(4) > B > BETA(5) ---> MODE V OPERATION
C ***** FOR BETA(5) > B > BETA(6) ---> MODE III OPERATION
C ***** FOR BETA(6) > B ---> MODE VI OPERATION
C *****
  IMPLICIT REAL*4 (A-H,O-Z)
  DIMENSION PAR(3), BETA(6), GUESS(3)
  PI = 4.*ATAN(1.)
10  READ(5,1000) WN, VON, INDEX
  READ(5,3000) ERREL, (GUESS(K), K = 1,3)
C ***
C *** A GOOD GUESS FOR GUESS(K), K = 1,3 ARE 1.1, 3.14, 1.57.
C ***
  IF(INDEX.NE.1) STOP
  INTL = 0
  WTS = PI/WN
C  ERREL = 0.0001
  ITMAX = 200
20  IF(VON.LT.0) GO TO 10
  IF(VON.EQ.0) VON = 0.0001
  INTL = INTL + 1
  PAR(1) = WTS
  PAR(2) = VON
  PAR(3) = PI
  WIN = PI/(PI + ACOS(VON))
  IF(WN.LE.WIN) THEN
    B1 = WTS - PI + ACOS(1 - 2*VON**2)
    IB1 = 1
  ELSE
    IB1 = 0
  ENDIF
  CALL SB2(PAR,ERREL,ITMAX,B2,INTL, FNORM,GUESS)
  BETA(2) = B2
  IF(IB1.EQ.1) THEN
    BETA(1) = B1
  ELSE
    BETA(1) = B2
  ENDIF
  B6 = ACOS(1 - 2*VON**2)
  BETA(6) = B6

```



```

W3N1=PI/(PI+2*ACOS((1+2*VON)**-1))
W3N2=PI/(PI+ACOS(VON)+ACOS(1-2*VON**2))
IF(VON.LE.0.5) THEN
  IF(WN.GE.W3N1) THEN
    IF(IB1.EQ.1) THEN
      ID=6
    ELSE
      ID=12
    ENDIF
    BETA(3)=B6
    BETA(4)=B6
    BETA(5)=B6
    GO TO 99
  ENDIF
  IF(WN.LT.W3N1.AND.WN.GE.W3N2) THEN
    RMAX=(1+2*VON)/2
    RMIN=VON
    SIGN=1
    CALL B34(RMAX,RMIN,RB3,VON,B3,WN,PI,SIGN)
    RMAX=1.
    RMIN=(1+2*VON)/2
    SIGN=-1
    CALL B34(RMAX,RMIN,RB4,VON,B4,WN,PI,SIGN)
    IF(RB3.I.E.(1-2*VON).AND.RB4.LE.(1-2*VON)) THEN
      IF(IB1.EQ.1) THEN
        ID=3
      ELSE
        ID=9
      ENDIF
      BETA(3)=B3
      BETA(4)=B4
      BETA(5)=B4
      GO TO 99
    ENDIF
    IF(RB3.GT.(1-2*VON).AND.RB4.GT.(1-2*VON)) THEN
      IF(IB1.EQ.1) THEN
        ID=4
      ELSE
        ID=10
      ENDIF
      BETA(3)=B3
      BETA(4)=B3
      BETA(5)=B4
      GO TO 99
    ENDIF
    IF(RB3.I.E.(1-2*VON).AND.RB4.GT.(1-2*VON)) THEN
      IF(IB1.EQ.1) THEN
        ID=1
      ELSE
        ID=7
      ENDIF
      B5=ACOS(1-6*VON**2/(1-2*VON))
      BETA(3)=B3
      BETA(4)=B5
      BETA(5)=B4
      GO TO 99
    ENDIF
  ENDIF
ENDIF

```

```

IF(WN.LT.W3N2) TIEN
  RMAX = (1 + 2*VON)/2
  RMIN = VON
  SIGN = 1
  CALL B34(RMAX,RMIN,RB3,VON,B3,WN,PI,SIGN)
  IF(RB3.LE.(1-2*VON)) THEN
    IF(IB1.EQ.1) THEN
      ID = 2
    ELSE
      ID = 8
    ENDIF
    B5 = ACOS(1-6*VON**2/(1-2*VON))
    BETA(3) = B3
    BETA(4) = B5
    BETA(5) = B6
  ELSE
    IF(IB1.EQ.1) THEN
      ID = 5
    ELSE
      ID = 11
    ENDIF
    BETA(3) = B3
    BETA(4) = B3
    BETA(5) = B6
  ENDIF
  GO TO 99
ENDIF
ELSE
IF(WN.GT.W3N2) TIEN
  IF(IB1.EQ.1) THEN
    ID = 6
  ELSE
    ID = 12
  ENDIF
  BETA(3) = B6
  BETA(4) = B6
  BETA(5) = B6
ELSE
  RMAX = 1
  RMIN = VON
  SIGN = 1
  CALL B34(RMAX,RMIN,RB3,VON,B3,WN,PI,SIGN)
  IF(IB1.EQ.1) THEN
    ID = 5
  ELSE
    ID = 11
  ENDIF
  BETA(3) = B3
  BETA(4) = B3
  BETA(5) = B6
ENDIF
ENDIF
99 DO 35 I = 1,6
  BETA(I) = BETA(I)*180/WTS
35 CONTINUE
WRITE(6,2000) ID, VON, (BETA(I), I = 1,6), FNORM
VON = VON-0.02

```

```

GO TO 20
1000 FORMAT(2F10.5,I1)
2000 FORMAT(1X,I2,3X,8F10.5)
3000 FORMAT(5F10.5)
END
C
C *****
C *****
C *****
C
SUBROUTINE SB2(PAR,ERREL,ITMAX,B2,INTL,FNORM,GUESS)
EXTERNAL FCN2
DIMENSION XGUESS(3),X(3),PAR(3),GUESS(3)
COMMON WTS,VON,PI
N=3
J=0
WTS = PAR(1)
VON = PAR(2)
PI = PAR(3)
IF(INTL.EQ.1) THEN
  X(1)=GUESS(1)
  X(2)=GUESS(2)
  X(3)=GUESS(3)
ENDIF
121 XGUESS(1)=X(1)-J*0.2
XGUESS(2)=X(2)-J*0.2
XGUESS(3)=X(3)+J*0.2
CALL NEQNF(FCN2,ERREL,N,ITMAX,XGUESS,X,FNORM)
IF(X(1).GE.0.AND.X(2).GE.0.AND.X(3).GE.0.AND.X(3).LE.PAR(3)
1 .AND.X(2).LE.3.1416) THEN
  B2=X(2)
  RETURN
ELSE
  IF(J.EQ.10) THEN
    WRITE(6,1200)
    STOP
  ELSE
    J=J+1
    GO TO 121
  ENDIF
ENDIF
1200 FORMAT(/,5X,'ERROR : CAN'T FIND B2',/)
END
C
C *****
C *****
C *****
C
SUBROUTINE B34(RMAX,RMIN,R,VON,BT,WN,PI,SIGN)
221 R=(RMAX+RMIN)/2.
BT=ACOS((1+R**2-(1-R+2*VON)**2)*0.5/R)
AL=ACOS((1+(1-R+2*VON)**2-R**2)*.5/(1-R+2*VON))
WCAL=PI/(AL+BT+PI)
IF(ABS(WN-WCAL).LT.0.0001) RETURN
IF(SIGN*WCAL.GT.SIGN*WN) THEN
  RMAX=R
ELSE
  RMIN=R

```

```

ENDIF
GO TO 221
END
C
C *****
C *****
C *****
C
SUBROUTINE FCN2(X,F,N)
DIMENSION X(N), F(N)
COMMON WTS, VON, PI
F(1) = -2*X(1)*COS(X(2)) - (1 + X(1)**2 - (1 - 2*VON + X(1))**2)
F(2) = -2*(1 - 2*VON + X(1))*COS(X(3))
1  -(1 + (1 - 2*VON + X(1))**2 - X(1)**2)
F(3) = X(2) + X(3) - WTS
RETURN
END

```

APPENDIX B.3

PREDICTION OF MODE TRANSITIONS OF A CM-SRC OPERATING ABOVE RESONANT FREQUENCY

Consider the boundary trajectories, T_{AB} , between Mode A and Mode B, and T_{AC} , between Mode A and Mode C, as shown in Figure B.3.1 and Figure B.3.2, respectively. These two trajectories are constructed via same topological mode sequence and can be represented by the same equations,

$$\begin{aligned}\cos \delta &= \frac{1 + (R_1 - 1 + 2V_{ON})^2 - R_1^2}{2(R_1 - 1 + 2V_{ON})}, \\ \cos \beta &= \frac{1 + R_1^2 - (R_1 - 1 + 2V_{ON})^2}{2R_1}, \\ \omega_{SN} &= \frac{\pi}{\delta + \beta}.\end{aligned}\tag{B.3.1}$$

The parameter R_1 can be used to distinguish between trajectories T_{AB} and T_{AC} . When $R_1 > 1$, equations (B.3.1) represent a T_{AB} . When $R_1 < 1$, equations (B.2.1) represent a T_{AC} .

As illustrated in Figure B.3.3, the frequency of a trajectory represented by equation (B.3.1) increases as R_1 decreases. Thus, the frequency, ω_{1N} , separating trajectory T_{AB} from trajectory T_{AC} occurs at $R_1 = 1$ and is calculated as

$$\omega_{1N} = \frac{\pi}{\delta + \beta}\tag{B.3.2}$$

where, $\delta = \cos^{-1}(V_{ON})$ and $\beta = \cos^{-1}(1 - 2V_{ON}^2)$.

If the converter's operating frequency, ω_{SN} , is greater than ω_{1N} , boundary trajectory T_{AC} exists. This implies that Mode B operation does not exist. As β_S decreases, the converter's operation transits from Mode A to Mode C, as indicated by SA in Figure 2.13(a). The boundary β_S angle, β_{AC} , can be calculated by solving equation (B.3.1). Angle β_{AC} is equal to $\beta \times \omega_{SN}$.

If $\omega_{SN} < \omega_{1N}$, boundary trajectory T_{AB} exists. Thus, as β_S decreases, the converter's operation transits from Mode A to Mode B to Mode C, as indicated by SB in Figure 2.13(a). The boundary β_S angle, β_{AB} , is calculated by solving equation (B.3.1). Angle β_{AB} is equal to $\beta \times \omega_{SN}$.

The boundary β_S angle, β_{BC} , between Mode B and Mode C can be calculated from trajectory T_{BC} , as shown in Figure B.3.4. Angle β_{BC} is equal to $\beta \times \omega_{SN}$, where $\beta = \cos^{-1}(1 - 2V_{ON})$.

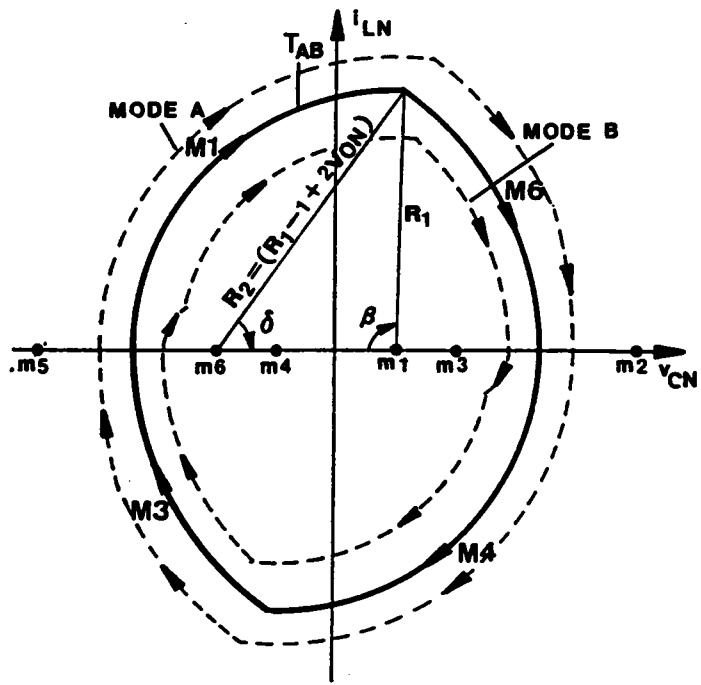


Figure B.3.1 Boundary Trajectory Between Mode A and Mode B

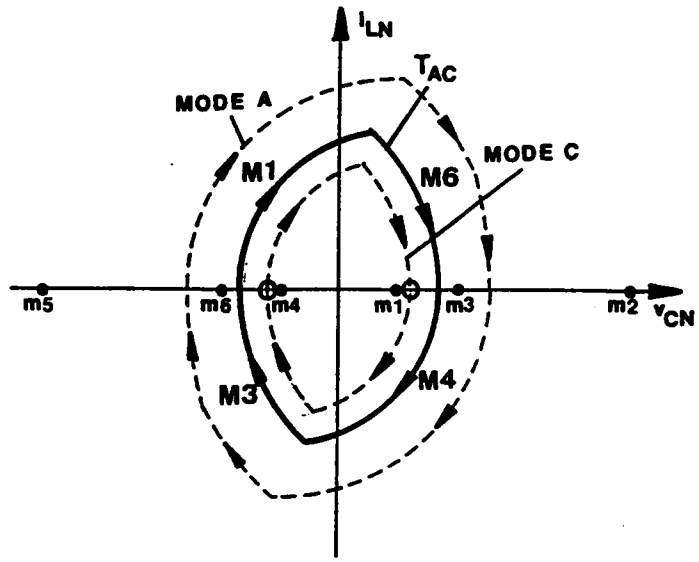


Figure B.3.2 Boundary Trajectory Between Mode A and Mode C

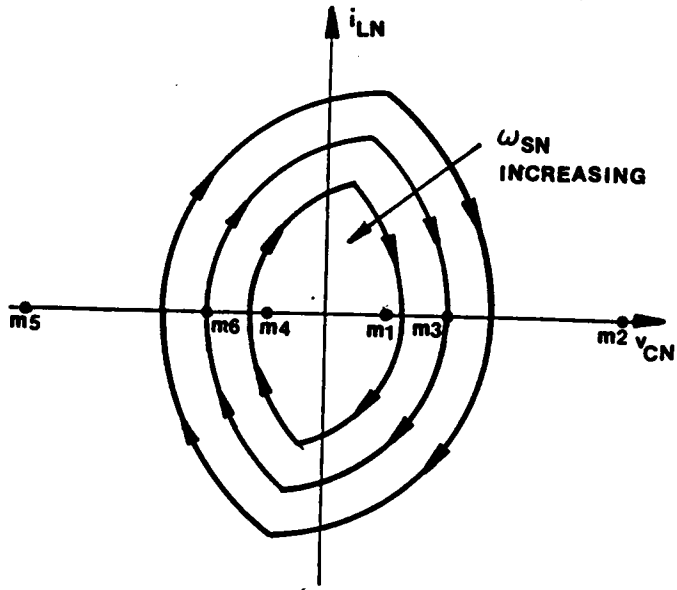


Figure B.3.3 Relationship Between Frequency of the Trajectory Described by Equation (B.3.1) and Radius R_1

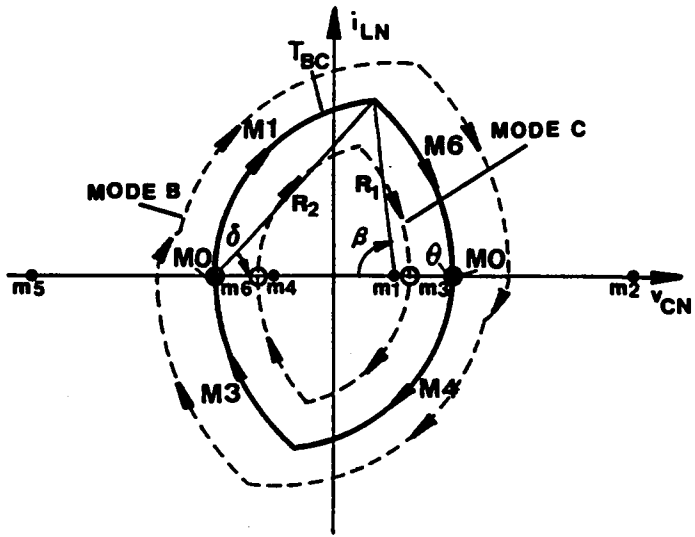


Figure B.3.4 Boundary Trajectory Between Mode B and Mode C

FORTRAN Program for Determining Mode Transitions and Mode Boundaries Above Resonant Frequency

```

C *****
C *****
C ***** PROGRAM NAME : SC10BD.FOR
C ***** FUNCTION : CALCULATE BOUNDARY B ANGLES AND PREDICT
C ***** MODE TRANSITIONS OF A CM-SRC OPERATING
C ***** ABOVE RESONANT FREQUENCY.
C *****
C *****
C *****
C *****
C ***** FOR B > BETA1 ---> MODE A OPERATION
C ***** FOR BETA1 > B > BETA2 ---> MODE B OPERATION
C ***** FOR BETA2 > B ---> MOCE C OPERATION
C *****
C      IMPLICIT REAL*4 (A-H,O-Z)
C      DIMENSION PAR(3)
C      COMMON WTS, VON, PI
C      PI=4.*ATAN(1.)
10  READ(5,1000) WN, VON, INDEX
C      IF(INDEX.NE.1) STOP
C      WTS=PI/WN
C      ERREL=0.0001
C      J=0
C      ITMAX=200
20  IF(VON.LT.0) GO TO 10
C      A3=ACOS(VON)
C      B3=ACOS(1-2*VON**2)
C      B3S=B3*180/WTS
C      W1N=PI/(A3+B3)
C      CALL BETA12(ERREL,ITMAX,B12,J)
C      J=J+1
C      IF(WN.LT.W1N) THEN
C          BETA1=B12*180/WTS
C          BETA2=B3S
C      ELSE
C          BETA1=B12*180/WTS
C          BETA2=BETA1
C      ENDIF
C      WRITE(6,2000) VON,BETA1,BETA2
C      WRITE(7,2000) VON,BETA2
C      VON=VON-0.01
C      GO TO 20
1000 FORMAT(2F10.5,I1)
2000 FORMAT(1X,3F14.5)
C      END
C *****
C *****
C *****
C *****
C
C      SUBROUTINE BETA12(ERREL,ITMAX,B12,JD)
C      EXTERNAL F12
C      DIMENSION X(2), XGUESS(2)

```

```

COMMON WTS,VON,PI
N=2
J=0
IF(JD.EQ.0) THEN
  X(1)=10.
  X(2)=PI
ENDIF
121 XGUESS(1)=X(1)-J*0.45
XGUESS(2)=X(2)-J*WTS/20.
CALL NEQNF(F12,ERREL,N,ITMAX,XGUESS,X,FNORM)
IF(X(1).GE.(1-VON).AND.X(2).GE.0.AND.
1 X(2).LE.WTS) THEN
  B12=X(2)
  RETURN
ELSE
  IF(J.EQ.20) THEN
    WRITE(6,1200)
    STOP
  ELSE
    J=J+1
    GO TO 121
  ENDIF
ENDIF
1200 FORMAT(/,5X,'ERROR : CAN'T FIND B12  ',/)
END
C
C *****
C *****
C *****
C
SUBROUTINE F12(X,F,N)
DIMENSION X(N), F(N)
COMMON WTS,VON,PI
F(1)=2*X(1)*COS(X(2))-(1+X(1)**2-(2*VON-1+X(1))**2)
F(2)=2*(2*VON-1+X(1))*COS(WTS-X(2))
1 -(1+(2*VON-1+X(1))**2-X(1)**2)
RETURN
END

```

APPENDIX B.4

CALCULATION OF TRAJECTORY PARAMETERS BELOW RESONANT FREQUENCY

The parameters for the equilibrium trajectories of a CM-SRC can be obtained by solving sets of nonlinear equations. The equations are derived from the geometrical relationship among the parameters. Notice that the distance between any two centers (m_1 - m_6) of topological modes are known.

The equations for solving the parameters of Mode-I Trajectory have already be shown in Section 2.3.7.1.

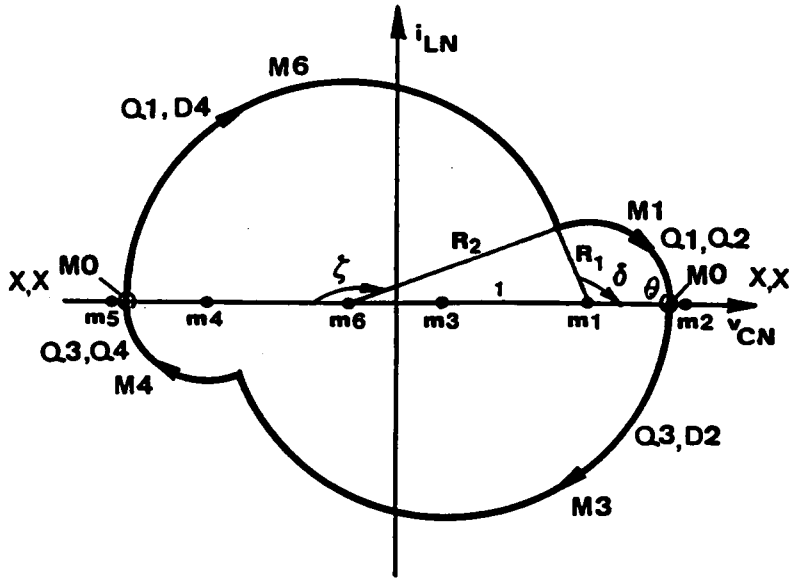
The equations for solving the parameters of Mode-II Trajectory are shown in Figure B.4.1.

The equations for solving the parameters of Mode-III Trajectory are shown in Figure B.4.2.

The equations for solving the parameters of Mode-IV Trajectory are shown in Figure B.4.3.

The equations for solving the parameters of Mode-V Trajectory are shown in Figure B.4.4.

The equations for solving the parameters of Mode-VI Trajectory are shown in Figure B.4.5.



$$\cos(\pi - \zeta) = \frac{1 + R_2^2 - R_1^2}{2R_2},$$

$$\cos(\pi - \delta) = \frac{1 + R_1^2 - R_2^2}{2R_1},$$

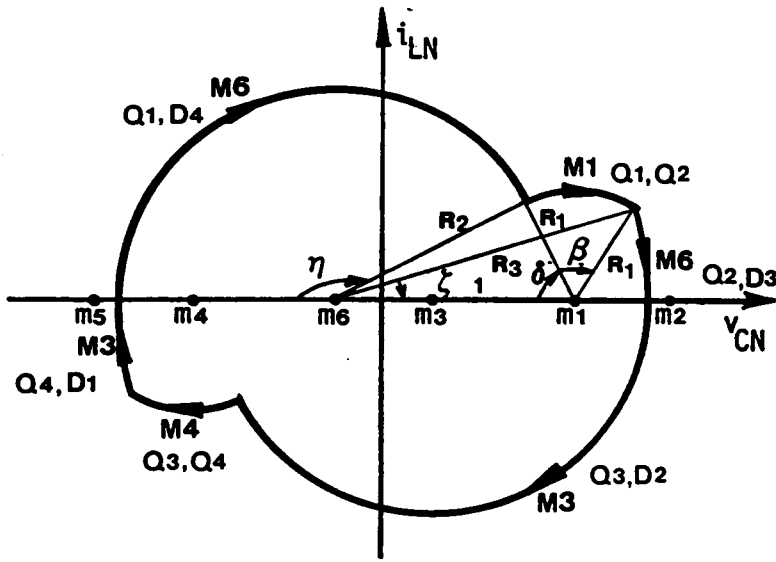
$$\frac{\beta_S}{\omega_{SN}} = \delta + \theta,$$

$$\frac{\pi}{\omega_{SN}} = \delta + \theta + \zeta,$$

$$R_2 = R_1 + 1 - 2V_{ON}.$$

$$0 \leq R_1 \leq 2V_{ON}, \quad 0 \leq R_2 \leq 1, \quad 0 \leq \zeta, \delta, \theta \leq \pi.$$

Figure B.4.1 Mode-II Trajectory Below Resonant Frequency



$$\cos(\pi - \eta) = \frac{1 + R_2^2 - R_1^2}{2R_2},$$

$$\cos \delta = \frac{1 + R_1^2 - R_2^2}{2R_1},$$

$$\cos \zeta = \frac{1 + R_3^2 - R_1^2}{2R_3},$$

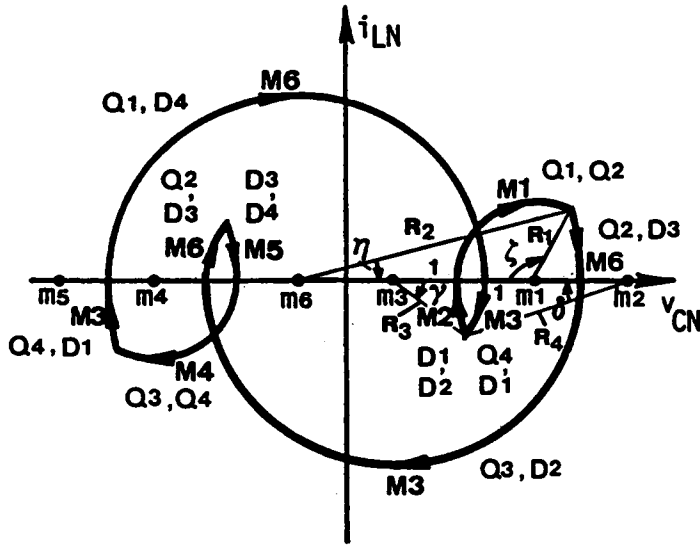
$$\cos\left(\delta + \frac{\beta_S}{\omega_{SN}}\right) = \frac{1 + R_1^2 - R_3^2}{2R_1},$$

$$\frac{\pi}{\omega_{SN}} = \zeta + \eta + \frac{\beta_S}{\omega_{SN}},$$

$$R_3 = R_2 + 2V_{ON}.$$

$$0 \leq R_1, R_2, R_3, \quad 0 \leq \eta, \zeta, \delta \leq \pi.$$

Figure B.4.2 Mode-III Trajectory Below Resonant Frequency



$$\cos \eta = \frac{1 + R_2^2 - R_1^2}{2R_2}, \quad \cos \zeta = \frac{1 + R_1^2 - R_2^2}{2R_1},$$

$$\cos \gamma = \frac{1 + R_3^2 - R_4^2}{2R_3}, \quad \cos \delta = \frac{1 + R_4^2 - R_3^2}{2R_4},$$

$$\frac{\beta_S}{\omega_{SN}} = \delta + \zeta,$$

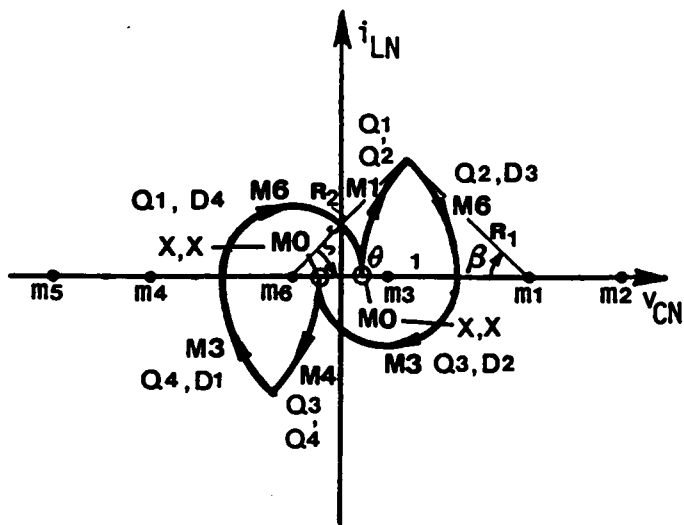
$$\frac{\pi}{\omega_{SN}} = \eta + \pi + \gamma + \frac{\beta_S}{\omega_{SN}},$$

$$R_4 = R_1 + 2V_{ON},$$

$$R_2 = R_3 + 4V_{ON}.$$

$$0 \leq R_1, R_2, R_3, R_4, \quad 0 \leq \eta, \zeta, \gamma, \delta \leq \pi.$$

Figure B.4.3 Mode-IV Trajectory Below Resonant Frequency



$$\cos \zeta = \frac{1 + R_2^2 - R_1^2}{2R_2},$$

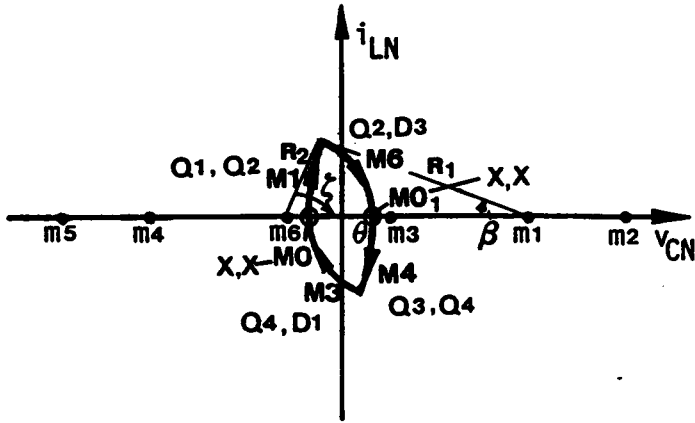
$$\cos\left(\frac{\beta_S}{\omega_{SN}}\right) = \frac{1 + R_1^2 - R_2^2}{2R_1},$$

$$\frac{\pi}{\omega_{SN}} = \pi + \theta + \zeta + \frac{\beta_S}{\omega_{SN}},$$

$$R_2 = 2V_{ON} + 1 - R_1.$$

$$0 \leq R_1 \leq 1, \quad 2V_{ON} \leq R_2, \quad 0 \leq \zeta, \theta \leq \pi.$$

Figure B.4.4 Mode-V Trajectory Below Resonant Frequency



$$\cos \zeta = \frac{1 + R_2^2 - R_1^2}{2R_2},$$

$$\cos\left(\frac{\beta_S}{\omega_{SN}}\right) = \frac{1 + R_1^2 - R_2^2}{2R_1},$$

$$\frac{\pi}{\omega_{SN}} = \theta + \zeta + \frac{\beta_S}{\omega_{SN}},$$

$$R_2 = R_1 - 1 + 2V_{ON}.$$

$$0 \leq R_1 \leq 1, \quad 0 \leq R_2 \leq 2V_{ON}, \quad 0 \leq \zeta \leq \pi, \quad 0 \leq \theta \leq 2\pi.$$

Figure B.4.5 Mode-VI Trajectory Below Resonant Frequency

FORTRAN Program for Calculating Trajectory Parameters Below Resonant Frequency

```

C *****
C *****
C ***** PROGRAM NAME : SCPAR.FOR
C ***** FUNCTION : CALCULATE PARAMETERS FOR THE EQUILIBRIUM STATE
C ***** TRAJECTORIES OF A CM-SRC OPERATING BELOW RESONANT
C ***** FREQUENCY.
C *****
C *****
C *****
C ***** REFER TO THE FIGURES IN APPENDIX B.4 FOR THE MEANINGS OF X(I)'S
C *****
C
C IMPLICIT REAL*4 (A-H,O-Z)
C DIMENSION BETA(6),X(6),XGUESS(6)
C COMMON WTS,VON,PI,BT
C EXTERNAL FCNA,FCNB,FCNC,FCND,FCNE,FCNF
C
C PI=4.*ATAN(1.)
10 READ(5,1000) WN, VON, BS, INDEX
   IF(INDEX.NE.1) STOP
   READ(5,3000) (XGUESS(K), K = 1,6)
   WTS = PI/WN
   BT = BS*WTS/180
   ERREL = 0.0001
   JOLD = 0
   ITMAX = 200
   CALL SCABD(WN,ERREL,ITMAX,BETA)
11 IF(BT.GE.BETA(1)) THEN
    J=1
  ELSE
    IF(BT.GE.BETA(2)) THEN
      J=2
    ELSE
      IF(BT.GE.BETA(3)) THEN
        J=3
      ELSE
        IF(BT.GE.BETA(4)) THEN
          J=4
        ELSE
          IF(BT.GE.BETA(5)) THEN
            J=5
          ELSE
            IF(BT.GE.BETA(6)) THEN
              J=6
            ELSE
              J=6
            ENDIF
          ENDIF
        ENDIF
      ENDIF
    ENDIF
  ENDIF
ENDIF
ENDIF
ENDIF
ENDIF

```

```

I=0
GO TO (100,200,300,400,500,600), J
100 N=6
101 IF(J.NE.JOLD) THEN
    X(1)=XGUESS(1)
    X(2)=XGUESS(2)
    X(3)=XGUESS(3)
    X(4)=XGUESS(4)
    X(5)=XGUESS(5)
    X(6)=XGUESS(6)
    ENDIF
    XGUESS(1)=X(1)-I*0.1
    XGUESS(2)=X(2)-I*0.05
    XGUESS(3)=X(3)-I*0.1
    XGUESS(4)=X(4)-I*0.1
    XGUESS(5)=X(5)+I*0.1
    XGUESS(6)=X(6)-I*0.1
    CALL NEQNF(FCNA,ERREL,N,ITMAX,XGUESS,X,FNORM)
    IF(X(1).GT.0.AND.X(2).GT.0.AND.X(3).GE.0.AND.X(4).GE.0
1 .AND.X(5).GE.0.AND.X(6).GE.0.AND.X(3).LE.PI.AND.X(4)
1 .LE.PI.AND.X(5).LE.PI.AND.X(6).LE.PI) GO TO 999
    IF(I.GE.20) STOP
    I=I+1
    GO TO 101
200 N=4
201 IF(J.NE.JOLD) THEN
    X(1)=2.
    X(2)=PI
    X(3)=0.
    X(4)=PI
    ENDIF
    XGUESS(1)=X(1)-I*0.2
    XGUESS(2)=X(2)-I*0.2
    XGUESS(3)=X(3)+I*0.1
    XGUESS(4)=X(4)-I*0.2
    CALL NEQNF(FCNB,ERREL,N,ITMAX,XGUESS,X,FNORM)
    IF(X(1).GT.0.AND.X(2).GT.0.AND.X(3).GE.0.AND.X(4).GE.0
1 .AND.X(2).LE.PI.AND.X(3).LE.PI.AND.X(4).LE.PI) GO TO 999
    IF(I.GE.20) STOP
    I=I+1
    GO TO 201
300 N=5
301 IF(J.NE.JOLD) THEN
    X(1)=1.5
    X(2)=2.
    X(3)=PI/2
    X(4)=PI
    X(5)=PI/2.
    ENDIF
    XGUESS(1)=X(1)-I*0.15
    XGUESS(2)=X(2)-I*0.2
    XGUESS(3)=X(3)
    XGUESS(4)=X(4)-I*0.2
    XGUESS(5)=X(5)-I*0.2
    CALL NEQNF(FCNC,ERREL,N,ITMAX,XGUESS,X,FNORM)
    IF(X(1).GT.0.AND.X(2).GT.0.AND.X(3).GE.0.AND.X(4).GE.0
1 .AND.X(5).GE.0.AND.X(3).LE.PI.AND.X(4)
1 .LE.PI.AND.X(5).LE.PI) GO TO 999

```

```

IF(I.GE.20) STOP
I=I+1
GO TO 301
400 N=6
401 IF(J.NE.JOLD) THEN
    X(1)=1.-2*VON
    X(2)=2*VON
    X(3)=PI/4
    X(4)=3*PI/4
    X(5)=PI/4
    X(6)=PI/4
ENDIF
XGUESS(1)=X(1)-I*0.1
XGUESS(2)=X(2)+I*0.15
XGUESS(3)=X(3)-I*0.1
XGUESS(4)=X(4)-I*0.15
XGUESS(5)=X(5)-I*0.1
XGUESS(6)=X(6)-I*0.1
CALL NEQNF(FCND,ERREL,N,ITMAX,XGUESS,X,FNORM)
IF(X(1).GT.0.AND.X(2).GT.0.AND.X(3).GE.0.AND.X(4).GE.0
1 .AND.X(5).GE.0.AND.X(6).GE.0.AND.X(3).LE.PI.AND.X(4)
1 .LE.PI.AND.X(5).LE.PI.AND.X(6).LE.PI) GO TO 999
IF(I.GE.20) STOP
I=I+1
GO TO 401
500 N=3
501 IF(J.NE.JOLD) THEN
    X(1)=1-2*VON
    X(3)=PI/2
ENDIF
XGUESS(1)=X(1)+I*0.1
XGUESS(3)=X(3)-I*0.1
XGUESS(2)=WTS-BT-XGUESS(3)
CALL NEQNF(FCNE,ERREL,N,ITMAX,XGUESS,X,FNORM)
IF(X(1).GT.0.AND.X(1).LE.1.AND.X(2).GE.0.AND.X(3).GE.0
1 .AND.X(2).LE.PI.AND.X(3).LE.PI) GO TO 999
IF(I.GE.20) STOP
I=I+1
GO TO 501
600 N=3
601 IF(J.NE.JOLD) THEN
    X(1)=1.
    X(3)=PI/2.
ENDIF
XGUESS(1)=X(1)-I*0.1
XGUESS(3)=X(3)-I*0.1
XGUESS(2)=WTS-BT-XGUESS(3)
CALL NEQNF(FCNF,ERREL,N,ITMAX,XGUESS,X,FNORM)
IF(X(1).GT.0.AND.X(2).GE.0.AND.X(3).GE.0.AND.X(1).LE.1
1 .AND.X(2).LE.(2*PI).AND.X(3).LE.PI) GO TO 999
IF(I.GE.20) STOP
I=I+1
GO TO 601
999 WRITE(6,2000) J, BT, VON, (X(K), K=1,N)
JOLD=J
IF(BT.EQ.0.001) GO TO 10
BT=BT-WTS/100
IF(BT.LE.0) BT=0.001

```

```

GO TO 11
3000 FORMAT(6F8.4)
2000 FORMAT(1X,I1,2X,8F8.4)
1000 FORMAT(3F10.5,I1)
END
C
C *****
C *****
C *****
C
SUBROUTINE SCABD(WN,ERREL,ITMAX,BETA)
DIMENSION X(3),BETA(6),XGUESS(3)
COMMON WTS,VON,PI,BT
C
INTL = 1
WIN = PI/(PI + ACOS(VON))
CALL SB2(ERREL,ITMAX,B2,INTL)
IF(WN.LE.WIN) THEN
  B1 = WTS-PI + ACOS(1-2*VON**2)
  ELSE
  B1 = B2
ENDIF
B6 = ACOS(1-2*VON**2)
BETA(1) = B1
BETA(2) = B2
BETA(6) = B6
IF(VON.LE.0.5) THEN
  VONR = ((COS(PI*(1-WN)*.5/WN))**-.1 - 1)*.5
  IF(VON.GT.VONR) THEN
    ID = 6
    BETA(3) = B6
    BETA(4) = B6
    BETA(5) = B6
    GO TO 99
  ENDIF
  WIN = PI/(PI + 2*ACOS((1 + 2*VON)**-.1))
  W2N = PI/(PI + ACOS(VON) + ACOS(1-2*VON**2))
  IF(WN.GE.WIN) THEN
    ID = 6
    BETA(3) = B6
    BETA(4) = B6
    BETA(5) = B6
    GO TO 99
  ENDIF
  IF(WN.LT.WIN.AND.WN.GE.W2N) THEN
    RMAX = (1 + 2*VON)/2
    RMIN = VON
    SIGN = 1
    CALL B34(RMAX,RMIN,RUP,VON,BUP,WN,PI,SIGN)
    RMAX = 1.
    RMIN = (1 + 2*VON)/2
    SIGN = -1
    CALL B34(RMAX,RMIN,RDN,VON,BDN,WN,PI,SIGN)
    IF(RUP.LE.(1-2*VON).AND.RDN.LE.(1-2*VON)) THEN
      ID = 3
      BETA(3) = BUP
      BETA(4) = BDN
      BETA(5) = BDN
    
```

```

    GO TO 99
ENDIF
IF(RUP.GT.(1-2*VON).AND.RDN.GT.(1-2*VON)) THEN
    ID = 5
    BETA(3) = BUP
    BETA(4) = BUP
    BETA(5) = BDN
    GO TO 99
ENDIF
IF(RUP.LE.(1-2*VON).AND.RDN.GT.(1-2*VON)) THEN
    ID = 1
    B5 = ACOS(1-6*VON**2/(1-2*VON))
    BETA(3) = BUP
    BETA(4) = B5
    BETA(5) = BDN
    GO TO 99
ENDIF
ENDIF
IF(WN.LT.W1N.AND.WN.LT.W2N) THEN
    RMAX = (1 + 2*VON)/2
    RMIN = VON
    SIGN = 1
    CALL B34(RMAX,RMIN,RUP,VON,BUP,WN,PI,SIGN)
    IF(RUP.LE.(1-2*VON)) THEN
        ID = 2
        B5 = ACOS(1-6*VON**2/(1-2*VON))
        BETA(3) = BUP
        BETA(4) = B5
        BETA(5) = B6
    ELSE
        ID = 4
        BETA(3) = BUP
        BETA(4) = BUP
        BETA(5) = B6
    ENDIF
    GO TO 99
ENDIF
ELSE
    WIN = PI/(PI + ACOS(1-2*VON**2) + ACOS(VON))
    IF(WN.GT.W1N) THEN
        ID = 6
        BETA(3) = B6
        BETA(4) = B6
        BETA(5) = B6
    ELSE
        ID = 4
        RMAX = 1
        RMIN = VON
        SIGN = 1
        CALL B34(RMAX,RMIN,RUP,VON,BUP,WN,PI,SIGN)
        BETA(3) = BUP
        BETA(4) = BUP
        BETA(5) = B6
    ENDIF
ENDIF
99 RETURN
END
C

```

```

C *****
C *****
C *****
C
SUBROUTINE SB2(ERREL,ITMAX,B2,INTL)
EXTERNAL FCN2
DIMENSION X(3),XGUESS(3)
COMMON WTS,VON,PI,BT
N=3
J=0
IF(INTL.EQ.1) THEN
  X(1)=1.1
  X(2)=3.14
  X(3)=1.57
ENDIF
121 XGUESS(1)=X(1)-J*0.1
XGUESS(2)=X(2)-J*0.15
XGUESS(3)=X(3)
CALL NEQNF(FCN2,ERREL,N,ITMAX,XGUESS,X,FNORM)
IF(X(1).GE.0.AND.X(2).GE.0.AND.X(3).GE.0.AND.X(3).LE.PI
1 .AND.X(2).LE.3.1416) THEN
  B2=X(2)
  RETURN
ELSE
  IF(J.EQ.10) THEN
    WRITE(6,1200)
    STOP
  ELSE
    J=J+1
    GO TO 121
  ENDIF
ENDIF
1200 FORMAT(/,5X,'ERROR : CAN'T FIND B2 ',/)
END
C *****
C *****
C *****
C
SUBROUTINE B34(RMAX,RMIN,R,VON,BT,WN,PI,SIGN)
221 R=(RMAX+RMIN)/2.
BT=ACOS((1+R**2-(1-R+2*VON)**2)*0.5/R)
AL=ACOS((1+(1-R+2*VON)**2-R**2)*.5/(1-R+2*VON))
WCAL=PI/(AL+BT+PI)
IF(ABS(WN-WCAL).LT.0.0001) RETURN
IF(SIGN*WCAL.GT.SIGN*WN) THEN
  RMAX=R
ELSE
  RMIN=R
ENDIF
GO TO 221
END
C *****
C *****
C *****
C
SUBROUTINE FCN2(X,F,N)

```



```

DIMENSION X(N), F(N)
COMMON WTS,VON,PI,BT
F(1)=-2*X(1)*COS(X(2))-(1+X(1)**2-(1-2*VON+X(1))**2)
F(2)=-2*(1-2*VON+X(1))*COS(X(3))
1 -(1+(1-2*VON+X(1))**2-X(1)**2)
F(3)=X(2)+X(3)-WTS
RETURN
END

```

C
C
C
C
C

```

SUBROUTINE FCNA(X,F,N)
DIMENSION X(N), F(N)
COMMON WTS,VON,PI,BT
F(1)=-2*X(1)*COS(X(6))-(1+X(1)**2-X(2)**2)
F(2)=-2*(X(1)-2*VON)*COS(X(5))-(1+(X(1)-2*VON)**2-X(2)**2)
F(3)=2*X(2)*COS(X(3))-(1+X(2)**2-(X(1)-2*VON)**2)
F(4)=2*X(2)*COS(X(4))-(1+X(2)**2-X(1)**2)
F(5)=X(5)+X(6)-BT
F(6)=PI-X(3)-X(4)+X(5)+X(6)-WTS
RETURN
END

```

C
C
C
C
C

```

SUBROUTINE FCNB(X,F,N)
DIMENSION X(N), F(N)
COMMON WTS,VON,PI,BT
F(1)=-2*X(1)*COS(X(2))-(1+X(1)**2-(1-2*VON+X(1))**2)
F(2)=-2*(1+X(1)-2*VON)*COS(X(4))-(1+(1+X(1)-2*VON)**2-
1 -X(1)**2)
F(3)=X(4)+X(2)+X(3)-WTS
F(4)=X(2)+X(3)-BT
RETURN
END

```

C
C
C
C
C

```

SUBROUTINE FCNC(X,F,N)
DIMENSION X(N), F(N)
COMMON WTS,VON,PI,BT
F(1)=-2*X(2)*COS(X(4))-(1+X(2)**2-X(1)**2)
F(2)=2*(X(2)+2*VON)*COS(X(5))-(1+(X(2)+2*VON)**2-X(1)**2)
F(3)=2*X(1)*COS(X(3)+BT)-(1+X(1)**2-(X(2)+2*VON)**2)
F(4)=2*X(1)*COS(X(3))-(1+X(1)**2-X(2)**2)
F(5)=X(4)+X(5)+BT-WTS
RETURN
END

```

C
C
C

```

C *****
C
SUBROUTINE FCND(X,F,N)
DIMENSION X(N), F(N)
COMMON WTS,VON,PI,BT
F(1)=2*X(1)*COS(X(4))-(1+X(1)**2-X(2)**2)
F(2)=2*(X(1)+2*VON)*COS(X(3))-(1+(X(1)+2*VON)**2
1 -(X(2)-4*VON)**2)
F(3)=2*X(2)*COS(X(6))-(1+X(2)**2-X(1)**2)
F(4)=2*(X(2)-4*VON)*COS(X(5))-(1+(X(2)-4*VON)**2
1 -(X(1)+2*VON)**2)
F(5)=X(3)+X(4)-BT
F(6)=X(5)+X(6)+BT+PI-WTS
RETURN
END

C *****
C *****
C *****
C
SUBROUTINE FCNE(X,F,N)
DIMENSION X(N), F(N)
COMMON WTS,VON,PI,BT
F(1)=2*X(1)*COS(BT)-(1+X(1)**2-(1-X(1)+2*VON)**2)
F(2)=2*(1-X(1)+2*VON)*COS(X(3))-(1+(1-X(1)+2*VON)**2
1 -X(1)**2)
F(3)=X(3)+BT+X(2)+PI-WTS
RETURN
END

C *****
C *****
C *****
C
SUBROUTINE FCNF(X,F,N)
DIMENSION X(N), F(N)
COMMON WTS,VON,PI,BT
F(1)=2*X(1)*COS(BT)-(1+X(1)**2-(X(1)-1+2*VON)**2)
F(2)=2*(X(1)-1+2*VON)*COS(X(3))-(1+(X(1)-1+2*VON)**2
1 -X(1)**2)
F(3)=X(3)+BT+X(2)-WTS
RETURN
END

```

EXPRESSIONS FOR CIRCUIT SALIENT FEATURES

BELOW RESONANT FREQUENCY

Circuit Salient Features	Circuit Operating Modes					
	Mode I	Mode II	Mode III	Mode IV	Mode V	Mode VI
V_{CPK}	$R_1 + 1 - V_{ON}$	$R_1 + 1 - V_{ON}$	$R_2 + V_{ON}$	$R_2 - V_{ON}$	$R_2 - V_{ON}$	$R_2 - V_{ON}$
I_{AV}	$\frac{Da + Db + Dc}{\omega_0 T_s}$	$\frac{Da + Db}{\omega_0 T_s}$	$\frac{Da + Db + Dc}{\omega_0 T_s}$	$\frac{Da + Db + Dc + Dd + De}{\omega_0 T_s}$	$\frac{Da + Db + Dc}{\omega_0 T_s}$	$\frac{Da + Db}{\omega_0 T_s}$
I_{RMS}	$\left[\frac{Ra + Rb + Rc}{\omega_0 T_s} \right]^{\frac{1}{2}}$	$\left[\frac{Ra + Rb}{\omega_0 T_s} \right]^{\frac{1}{2}}$	$\left[\frac{Ra + Rb + Rc}{\omega_0 T_s} \right]^{\frac{1}{2}}$	$\left[\frac{Ra + Rb + Rc + Rd + Re}{\omega_0 T_s} \right]^{\frac{1}{2}}$	$\left[\frac{Ra + Rb + Rc}{\omega_0 T_s} \right]^{\frac{1}{2}}$	$\left[\frac{Ra + Rb}{\omega_0 T_s} \right]^{\frac{1}{2}}$
I_{Q1RMS}	$\left[\frac{Rb + Rc}{\omega_0 T_s} \right]^{\frac{1}{2}}$	$\left[\frac{Ra + Rb}{\omega_0 T_s} \right]^{\frac{1}{2}}$	$\left[\frac{Ra + Rb}{\omega_0 T_s} \right]^{\frac{1}{2}}$	$\left[\frac{Ra + Rd}{\omega_0 T_s} \right]^{\frac{1}{2}}$	$\left[\frac{Ra + Rb}{\omega_0 T_s} \right]^{\frac{1}{2}}$	$\left[\frac{Ra}{\omega_0 T_s} \right]^{\frac{1}{2}}$
I_{Q2RMS}	$\left[\frac{Rc}{\omega_0 T_s} \right]^{\frac{1}{2}}$	$\left[\frac{Rb}{\omega_0 T_s} \right]^{\frac{1}{2}}$	$\left[\frac{Ra + Rc}{\omega_0 T_s} \right]^{\frac{1}{2}}$	$\left[\frac{Rb + Rd + Re}{\omega_0 T_s} \right]^{\frac{1}{2}}$	$\left[\frac{Rb + Rc}{\omega_0 T_s} \right]^{\frac{1}{2}}$	$\left[\frac{Ra + Rb}{\omega_0 T_s} \right]^{\frac{1}{2}}$
I_{D1AV}	$\frac{Da}{\omega_0 T_s}$	0	$\frac{Dc}{\omega_0 T_s}$	$\frac{Db + Dc + De}{\omega_0 T_s}$	$\frac{Dc}{\omega_0 T_s}$	$\frac{Db}{\omega_0 T_s}$
I_{D2AV}	$\frac{Da + Db}{\omega_0 T_s}$	$\frac{Da}{\omega_0 T_s}$	$\frac{Da}{\omega_0 T_s}$	$\frac{Da + Dc}{\omega_0 T_s}$	$\frac{Da}{\omega_0 T_s}$	0
I_{Q1off}	0	0	$R_3 \sin \zeta$	0, $R_2 \sin \eta$	0, $R_2 \sin \zeta$	$R_1 \sin \beta$
I_{Q2off}	0	0	0	0, $R_4 \sin \delta$	0	0
I_{Q1on}	$R_2 \sin \zeta$	0	0	0, 0	0, 0	0
I_{Q2on}	$R_2 \sin \delta$	$R_1 \sin \delta$	$R_1 \sin \delta$	0, 0	0	0

EXPRESSIONS FOR CIRCUIT SALIENT FEATURES

BELOW RESONANT FREQUENCY (CONTINUED)

Parameter	Circuit Operating Modes					
	Mode I	Mode II	Mode III	Mode IV	Mode V	Mode VI
Values						
$Da =$	$R_3(1 - \cos \eta)$	$R_2(1 - \cos \zeta)$	$R_2(1 - \cos \eta)$	$2(R_2 - 2V_{on})$	$2(1 - R_1)$	$R_1(1 - \cos \beta)$
$Db =$	$R_2(\cos \zeta + \cos \delta)$	$R_1(1 - \cos \delta)$	$R_1(\cos \delta - \cos(\delta + \beta))$	$R_3(1 - \cos \gamma)$	$R_1(1 - \cos \beta)$	$R_3(1 - \cos \zeta)$
$Dc =$	$R_1(1 - \cos \gamma)$		$R_3(1 - \cos \zeta)$	$R_4(1 - \cos \delta)$	$R_3(1 - \cos \zeta)$	
$Dd =$				$R_1(1 - \cos \zeta)$		
$De =$				$R_3(1 - \cos \eta)$		
$Ra =$	$\frac{R_3}{2} (\eta - \frac{\sin 2\eta}{2})$	$\frac{R_3}{2} (\zeta - \frac{\sin 2\zeta}{2})$	$\frac{R_3}{2} (\eta - \frac{\sin 2\eta}{2})$	$\frac{\pi(R_2 - 2V_{on})^2}{2}$	$\frac{\pi(1 - R_1)^2}{2}$	$\frac{R_1^2}{2} (\beta - \frac{\sin 2\beta}{2})$
$Rb =$	$\frac{R_3}{2} (\pi - \zeta - \delta + \frac{\sin 2\zeta + \sin 2\delta}{2})$	$\frac{R_1^2}{2} (\delta - \frac{\sin 2\delta}{2})$	$\frac{R_1^2}{2} (\beta + \frac{\sin 2\delta}{2} - \frac{\sin(2\delta + 2\beta)}{2})$	$\frac{R_3}{2} (\gamma - \frac{\sin 2\gamma}{2})$	$\frac{R_1^2}{2} (\beta - \frac{\sin 2\beta}{2})$	$\frac{R_3^2}{2} (\zeta - \frac{\sin 2\zeta}{2})$
$Rc =$	$\frac{R_1^2}{2} (\gamma - \frac{\sin 2\gamma}{2})$		$\frac{R_3}{2} (\zeta - \frac{\sin 2\zeta}{2})$	$\frac{R_4^2}{2} (\delta - \frac{\sin 2\delta}{2})$		$\frac{R_3^2}{2} (\zeta - \frac{\sin 2\zeta}{2})$
$Rd =$				$\frac{R_1^2}{2} (\zeta - \frac{\sin 2\zeta}{2})$		
$Re =$				$\frac{R_3^2}{2} (\eta - \frac{\sin 2\eta}{2})$		


```

B2 = X(4)
AL = X(5)
GA = X(6)
IAV = (2*(R1-2*VON) + (R1-4*VON)*(1-COS(AL)) + (R + 2*VON)*(1-COS(B1))
1   + R*(1-COS(B2)) + R1*(1-COS(GA)))/WTS
ILRMS = ((.5*(R1-2*VON)**2*PI + .5*(R1-4*VON)**2*(AL-.5*SIN(2*AL))
1   + .5*(R + 2*VON)**2*(B1-.5*SIN(2*B1)) + .5*R**2*(B2-.5*SIN(2*B2))
1   + .5*R1**2*(GA-.5*SIN(2*GA)))/WTS)**0.5
VPK = R1-VON
GO TO 999
500 R = X(1)
FI = X(2)
AL = X(3)
IAV = (2*(1-R) + R*(1-COS(BT)) + (1-R + 2*VON)*(1-COS(AL)))/WTS
ILRMS = ((.5*PI*(1-R)**2 + .5*R**2*(BT-.5*SIN(2*BT))
1   + .5*(1-R + 2*VON)**2*(AL-.5*SIN(2*AL)))/WTS)**0.5
VPK = 1-R + VON
GO TO 999
600 R = X(1)
FI = X(2)
AL = X(3)
IAV = (R*(1-COS(BT)) + (R-1 + 2*VON)*(1-COS(AL)))/WTS
ILRMS = ((.5*R**2*(BT-.5*SIN(2*BT)) + .5*(R-1 + 2*VON)**2*
1   (AL-.5*SIN(2*AL)))/WTS)**0.5
VPK = R-1 + VON
999 BS = BT*180/WTS
WRITE(6,2000) BS, IAV, ILRMS, VPK
GO TO 11
1050 FORMAT(F10.5)
1000 FORMAT(1X,I1,2X,8F8.4)
2000 FORMAT(4F14.5)
END

```

```

C *****
C *****
C ***** PROGRAM NAME : SCOUT2.FOR
C ***** FUNCTION : CALCULATE AVERAGE CURRENTS FOR D1,D2, RMS
C ***** CURRENTS, TURN-ON CURRENTS AND TURN-OFF CUR-
C ***** RENTS FOR Q1,Q2.
C *****
C *****
C *****
C
REAL IQA, IDA, IAOFF, IAON
DIMENSION X(6)
PI=4.*ATAN(1.)
10 READ(5,1050) WN
WTS=PI/WN
11 READ(5,1000) J,BT,VON,(X(K), K=1,6)
C
C ***** THE INPUTS AERE OBTAINED FROM PROGRAM SCPAR.FOR
C
IF(J.EQ.0) STOP
GO TO (100,200,300,400,500,600), J
100 R=X(1)
R1=X(2)
B1=X(3)
B2=X(4)
AL=X(5)
GA=X(6)
IDA=(R-2*VON)*(1-COS(AL))/WTS
IQA=((0.5*R1**2*(PI-B1-B2+0.5*SIN(2*B1)+0.5*SIN(2*B2))
1 +0.5*R**2*(GA-0.5*SIN(2*GA)))/WTS)**0.5
IAOFF=0.
IAON=R1*SIN(B1)
GO TO 999
200 R=X(1)
B1=X(2)
FI=X(3)
AL=X(4)
IDA=0.
IQA=((0.5*(1-2*VON+R)**2*(AL-.5*SIN(2*AL))
1 +.5*R**2*(B1-.5*SIN(2*B1)))/WTS)**0.5
IAOFF=0.
IAON=0.
GO TO 999
300 R=X(1)
R1=X(2)
B1=X(3)
AL=X(4)
GA=X(5)
IDA=(R1+2*VON)*(1-COS(GA))/WTS
IQA=((0.5*R1**2*(AL-.5*SIN(2*AL))+.5*R**2*(BT+.5*SIN(2*B1)
1 -.5*SIN(2*(B1+BT)))/WTS)**0.5
IAOFF=(R1+2*VON)*SIN(GA)
IAON=0.
GO TO 999
400 R=X(1)
R1=X(2)
B1=X(3)
B2=X(4)
AL=X(5)
GA=X(6)
IDA=((R1-4*VON)*(1-COS(AL))+(R+2*VON)*(1-COS(B1))+R1*(1-COS(GA)))
1 /WTS

```

```

IQA = ((.5*(R1-2*VON)**2*PI + .5*R**2*(B2-.5*SIN(2*B2)))/WTS)**0.5
IAOFF = R1*SIN(GA)
IAON = 0.
GO TO 999
500 R = X(1)
FI = X(2)
AL = X(3)
IDA = (1-R + 2*VON)*(1-COS(AL))/WTS
IQA = ((.5*PI*(1-R)**2 + .5*R**2*(BT-.5*SIN(2*BT)))/WTS)**0.5
IAOFF = (1-R + 2*VON)*SIN(AL)
IAON = 0.
GO TO 999
600 R = X(1)
FI = X(2)
AL = X(3)
IDA = (R-1 + 2*VON)*(1-COS(AL))/WTS
IQA = (.5*R**2*(BT-.5*SIN(2*BT))/WTS)**0.5
IAOFF = R*SIN(BT)
IAON = 0.
999 BS = BT*180/WTS
WRITE(6,2000) BS, IDA, IQA, IAOFF, IAON
GO TO 11
1050 FORMAT(F10.5)
1000 FORMAT(1X,I1,2X,8F8.4)
2000 FORMAT(5F14.5)
END

```



```

C *****
C *****
C ***** PROGRAM NAME : SCOUT3.FOR
C ***** FUNCTION : CALCULATE AVERAGE CURRENTS FOR D3,D4, RMS
C ***** CURRENTS, TURN-ON CURRENTS AND TURN-OFF CUR-
C ***** RENTS FOR Q3,Q4.
C *****
C *****
C *****
C
REAL IDB, IQB, IBOFF, IBON
DIMENSION X(6)
PI=4.*ATAN(1.)
10 READ(5,1050) WN
WTS=PI/WN
11 READ(5,1000) J,BT,VON,(X(K), K=1,6)
C ***** THE INPUTS ARE OBTAINED FROM PROGRAM SCPAR.FOR
C
IF(J.EQ.0) STOP
GO TO (100,200,300,400,500,600), J
100 R=X(1)
R1=X(2)
B1=X(3)
B2=X(4)
AL=X(5)
GA=X(6)
IDB=((R-2*VON)*(1-COS(AL))+R1*(COS(B1)+COS(B2)))/WTS
IQB=(0.5*R**2*(GA-0.5*SIN(2*GA))/WTS)**0.5
IBOFF=0.
IBON=R1*SIN(B2)
GO TO 999
200 R=X(1)
B1=X(2)
FI=X(3)
AL=X(4)
IDB=(1-2*VON+R)*(1-COS(AL))/WTS
IQB=(.5*R**2*(B1-.5*SIN(2*B1))/WTS)**0.5
IBOFF=0.
IBON=R*SIN(B1)
GO TO 999
300 R=X(1)
R1=X(2)
B1=X(3)
AL=X(4)
GA=X(5)
IDB=R1*(1-COS(AL))/WTS
IQB=((.5*R**2*(BT+.5*SIN(2*B1)-.5*SIN(2*(B1+BT)))
1 +.5*(R1+2*VON)**2*(GA-.5*SIN(2*GA)))/WTS)**0.5
IBOFF=0.
IBON=R*SIN(B1)
GO TO 999
400 R=X(1)
R1=X(2)
B1=X(3)
B2=X(4)
AL=X(5)
GA=X(6)
IDB=(2*(R1-2*VON)+(R+2*VON)*(1-COS(B1)))/WTS
IQB=((.5*(R1-4*VON)**2*(AL-.5*SIN(2*AL))+.5*R**2*(B2-.5*SIN(2*B2))
1 +.5*R1**2*(GA-.5*SIN(2*GA)))/WTS)**0.5
IBOFF=(R+2*VON)*SIN(B1)

```

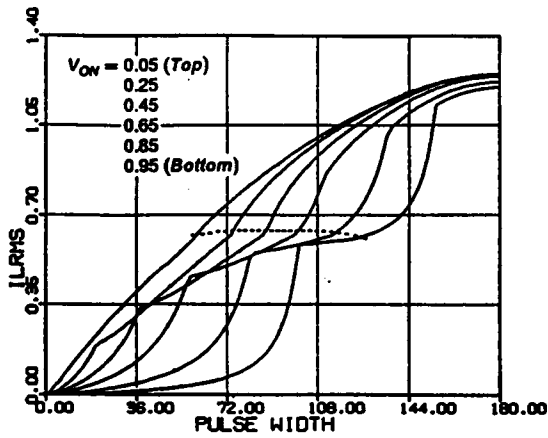
```

IBON = 0.
GO TO 999
500 R = X(1)
    FI = X(2)
    AL = X(3)
    IDB = 2*(1-R)/WTS
    IQB = ((.5*R**2*(BT-.5*SIN(2*BT)) + .5*(1-R + 2*VON)**2*(AL-
1    .5*SIN(2*AL)))/WTS)**0.5
    IBOFF = 0.
    IBON = 0.
    GO TO 999
600 R = X(1)
    FI = X(2)
    AL = X(3)
    IDB = 0.
    IQB = ((.5*R**2*(BT-.5*SIN(2*BT)) + .5*(R-1 + 2*VON)**2*
1    (AL-.5*SIN(2*AL)))/WTS)**0.5
    IBOFF = 0.
    IBON = 0.
999 BS = BT*180/WTS
    WRITE(6,2000) BS, IDB, IQB, IBOFF, IBON
    GO TO 11
1050 FORMAT(F10.5)
1000 FORMAT(1X,I1,2X,8F8.4)
2000 FORMAT(5F14.5)
END

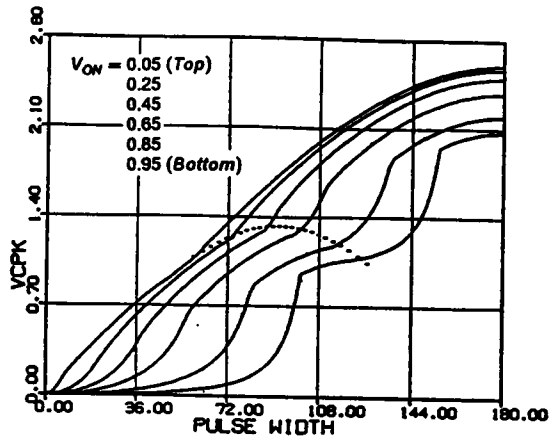
```

APPENDIX B.6

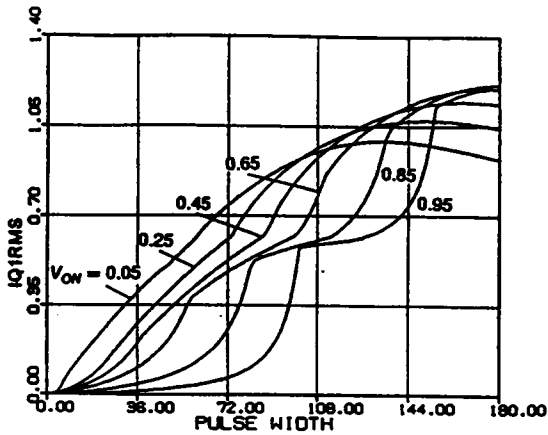
DC CHARACTERISTICS BELOW RESONANT FREQUENCY



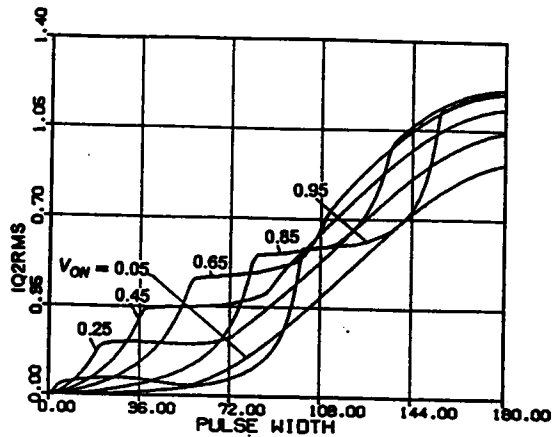
• RMS switch current ($Q2, Q4$)



• Peak capacitor voltage

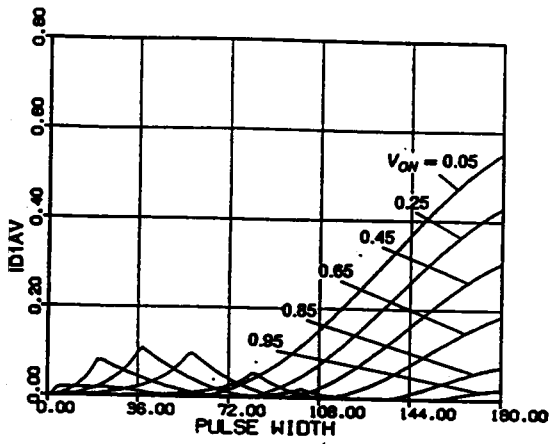


• RMS switch current ($Q1, Q3$)

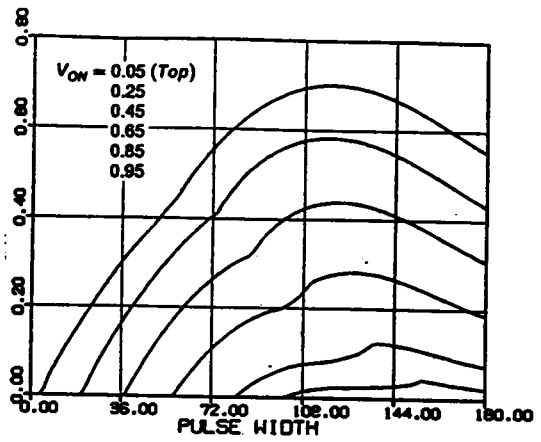


• RMS switch current ($Q2, Q4$)

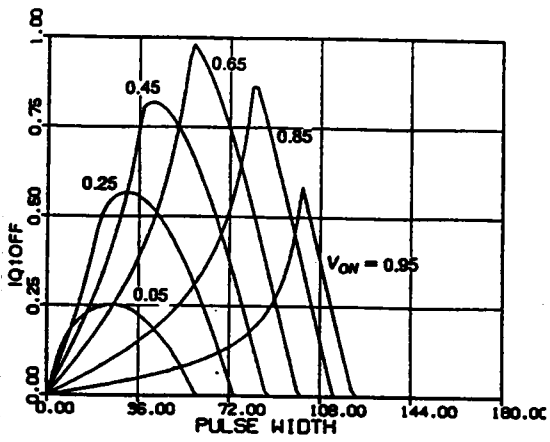
Figure B.6.1 DC Characteristics for $\omega_{SN} = 0.7$.



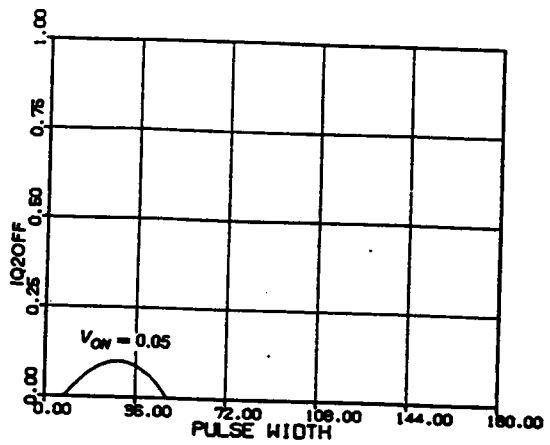
• Average diode current (*D1,D3*)



• Average diode current (*D2,D4*)

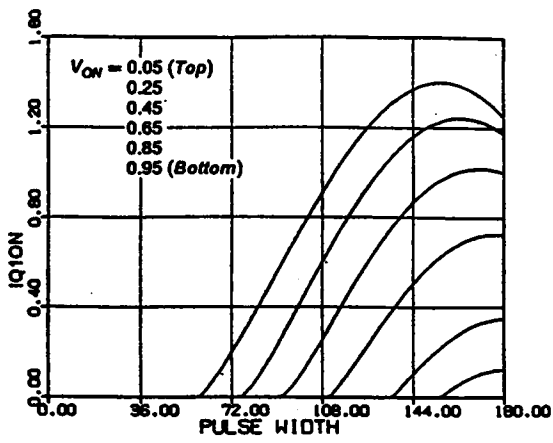


• Switch turn-off current (*Q1,Q3*)

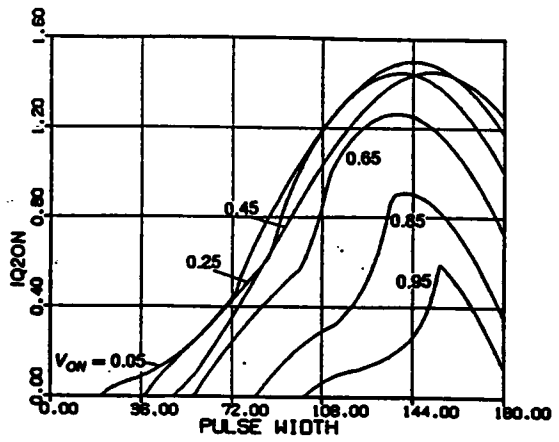


• Switch turn-off current (*Q2,Q4*)

Figure B.6.1 Continued

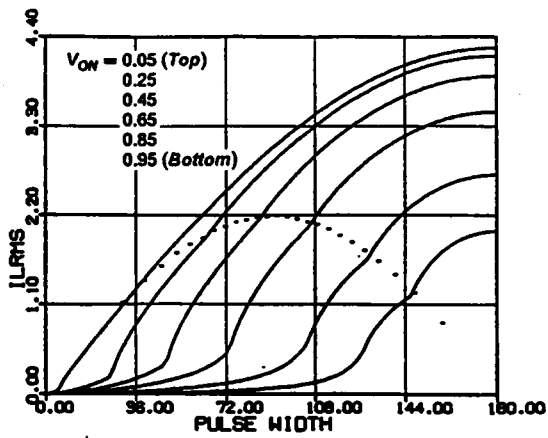


• Switch turn-on current (Q1,Q3)

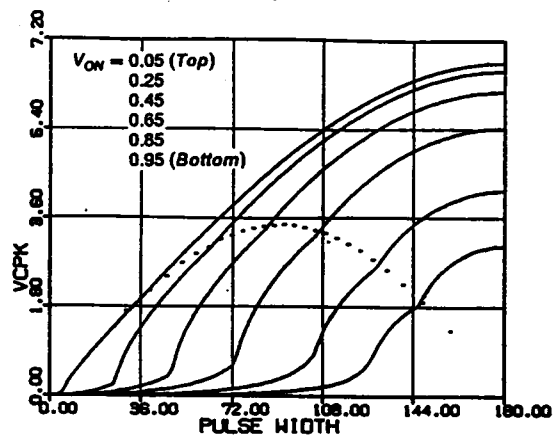


• Switch turn-on current (Q2,Q4)

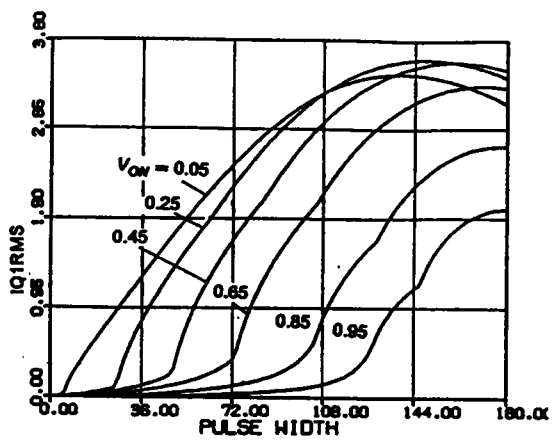
Figure B.6.1 Continued



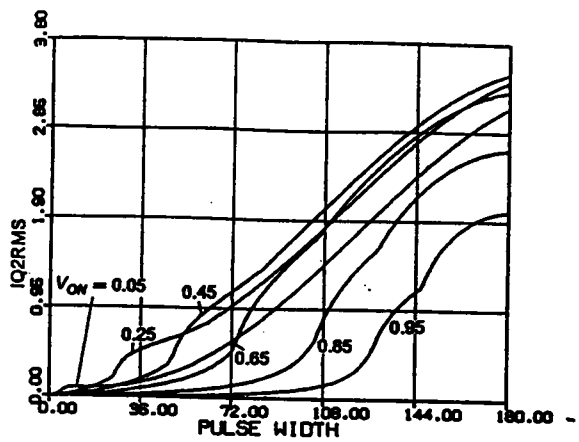
• *RMS inductor current*



• *Peak capacitor voltage*

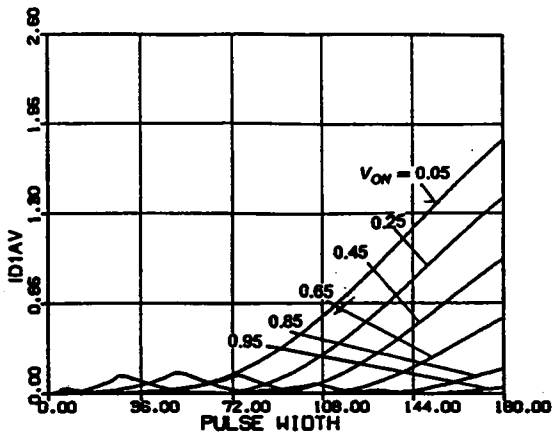


• *RMS switch current (Q1,Q3)*

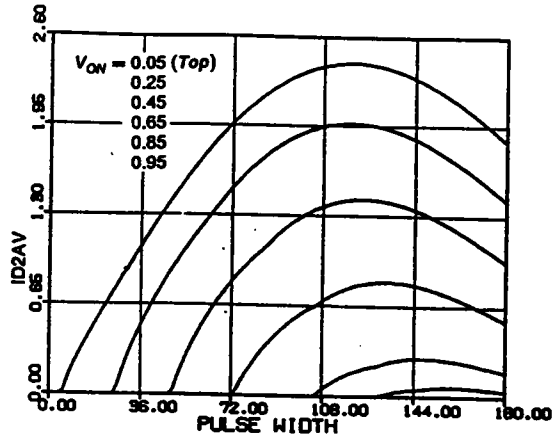


• *RMS switch current (Q2,Q4)*

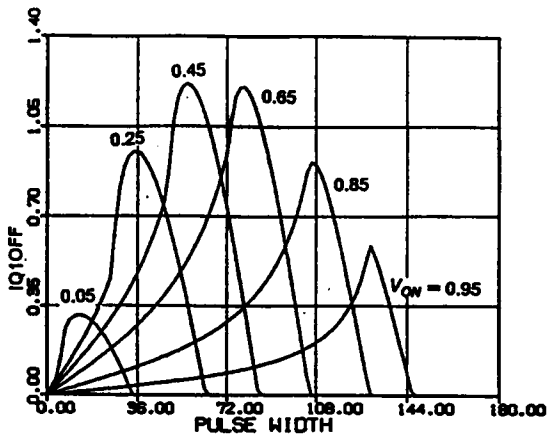
Figure B.6.2 DC Characteristics for $\omega_{SN} = 0.9$.



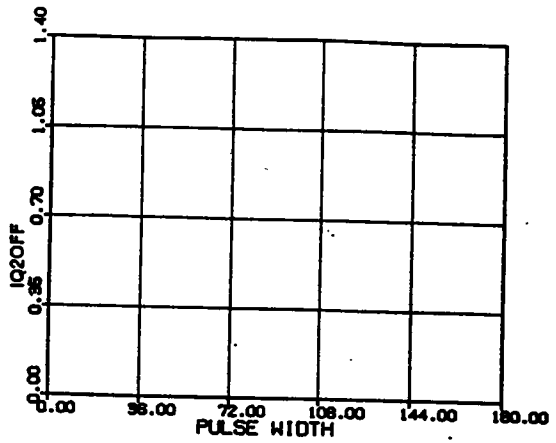
• Average diode current (D1,D3)



• Average diode current (D2,D4)

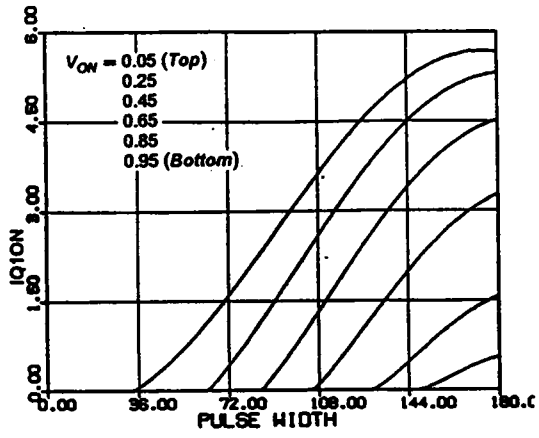


• Switch turn-off current (Q1,Q3)

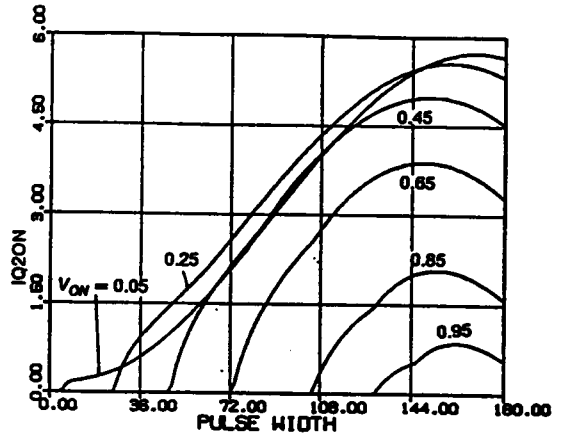


• Switch turn-off current (Q2,Q4)

Figure B.6.2 Continued



• Switch turn-on current ($Q1, Q3$)



• Switch turn-on current ($Q2, Q4$)

Figure B.6.2 Continued

APPENDIX B.7

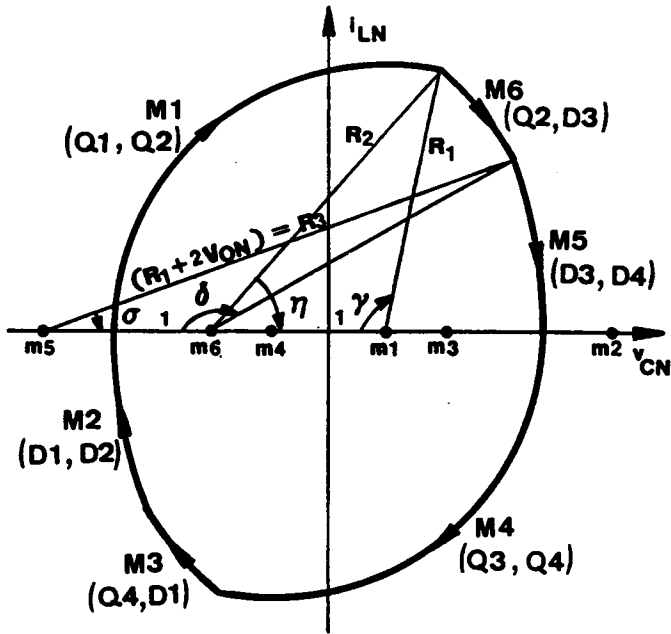
CALCULATION OF TRAJECTORY PARAMETERS ABOVE RESONANT FREQUENCY

The equations for solving the parameters of the equilibrium trajectories of a CM-SRC operating above resonant frequency are included in this section.

The equations for solving the parameters of Mode-A Trajectory are shown in Figure B.7.1.

The equations for solving the parameters of Mode-B Trajectory are shown in Figure B.7.2.

The equations for solving the parameters of Mode-C Trajectory are shown in Figure B.7.3.



$$\cos \gamma = \frac{1 + R_1^2 - R_2^2}{2R_1},$$

$$\cos \eta = \frac{1 + R_2^2 - R_1^2}{2R_2},$$

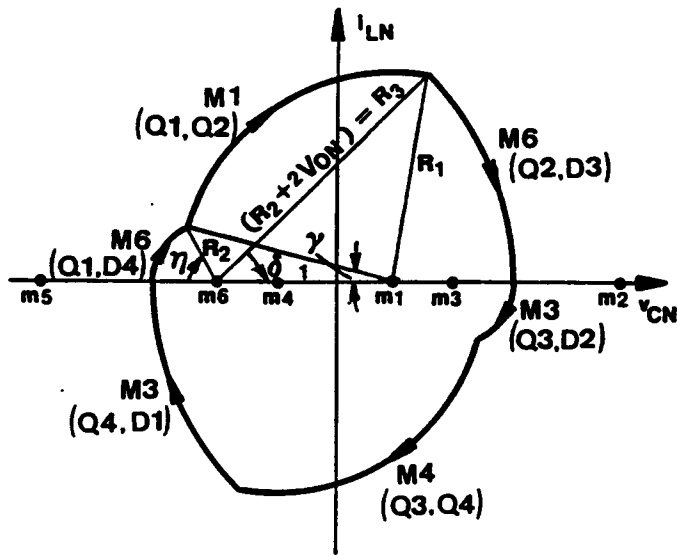
$$\cos \delta = \frac{1 + R_1^2 - (R_1 + 2V_{ON})^2}{2R_1},$$

$$\cos\left(\frac{\beta_S}{\omega_{SN}} - \gamma\right) = \frac{1 + (R_1 + 2V_{ON})^2 - R_2^2}{2(R_1 + 2V_{ON})},$$

$$\frac{\pi}{\omega_{SN}} = \delta + \eta - \pi + \frac{\beta_S}{\omega_{SN}}.$$

$$(1 - V_{ON}) \leq R_1, \quad 0 \leq R_2, \quad 0 \leq \eta, \quad \delta \leq \pi, \quad 0 \leq \gamma \leq \frac{\pi}{\omega_{SN}}.$$

Figure B.7.1 Mode-A Trajectory Above Resonant Frequency



$$\cos \gamma = \frac{1 + R_1^2 - R_2^2}{2R_1},$$

$$\cos(\pi - \eta) = \frac{1 + R_2^2 - R_1^2}{2R_2},$$

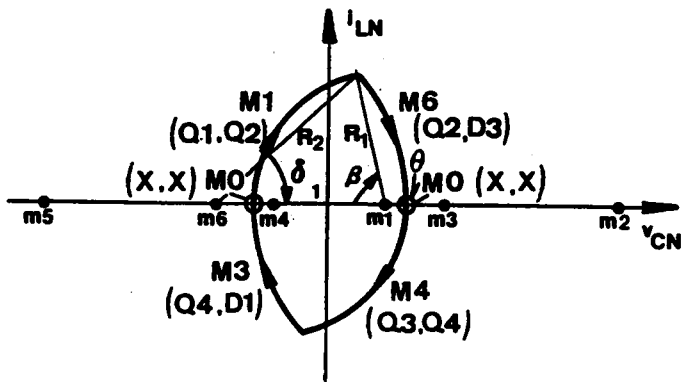
$$\cos\left(\gamma + \frac{\beta_S}{\omega_{SN}}\right) = \frac{1 + R_1^2 - (R_2 + 2V_{ON})^2}{2R_1},$$

$$\cos \delta = \frac{1 + (R_2 + 2V_{ON})^2 - R_1^2}{2(R_2 + 2V_{ON})},$$

$$\frac{\pi}{\omega_{SN}} = \delta + \eta + \frac{\beta_S}{\omega_{SN}}.$$

$$0 \leq R_1, R_2, \quad 0 \leq \gamma \leq \pi, \quad 0 \leq \eta, \delta \leq \frac{\pi}{\omega_{SN}}.$$

Figure B.7.2 Mode-B Trajectory Above Resonant Frequency



$$\cos\left(\frac{\beta_S}{\omega_{SN}}\right) = \frac{1 + R_1^2 - R_2^2}{2R_1},$$

$$\cos \delta = \frac{1 + R_2^2 - R_1^2}{2R_2},$$

$$\frac{\pi}{\omega_{SN}} = \delta + \theta + \frac{\beta_S}{\omega_{SN}},$$

$$R_2 = R_1 - 1 + 2V_{ON}.$$

$$(1 - V_{ON}) \leq R_1 \leq 1, \quad V_{ON} \leq R_2 \leq 2V_{ON}, \quad 0 \leq \theta, \delta \leq \frac{\pi}{\omega_{SN}}.$$

Figure B.7.3 Mode-C Trajectory Above Resonant Frequency

FORTRAN Program for Calculating Trajectory Parameters Above Resonant Frequency

```

C *****
C *****
C ***** PROGRAM NAME : SC10PAR.FOR
C *****
C ***** FUNCTION : CALCULATE EQUILIBRIUM STATE TRAJECTORY PARAMETERS
C ***** FOR A GIVEN OUTPUT VOLTAGE, VON, AND OPERATING
C ***** FREQUENCY, WN. B ANGLE : VARYING.
C *****
C *****
C *****
C ***** REFER TO THE FIGURES IN APPENDIX B.7 FOR THE MEANINGS OF X(I)'S
C *****
C IMPLICIT REAL*4 (A-H,O-Z)
C EXTERNAL FCNA, FCNB, FCNC
C COMMON WTS, VON, PI, BT
C DIMENSION X(5), XGUESS(5), Y(5), YY(5)
C PI=4.*ATAN(1.)
C J=0
10 READ(5,1000) WN, VON, INDEX
C IF(INDEX.NE.1) STOP
C READ(5,2100) (XGUESS(K), K = 1,5)
C
C *** A GOOD GUESS FOR X(K), K = 1,5 IS
C *** 6.6, 6.8, 1.9, 1.4, 1.7 FOR WN= 1.1, 1.2,
C *** 4., 4., 2., 2., 1.5 FOR WN= 1.3,
C *** 2.8, 2.8, 1.7, 1.7, 1.3 FOR WN= 1.4.
C
C JA = 0
C JB = 0
C JC = 0
C WTS = PI/WN
C ERREL = .0001
C ITMAX = 200
C A3 = ACOS(VON)
C B3 = ACOS(1-2*VON**2)
C W1N = PI/(A3 + B3)
C CALL BETA12(ERREL,ITMAX,B12,J)
C J = J + 1
C IF(WN.LT.W1N) THEN
C BETA1 = B12
C BETA2 = B3
C ELSE
C BETA1 = B12
C BETA2 = B12
C ENDIF
C BT = WTS
99 IF(BT.GE.BETA1) THEN
C JJ = 1
C ELSE
C IF(BT.GE.BETA2) THEN
C JJ = 2
C ELSE

```

```

        JJ=3
        ENDIF
        ENDIF
        GO TO (100,200,300), JJ
100 N=5
    IC=0
    IF(JA.EQ.0) THEN
        Y(1)=XGUESS(1)
        Y(2)=XGUESS(2)
        Y(3)=XGUESS(3)
        Y(4)=XGUESS(4)
        Y(5)=XGUESS(5)
    ENDIF
110 XGUESS(1)=Y(1)-IC*.5
    XGUESS(2)=Y(2)-IC*.5
    XGUESS(3)=Y(3)-IC*WTS/20
    XGUESS(4)=Y(4)-IC*WTS/20
    XGUESS(5)=Y(5)-IC*WTS/20
    CALL NEQNF(FCNA,ERREL,N,ITMAX,XGUESS,X,FNORM)
    IF(X(1).GE.(1-VON).AND.X(2).GE.VON.AND.
1 X(3).LE.PI.AND.X(3).GE.0.AND.X(4).GE.0
1 .AND.X(4).LE.PI.AND.X(5).GE.0.AND.
1 X(5).LE.PI) THEN
        ID=1
        JA=JA+1
        DO 115 K=1,N
115 Y(K)=X(K)
        BS=BT*180/WTS
        WRITE(6,2000) ID,WTS,VON,BS,(X(I), I=1,N)
        GO TO 999
    ELSE
        IF(IC.GE.20) STOP
        IC=IC+1
        GO TO 110
    ENDIF
200 N=5
    IC=0
    IF(JB.EQ.0) THEN
        YY(2)=Y(1)
        YY(1)=Y(1)-1
        YY(5)=Y(4)
        YY(3)=0.
        YY(4)=0.
    ENDIF
235 XGUESS(1)=YY(1)
    XGUESS(2)=YY(2)
    XGUESS(3)=YY(3)
    XGUESS(4)=YY(4)+IC*0.1
    XGUESS(5)=YY(5)
    DO 236 JK=1,N
236 IF(XGUESS(JK).LT.0) XGUESS(JK)=0
    CALL NEQNF(FCNB,ERREL,N,ITMAX,XGUESS,X,FNORM)
    IF(X(1).GE.0.AND.X(2).GE.0.AND.X(3).GE.0.AND.
1 X(3).LE.PI.AND.X(4).LE.WTS.AND.X(4).GE.0.AND.
1 X(5).LE.WTS.AND.X(5).GE.0) THEN
        ID=2
        JB=JB+1
        DO 250 K=1,N

```

```

250  YY(K) = X(K)
      BS = BT*180/WTS
      WRITE(6,2000) ID,WTS,VON,BS,(X(I), I = 1,N)
      IC = 0
      GO TO 999
      ELSE
      IF(XGUESS(4).GE.WTS) THEN
        BT = BT + 0.015
        IC = 0.
        GO TO 99
      ELSE
        IC = IC + 1
        GO TO 235
      ENDIF
    ENDIF
300  N = 3
      IC = 0
      IF(JC.EQ.0) THEN
        Y(1) = 1
        Y(3) = ACOS(VON)
        Y(2) = WTS - Y(3) - ACOS(1 - 2*VON**2)
      ENDIF
360  XGUESS(1) = Y(1) - IC*0.1
      XGUESS(2) = Y(2) + IC*0.1
      XGUESS(3) = Y(3) - IC*0.1
      DO 361 JK = 1,N
361  IF(XGUESS(JK).LT.0) XGUESS(JK) = 0
      CALL NEQNF(FCNC,ERREL,N,ITMAX,XGUESS,X,FNORM)
      IF(X(1).LE.1.AND.X(2).LE.WTS.AND.X(2).GE.0.AND.
1  X(3).LT.WTS.AND.X(3).GE.0) THEN
        ID = 3
        JC = JC + 1
        DO 350 K = 1,N
350  Y(K) = X(K)
        BS = BT*180/WTS
        WRITE(6,2000) ID,WTS,VON,BS,(X(I), I = 1,N)
        IC = 0
        GO TO 999
        ELSE
        IF(IC.GE.20) STOP
        IC = IC + 1
        GO TO 360
      ENDIF
999  IF(BT.LE.0) GO TO 10
      BT = BT - WTS/100
      IF(BT.LT.0) BT = 0
      GO TO 99
1000 FORMAT(2F10.5,I1)
2000 FORMAT(1X,I1,F8.5,F7.4,F10.5,5F9.5)
2100 FORMAT(5F9.5)
      END
C
C *****
C *****
C *****
C
      SUBROUTINE FCNA(X,F,N)
      DIMENSION X(N), F(N)

```

```

COMMON WTS, VON, PI, BT
F(1) = 2*(X(1) + 2*VON)*COS(BT-X(5)) - (1 + (X(1) +
1 2*VON)**2-X(2)**2)
F(2) = 2*X(2)*COS(X(3)) - (1 + X(2)**2 - (X(1) + 2*VON)**2)
F(3) = 2*X(2)*COS(X(4)) - (1 + X(2)**2 - X(1)**2)
F(4) = 2*X(1)*COS(X(5)) - (1 + X(1)**2 - X(2)**2)
F(5) = WTS - BT - X(3) - X(4) + PI
RETURN
END

```

C
C
C
C
C

```

SUBROUTINE FCNB(X,F,N)
DIMENSION X(N), F(N)
COMMON WTS, VON, PI, BT
F(1) = -2*X(1)*COS(X(5)) - (1 + X(1)**2 - X(2)**2)
F(2) = 2*(X(1) + 2*VON)*COS(X(4))
1 -(1 + (X(1) + 2*VON)**2 - X(2)**2)
F(3) = 2*X(2)*COS(X(3)) - (1 + X(2)**2 - X(1)**2)
F(4) = 2*X(2)*COS(X(3) + BT) - (1 + X(2)**2 - (X(1) + 2*VON)**2)
F(5) = X(5) + X(4) - WTS + BT
RETURN
END

```

C
C
C
C
C

```

SUBROUTINE FCNC(X,F,N)
DIMENSION X(N), F(N)
COMMON WTS, VON, PI, BT
F(1) = 2*X(1)*COS(BT) - (1 + X(1)**2 - (X(1) - 1 + 2*VON)**2)
F(2) = 2*(X(1) - 1 + 2*VON)*COS(X(2))
1 -(1 + (X(1) - 1 + 2*VON)**2 - X(1)**2)
F(3) = X(2) + X(3) + BT - WTS
RETURN
END

```

C
C
C
C
C

```

SUBROUTINE BETA12(ERREL,ITMAX,B12,JD)
EXTERNAL F12
COMMON WTS, VON, PI, BT
DIMENSION X(2), XGUESS(2)
N = 2
J = 0
IF(JD.EQ.0) THEN
  X(1) = 10.
  X(2) = WTS
ENDIF
121 XGUESS(1) = X(1) - J*0.45
XGUESS(2) = X(2) - J*WTS/20.
CALL NEQNF(F12,ERREL,N,ITMAX,XGUESS,X, FNORM)
IF(X(1).GE.(1-VON).AND.X(2).GE.0.AND.

```



```

1  X(2).LE.WTS) THEN
   B12= X(2)
   RETURN
  ELSE
   IF(J.EQ.20) THEN
    WRITE(6,1200)
    STOP
   ELSE
    J=J+1
    GO TO 121
   ENDIF
  ENDIF
1200 FORMAT(/,5X,'ERROR : CAN'T FIND B12  ',/)
END

C
C *****
C *****
C *****
C

SUBROUTINE F12(X,F,N)
DIMENSION X(N), F(N)
COMMON WTS, VON, PI, BT
F(1)= 2*X(1)*COS(X(2))-(1+X(1)**2-(2*VON-1+X(1))**2)
F(2)= 2*(2*VON-1+X(1))*COS(WTS-X(2))
1  -(1+(2*VON-1+X(1))**2-X(1)**2)
RETURN
END

```

APPENDIX B.8
EXPRESSIONS FOR CIRCUIT SALIENT FEATURES
ABOVE RESONANT FREQUENCY

Circuit Salient Features	Circuit Operating Modes		
	Mode A	Mode B	Mode C
V_{CPK}	$R_1 - 1 + V_{ON}$	$R_2 + V_{ON}$	$R_1 - 1 + V_{ON}$
I_{AV}	$\frac{Da + Db + Dc}{\omega_0 T_s}$	$\frac{Da + Db + Dc}{\omega_0 T_s}$	$\frac{Da + Db}{\omega_0 T_s}$
I_{RMS}	$\left[\frac{Ra + Rb + Rc}{\omega_0 T_s} \right]^{\frac{1}{2}}$	$\left[\frac{Ra + Rb + Rc}{\omega_0 T_s} \right]^{\frac{1}{2}}$	$\left[\frac{Ra + Rb}{\omega_0 T_s} \right]^{\frac{1}{2}}$
I_{Q1RMS}	$\left[\frac{Ra}{\omega_0 T_s} \right]^{\frac{1}{2}}$	$\left[\frac{Ra + Rb}{\omega_0 T_s} \right]^{\frac{1}{2}}$	$\left[\frac{Ra}{\omega_0 T_s} \right]^{\frac{1}{2}}$
I_{Q2RMS}	$\left[\frac{Ra + Rb}{\omega_0 T_s} \right]^{\frac{1}{2}}$	$\left[\frac{Rb + Rc}{\omega_0 T_s} \right]^{\frac{1}{2}}$	$\left[\frac{Ra + Rb}{\omega_0 T_s} \right]^{\frac{1}{2}}$
I_{D1AV}	$\frac{Db + Dc}{\omega_0 T_s}$	$\frac{Dc}{\omega_0 T_s}$	$\frac{Db}{\omega_0 T_s}$
I_{D2AV}	$\frac{Dc}{\omega_0 T_s}$	$\frac{Da}{\omega_0 T_s}$	0
I_{Q1off}	$R_2 \sin \eta$	$R_3 \sin \delta$	$R_2 \sin \delta$
I_{Q2off}	$R_3 \sin \sigma$	0	0
I_{Q1on}	0	0	0
I_{Q2on}	0	$R_1 \sin \gamma$	0
$Da =$	$R_1(1 - \cos \gamma)$	$R_2(1 - \cos \eta)$	$R_1(1 - \cos \beta)$
$Db =$	$-R_2(\cos \eta + \cos \delta)$	$R_1(\cos \gamma - \cos(\gamma + \beta))$	$R_2(1 - \cos \delta)$
$Dc =$	$R_3(1 - \cos \sigma)$	$R_3(1 - \cos \delta)$	
$Ra =$	$\frac{R_1^2}{2} \left(\gamma - \frac{\sin 2\gamma}{2} \right)$	$\frac{R_2^2}{2} \left(\eta - \frac{\sin 2\eta}{2} \right)$	$\frac{R_1^2}{2} \left(\beta - \frac{\sin 2\beta}{2} \right)$
$Rb =$	$\frac{R_2^2}{2} \left(\delta + \eta - \pi - \left(\frac{\sin 2\delta}{2} + \frac{\sin 2\eta}{2} \right) \right)$	$\frac{R_1^2}{2} \left(\beta + \frac{\sin 2\gamma}{2} - \frac{\sin(2\gamma + 2\beta)}{2} \right)$	$\frac{R_2^2}{2} \left(\delta - \frac{\sin 2\delta}{2} \right)$
$Rc =$	$\frac{R_3^2}{2} \left(\sigma - \frac{\sin 2\sigma}{2} \right)$	$\frac{R_3^2}{2} \left(\delta - \frac{\sin 2\delta}{2} \right)$	

FORTRAN Programs for Calculating Circuit Salient Features of a CM-SRC Operating Above Resonant Frequency

```

C *****
C *****
C ***** PROGRAM NAME : SC100OUT.FOR
C *****
C ***** FUNCTION : CALCULATE IAV, IRMS, VPK, IQARMS, IQBRMS,
C ***** IDA, IDB, IAOFF, IBOFF, IAON, IBON. SRC,
C ***** ABOVE RESONANT FREQUENCY.
C *****
C *****
C *****
C
REAL IAV, IRMS, IQARMS, IQBRMS, IDA, IDB, IAOFF, IBOFF,
1 IAON, IBON
DIMENSION X(5)
PI=4.*ATAN(1.)
10 READ(5,1000) ID,WTS,VON,BS, (X(I),I= 1,5)
GO TO (100,200,300), ID
100 R = X(1)
R1 = X(2)
B1 = X(3)
B2 = X(4)
AL = X(5)
B = WTS-X(3)-X(4) + PI
GA = B-AL
IAV = (R*(1-COS(AL))-R1*(COS(B1) + COS(B2))
1 + (R + 2*VON)*(1-COS(GA)))/WTS
IRMS = ((R**2*.5*(AL-.5*SIN(2*AL)) + R1**2*.5*(B2 + B1-PI
1 -.5*(SIN(2*B2) + SIN(2*B1))) + (R + 2*VON)**2*.5*
1 (GA-.5*SIN(2*GA)))/WTS)**.5
VPK = R-1 + VON
IDA = (-R1*(COS(B1) + COS(B2)) + (R + 2*VON)*(1-COS(GA)))/WTS
IQARMS = (R**2*.5*(AL-.5*SIN(2*AL))
1 /WTS)**.5
IAOFF = R1*SIN(B2)
IAON = 0.
IDB = (R + 2*VON)*(1-COS(GA))/WTS
IQBRMS = ((R**2*.5*(AL-.5*SIN(2*AL)) + R1**2*.5*(B2 + B1-PI
1 -.5*(SIN(2*B1) + SIN(2*B2))))/WTS)**.5
IBOFF = (R + 2*VON)*SIN(GA)
IBON = 0.
GO TO 20
200 R = X(1)
R1 = X(2)
B1 = X(3)
GA = X(4)
AL = X(5)
B = WTS-GA-AL
IAV = (R*(1-COS(AL)) + R1*(COS(B1)-
1 COS(B1 + B)) + (R + 2*VON)*(1-COS(GA)))/WTS
IRMS = ((R**2*.5*(AL-.5*SIN(2*AL)) + R1**2*
1 .5*(B + .5*SIN(2*B1)-.5*SIN(2*B1 + 2*B)) +
1 (R + 2*VON)**2*.5*(GA-.5*SIN(2*GA)))/
1 /WTS)**.5
VPK = R + VON

```

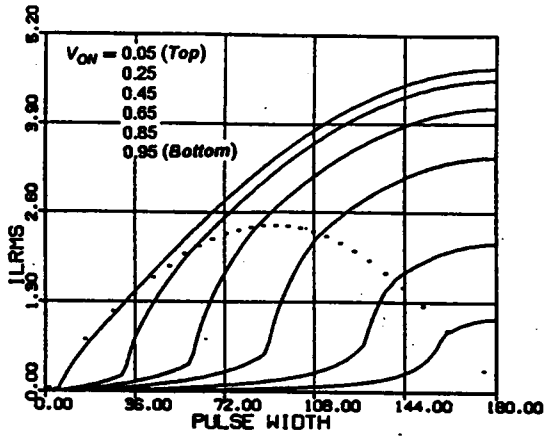
```

IDA = (R + 2*VON)*(1-COS(GA))/WTS
IQARMS = ((R**2*.5*(AL-.5*SIN(2*AL)) + R1**2*
1 .5*(B + .5*SIN(2*B1)-.5*SIN(2*B1 + 2*B)))
1 /WTS)**.5
IAOFF = (R + 2*VON)*SIN(GA)
IAON = 0.
IDB = R*(1-COS(AL))/WTS.
IQBRMS = ((R1**2*
1 .5*(B + .5*SIN(2*B1)-.5*SIN(2*B1 + 2*B)) +
1 (R + 2*VON)**2*.5*(GA-.5*SIN(2*GA)))
1 /WTS)**.5
IBOFF = 0.
IBON = R1*SIN(B1)
GO TO 20
300 R = X(1)
GA = X(2)
FI = X(3)
B = WTS-GA-FI
IAV = (R*(1-COS(B)) + (R-1 + 2*VON)*(1-COS(GA)))
1 /WTS
IRMS = ((R**2*.5*(B-.5*SIN(2*B)) + (R-1 + 2*VON)**2
1 *.5*(GA-.5*SIN(2*GA)))/WTS)**.5
VPK = R-1 + VON
IDA = (R-1 + 2*VON)*(1-COS(GA))/WTS
IQARMS = (R**2*.5*(B-.5*SIN(2*B))/WTS)**.5
IAOFF = (R-1 + 2*VON)*SIN(GA)
IAON = 0
IDB = 0.
IQBRMS = IRMS
IBOFF = 0.
IBON = 0.
20 WRITE(6,2000) BS,IAV,IRMS,VPK
WRITE(7,2000) BS,IQARMS,IDA,IAOFF,IAON
WRITE(8,2000) BS,IQBRMS,IDB,IBOFF,IBON
GO TO 10
1000 FORMAT(1X,I1,F8.5,F7.4,F10.5,5F9.5)
2000 FORMAT(5F14.5)
END

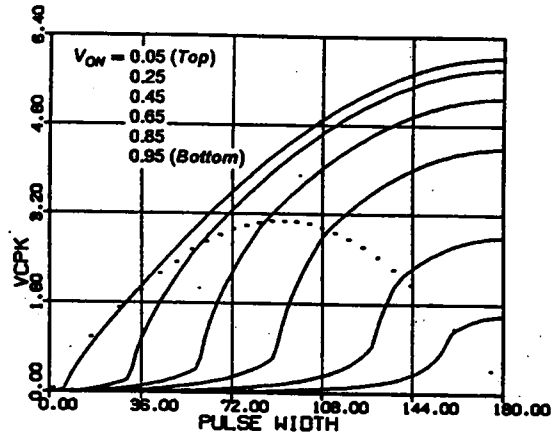
```

APPENDIX B.9

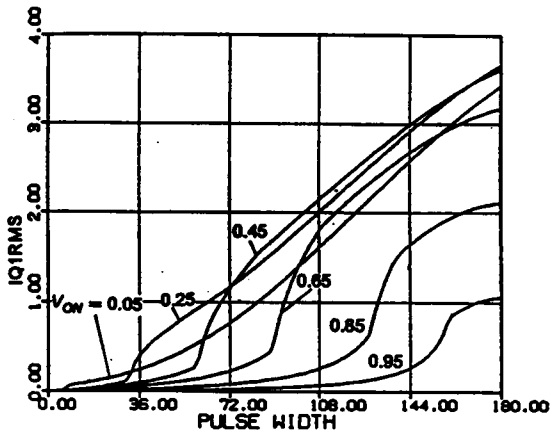
DC CHARACTERISTICS ABOVE RESONANT FREQUENCY



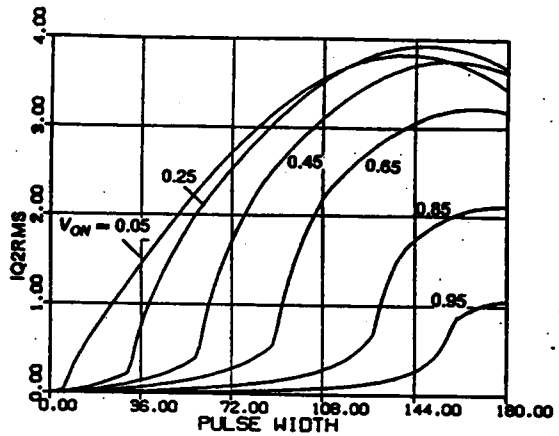
• *RMS inductor current*



• *Peak capacitor voltage*

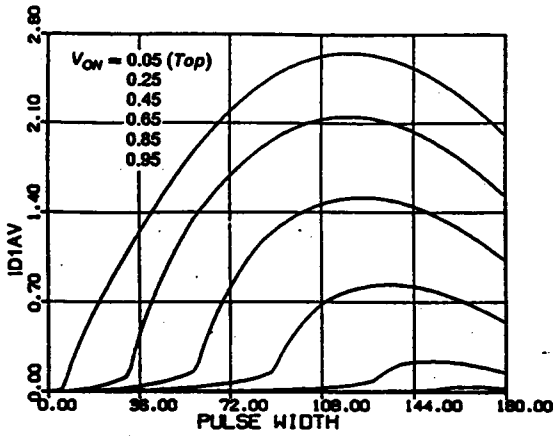


• *RMS switch current (Q1,Q3)*

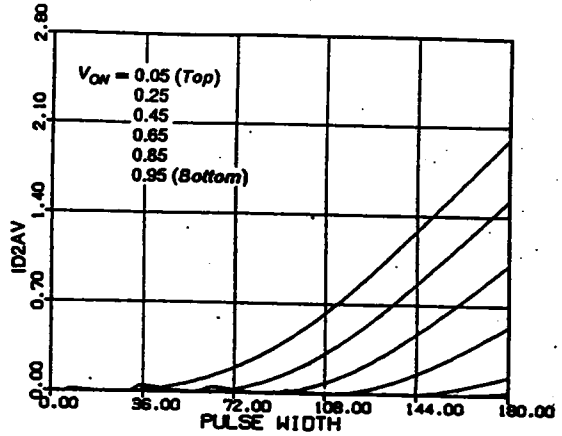


• *RMS switch current (Q2,Q4)*

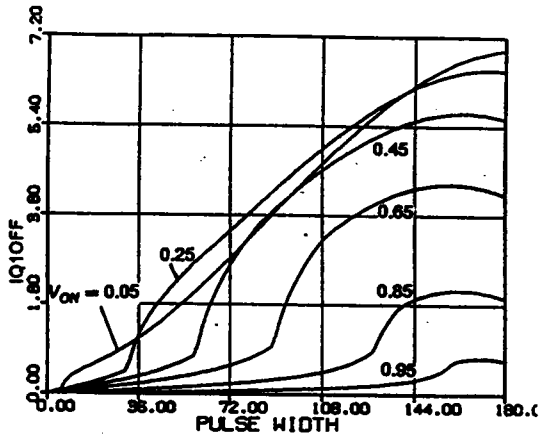
Figure B.9.1 DC Characteristics for $\omega_{SN} = 1.1$



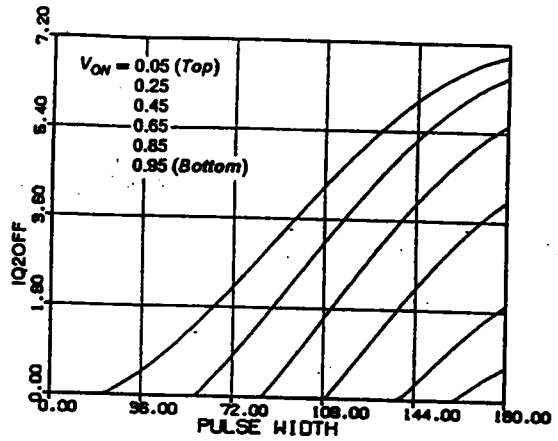
• Average diode current (D1,D3)



• Average diode current (D2,D4)

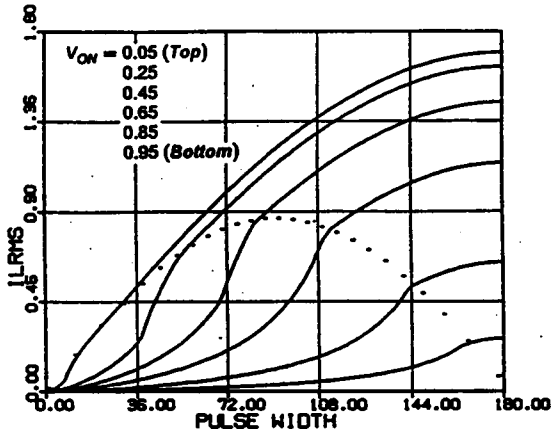


• Switch turn-off current (Q1,Q3)

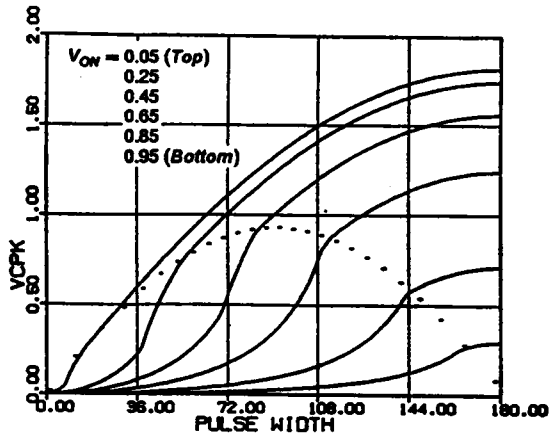


• Switch turn-off current (Q2,Q4)

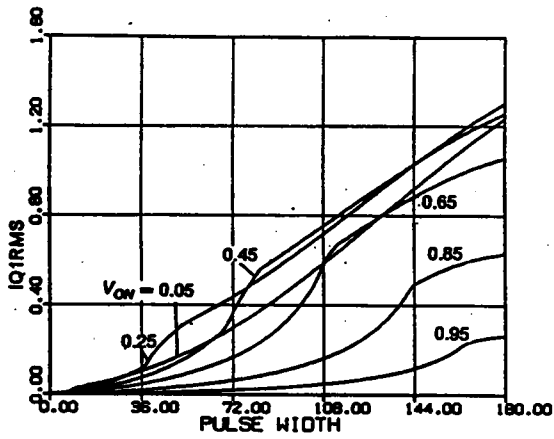
Figure B.9.1 Continued



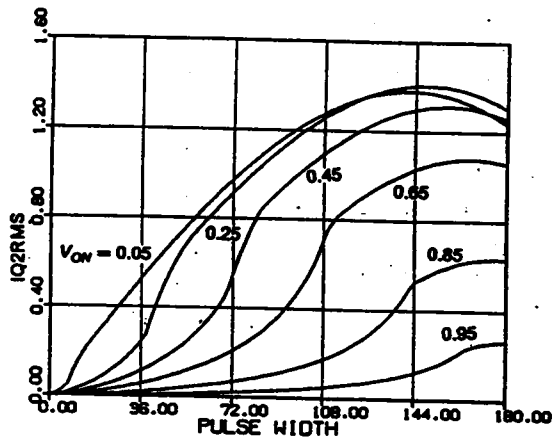
• *RMS inductor current*



• *Peak capacitor voltage*

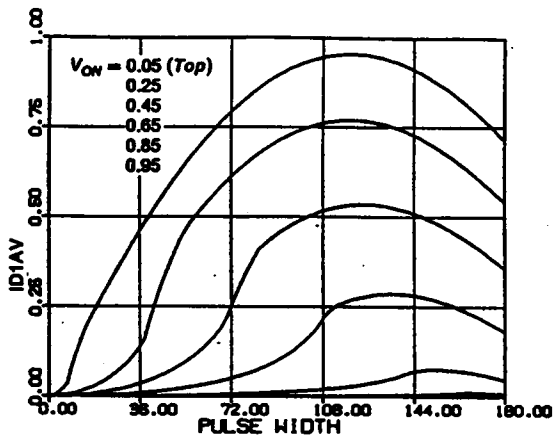


• *RMS switch current (Q1,Q3)*

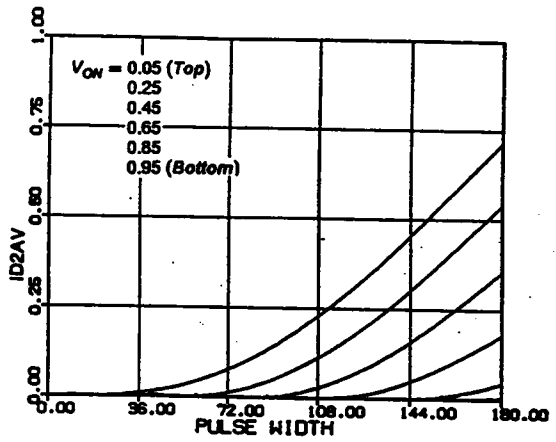


• *RMS switch current (Q2,Q4)*

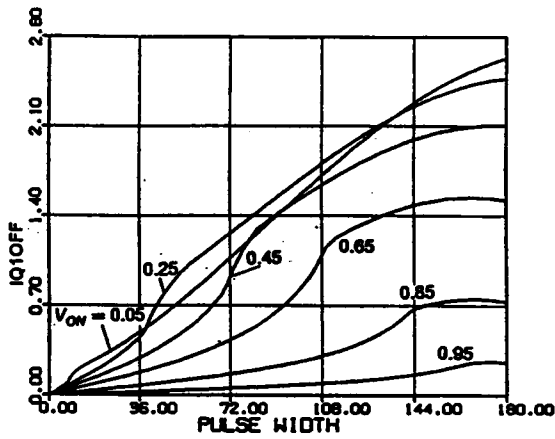
Figure B.9.2 DC Characteristics for $\omega_{SN} = 1.3$



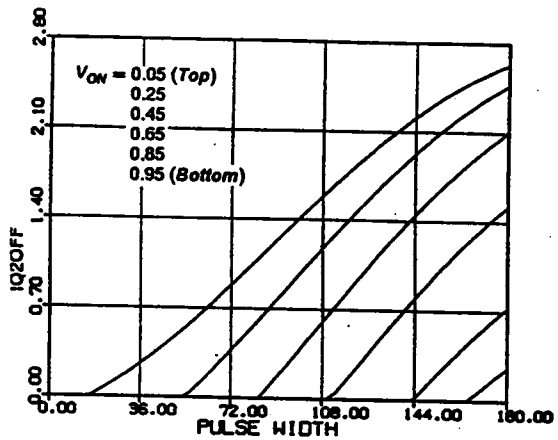
• Average diode current (*D1,D3*)



• Average diode current (*D2,D4*)

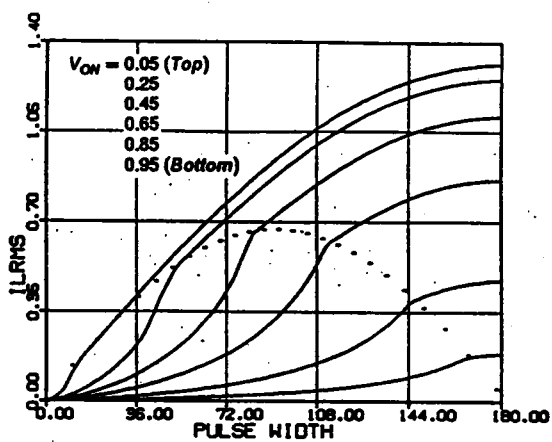


• Switch turn-off current (*Q1,Q3*)

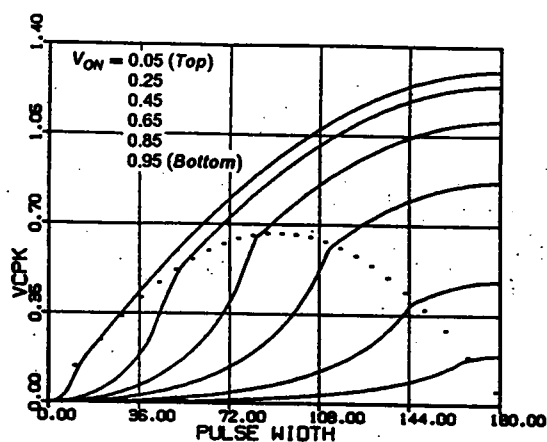


• Switch turn-off current (*Q2,Q4*)

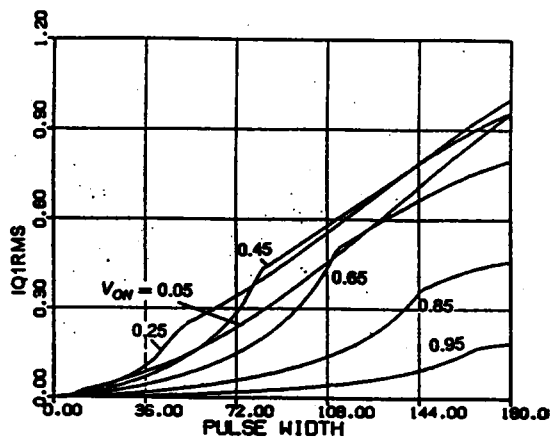
Figure B.9.2 Continued



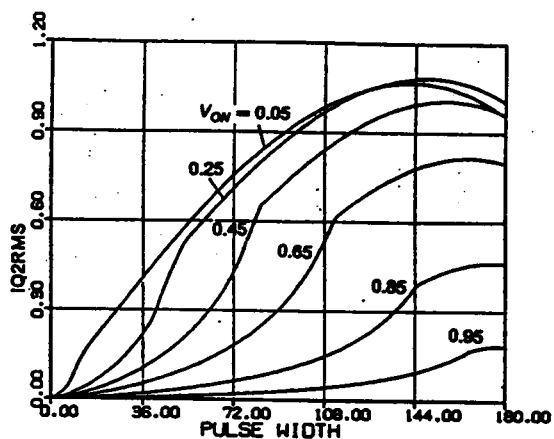
• RMS inductor current



• Peak capacitor voltage

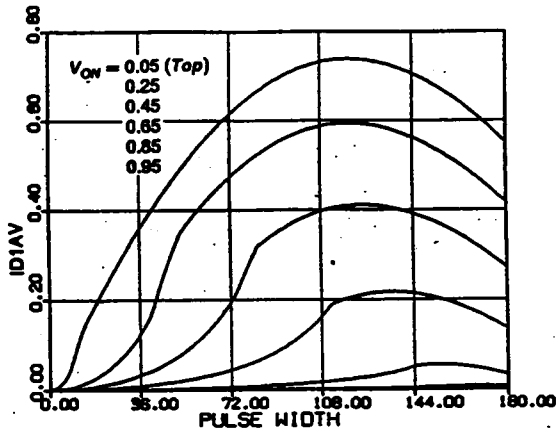


• RMS switch current (Q1,Q3)

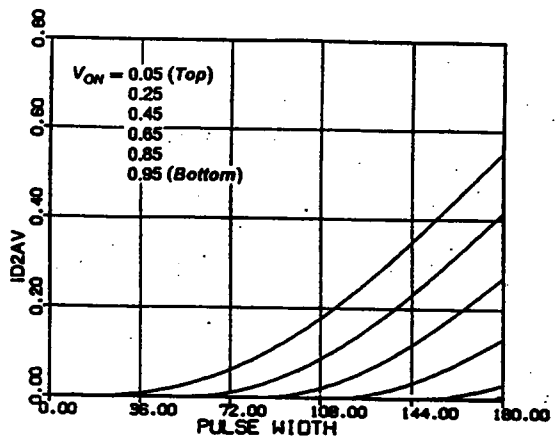


• RMS switch current (Q2,Q4)

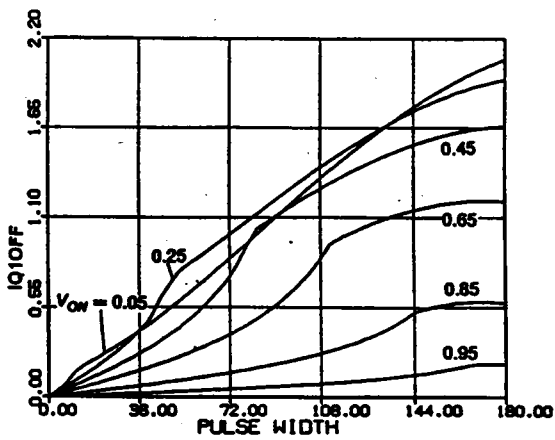
Figure B.9.3 DC Characteristics for $\omega_{SN} = 1.4$



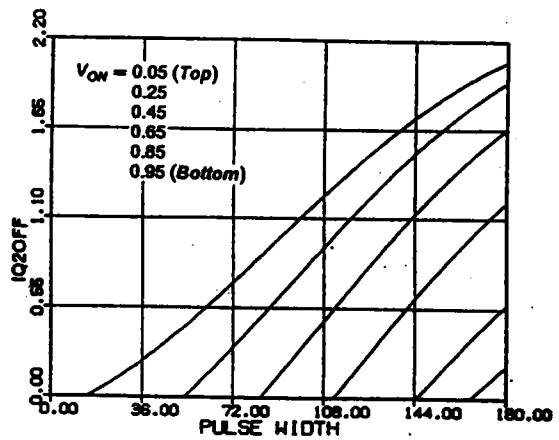
• Average diode current ($D1, D3$)



• Average diode current ($D2, D4$)



• Switch turn-off current ($Q2, Q4$)



• Switch turn-off current ($Q1, Q3$)

Figure B.9.3 Continued

APPENDIX B.10

GENERATION OF CIRCUIT WAVEFORMS OF A CM-SRC

Fortran Program for Generating Capacitor Voltage and Inductor Current Waveforms (Below Resonant Frequency)

```
C *****
C *****
C ***** PROGRAM NAME : SCWAVE.FOR
C ***** FUNCTION : GENERATE STEADY-STATE WAVEFORMS FOR THE INDUCTOR
C ***** CURRENT AND CAPACITOR VOLTAGE OF A CM-SRC
C ***** OPERATING ABOVE RESONANT FREQUENCY.
C *****
C *****
C
REAL ILN, VCN
DIMENSION X(6)
PI = 4.*ATAN(1.)
10 READ(5,1050) WN
11 READ(5,1000) J,BT,VON,(X(K), K = 1,6)
C
C ***** THE INPUTS ARE OBTAINED FROM PROGRAM SCPAR.FOR
C
IF(J.EQ.0) STOP
WT = 0.
YT = 0.
GO TO (100,200,300,400,500,600), J
100 R = X(1)
R1 = X(2)
B1 = X(3)
B2 = X(4)
AL = X(5)
GA = X(6)
T = PI-B1
101 IF(T.LT.B2) GO TO 102
ILN = R1*SIN(T)
VCN = R1*COS(T)-VON
WRITE(7,2000) WT, ILN
WRITE(6,2000) WT,VCN,ILN
T = T-(PI-B2-B1)/30.
WT = WT + (PI-B2-B1)*180*WN/PI/30.
GO TO 101
102 T = GA
YT = YT + (PI-B2-B1)
WT = YT*180*WN/PI
103 IF(T.LT.0) GO TO 104
ILN = R*SIN(T)
VCN = R*COS(T) + 1-VON
WRITE(7,2000) WT, ILN
WRITE(6,2000) WT,VCN,ILN
T = T-GA/50.
WT = WT + GA*180*WN/PI/50.
```

```

GO TO 103
104 T=0.
   YT=YT+GA
   WT=YT*180*WN/PI
105 IF(T.LT.-AL) GO TO 106
   ILN=(R-2*VON)*SIN(T)
   VCN=(R-2*VON)*COS(T)+1+VON
   WRITE(7,2000) WT, ILN
   WRITE(6,2000) WT,VCN,ILN
   T=T-AL/30.
   WT=WT+AL*180*WN/PI/30.
   GO TO 105
106 T=-B1
   YT=YT+AL
   WT=YT*180*WN/PI
107 IF(T.LT.(-PI+B2)) GO TO 108
   ILN=R1*SIN(T)
   VCN=R1*COS(T)+VON
   WRITE(7,2000) WT, ILN
   WRITE(6,2000) WT,VCN,ILN
   T=T-(PI-B2-B1)/30.
   WT=WT+(PI-B2-B1)*180*WN/PI/30.
   GO TO 107
108 T=-PI+GA
   YT=YT+(PI-B2-B1)
   WT=YT*180*WN/PI
109 IF(T.LT.-PI) GO TO 110
   ILN=R*SIN(T)
   VCN=R*COS(T)-1+VON
   WRITE(7,2000) WT, ILN
   WRITE(6,2000) WT,VCN,ILN
   T=T-GA/50.
   WT=WT+GA*180*WN/PI/50.
   GO TO 109
110 T=PI
   YT=YT+GA
   WT=YT*180*WN/PI
111 IF(T.LT.(PI-AL)) GO TO 112
   ILN=(R-2*VON)*SIN(T)
   VCN=(R-2*VON)*COS(T)-1-VON
   WRITE(7,2000) WT, ILN
   WRITE(6,2000) WT,VCN,ILN
   T=T-AL/30.
   WT=WT+AL*180*WN/PI/30.
   GO TO 111
112 T=PI-B1
   YT=YT+AL
   WT=YT*180*WN/PI
113 IF(T.LT.B2) GO TO 10
   ILN=R1*SIN(T)
   VCN=R1*COS(T)-VON
   WRITE(7,2000) WT, ILN
   WRITE(6,2000) WT,VCN,ILN
   T=T-(PI-B1-B2)/30.
   WT=WT+(PI-B1-B2)*180*WN/PI/30.
   GO TO 113
200 R=X(1)
   B1=X(2)

```

```

FI = X(3)
AL = X(4)
T = PI
201 IF(T.LT.(PI-AL)) GO TO 202
ILN = (R + 1-2*VON)*SIN(T)
VCN = (R + 1-2*VON)*COS(T)-VON
WRITE(7,2000) WT, ILN
WRITE(6,2000) WT,VCN,ILN
T = T-AL/50.
WT = WT + AL*180*WN/PI/50.
GO TO 201
202 T = B1
YT = YT + AL
WT = YT*180*WN/PI
203 IF(T.LT.0) GO TO 204
ILN = R*SIN(T)
VCN = R*COS(T) + 1-VON
WRITE(7,2000) WT, ILN
WRITE(6,2000) WT,VCN,ILN
T = T-B1/30.
WT = WT + B1*180*WN/PI/30.
GO TO 203
204 T = FI
YT = YT + B1
WT = YT*180*WN/PI
205 IF(T.LT.0) GO TO 206
ILN = 0.
VCN = R + 1-VON
WRITE(7,2000) WT,ILN
WRITE(6,2000) WT,VCN,ILN
T = T-FI/30.
WT = WT + FI*180*WN/PI/30.
GO TO 205
206 T = 0.
YT = YT + FI
WT = YT*180*WN/PI
207 IF(T.LT.-AL) GO TO 208
ILN = (R + 1-2*VON)*SIN(T)
VCN = (R + 1-2*VON)*COS(T) + VON
WRITE(7,2000) WT, ILN
WRITE(6,2000) WT,VCN,ILN
T = T-AL/50.
WT = WT + AL*180*WN/PI/50.
GO TO 207
208 T = -PI + B1
YT = YT + AL
WT = YT*180*WN/PI
209 IF(T.LT.-PI) GO TO 210
ILN = R*SIN(T)
VCN = R*COS(T)-1 + VON
WRITE(7,2000) WT, ILN
WRITE(6,2000) WT,VCN,ILN
T = T-B1/30.
WT = WT + B1*180*WN/PI/30.
GO TO 209
210 T = FI
YT = YT + B1
WT = YT*180*WN/PI

```

```

211 IF(T.LT.0.) GO TO 212
    ILN=0.
    VCN=-R-1+VON
    WRITE(7,2000) WT, ILN
    WRITE(6,2000) WT,VCN,ILN
    T=T-FI/30.
    WT=WT+FI*180*WN/PI/30.
    GO TO 211
212 T=PI
    YT=YT+FI
    WT=YT*180*WN/PI
213 IF(T.LT.(PI-AL)) GO TO 10
    ILN=(R+1-2*VON)*SIN(T)
    VCN=(R+1-2*VON)*COS(T)-VON
    WRITE(7,2000) WT, ILN
    WRITE(6,2000) WT,VCN,ILN
    T=T-AL/50.
    WT=WT+AL*180*WN/PI/50.
    GO TO 213
300 R=X(1)
    R1=X(2)
    B1=X(3)
    AL=X(4)
    GA=X(5)
    T=-PI+GA
301 IF(T.LT.-PI) GO TO 302
    ILN=(R1+2*VON)*SIN(T)
    VCN=(R1+2*VON)*COS(T)+VON
    WRITE(7,2000) WT, ILN
    WRITE(6,2000) WT,VCN,ILN
    T=T-GA/30.
    WT=WT+GA*180*WN/PI/30.
    GO TO 301
302 T=PI
    YT=YT+GA
    WT=YT*180*WN/PI
303 IF(T.LT.(PI-AL)) GO TO 304
    ILN=R1*SIN(T)
    VCN=R1*COS(T)-VON
    WRITE(7,2000) WT,ILN
    WRITE(6,2000) WT,VCN,ILN
    T=T-AL/50.
    WT=WT+AL*180*WN/PI/50.
    GO TO 303
304 T=PI-B1
    YT=YT+AL
    WT=YT*180*WN/PI
305 IF(T.LT.(PI-B1-BT)) GO TO 306
    ILN=R*SIN(T)
    VCN=R*COS(T)+1-VON
    WRITE(7,2000) WT, ILN
    WRITE(6,2000) WT,VCN,ILN
    T=T-BT/30.
    WT=WT+BT*180*WN/PI/30.
    GO TO 305
306 T=GA
    YT=YT+BT
    WT=YT*180*WN/PI

```

```

307 IF(T.LT.0) GO TO 308
    ILN=(R1+2*VON)*SIN(T)
    VCN=(R1+2*VON)*COS(T)-VON
    WRITE(7,2000) WT,ILN
    WRITE(6,2000) WT,VCN,ILN
    T=T-GA/30.
    WT=WT+GA*180*WN/PI/30.
    GO TO 307
308 T=0.
    YT=YT+GA
    WT=YT*180*WN/PI
309 IF(T.LT.-AL) GO TO 310
    ILN=R1*SIN(T)
    VCN=R1*COS(T)+VON
    WRITE(7,2000) WT,ILN
    WRITE(6,2000) WT,VCN,ILN
    T=T-AL/50.
    WT=WT+AL*180*WN/PI/50.
    GO TO 309
310 T=-B1
    YT=YT+AL
    WT=YT*180*WN/PI
311 IF(T.LT.(-B1-BT)) GO TO 312
    ILN=R*SIN(T)
    VCN=R*COS(T)-1+VON
    WRITE(7,2000) WT,ILN
    WRITE(6,2000) WT,VCN,ILN
    T=T-BT/30.
    WT=WT+BT*180*WN/PI/30.
    GO TO 311
312 T=-PI+GA
    YT=YT+BT
    WT=YT*180*WN/PI
313 IF(T.LT.-PI) GO TO 10
    ILN=(R1+2*VON)*SIN(T)
    VCN=(R1+2*VON)*COS(T)+VON
    WRITE(7,2000) WT,ILN
    WRITE(6,2000) WT,VCN,ILN
    T=T-GA/30.
    WT=WT+GA*180*WN/PI/30.
    GO TO 313
400 R=X(1)
    R1=X(2)
    B1=X(3)
    B2=X(4)
    AL=X(5)
    GA=X(6)
    T=-PI+GA
401 IF(T.LT.-PI) GO TO 402
    ILN=R1*SIN(T)
    VCN=R1*COS(T)+VON
    WRITE(7,2000) WT,ILN
    WRITE(6,2000) WT,VCN,ILN
    T=T-GA/30.
    WT=WT+GA*180*WN/PI/30.
    GO TO 401
402 T=PI
    YT=YT+GA

```

```

WT = YT*180*WN/PI
403 IF(T.LT.0) GO TO 404
ILN = (R1-2*VON)*SIN(T)
VCN = (R1-2*VON)*COS(T)-VON
WRITE(7,2000) WT, ILN
WRITE(6,2000) WT,VCN,ILN
T = T-PI/60.
WT = WT + PI*180*WN/PI/60.
GO TO 403
404 T = 0.
YT = YT + PI
WT = YT*180*WN/PI
405 IF(T.LT.-AL) GO TO 406
ILN = (R1-4*VON)*SIN(T)
VCN = (R1-4*VON)*COS(T) + VON
WRITE(7,2000) WT, ILN
WRITE(6,2000) WT,VCN,ILN
T = T-AL/20.
WT = WT + AL*180*WN/PI/20.
GO TO 405
406 T = -PI + B1
YT = YT + AL
WT = YT*180*WN/PI
407 IF(T.LT.-PI) GO TO 408
ILN = (R + 2*VON)*SIN(T)
VCN = (R + 2*VON)*COS(T) + 1 + VON
WRITE(7,2000) WT, ILN
WRITE(6,2000) WT,VCN,ILN
T = T-B1/20.
WT = WT + B1*180*WN/PI/20.
GO TO 407
408 T = PI
YT = YT + B1
WT = YT*180*WN/PI
409 IF(T.LT.(PI-B2)) GO TO 410
ILN = R*SIN(T)
VCN = R*COS(T) + 1-VON
WRITE(7,2000) WT, ILN
WRITE(6,2000) WT,VCN,ILN
T = T-B2/40.
WT = WT + B2*180*WN/PI/40.
GO TO 409
410 T = GA
YT = YT + B2
WT = YT*180*WN/PI
411 IF(T.LT.0.) GO TO 412
ILN = R1*SIN(T)
VCN = R1*COS(T)-VON
WRITE(7,2000) WT, ILN
WRITE(6,2000) WT,VCN,ILN
T = T-GA/30.
WT = WT + GA*180*WN/PI/30.
GO TO 411
412 T = 0.
YT = YT + GA
WT = YT*180*WN/PI
413 IF(T.LT.-PI) GO TO 414
ILN = (R1-2*VON)*SIN(T)

```



```

VCN=(R1-2*VON)*COS(T)+VON
WRITE(7,2000) WT, ILN
WRITE(6,2000) WT,VCN,ILN
T=T-PI/60.
WT=WT+PI*180*WN/PI/60.
GO TO 413
414 T=PI
YT=YT+PI
WT=YT*180*WN/PI
415 IF(T.LT.(PI-AL)) GO TO 416
ILN=(R1-4*VON)*SIN(T)
VCN=(R1-4*VON)*COS(T)-VON
WRITE(7,2000) WT, ILN
WRITE(6,2000) WT,VCN,ILN
T=T-AL/20.
WT=WT+AL*180*WN/PI/20.
GO TO 415
416 T=B1
YT=YT+AL
WT=YT*180*WN/PI
417 IF(T.LT.0.) GO TO 418
ILN=(R+2*VON)*SIN(T)
VCN=(R+2*VON)*COS(T)-1-VON
WRITE(7,2000) WT, ILN
WRITE(6,2000) WT,VCN,ILN
T=T-B1/20.
WT=WT+B1*180*WN/PI/20.
GO TO 417
418 T=0.
YT=YT+B1
WT=YT*180*WN/PI
419 IF(T.LT.-B2) GO TO 420
ILN=R*SIN(T)
VCN=R*COS(T)-1+VON
WRITE(7,2000) WT, ILN
WRITE(6,2000) WT,VCN,ILN
T=T-B2/40.
WT=WT+B2*180*WN/PI/40.
GO TO 419
420 T=-PI+GA
YT=YT+B2
WT=YT*180*WN/PI
421 IF(T.LT.-PI) GO TO 10
ILN=R1*SIN(T)
VCN=R1*COS(T)+VON
WRITE(7,2000) WT, ILN
WRITE(6,2000) WT,VCN,ILN
T=T-GA/30.
WT=WT+GA*180*WN/PI/30.
GO TO 421
500 R=X(1)
FI=X(2)
AL=X(3)
T=-PI+AL
501 IF(T.LT.-PI) GO TO 502
ILN=(1-R+2*VON)*SIN(T)
VCN=(1-R+2*VON)*COS(T)+VON
WRITE(7,2000) WT, ILN

```

```

WRITE(6,2000) WT,VCN,ILN
T = T-AL/30.
WT = WT + AL*180*WN/PI/30.
GO TO 501
502 T = PI
YT = YT + AL
WT = YT*180*WN/PI
503 IF(T.LT.0) GO TO 504
ILN = (1-R)*SIN(T)
VCN = (1-R)*COS(T)-VON
WRITE(7,2000) WT, ILN
WRITE(6,2000) WT,VCN,ILN
T = T-PI/50.
WT = WT + PI*180*WN/PI/50.
GO TO 503
504 T = FI
YT = YT + PI
WT = YT*180*WN/PI
505 IF(T.LT.0.) GO TO 506
ILN = 0.
VCN = 1-R-VON
WRITE(7,2000) WT, ILN
WRITE(6,2000) WT,VCN,ILN
T = T-FI/30.
WT = WT + FI*180*WN/PI/30.
GO TO 505
506 T = PI
YT = YT + FI
WT = YT*180*WN/PI
507 IF(T.LT.(PI-BT)) GO TO 508
ILN = R*SIN(T)
VCN = R*COS(T) + 1-VON
WRITE(7,2000) WT, ILN
WRITE(6,2000) WT,VCN,ILN
T = T-BT/30.
WT = WT + BT*180*WN/PI/30.
GO TO 507
508 T = AL
YT = YT + BT
WT = YT*180*WN/PI
509 IF(T.LT.0.) GO TO 510
ILN = (1-R + 2*VON)*SIN(T)
VCN = (1-R + 2*VON)*COS(T)-VON
WRITE(7,2000) WT, ILN
WRITE(6,2000) WT,VCN,ILN
T = T-AL/30.
WT = WT + AL*180*WN/PI/30.
GO TO 509
510 T = 0.
YT = YT + AL
WT = YT*180*WN/PI
511 IF(T.LT.-PI) GO TO 512
ILN = (1-R)*SIN(T)
VCN = (1-R)*COS(T) + VON
WRITE(7,2000) WT, ILN
WRITE(6,2000) WT,VCN,ILN
T = T-PI/50.
WT = WT + PI*180*WN/PI/50.

```

```

GO TO 511
512 T=FI
    YT=YT+PI
    WT=YT*180*WN/PI
513 IF(T.LT.0.) GO TO 514
    ILN=0.
    VCN=-1+R+VON
    WRITE(7,2000) WT, ILN
    WRITE(6,2000) WT,VCN,ILN
    T=T-FI/30.
    WT=WT+FI*180*WN/PI/30.
    GO TO 513
514 T=0.
    YT=YT+FI
    WT=YT*180*WN/PI
515 IF(T.LT.-BT) GO TO 516
    ILN=R*SIN(T)
    VCN=R*COS(T)-1+VON
    WRITE(7,2000) WT, ILN
    WRITE(6,2000) WT,VCN,ILN
    T=T-BT/30.
    WT=WT+BT*180*WN/PI/30.
    GO TO 515
516 T=-PI+AL
    YT=YT+BT
    WT=YT*180*WN/PI
517 IF(T.LT.-PI) GO TO 10
    ILN=(1-R+2*VON)*SIN(T)
    VCN=(1-R+2*VON)*COS(T)+VON
    WRITE(7,2000) WT, ILN
    WRITE(6,2000) WT,VCN,ILN
    T=T-AL/30.
    WT=WT+AL*180*WN/PI/30.
    GO TO 517
600 R=X(1)
    FI=X(2)
    AL=X(3)
    T=-PI+AL
601 IF(T.LT.-PI) GO TO 602
    ILN=(R-1+2*VON)*SIN(T)
    VCN=(R-1+2*VON)*COS(T)+VON
    WRITE(7,2000) WT, ILN
    WRITE(6,2000) WT,VCN,ILN
    T=T-AL/30.
    WT=WT+AL*180*WN/PI/30.
    GO TO 601
602 T=FI
    YT=YT+AL
    WT=YT*180*WN/PI
603 IF(T.LT.0) GO TO 604
    ILN=0.
    VCN=-R+1-VON
    WRITE(7,2000) WT, ILN
    WRITE(6,2000) WT,VCN,ILN
    T=T-FI/20.
    WT=WT+FI*180*WN/PI/20.
    GO TO 603
604 T=PI

```

```

YT = YT + FI
WT = YT*180*WN/PI
605 IF(T.LT.(PI-BT)) GO TO 606
ILN = R*SIN(T)
VCN = R*COS(T) + 1-VON
WRITE(7,2000) WT, ILN
WRITE(6,2000) WT,VCN,ILN
T = T-BT/30.
WT = WT + BT*180*WN/PI/30.
GO TO 605
606 T = AL
YT = YT + BT
WT = YT*180*WN/PI
607 IF(T.LT.0) GO TO 608
ILN = (R-1 + 2*VON)*SIN(T)
VCN = (R-1 + 2*VON)*COS(T)-VON
WRITE(7,2000) WT, ILN
WRITE(6,2000) WT,VCN,ILN
T = T-AL/30.
WT = WT + AL*180*WN/PI/30.
GO TO 607
608 T = FI
YT = YT + AL
WT = YT*180*WN/PI
609 IF(T.LT.0.) GO TO 610
ILN = 0.
VCN = R-1 + VON
WRITE(7,2000) WT, ILN
WRITE(6,2000) WT,VCN,ILN
T = T-FI/20.
WT = WT + FI*180*WN/PI/20.
GO TO 609
610 T = 0.
YT = YT + FI
WT = YT*180*WN/PI
611 IF(T.LT.-BT) GO TO 612.
ILN = R*SIN(T)
VCN = R*COS(T)-1 + VON
WRITE(7,2000) WT, ILN
WRITE(6,2000) WT,VCN,ILN
T = T-BT/30.
WT = WT + BT*180*WN/PI/30.
GO TO 611
612 T = -PI + AL
YT = YT + BT
WT = YT*180*WN/PI
613 IF(T.LT.-PI) GO TO 10
ILN = (R-1 + 2*VON)*SIN(T)
VCN = (R-1 + 2*VON)*COS(T) + VON
WRITE(7,2000) WT, ILN
WRITE(6,2000) WT,VCN,ILN
T = T-AL/30.
WT = WT + AL*180*WN/PI/30.
GO TO 613
1050 FORMAT(F10.5)
1000 FORMAT(1X,I1,2X,8F8.4)
2000 FORMAT(3F14.5)
END

```

Fortran Program for Generating Capacitor Voltage and Inductor Current Waveforms (Above Resonant Frequency)

```

C *****
C *****
C ***** PROGRAM : SC10WAVE.FOR
C *****
C ***** FUNCTION : GENERATE DATA FOR ILN AND VCN FOR A COMPLETE
C ***** SWITCHING CYCLE UNDER STEADY-STATE. SRC, ABOVE
C ***** RESONANT FREQUENCY.
C *****
C *****
C *****
REAL ILN, VCN
DIMENSION X(5)
PI=4.*ATAN(1)
10 READ(5,1000) ID,WTS,VON,BS,(X(K), K = 1,5)
C ***** THE INPUTS ARE GENERATED BY THE FILE SC10PAR.FOR
C *****
WN = PI/WTS
BT = BS/WN
IF(ID.EQ.0) STOP
WT=0.
YT=0.
GO TO (100,200,300), ID
100 R = X(1)
R1 = X(2)
B1 = X(3)
B2 = X(4)
AL = X(5)
GA = BT-AL
T = -PI + B2
101 IF(T.LT.-B1) GO TO 102
ILN = R1*SIN(T)
VCN = R1*COS(T) + VON
WRITE(6,2000) WT,VCN,ILN
WRITE(7,2000) WT,ILN
T = T - (B1 + B2 - PI)/30.
WT = WT + (-PI + B2 + B1)*180*WN/PI/30.
GO TO 101
102 T = -PI + GA
YT = YT - (PI - B2 - B1)
WT = YT*180*WN/PI
103 IF(T.LT.-PI) GO TO 104
ILN = (R + 2*VON)*SIN(T)
VCN = (R + 2*VON)*COS(T) + 1 + VON
WRITE(6,2000) WT,VCN,ILN
WRITE(7,2000) WT,ILN
T = T - GA/30.
WT = WT + GA*180*WN/PI/30.
GO TO 103
104 T = PI
YT = YT + GA
WT = YT*180*WN/PI
105 IF(T.LT.(PI-AL)) GO TO 106
ILN = R*SIN(T)

```

```

VCN = R * COS(T) + 1 - VON
WRITE(6,2000) WT,VCN,ILN
WRITE(7,2000) WT,ILN
T = T - AL / 30.
WT = WT + AL * 180 * WN / PI / 30.
GO TO 105
106 T = B2
YT = YT + AL
WT = YT * 180 * WN / PI
107 IF(T.LT.(PI-B1)) GO TO 108
ILN = R1 * SIN(T)
VCN = R1 * COS(T) - VON
WRITE(6,2000) WT,VCN,ILN
WRITE(7,2000) WT,ILN
T = T - (-PI + B2 + B1) / 30.
WT = WT - (PI - B2 - B1) * 180 * WN / PI / 30.
GO TO 107
108 T = GA
YT = YT - (PI - B2 - B1)
WT = YT * 180 * WN / PI
109 IF(T.LT.0) GO TO 110
ILN = (R + 2 * VON) * SIN(T)
VCN = (R + 2 * VON) * COS(T) - 1 - VON
WRITE(6,2000) WT,VCN,ILN
WRITE(7,2000) WT,ILN
T = T - GA / 30.
WT = WT + GA * 180 * WN / PI / 30.
GO TO 109
110 T = 0
YT = YT + GA
WT = YT * 180 * WN / PI
111 IF(T.LT.-AL) GO TO 112
ILN = R * SIN(T)
VCN = R * COS(T) - 1 + VON
WRITE(6,2000) WT,VCN,ILN
WRITE(7,2000) WT,ILN
T = T - AL / 30.
WT = WT + AL * 180 * WN / PI / 30.
GO TO 111
112 T = -PI + B2
YT = YT + AL
WT = YT * 180 * WN / PI
113 IF(T.LT.-B1) GO TO 10
ILN = R1 * SIN(T)
VCN = R1 * COS(T) + VON
WRITE(6,2000) WT,VCN,ILN
WRITE(7,2000) WT,ILN
T = T + (PI - B1 - B2) / 30.
WT = WT - (PI - B1 - B2) * 180 * WN / PI / 30.
GO TO 113
200 R = X(1)
R1 = X(2)
B1 = X(3)
GA = X(4)
AL = X(5)
T = -PI + GA
201 IF(T.LT.-PI) GO TO 202
ILN = (R + 2 * VON) * SIN(T)

```

```

VCN=(R + 2*VON)*COS(T) + VON
WRITE(6,2000) WT,VCN,ILN
WRITE(7,2000) WT,ILN
T=T-GA/30.
WT=WT + GA*180*WN/PI/30.
GO TO 201
202 T=PI
YT=YT + GA
WT=YT*180*WN/PI
203 IF(T.LT.(PI-AL)) GO TO 204
ILN=R*SIN(T)
VCN=R*COS(T)-VON
WRITE(6,2000) WT,VCN,ILN
WRITE(7,2000) WT,ILN
T=T-AL/30.
WT=WT + AL*180*WN/PI/30.
GO TO 203
204 T=PI-B1
YT=YT + AL
WT=YT*180*WN/PI
205 IF(T.LT.(PI-B1-BT)) GO TO 206
ILN=R1*SIN(T)
VCN=R1*COS(T) + 1-VON
WRITE(6,2000) WT,VCN,ILN
WRITE(7,2000) WT,ILN
T=T-BT/30.
WT=WT + BT*180*WN/PI/30.
GO TO 205
206 T=GA
YT=YT + BT
WT=YT*180*WN/PI
207 IF(T.LT.0) GO TO 208
ILN=(R + 2*VON)*SIN(T)
VCN=(R + 2*VON)*COS(T)-VON
WRITE(6,2000) WT,VCN,ILN
WRITE(7,2000) WT,ILN
T=T-GA/30.
WT=WT + GA*180*WN/PI/30.
GO TO 207
208 T=0.
YT=YT + GA
WT=YT*180*WN/PI
209 IF(T.LT.-AL) GO TO 210
ILN=R*SIN(T)
VCN=R*COS(T) + VON
WRITE(6,2000) WT,VCN,ILN
WRITE(7,2000) WT,ILN
T=T-AL/30.
WT=WT + AL*180*WN/PI/30.
GO TO 209
210 T=-B1
YT=YT + AL
WT=YT*180*WN/PI
211 IF(T.LT.(-B1-BT)) GO TO 212
ILN=R1*SIN(T)
VCN=R1*COS(T)-1 + VON
WRITE(6,2000) WT,VCN,ILN
WRITE(7,2000) WT,ILN

```

```

T = T-BT/30.
WT = WT + BT*180*WN/PI/30.
GO TO 211
212 T = -PI + GA
    YT = YT + BT
    WT = YT*180*WN/PI
213 IF(T.LT.-PI) GO TO 10
    ILN = (R + 2*VON)*SIN(T)
    VCN = (R + 2*VON)*COS(T) + VON
    WRITE(6,2000) WT,VCN,ILN
    WRITE(7,2000) WT,ILN
    T = T-GA/30.
    WT = WT + GA*180*WN/PI/30.
    GO TO 213
300 R = X(1)
    GA = X(2)
    FI = X(3)
    T = -PI + GA
301 IF(T.LT.-PI) GO TO 302
    ILN = (R-1 + 2*VON)*SIN(T)
    VCN = (R-1 + 2*VON)*COS(T) + VON
    WRITE(6,2000) WT,VCN,ILN
    WRITE(7,2000) WT,ILN
    T = T-GA/30.
    WT = WT + GA*180*WN/PI/30.
    GO TO 301
302 T = 0
    YT = YT + GA
    WT = YT*180*WN/PI
303 IF(T.GT.FI) GO TO 304
    ILN = 0.
    VCN = -R + 1-VON
    WRITE(6,2000) WT,VCN,ILN
    WRITE(7,2000) WT,ILN
    T = T + FI/30.
    WT = WT + FI*180*WN/PI/30.
    GO TO 303
304 T = PI
    YT = YT + FI
    WT = YT*180*WN/PI
305 IF(T.LT.(PI-BT)) GO TO 306
    ILN = R*SIN(T)
    VCN = R*COS(T) + 1-VON
    WRITE(6,2000) WT,VCN,ILN
    WRITE(7,2000) WT,ILN
    T = T-BT/30.
    WT = WT + BT*180*WN/PI/30.
    GO TO 305
306 T = GA
    YT = YT + BT
    WT = YT*180*WN/PI
307 IF(T.LT.0) GO TO 308
    ILN = (R-1 + 2*VON)*SIN(T)
    VCN = (R-1 + 2*VON)*COS(T)-VON
    WRITE(6,2000) WT,VCN,ILN
    WRITE(7,2000) WT,ILN
    T = T-GA/30
    WT = WT + GA*180*WN/PI/30.

```



```

GO TO 307
308 T=0
    YT=YT+GA
    WT=YT*180*WN/PI
309 IF(T.GT.FI) GO TO 310
    ILN=0.
    VCN=R-1+VON
    WRITE(6,2000) WT,VCN,ILN
    WRITE(7,2000) WT,ILN
    T=T+FI/30.
    WT=WT+FI*180*WN/PI/30.
    GO TO 309
310 T=0.
    YT=YT+FI
    WT=YT*180*WN/PI
311 IF(T.LT.-BT) GO TO 312
    ILN=R*SIN(T)
    VCN=R*COS(T)-1+VON
    WRITE(6,2000) WT,VCN,ILN
    WRITE(7,2000) WT,ILN
    T=T-BT/30.
    WT=WT+BT*180*WN/PI/30.
    GO TO 311
312 T=-PI+GA
    YT=YT+BT
    WT=YT*180*WN/PI
313 IF(T.LT.-PI) GO TO 10
    ILN=(R-1+2*VON)*SIN(T)
    VCN=(R-1+2*VON)*COS(T)+VON
    WRITE(6,2000) WT,VCN,ILN
    WRITE(7,2000) WT,ILN
    T=T-GA/30.
    WT=WT+GA*180*WN/PI/30.
    GO TO 313
1000 FORMAT(1X,11,2X,8F8.4)
2000 FORMAT(3F14.5)
END

```

APPENDIX C.1

RULES FOR CONSTRUCTING EQUILIBRIUM STATE TRAJECTORIES OF A CM-PRC

An equilibrium state trajectory constructed in the composite diagram discussed in Section 3.3.4 must satisfy the following rules. These rules are obtained from the converter's operation.

- On the left half plane ($v_{CN} < 0$),
 - triggering of Q1 initiates M6;
 - triggering of Q2 initiates M1;
 - triggering of Q4 initiates M5.
- On the right half plane ($v_{CN} > 0$),
 - triggering of Q3 initiates M3;
 - triggering of Q4 initiates M4;
 - triggering of Q2 initiates M2.
- On the i_{LN} -axis ($v_{CN} = 0$),
 - if the magnitude of i_{LN} is greater than I_{ON} ,

- ▲ triggering of Q2 initiates M2;
 - ▲ triggering of Q4 initiates M5;
- if the magnitude of i_{LN} is greater than I_{ON} and no triggering event occurs,
 - ▲ M2 is initiated if the previous topological mode is M1;
 - ▲ M3 is initiated if the previous topological mode is M6;
 - ▲ M5 is initiated if the previous topological mode is M4;
 - ▲ M6 is initiated if the previous topological mode is M3;
- if the magnitude of i_{LN} is equal to I_{ON} ,
 - ▲ M0 is initiated if the previous topological mode is M3 or M6; M0 will be terminated when Q2 or Q4 is triggered which initiates M2 or M5, respectively;
 - ▲ M2 is initiated if the previous topological mode is ML and $i_{LN} > 0$;
 - ▲ M5 is initiated if the previous topological mode is ML and $i_{LN} < 0$;
- if the magnitude of i_{LN} is less than I_{ON} ,
 - ▲ M0 is initiated if the previous topological mode is M3 or M6; M0 will be terminated when Q2 or Q4 is triggered which initiates ML;
 - ▲ ML is initiated if previous topological mode is M1 or M4.

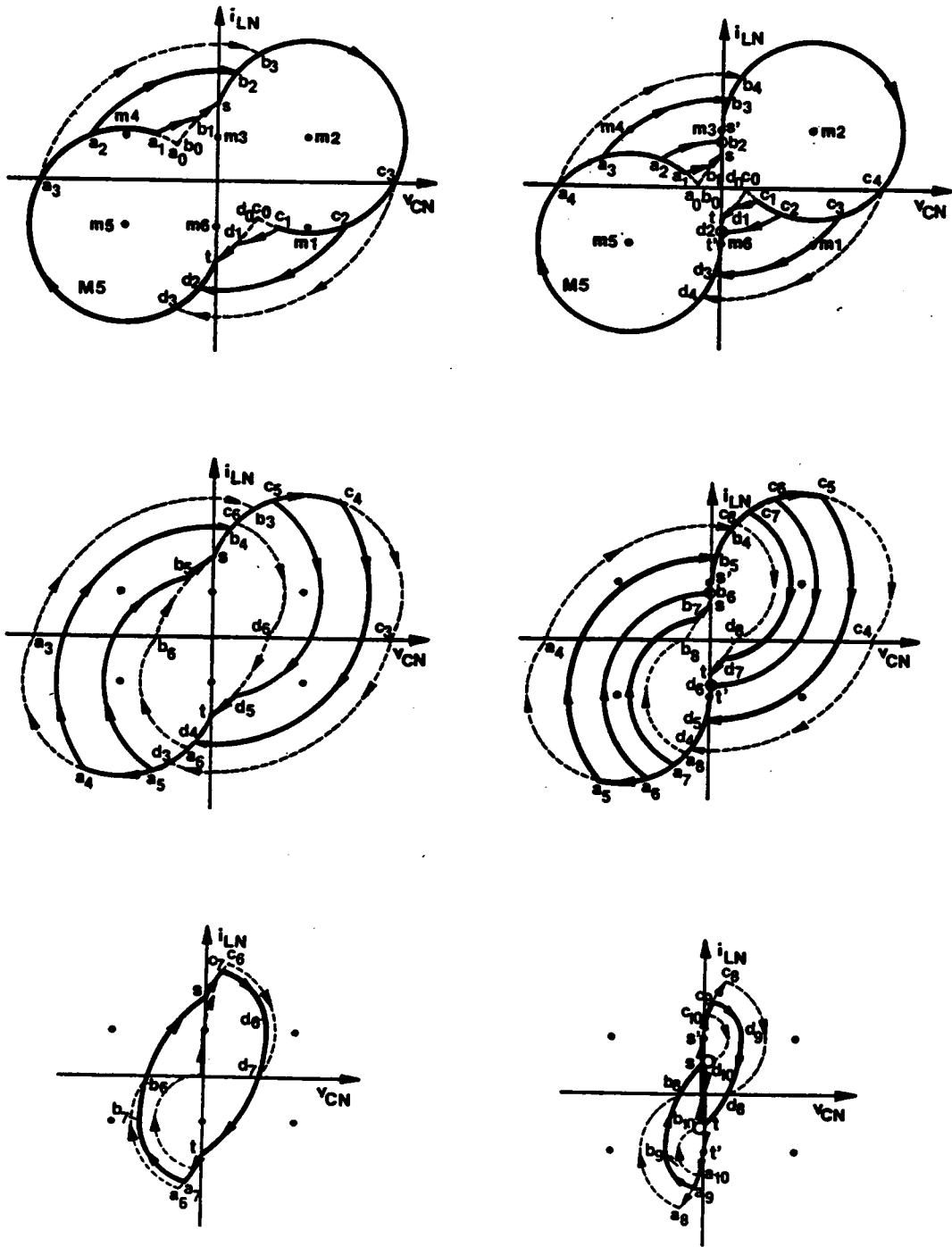
A systematic way to construct equilibrium trajectories of a CM-PRC is illustrated in Figure C.1.1. Starting with an equilibrium trajectory ($a_0sc_0ta_0$ in Figure C.1.1(a) or $a_0ss'c_0t't'a_0$ in Figure C.1.1(b)) corresponding to conventional PRC operation, the triggering instant of Q1(Q3), $a_0, a_1, a_2, \dots (c_0, c_1, c_2, \dots)$, is gradually moved counterclockwise along the trajectory of M5(M2). By doing so, the effective duty ratio of the quasi-square-wave voltage is gradually reduced and various equilibrium trajectories can be obtained.

In Figure C.1.1(a), trajectory $a_1b_1sc_1d_1ta_1$ corresponds to a mode- I_N operation. Trajectory $a_2b_2c_2d_2a_2$ corresponds to a mode- II_N operation. Trajectory $a_4b_4c_4d_4a_4$ corresponds to a mode- III_S operation. Trajectory $a_5b_5sc_5d_5ta_5$ corresponds to a mode- I_S operation. Trajectory $a_7b_7sc_7d_7ta_7$ corresponds to a mode- I_F operation.

In Figure C.1.1(b), trajectory $a_1b_1ss'c_1d_1t't'a_1$ corresponds to a mode- III_N operation. Trajectory $a_2b_2s'c_2d_2t'a_2$ corresponds to a mode- IV_N operation. Trajectory $a_6b_6s'c_6d_6t'a_6$ corresponds to a mode- IV_S operation. Trajectory $a_7b_7ss'c_7d_7t't'a_7$ corresponds to a mode- III_S operation. Trajectory $a_9b_9ss'c_9d_9t't'a_9$ corresponds to a mode- III_F operation. Trajectory $a_{10}b_{10}s'c_{10}d_{10}t'a_{10}$ corresponds to a mode- IV_F operation.

Figure C.1.2 shows the construction of equilibrium trajectories above resonant frequency. In Figure C.1.2(a), trajectory $a_1b_1sc_1d_1ta_1$ represents a mode- I_F operation. Trajectory $a_1b_1sc_1d_1ta_1$ represents a mode- I_S operation. Trajectory $a_2b_2c_2d_2a_2$ represents a mode- IIA_F operation. Trajectory $a_2b_2c_2d_2a_2$ represents a mode- IIA_S operation.

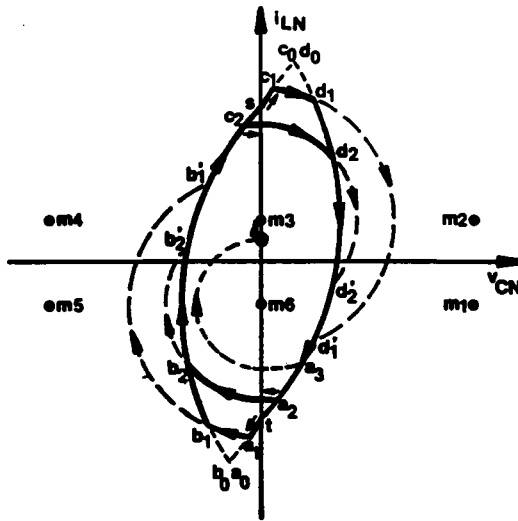
In Figure C.1.2(b), trajectory $a_1b_1ss'c_1d_1t't'a_1$ represents a mode- III_F operation. Trajectory $a_2b_2s'c_2d_2t'a_2$ represents a mode- IV_F operation. It can be shown, however, that mode-IV operation cannot exist at frequencies above resonant frequency.



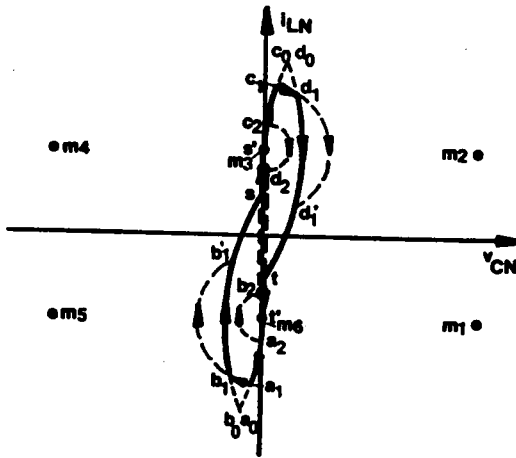
(a) Trajectories for continuous v_{CN}

(b) Trajectories for discontinuous v_{CN}

Figure C.1.1 Systematical Construction of Equilibrium Trajectories Below Resonant Frequency



(a) Trajectories for continuous v_{CN}



(b) Trajectories for discontinuous v_{CN}

Figure C.1.2 Systematical Construction of Equilibrium Trajectories Above Resonant Frequency

APPENDIX C.2

PREDICTION OF MODE TRANSITIONS OF A CM-PRC OPERATING BELOW RESONANT FREQUENCY

Assume the waveform for the capacitor voltage is continuous when β_S is equal to 180° (PRC operation). This requires [...]

$$I_{ON} \leq -0.5 \times \sin\left(\frac{\pi}{\omega_{SN}}\right) \times \sqrt{\frac{1 + (1 - 2(\cos(\frac{\pi}{\omega_{SN}}) - 1))}{\sin^2(\frac{\pi}{\omega_{SN}})}} \quad (C.2.1)$$

As β_S decreases, the first operating mode for the converter is mode I.

Further decreasing β_S , the converter's operation may transit into mode II or mode III. Consider the boundary trajectories, T_{A12} and T_{B12} , between mode I and mode II, as shown in Figure C.2.1. These trajectories can be represented by the equations

$$\left[\begin{array}{l} \cos \rho = \frac{1}{R}, \\ \cos \sigma = \frac{1 + R^2 - R_1^2}{2R}, \\ \cos \gamma = \frac{1 + R_1^2 - R^2}{2R_1}, \\ \frac{\pi}{\omega_{SN}} = \sigma - \rho + \frac{\pi}{2} - \gamma, \\ R_1 = 2I_{ON} + \sqrt{R^2 - 1}, \end{array} \right. \quad (C.2.2)$$

and can be constructed only when $R + 1 \geq R_1$ which leads to

$$2I_{ON} \leq R_1 \leq R_{1max}, \quad R_{1max} = \begin{cases} \text{infinite} & \text{when } I_{ON} \leq 0.5, \\ \frac{2I_{ON}^2}{2I_{ON} - 1} & \text{when } I_{ON} > 0.5. \end{cases}$$

The corresponding frequency to these trajectories are shown in Figure C.2.2 as a function of radius R , where

$$\begin{aligned}\omega_1 &= \frac{\pi}{\pi + \sigma/2}, & \sigma &= \cos^{-1}(1 - 2I_{ON}^2), \\ \omega_2 &= \frac{\pi}{\pi + \sigma/2}, & \sigma &= 2\pi - \cos^{-1}(1 - 2I_{ON}^2),\end{aligned}\tag{C.2.3}$$

ω_3 is the frequency occurs at $R_{\max} = R_{1\max} - 1$, and ω_H is the highest possible frequency which can be numerically determined. If we define

$$\omega_{12\max} = \begin{cases} 1 & \text{for } I_{ON} \leq 0.5, \\ \omega_H & \text{for } I_{ON} > 0.5, \end{cases}$$

from Figure C.2.2, the transition of the operating mode can be determined as follows.

(a). If $\omega_{12\max} < \omega_{SN}$, the converter's operation transits form mode I to mode III since there is no boundary trajectory exists between mode I and mode II. The boundary β_S angle, β_{13} , between mode I and mode III can be calculated by solving equation C.2.7, $\beta_{13} = (\alpha_2 - \alpha_1 + \sigma) \times \omega_{SN}$.

(b). If $\omega_1 \leq \omega_{SN} < \omega_{12\max}$, the converter's operation transits form mode I to mode II back to mode I to mode III since two boundary trajectories between mode I and mode II exist. Two sets of solutions, $(R, R_1, \sigma, \rho, \gamma)$ and $(R', R_1', \sigma', \rho', \gamma')$, can be obtained when equation C.2.2 is solved. The boundary β_S angles between mode I and mode II are $\beta_{12A} = (\sigma - \rho) \times \omega_{SN}$ and $\beta_{12B} = (\sigma' - \rho') \times \omega_{SN}$. The boundary β_{SN} angle between mode I and mode III is calculated as in (a).

(c). If $\omega_2 \leq \omega_{SN} < \omega_1$, the converter's operation transits from mode I to mode II to mode IV, since there is one boundary trajectory between mode I and mode II exists. The transition from mode II to mode IV can be easily justified since, besides mode I,

mode IV is the only possible operating mode for the converter to transit into from mode II. One solution, $(R, R_1, \sigma, \rho, \gamma)$, for equation C.2.2 exists. The boundary β_S angle between mode I and mode II is $\beta_{12} = (\sigma - \rho) \times \omega_{SN}$. The boundary β_S angle between mode II and mode IV is $\beta_{24} = \sigma \times \omega_{SN}$, $\sigma = \cos^{-1}(1 - 2I_{ON}^2)$, which is calculated from Figure C.2.5(b).

(d). If $\omega_{SN} < \omega_2$, the converter's operation transits from mode I to mode III, since there is no boundary trajectory exists between mode I and mode II. The boundary β_S angle, β_{13} , between mode I and mode III is calculated as in (a).

Before proceeding to determine the mode transitions as β_S is further decreased, consider the boundary trajectories, T_{A34} and T_{B34} , between mode III and Mode IV, as shown in Figure C.2.3. These trajectories can be described by equations

$$\begin{cases} \cos \sigma = \frac{2 - R^2}{2}, \\ \ell = 2I_{ON} - R, \\ \frac{\pi}{\omega_{SN}} = \pi + \frac{\sigma}{2} + \ell. \end{cases} \quad (C.2.4)$$

The corresponding frequency to these trajectories are shown in Figure C.2.4 as a function of radius R , where

$$\begin{aligned} \omega_{LA} &= \frac{\pi}{2\pi + 2I_{ON}}, \\ \omega_{LB} &= \frac{\pi}{\pi + 2I_{ON}}, \end{aligned} \quad (C.2.5)$$

$$\omega_M = \begin{cases} \omega_1 & \text{for } I_{ON} \leq \frac{\sqrt{3}}{2}, \\ \frac{\pi}{2I_{ON} + 2.4567} & \text{for } I_{ON} > \frac{\sqrt{3}}{2}, \end{cases} \quad (C.2.6)$$

and ω_1, ω_2 are the same as in equation (C.2.3).

Figure C.2.5 shows the boundary trajectories mode I and mode III, and mode II and mode IV. The boundary trajectory between mode I and mode III can be described by equations

$$\left[\begin{array}{l} \cos \sigma = \frac{2 - R_1^2}{2}, \\ \cos \eta = \frac{1 + R_1^2 - R_2^2}{2R_1}, \\ \cos \alpha_1 = \frac{1 + R_2^2 - R_1^2}{2}, \\ \cos \alpha_2 = \frac{1}{R_2}, \\ -\gamma = \frac{\pi - \sigma}{2}, \\ R_2^2 = 1 + 4I_{ON}^2, \\ \frac{\pi}{\omega_{SN}} = \sigma - \gamma + \pi - \eta + \alpha_2 - \alpha_1. \end{array} \right. \quad (C.2.7)$$

The boundary trajectory between mode II and mode IV can be described by equations

$$\left[\begin{array}{l} \cos \sigma = 1 - 2I_{ON}^2, \\ \frac{\pi}{\omega_{SN}} = \pi + \frac{\sigma}{2} + \theta. \end{array} \right. \quad (C.2.8)$$

For $\omega_{SN} \leq \omega_2$, two boundary trajectories between mode II and mode IV exist, and one boundary trajectory between mode I and mode III exists.

For $\omega_2 < \omega_{SN} \leq \omega_1$, one boundary trajectory between mode II and mode IV exists, while no boundary trajectory exists between mode I and mode III.

For $\omega_1 < \omega_{SN}$, no boundary trajectory exists between mode II and mode IV, while one boundary trajectory between mode I and mode III exists.

From Figure C.2.4, as β_S is further decreases, the transitions of the converter's operating mode can be determined as follows.

For the sequence in (a),

(a).1 if $\omega_M \leq \omega_{SN}$, the converter's operation transits from mode III to mode V since no boundary trajectory exists between mode III and mode IV; the boundary β_S angle between mode III and mode V is $\beta_{35} = 2I_{ON} \times \omega_{SN}$;

(a).2 if $\omega_M > \omega_{SN}$, the converter's operation transits from mode III to mode IV back to mode III to mode V since two boundary trajectories between mode III and mode IV exists; two sets of solutions, (R, σ, ℓ) and (R', σ', ℓ') , can be obtained from equation (C.2.4); the boundary β_S angles between mode III and mode IV are $\beta_{34A} = (\sigma + \ell) \times \omega_{SN}$ and $\beta_{34B} = (\sigma' - \ell') \times \omega_{SN}$; the boundary β_{SN} angle between mode III and mode V is calculated as in (a).1.

For the sequence in (b),

(b).1 if $\omega_M \leq \omega_{SN}$, the converter's operation transits from mode III to mode V since no boundary trajectory exists between mode III and mode IV; the boundary β_S angle between mode III and mode V is calculated as in (a).1;

(b).2 if $\omega_M > \omega_{SN}$, the converter's operation transits from mode III to mode IV back to mode III to mode V since two boundary trajectories between mode III and mode IV exists; the boundary β_S angles between mode III and mode IV, and the boundary β_{SN} angle between mode III and mode V, are calculated as in (a).2.

For the sequence in (c),

(c).1 if $\omega_{LB} \geq \omega_2$ and $\omega_{LB} \leq \omega_{SN}$, the converter's operation transits from mode IV to mode III to mode V since one boundary trajectory between mode III and mode IV exists; the boundary β_S angle between mode III and mode IV, and the boundary β_{SN} angle between mode III and mode V, are calculated as in (a).2;

(c).2 if $\omega_{LB} \geq \omega_2$ and $\omega_{LB} > \omega_{SN}$, the converter's operation transits from mode IV to mode V since no boundary trajectory exists between mode III and mode IV; the boundary β_S angle between mode IV and mode V is $\beta_{45} = 2I_{ON} \times \omega_{SN}$;

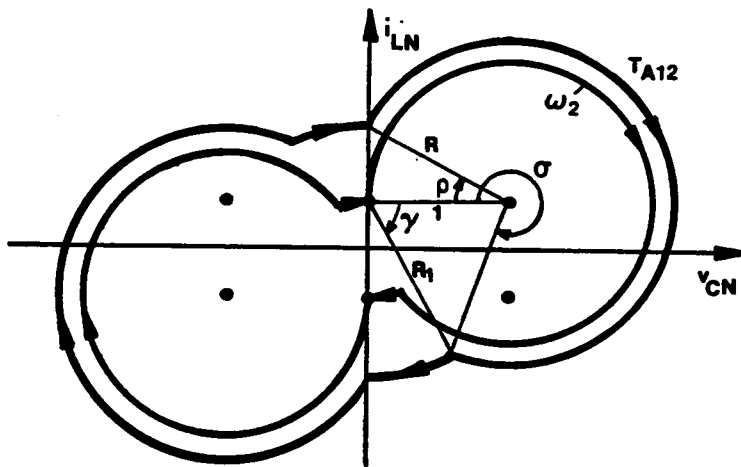
(c).3 if $\omega_{LB} < \omega_2$, the converter's operation transits from mode IV to mode III to mode V since one boundary trajectory between mode III and mode IV exists; the boundary β_S angles are calculated as in (a).2.

The case for the sequence in (d) is special since two boundary trajectories between mode II and mode IV exist.

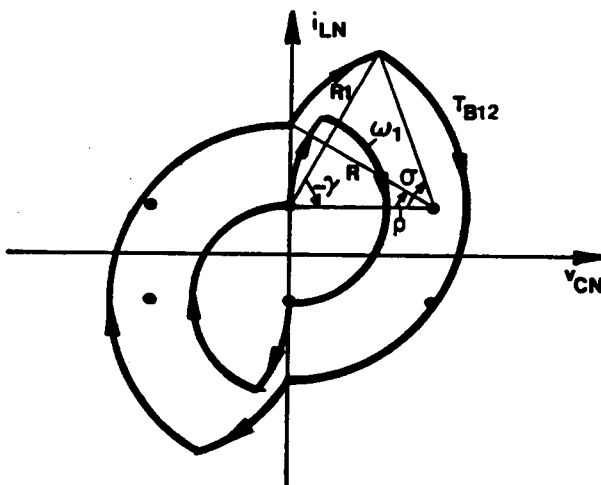
(d).1 If $\omega_{LB} \geq \omega_2$, the converter's operation transits from mode III to mode IV to mode II back to mode IV to mode V since one boundary trajectory between mode III and mode IV and two boundary trajectories between mode II and mode IV exist. The boundary β_S angle between mode III and mode IV is calculated as in (a).2. The boundary β_{SN} angle between mode IV and mode V is calculated as in (c).2. The boundary β_{SN} angles between mode II and mode IV are $\beta_{24A} = \omega_{SN} \times \cos^{-1}(1 - 2I_{ON}^2)$ and $\beta_{24B} = \omega_{SN} \times (2\pi - \cos^{-1}(1 - 2I_{ON}^2))$.

(d).2 If $\omega_{LB} < \omega_2$ and $\omega_{LB} \leq \omega_{SN}$, the converter's operation transits from mode III to mode IV to mode II back to mode IV to mode III to mode V since two boundary trajectories between mode III and mode IV and two boundary trajectories between mode II and mode IV exist. The boundary β_S angle between mode III and mode IV and the boundary β_{SN} angle between mode III and mode V is calculated as in (a).2. The boundary β_{SN} angles between mode II and mode IV are calculated as in (d).1.

(d).3 If $\omega_{LB} < \omega_2$ and $\omega_{LB} > \omega_{SN}$, the converter's operation transits from mode III to mode IV to mode II back to mode IV to mode V since one boundary trajectory between mode III and mode IV and two boundary trajectories between mode II and mode IV exist. The boundary β_S angles are calculated as in (d)1

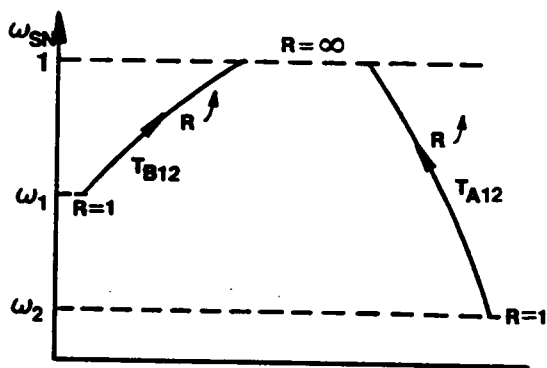


(a) $\sigma \geq \pi (\gamma \geq 0)$

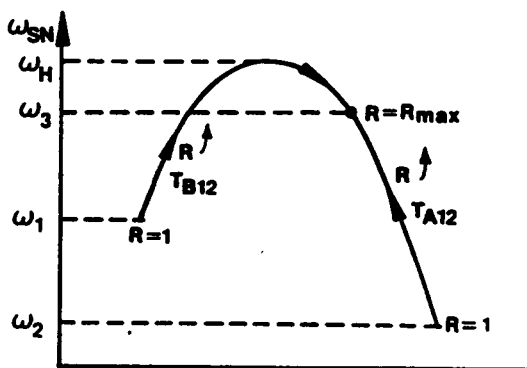


(b) $\sigma < \pi (\gamma < 0)$

Figure C.2.1 Boundary Trajectories Between Mode I and Mode II

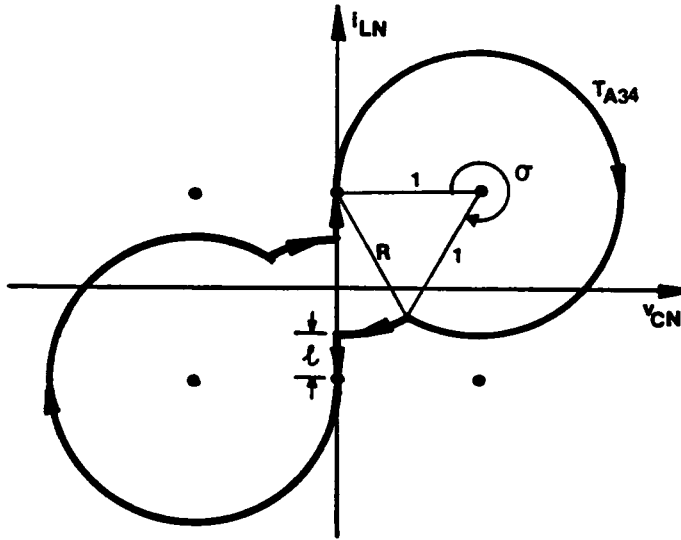


(a) $I_{ON} \leq 0.5$

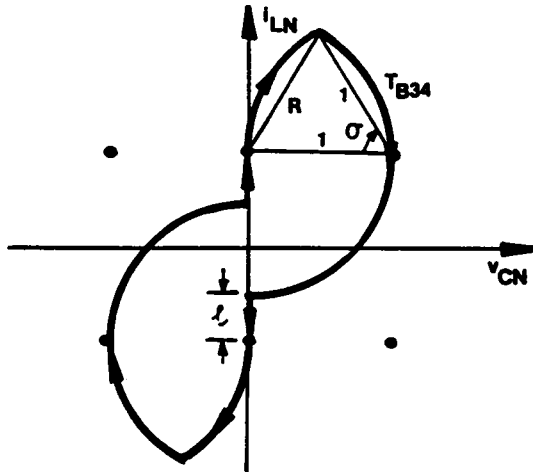


(b) $I_{ON} > 0.5$

Figure C.2.2 Corresponding Frequency for the Trajectories in Figure C.2.1

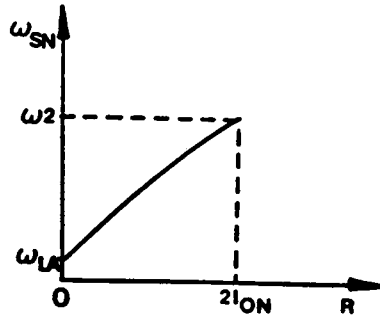


(a) $\sigma \geq \pi$

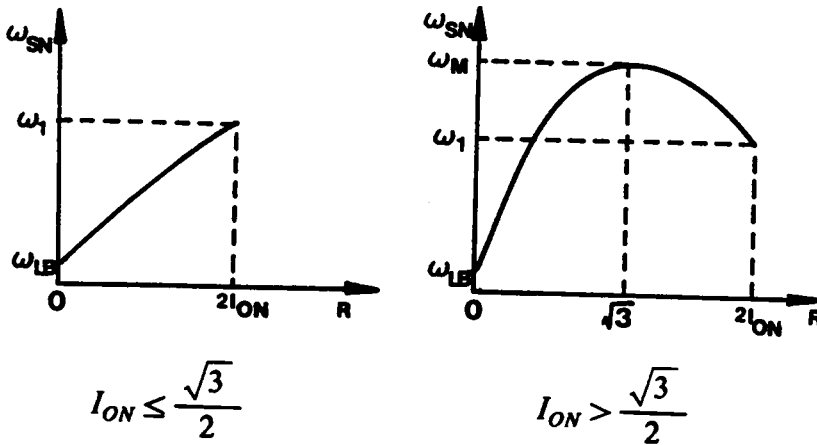


(b) $\sigma < \pi$

Figure C.2.3 Boundary Trajectories Between Mode III and Mode IV



(a) Frequency for T_{A34}

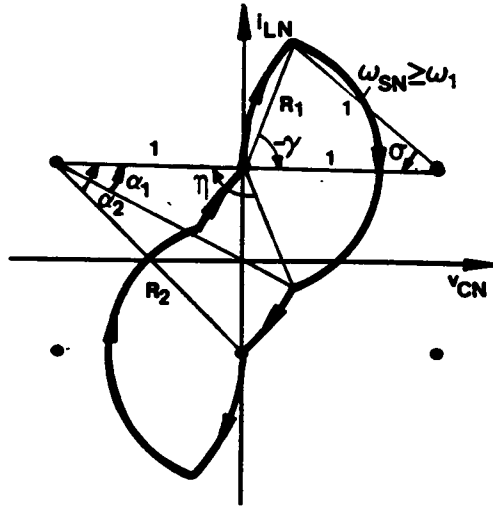


$$I_{ON} \leq \frac{\sqrt{3}}{2}$$

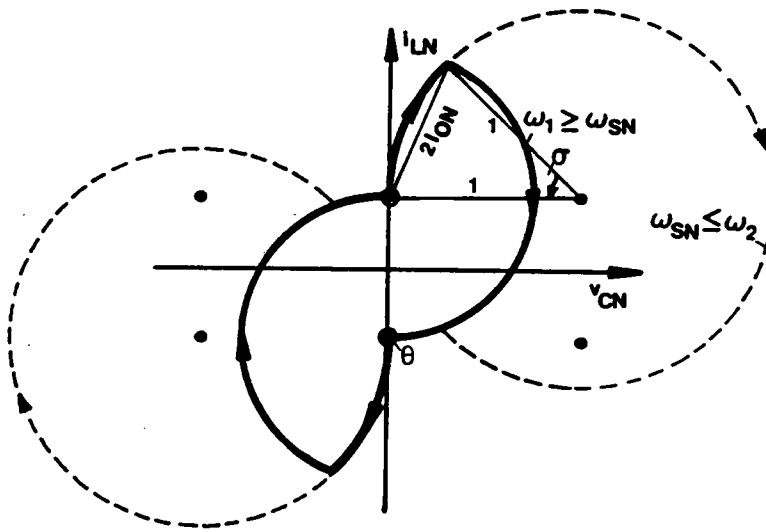
$$I_{ON} > \frac{\sqrt{3}}{2}$$

(b) Frequency for T_{B34}

Figure C.2.4 Corresponding Frequency for the Trajectories in Figure C.2.3



(a) Boundary between Mode I and Mode III



(b) Boundary between Mode II and Mode IV

Figure C.2.5 Boundary Trajectories for Discontinuous Capacitor Voltage Waveform

APPENDIX C.3

PREDICTION OF MODE TRANSITIONS OF A CM-PRC OPERATING ABOVE RESONANT FREQUENCY

Depending upon the switching frequency, the capacitor voltage waveform of a CM-PRC at $\beta_S = 180^\circ$ can be continuous or discontinuous. The boundary frequency for continuous capacitor voltage waveform is

$$\omega_D = \frac{\pi}{\rho + \sigma + \gamma},$$

$$\rho = \cos^{-1}(1 - I_{ON}^2), \quad \sigma = \cos^{-1}\left(\frac{1 + I_{ON}^2}{\sqrt{1 + 4I_{ON}^2}}\right), \quad \gamma = \cos^{-1}\left(\frac{1}{\sqrt{1 + 4I_{ON}^2}}\right). \quad (\text{C.3.1})$$

If $\omega_{SN} \geq \pi/2I_{ON}$, the converter operates only in mode V.

If $\omega_D \leq \omega_{SN} < \pi/2I_{ON}$, the converter first operates in mode III then transits to mode V. The boundary β_S angle between mode III and mode V is $\beta_{35} = 2I_{ON} \times \omega_{SN}$.

If $\omega_{SN} < \omega_D$, the converter operates in mode I when β_S is decreased from 180° . As β_S is further decreased, the converter's operation may transit into mode IIA or mode III.

Consider the boundary trajectories, T_{A12A} and T_{B12A} , between mode I and mode IIA, as shown in Figure C.3.1. These trajectories can be described by equations

$$\left[\begin{array}{l} \cos \alpha_1 = \frac{1 + R_3^2 - R_2^2}{2R_3}, \\ \cos \alpha_2 = \frac{1}{R_3}, \\ \cos \eta = \frac{1 + R_2^2 - R_3^2}{2R_2}, \\ R_3^2 = (R_2 + 2I_{ON})^2 + 1, \\ \frac{\pi}{\omega_{SN}} = \alpha_2 - \alpha_1 + \pi - \eta + \frac{\pi}{2}, \end{array} \right. \quad (C.3.2)$$

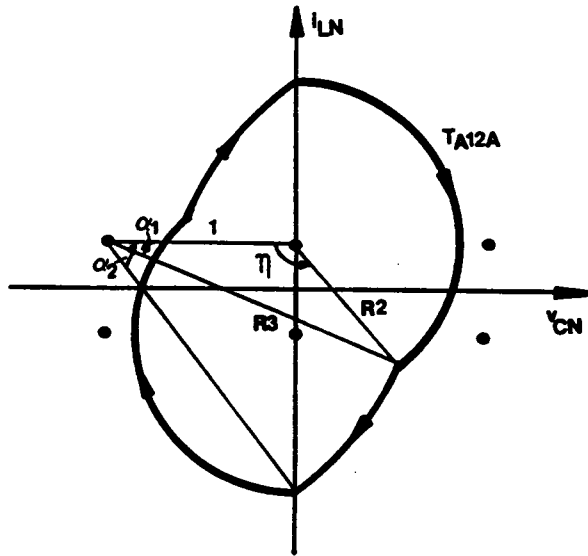
and can be constructed only when $I_{ON} \leq 0.5$ and $R_2 \geq R_S$, where $R_S = \frac{2I_{ON}}{1 - 2I_{ON}}$. The corresponding frequency for these trajectories are shown as a function of radius R_2 in Figure C.3.2, where ω_S is the frequency occurs at $R_2 = R_S$ and ω_M is the highest possible frequency which can be calculated numerically. From Figure C.3.2, the transitions of the operating mode can be determined as follows.

(a). If $\omega_{SN} \geq \omega_M$, the converter's operation transits from mode I to mode III to mode V since no boundary trajectory exists between mode I and mode IIA. The boundary β_S angle between mode I and mode III and the boundary β_S angle between mode III and mode V are calculated as in Appendix C.2.

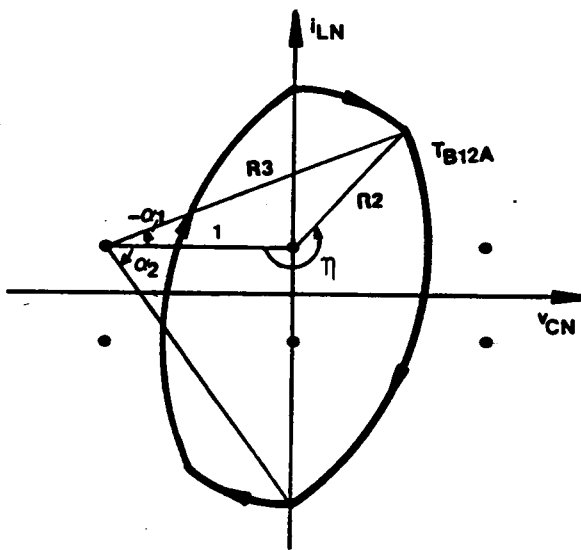
(b). If $\omega_{SN} < \omega_M$, the converter's operation transits from mode I to mode IIA back to mode I to mode V since two boundary trajectories between mode I and mode IIA exist. Two sets of solutions, $(R_2, R_3, \eta, \alpha_1, \alpha_2)$ and $(R_2', R_3', \eta', \alpha_1', \alpha_2')$, can be obtained from equation C.3.1. The boundary β_S angles between mode I and mode IIA are $\beta_{12AA} = (\alpha_2 - \alpha_1) \times \omega_{SN}$ and $\beta_{12AB} = (\alpha_2' - \alpha_1') \times \omega_{SN}$. The boundary β_S angle between mode I and mode III and the boundary β_S between mode III and mode V are calculated as in Appendix C.2.

A Fortran program for determining the mode transitions and mode boundaries in this frequency range is included in the following. The program requires inputs for ω_{SN} and

I_{ON} and generates outputs for four boundary angles, $BA1$, $BA2$, $BC1$, and $BC2$. When $\beta_S \geq BA1$, the converter operates in mode I. When $BA1 > \beta_S \geq BA2$, the converter operates in mode II Λ . When $BA2 > \beta_S \geq BC1$, the converter operates in mode I. When $BC1 > \beta_S \geq BC2$, the converter operates in mode III. When $BC2 > \beta_S$, the converter operates in mode V.

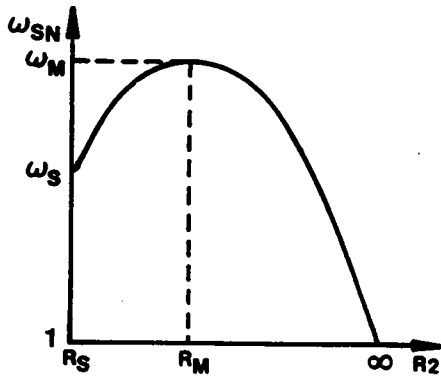


(a) $\eta \leq \pi (\alpha_1 \geq 0)$

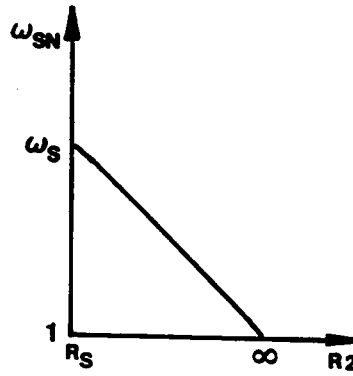


(b) $\eta > \pi (\alpha_1 < 0)$

Figure C.3.1 Boundary Trajectories Between Mode I and Mode IIA



(a) Frequency for T_{B12A}



(b) Frequency for T_{A12A}

Figure C.3.2 Corresponding Frequency for the Trajectories in Figure C.3.1

Fortran Program for Determining Mode Transitions and Mode Boundaries Above Resonant Frequency

```

C *****
C *****
C ***** PROGRAM NAME : PC10BD.FOR
C *****
C ***** FUNCTION : CALCULATE THE MODE BOUNDARIES OF A CLAMPED-MODE
C ***** PRC OPERATING ABOVE THE RESONANT FREQUENCY.
C *****
C *****
C *****
C ***** FOR BS > BA1 ---> MODE I OPERATION
C ***** FOR BA1 > BS > BA2 ---> MODE IIA OPERATION
C ***** FOR BA2 > BS > BC1 ---> MODE I OPERATION
C ***** FOR BC1 > BS > BC2 ---> MODE III OPERATION
C ***** FOR BC2 > BS ---> MODE V OPERATION
C *****
IMPLICIT REAL*8 (A-H,O-Z)
COMMON WN, OI, PI
PI=4.*DATAN(1.D0)
11 READ(5,*) WN, OI
IF(WN.LT.0) STOP
WTS=PI/WN
10 A=DACOS(1-OI**2)
B=DACOS((1+OI**2)/(1+4*OI**2)**0.5)
C=DACOS(1/(1+4*OI**2)**0.5)
WN1=PI/(A+B+C)
WN2=PI/(2*OI)
IF(WN.GE.WN2) THEN
BC1=WTS
BC2=WTS
ELSE
IF(WN.GE.WN1) THEN
BC1=WTS
BC2=2*OI
ELSE
BC2=2*OI
Lambda=DACOS(-2*OI**2+(1+4*OI**2)**0.5)
B=DACOS(1/(1+4*OI**2)**0.5)
WN3=PI/(0.5*(PI+Lambda)+B)
IF(WN.GE.WN3) THEN
R11=(2**0.5)*OI
RL=(1+4*OI**2)**0.5-1
15 R=(R11+RL)/2.
CALL FQBDIII(R,AL,BE1,BE2,GA1,GA2)
WNC=PI/(AL+BE1-BE2+GA2+GA1)
IF(DABS(WNC-WN).LE.1.D-4) THEN
BC1=(GA2+GA1+AL)
ELSE
IF(WNC.GT.WN) THEN
RH=R
ELSE
RL=R
ENDIF
GO TO 15

```

```

        ENDIF
    ELSE
        RH = 2*OI
        RL = (1 + 4*OI**2)**0.5 - 1
25      R = (RH + RL)/2.
        CALL FQBDIII(R,AL,BE1,BE2,GA1,GA2)
        WNC = PI/(AL + BE1 + BE2 + GA2 - GA1)
        IF(DABS(WNC - WN).LE.1.D-4) THEN
            BC1 = (GA2 - GA1 + AL)
        ELSE
            IF(WNC.GT.WN) THEN
                RL = R
            ELSE
                RH = R
            ENDIF
        GO TO 25
    ENDIF
ENDIF
ENDIF
ENDIF
CALL BDIIA(BA1,BA2)
WRITE(6,2000) WN, OI, BA1, BA2, BC1, BC2
2000 FORMAT(6F12.5)
GO TO 11
END
C
C *****
C *****
C *****
C
SUBROUTINE FQBDIII(R1,AL,BE1,BE2,GA1,GA2)
IMPLICIT REAL*8 (A-H,O-Z)
COMMON WN, OI, PI
R2 = (1 + 4*OI**2)**0.5
AL = DACOS(1 - 0.5*R1**2)
BE1 = (PI - AL)*0.5
BE2 = PI - DACOS((1 + R1**2 - R2**2)/(2*R1))
GA1 = DACOS((1 + R2**2 - R1**2)/(2*R2))
GA2 = DACOS(1/R2)
RETURN
END
C
C *****
C *****
C *****
C
SUBROUTINE BDIIA(BA1,BA2)
IMPLICIT REAL*8 (A-H,O-Z)
COMMON WN, OI, PI
WTS = PI/WN
11 IF(OI.GE.0.5) THEN
    BA1 = WTS
    BA2 = WTS
    RETURN
ENDIF
R2A1 = 2*OI**2/(1 - 2*OI)
CALL FQIIA(R2A1,AL1,AL2,ET2,WA1,WA11)
R2 = R2A1 + 25.

```



```

12 CALL FQIIA(R2,AL1,AL2,ET2,WNC1,WNC2)
   IF(WNC1.GE.WA1) THEN
     R2=R2*2.
     GO TO 12
   ENDIF
   R2A2=R2
   WA2=WNC1
   RH=R2A2
   RL=R2A1
14 R2=(RH+RL)/2.
   R2P=R2+1.D-4
   CALL FQIIA(R2,AL1,AL2,ET2,WNC1,WNC2)
   CALL FQIIA(R2P,AL1,AL2,ET2,WNC1,WNC2)
   IF(DABS(RH-RL).LE.1.D-4) THEN
     R2AMAX=R2
     WAMAX=WNC1
   ELSE
     IF(WNC1.LE.WNC1) THEN
       RL=R2
     ELSE
       RH=R2
     ENDIF
     GO TO 14
   ENDIF
   IF(WN.GE.WAMAX) THEN
     BA1=WTS
     BA2=WTS
     RETURN
   ENDIF
   IF(WN.GE.WA1) THEN
     RH=R2A2
     RL=R2AMAX
22 R2=(RH+RL)/2.
   CALL FQIIA(R2,AL1,AL2,ET2,WNC1,WNC2)
   IF(DABS(RH-RL).LE.1.D-4) THEN
     BA1=(AL2+AL1)
   ELSE
     IF(WNC1.GT.WN) THEN
       RL=R2
     ELSE
       RH=R2
     ENDIF
     GO TO 22
   ENDIF
   RH=R2AMAX
   RL=R2A1
24 R2=(RH+RL)/2.
   CALL FQIIA(R2,AL1,AL2,ET2,WNC1,WNC2)
   IF(DABS(RH-RL).LE.1.D-4) THEN
     BA2=(AL2+AL1)
   ELSE
     IF(WNC1.GT.WN) THEN
       RH=R2
     ELSE
       RL=R2
     ENDIF
     GO TO 24
   ENDIF

```

```

ELSE
  IF(WN.GE.WA2) THEN
    R2A3 = R2A2
  ELSE
    R2 = R2A2*2
26  CALL FQIIA(R2,AL1,AL2,ET2,WNC1,WNC2)
    IF(WN.GT.WNC1) THEN
      R2A3 = R2
    ELSE
      R2 = R2*2
      GO TO 26
    ENDIF
  ENDIF
  RH = R2A3
  RL = R2AMAX
28  R2 = (RH + RL)/2.
  CALL FQIIA(R2,AL1,AL2,ET2,WNC1,WNC2)
  IF(DABS(RII-RL).LE.1.D-4) THEN
    BA1 = (AI.2 + AI.1)
  ELSE
    IF(WNC1.GT.WN) THEN
      RL = R2
    ELSE
      RII = R2
    ENDIF
    GO TO 28
  ENDIF
  R2 = R2A1 + 5.
32  CALL FQIIA(R2,AL1,AL2,ET2,WNC1,WNC2)
  IF(WNC2.LE.WN) THEN
    R2A4 = R2
  ELSE
    R2 = R2*2.
    GO TO 32
  ENDIF
  RH = R2A4
  RL = R2A1
34  R2 = (RH + RL)/2.
  CALL FQIIA(R2,AL1,AL2,ET2,WNC1,WNC2)
  IF(DABS(RII-RL).LE.1.D-4) THEN
    BA2 = (AL2-AL1)
  ELSE
    IF(WNC2.GT.WN) THEN
      RL = R2
    ELSE
      RII = R2
    ENDIF
    GO TO 34
  ENDIF
  ENDIF
  ENDIF
  RETURN
  END
C
C *****
C *****
C *****
C
SUBROUTINE FQIIA(R2,AL1,AL2,ET2,WNC1,WNC2)

```

```
IMPLICIT REAL*8 (A-H,O-Z)
COMMON WN, OI, PI
R3 = ((R2 + 2*OI)**2 + 1.)**0.5
AL2 = DACOS(1/R3)
AL1 = DACOS((1 + R3**2 - R2**2)/(2*R3))
ET1 = 2*PI - DACOS((1 + R2**2 - R3**2)/(2*R2))
ET2 = 2*PI - ET1
WNC1 = PI/(AL2 + AL1 + 1.5*PI - ET1)
WNC2 = PI/(AL2 - AL1 + 1.5*PI - ET2)
RETURN
END
```

APPENDIX C.4

CALCULATION OF TRAJECTORY PARAMETERS OF A CM-PRC

The parameters for the equilibrium trajectories of a CM-PRC can be obtained by solving sets of nonlinear equations. The equations are shown in Figures C.4.1 ~ C.4.6.

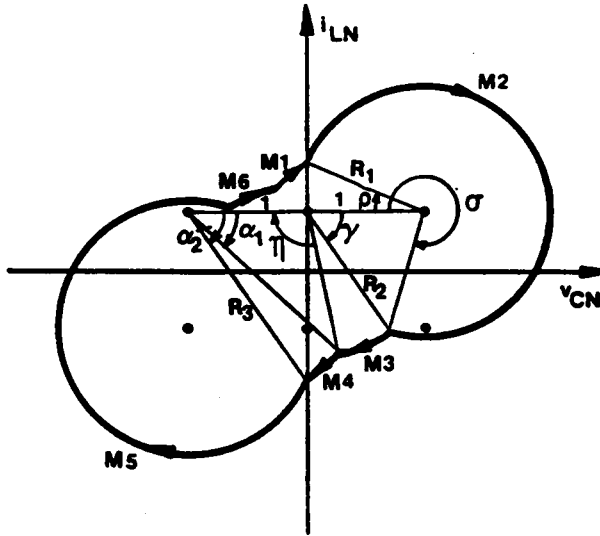
There are different equilibrium trajectories shown for each operating mode. All the equilibrium trajectories can be described by the same sets of equations shown. However, all the trajectories must be considered when the circuit salient features are calculated. For example, the natural-commutation trajectory and the semi-commutation trajectories in an operating mode have different device conduction sequences. Thus, the expressions for calculating switch currents and diode currents are derived from different conduction intervals, which results in different expressions. The expressions for calculating peak capacitor voltage in the trajectories with the same commutation features are also different. As shown in Figure C.4.1(b) and Figure C.4.1(c), the peak capacitor voltage for the trajectories are $R_1 + 1$ and R_2 , respectively.

The FORTRAN programs for calculating trajectory parameters at frequencies below and above resonant frequency are included at the end of this section. The outputs generated by the programs are defined in the following:

- For mode-I trajectory in Figure C.4.1, $ID = 1$, $X(1) = R_1$, $X(2) = R_2$, $X(3) = R_3$, $X(4) = \rho$, $X(5) = \sigma$, $X(6) = \eta$, $X(7) = \alpha_1$, $X(8) = \alpha_2$; $IDD = 11$ for Trajectory C.4.1(a), $IDD = 12$ for Trajectory C.4.1(b), $IDD = 13$ for Trajectory C.4.1(c), $IDD = 14$ for Trajectory C.4.1(d), $IDD = 15$ for Trajectory C.4.1(e).
- For mode-II trajectory in Figure C.4.2, $ID = 2$, $X(1) = R_1$, $X(2) = R_2$, $X(3) = \rho$, $X(4) = \sigma$, $X(5) = \alpha$, $X(6) \sim X(8) = \text{dummy}$; $IDD = 21$ for Trajectory C.4.2(a), $IDD = 22$ for

Trajectory C.4.2(b), IDD= 23 for Trajectory C.4.2(c), IDD= 29 for Trajectory C.4.2(d).

- For mode-III trajectory in Figure C.4.3, ID= 3, $X(1)=R_{1:ef}$, $X(2)=:f.R_2$, $X(3)=\sigma$, $X(4)=\eta$, $X(5)=\alpha_1$, $X(6)=\alpha_2$, $X(7)\sim X(8)=$ dummy ; IDD= 31 for Trajectory C.4.3(a), IDD= 32 for Trajectory C.4.3(b), IDD= 33 for Trajectory C.4.3(c), IDD= 34 for Trajectory C.4.3(d), IDD= 35 for Trajectory C.4.3(e). IDD= 36 for Trajectory C.4.3(f), IDD= 37 for Trajectory C.4.3(g).
- For mode-IV trajectory in Figure C.4.4, ID= 4, $X(1)=R_1$, $X(2)=\sigma$, $X(3)=\theta$, $X(4)\sim X(8)=$ dummy ; IDD= 41 for Trajectory C.4.4(a), IDD= 42 for Trajectory C.4.4(b), IDD= 43 for Trajectory C.4.4(c), IDD= 44 for Trajectory C.4.4(d).
- For mode-V trajectory in Figure C.4.5, ID= 5, $X(1)\sim X(8)=$ dummy ; IDD= 55.
- For mode-IIA trajectory in Figure C.4.6, ID= 21, $X(1)=R_1$, $X(2)=R_2$, $X(3)=R_3$, $X(4)=\rho$, $X(5)=\eta$, $X(6)=\alpha_1$, $X(7)=\alpha_2$, $X(8)=$ dummy; IDD= 23 for Trajectory C.4.6(a), IDD= 24 for Trajectory C.4.6(b), IDD= 25 for Trajectory C.4.6(c).



(a) Natural-commutation trajectory

$$\cos \rho = \frac{1}{R_1}, \quad \cos \alpha_2 = \frac{1}{R_3}, \quad R_3^2 = 1 + (2I_{ON} + \sqrt{R_1^2 - 1})^2,$$

$$\cos \sigma = \frac{1 + R_1^2 - R_2^2}{2R_1}, \quad \cos \gamma = \frac{1 + R_2^2 - R_1^2}{2R_2},$$

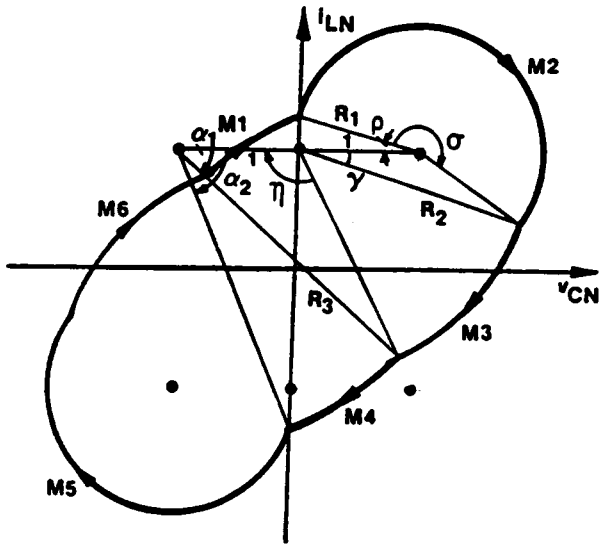
$$\cos \eta = \frac{1 + R_2^2 - R_3^2}{2R_2}, \quad \cos \alpha_1 = \frac{1 + R_3^2 - R_2^2}{2R_3},$$

$$\frac{\beta_S}{\omega_{SN}} = \alpha_2 - \alpha_1 + \sigma - \rho, \quad \frac{\pi}{\omega_{SN}} = \sigma - \rho + \pi - \gamma - \eta + \alpha_2 - \alpha_1.$$

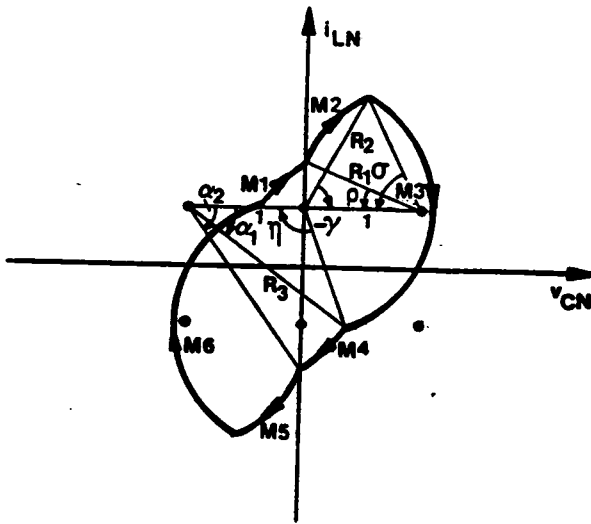
$$1 \leq R_1, \quad 0 \leq R_2, \quad \sqrt{1 + 4I_{ON}^2} \leq R_3, \quad 0 \leq \alpha_2, \quad \rho \leq \frac{\pi}{2},$$

$$-\frac{\pi}{2} \leq \alpha_1, \quad \gamma \leq \frac{\pi}{2}, \quad 0 \leq \eta \leq \frac{3\pi}{2}, \quad 0 \leq \sigma \leq 2\pi.$$

Figure C.4.1 Mode-I Trajectories

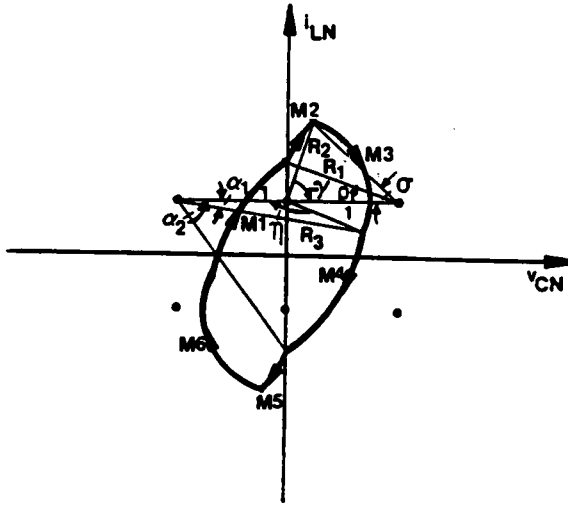


(b) Mixed-commutation trajectory ($\sigma \geq \pi$)

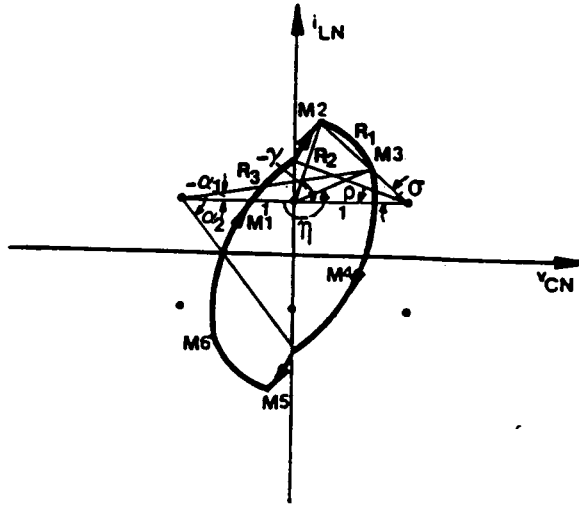


(c) Mixed-commutation trajectory ($\sigma < \pi$)

Figure C.4.1 Continued

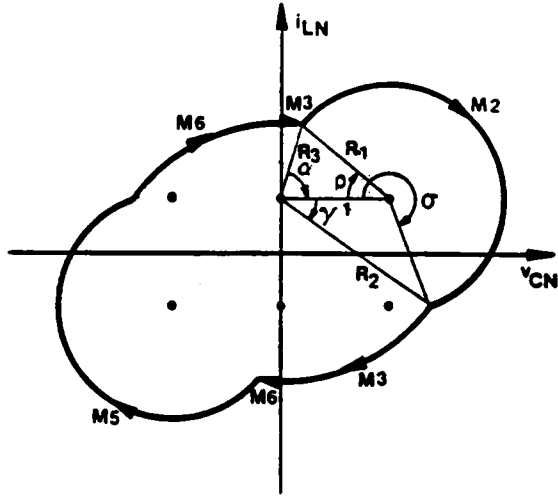


(d) Force-commutation trajectory ($\eta \leq \pi$)



(e) Force-commutation trajectory ($\eta > \pi$)

Figure C.4.1 Continued



(a) Natural-commutation trajectory

$$\cos \sigma = \frac{1 + R_1^2 - R_2^2}{2R_1}, \quad \cos \gamma = \frac{1 + R_2^2 - R_1^2}{2R_2},$$

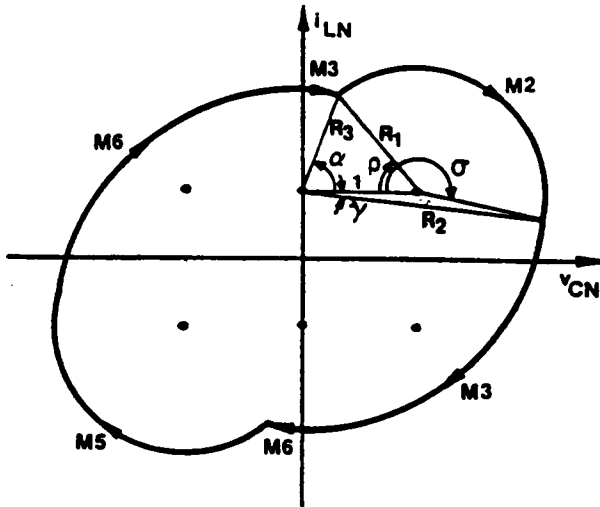
$$\cos \rho = \frac{1 + R_1^2 - R_3^2}{2R_1}, \quad \cos \alpha = \frac{1 + R_3^2 - R_1^2}{2R_3},$$

$$\frac{\beta_S}{\omega_{SN}} = \sigma - \rho, \quad R_3 = R_2 - 2I_{ON},$$

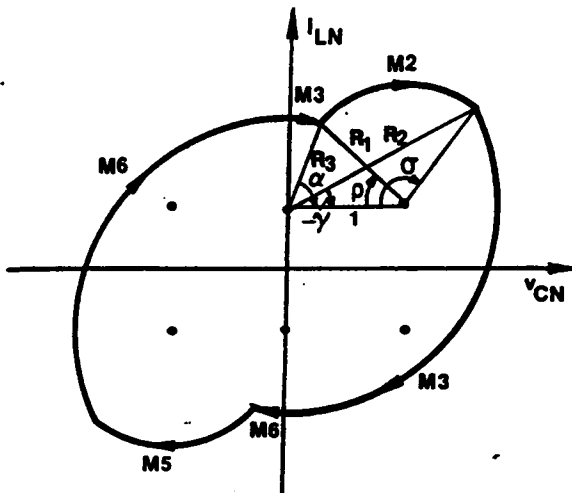
$$\frac{\pi}{\omega_{SN}} = \sigma - \rho + \frac{\pi}{2} - \gamma + \frac{\pi}{2} - \alpha.$$

$$0 \leq R_1, R_3, 2I_{ON} \leq R_2, \quad -\frac{\pi}{2} \leq \alpha, \gamma, \rho \leq \frac{\pi}{2}, \quad 0 \leq \sigma \leq 2\pi.$$

Figure C.4.2 Mode-II Trajectories

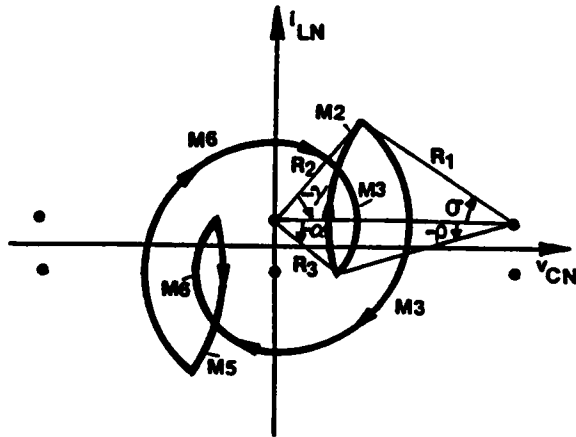


(b) Mixed-commutation trajectory ($\sigma \geq \pi$)



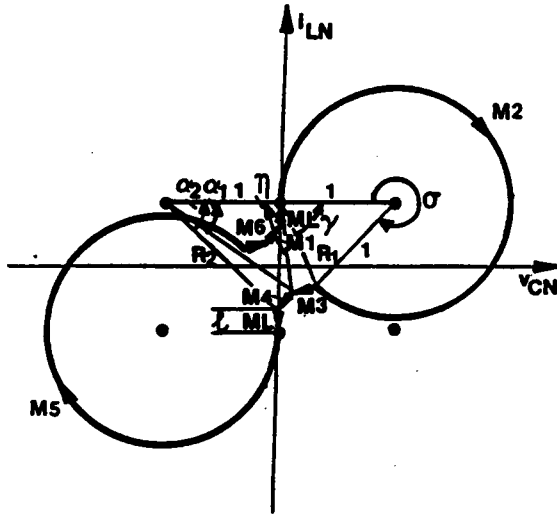
(c) Mixed-commutation trajectory ($\sigma < \pi$)

Figure C.4.2 Continued



(d) Force-commutation trajectory (multiple conduction)

Figure C.4.2 Continued



(a) Natural-commutation trajectory

$$\cos \sigma = \frac{2 - R_1^2}{2}, \quad \gamma = \frac{\sigma - \pi}{2},$$

$$\cos \eta = \frac{1 + R_1^2 - R_2^2}{2R_1}, \quad \cos \alpha_1 = \frac{1 + R_2^2 - R_1^2}{2R_2},$$

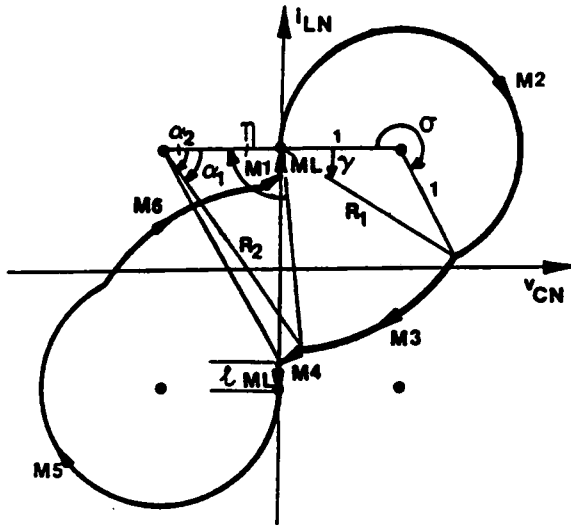
$$\cos \alpha_2 = \frac{1}{R_2}, \quad \sqrt{R_2^2 - 1} + \ell = 2I_{ON},$$

$$\frac{\beta_S}{\omega_{SN}} = \alpha_2 - \alpha_1 + \sigma + \ell, \quad \frac{\pi}{\omega_{SN}} = \sigma + \pi - \gamma - \eta + \alpha_2 - \alpha_1 + \ell.$$

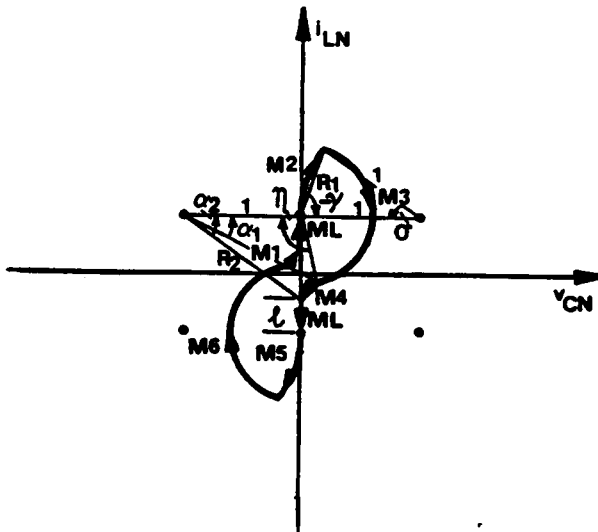
$$0 \leq R_1, \quad 1 \leq R_2 \leq \sqrt{1 + 4I_{ON}^2}, \quad 0 \leq \alpha_2 \leq \frac{\pi}{2},$$

$$-\frac{\pi}{2} \leq \alpha_1, \quad \gamma \leq \frac{\pi}{2}, \quad 0 \leq \eta \leq \frac{3\pi}{2}, \quad 0 \leq \sigma \leq 2\pi, \quad 0 \leq \ell \leq 2I_{ON}.$$

Figure C.4.3 Mode-III Trajectories

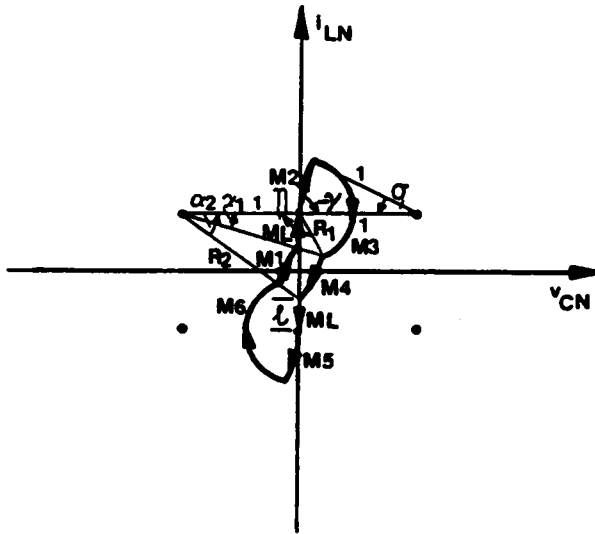


(b) Mixed-commutation trajectory ($\sigma \geq \pi$)

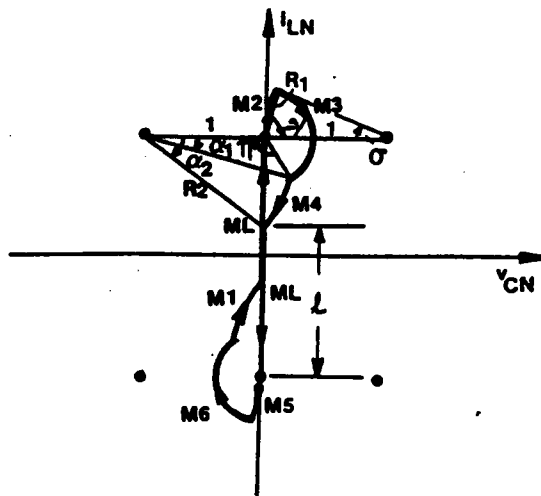


(c) Mixed-commutation trajectory ($\sigma < \pi$)

Figure C.4.3 Continued

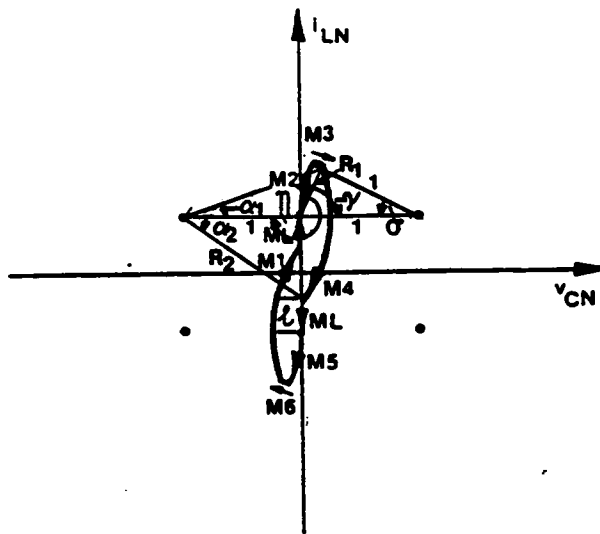


(d) Force-commutation trajectory ($\eta \leq \pi, R_2 \sin \alpha_2 \geq I_{ON}$)

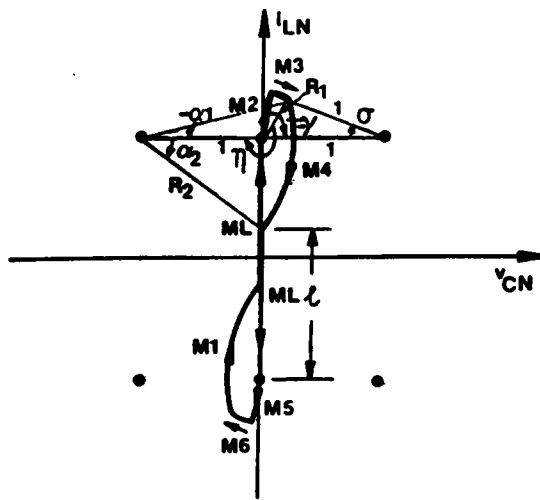


(e) Force-commutation trajectory ($\eta \leq \pi, R_2 \sin \alpha_2 < I_{ON}$)

Figure C.4.3 Continued

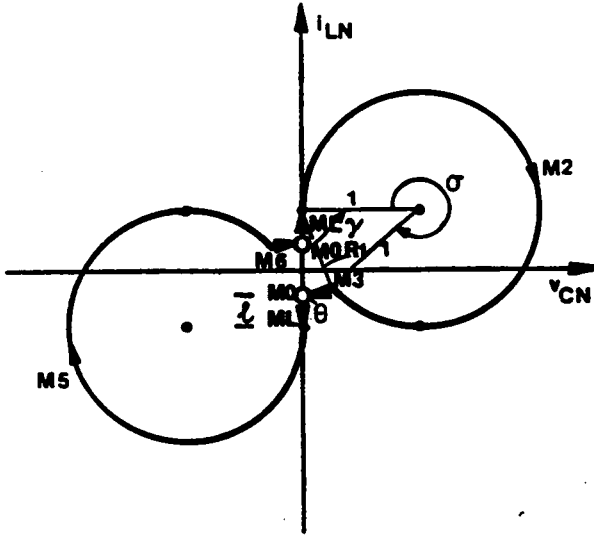


(f) Force-commutation trajectory ($\eta > \pi$, $R_2 \sin \alpha_2 \geq I_{ON}$)



(g) Force-commutation trajectory ($\eta > \pi$, $R_2 \sin \alpha_2 < I_{ON}$)

Figure C.4.3 Continued



(a) Natural-commutation trajectory

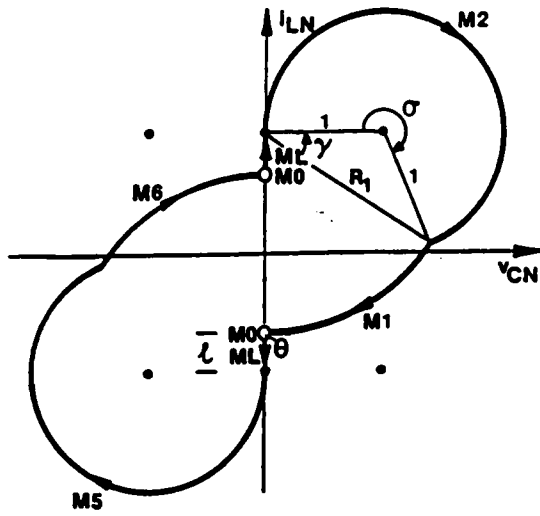
$$\cos \sigma = \frac{2 - R_1^2}{2}, \quad \gamma = \frac{\sigma - \pi}{2},$$

$$\frac{\beta_S}{\omega_{SN}} = \sigma + \ell, \quad R_1 = 2I_{ON} - \ell,$$

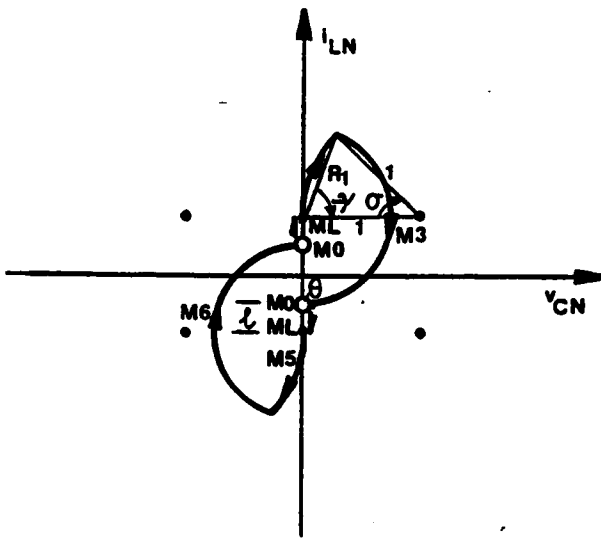
$$\frac{\pi}{\omega_{SN}} = \sigma + \frac{\pi}{2} - \gamma + \theta + \ell.$$

$$0 \leq R_1 \leq 2I_{ON}, \quad -\frac{\pi}{2} \leq \gamma \leq \frac{\pi}{2}, \quad 0 \leq \sigma \leq 2\pi, \quad 0 \leq \ell \leq 2I_{ON}.$$

Figure C.4.4 Mode-IV Trajectories

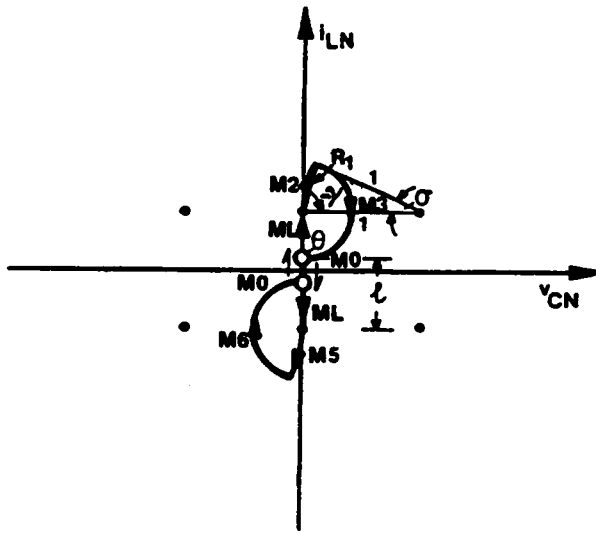


(b) Mixed-commutation trajectory ($\sigma \geq \pi$)



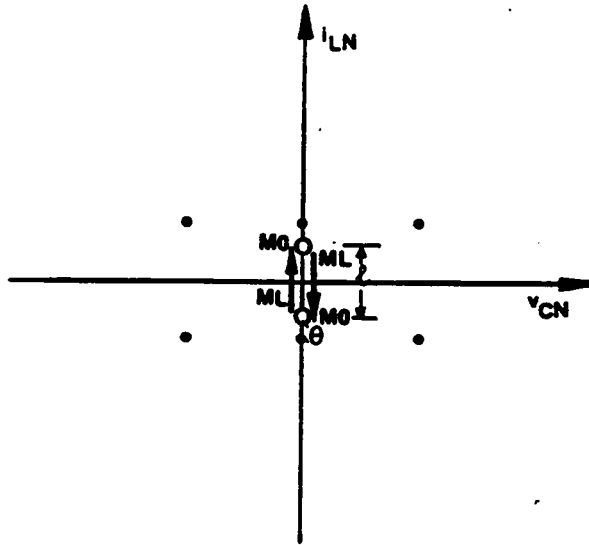
(c) Mixed-commutation trajectory ($\sigma < \pi$)

Figure C.4.4 Continued



(d) Force-commutation trajectory

Figure C.4.4 Continued

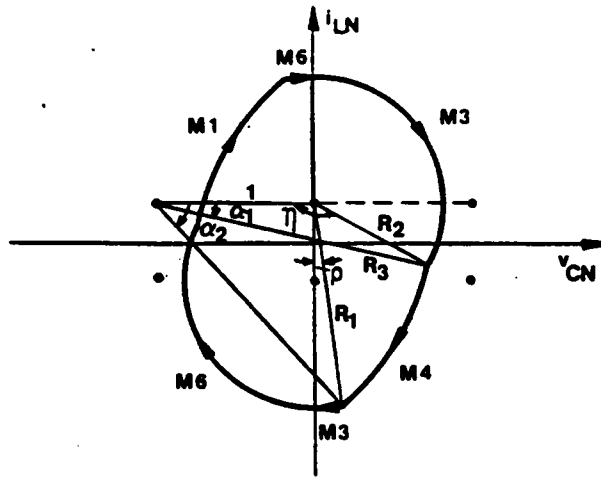


$$\frac{\beta_S}{\omega_{SN}} = \ell,$$

$$\frac{\pi}{\omega_{SN}} = \theta + \ell.$$

$$0 \leq \theta \leq 2\pi, \quad 0 \leq \ell \leq 2I_{ON}.$$

Figure C.4.5 Mode-V Trajectory



(a) Mixed-commutation trajectory

$$\cos\left(\frac{\pi}{2} + \rho\right) = \frac{1 + R_1^2 - R_3^2}{2R_1}, \quad \cos \alpha_2 = \frac{1 + R_3^2 - R_1^2}{2R_3},$$

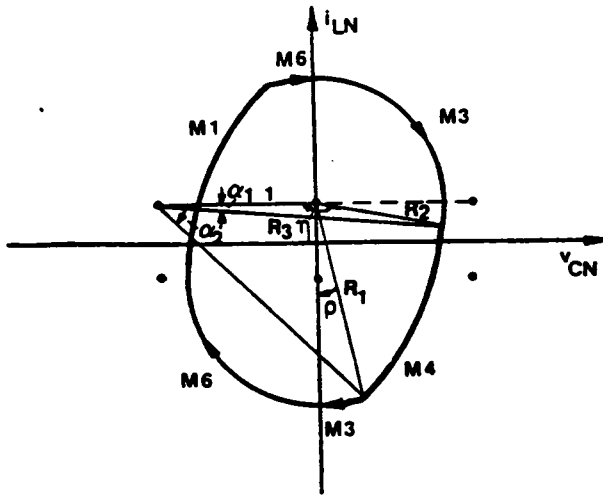
$$\cos \eta = \frac{1 + R_2^2 - R_3^2}{2R_2}, \quad \cos \alpha_1 = \frac{1 + R_3^2 - R_2^2}{2R_3},$$

$$\frac{\beta_S}{\omega_{SN}} = \alpha_2 - \alpha_1, \quad R_2 = R_1 + 2I_{ON},$$

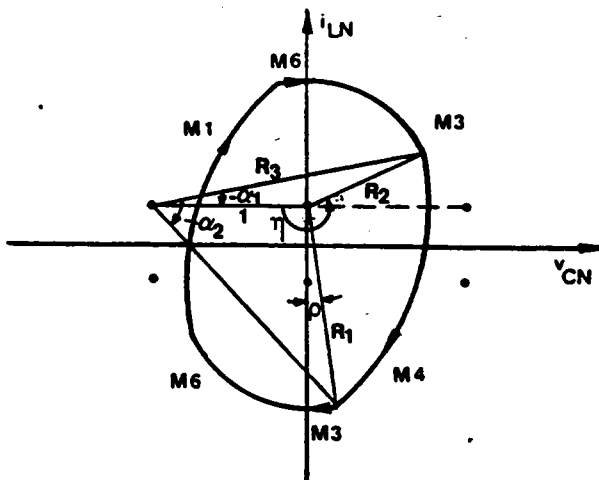
$$\frac{\pi}{\omega_{SN}} = \frac{3\pi}{2} - \eta + \alpha_2 - \alpha_1 + \rho.$$

$$2I_{ON} \leq R_1, \quad 0 \leq R_2, \quad 1 \leq R_3, \quad 0 \leq \alpha_2, \quad \rho \leq \frac{\pi}{2}, \quad -\frac{\pi}{2} \leq \alpha_1 \leq \frac{\pi}{2}, \quad 0 \leq \eta \leq \frac{3\pi}{2}.$$

Figure C.4.6 Mode-IIA Trajectories



(b) Force-commutation trajectory ($\eta \geq \pi$)



(c) Force-commutation trajectory ($\eta < \pi$)

Figure C.4.6 Continued

FORTRAN Program for Calculating Trajectory Parameters Below Resonant Frequency

```

C *****
C *****
C ***** PROGRAM NAME : PCPAR.FOR
C ***** FUNCTION : CALCULATE PARAMETERS FOR THE STEADY-STATE STATE
C ***** TRAJECTORIES BELOW RESONANT FREQUENCY.
C *****
C *****
C
DIMENSION X(8),Y(8),YY(8),XGUESS(8),BD(8),ID(8)
COMMON WN,OI,PI,BT,WTS
EXTERNAL FCN1,FCN2,FCN3,FCN4
PI=4.*ATAN(1.)
ERREL=0.0001
ITMAX=200
10 READ(5,*) WN,OI,ND
IF(WN.LT.0) STOP
WRITE(6,1000) WN,OI
IC=1
WTS=PI/WN
12 READ(5,*) (BD(K), K=1,8)
J=0
DO 14 K=1,8
IF(BD(K).NE.0.) J=J+1
BD(K)=BD(K)*WTS/180.
14 CONTINUE
READ(5,*) (ID(K), K=1,J+1)
BT=WTS
15 DO 22 K=1,J
IF(BT.GE.BD(K)) THEN
II=ID(K)
GO TO 35
ENDIF
22 CONTINUE
II=ID(J+1)
35 GO TO (100,200,300,400,500),II
100 IF(IC.EQ.1) THEN
CALL INITIAL1(XGUESS)
IC=0
Y(1)=XGUESS(2)
Y(2)=XGUESS(1)
Y(3)=XGUESS(3)
Y(4)=XGUESS(4)
Y(5)=2*PI-XGUESS(5)
Y(6)=XGUESS(8)
Y(7)=XGUESS(7)
Y(8)=XGUESS(6)
ELSE
IF(IOD.FQ.2) THEN
DO 103 I=1,5
103 YY(I)=Y(I)
Y(1)=YY(2)
Y(2)=YY(1)
Y(3)=(1+YY(2)**2)**0.5

```

```

        Y(4)=YY(3)
        Y(5)=YY(4)
        Y(6)=ACOS(1/Y(3))
        Y(7)=Y(6)
        Y(8)=PI/2.
    ENDIF
ENDIF
I=0
N=8
105 XGUESS(1)=Y(1)-I*0.2
    XGUESS(2)=Y(2)-I*0.2
    XGUESS(3)=Y(3)+I*0.2
    XGUESS(4)=Y(4)
    XGUESS(5)=Y(5)
    XGUESS(6)=Y(6)
    XGUESS(7)=Y(7)
    XGUESS(8)=Y(8)
    CALL NEQNF(FCN1,ERREL,N,ITMAX,XGUESS,X,FNORM)
    IF(X(1).GE.0.AND.X(2).GE.1.AND.X(3).GE.1.AND.
1   X(4).GE.0.AND.X(4).LE.1.5708.AND.X(5).GE.0.AND.X(5).LE.6.2832
1   .AND.X(6).GE.X(7).AND.X(7).GE.0.AND.X(6).LE.1.5708.AND.
1   X(8).GE.1.57079.AND.X(8).LE.3.1416) THEN
        IFLAG=1
        IOD=1
        DO 150 K=1,N
            Y(K)=X(K)
150    CONTINUE
            X(1)=Y(2)
            X(2)=Y(1)
            X(3)=Y(3)
            X(4)=Y(4)
            X(5)=2*PI-Y(5)
            X(6)=Y(8)
            X(7)=Y(7)
            X(8)=Y(6)
            IF(X(5).GE.PI) THEN
                GA=(1-1/WN)*PI-X(6)+BT
                IF(X(2)*SIN(GA).GT.O1) THEN
                    IDD=11
                ELSE
                    IDD=12
                ENDIF
            ELSE
                IF(X(6).LE.PI) THEN
                    IF(X(3)*SIN(X(7)).GT.O1) THEN
                        IDD=13
                    ELSE
                        IDD=14
                    ENDIF
                ELSE
                    IDD=15
                ENDIF
            ENDIF
            BS=BT*180/WTS
            WRITE(6,9999) II,IDD,BS,(X(K),K=1,8)
9999    FORMAT(1X,I2,1X,I2,F10.4,8F7.4)
            GO TO 999
        ELSE

```

```

      IF(I.GE.8) THEN
C      BS = BT*180/WTS
C      WRITE(6,8888) BS
C8888  FORMAT(/,'ERROR OCCUR AT BS = ',F10.4)
      BT = BT + WTS/(3*ND)
      GO TO 15
      ELSE
      I = I + 1
      GO TO 105
      ENDIF
    ENDIF
  200 I = 0
      IF(IOD.EQ.1) THEN
      TEMP = Y(1)
      Y(1) = Y(2)
      Y(2) = TEMP
      Y(3) = Y(4)
      Y(4) = Y(5)
      Y(5) = PI/2.
      ENDIF
      IF(IOD.EQ.4) THEN
      Y(1) = 2*OI
      Y(2) = 1.
      Y(3) = 0.
      Y(4) = ACOS(1-2*OI**2)
      Y(5) = PI/2.
      ENDIF
      N = 5
  205 XGUESS(1) = Y(1)-I*0.15
      XGUESS(2) = Y(2)-I*0.15
      XGUESS(3) = Y(3)-I*0.05
      XGUESS(4) = Y(4) + I*.15
      XGUESS(5) = Y(5)-I*0.05
      CALL NEQNF(FCN2,ERREL,N,ITMAX,XGUESS,X,FNORM)
      IF(X(1).GE.0.AND.X(2).GE.2*OI.AND.X(3).GE.
1 -1.57079.AND.X(3)*X(5).GE.0.
1 .AND.X(3).LE.3.1416.AND.X(4).GE.0.AND.X(4).LE.6.2832.AND.
1 X(5).GE.-1.57079.AND.X(5).LE.3.1416) THEN
      IOD = 2
      DO 250 K = 1,N
      Y(K) = X(K)
  250  CONTINUE
      X(1) = Y(1)
      X(2) = Y(2)
      X(3) = Y(3)
      X(4) = 2*PI-Y(4)
      X(5) = Y(5)
      X(6) = 0.
      X(7) = 0.
      X(8) = 0.
      IF(X(4).GE.PI) THEN
      GA = (1-1/WN)*PI-X(5) + BT
      IF(X(2)*SIN(GA).GT.OI) THEN
      IDD = 21
      ELSE
      IDD = 22
      ENDIF
      ELSE

```



```

        IDD = 23
        ENDIF
        BS = BT*180/WTS
        WRITE(6,9999) II,IDD,BS,(X(K),K = 1,8)
        GO TO 999
    ELSE
        IF(I.GE.8) THEN
C          BS = B*180/WTS
C          WRITE(6,8888) BS
          BT = BT + WTS/(3*ND)
          IF(IOD.EQ.1) THEN
              TEMP = Y(1)
              Y(1) = Y(2)
              Y(2) = TEMP
          ENDIF
          GO TO 15
        ELSE
          I = I + 1
          GO TO 205
        ENDIF
    ENDIF
    ENDIF
300 I = 0
    IF(IFLAG.EQ.0) THEN
        Y(1) = 2*OI
        Y(2) = (1 + 4*OI**2)**0.5
        Y(3) = PI/2.
        Y(4) = PI/3.
        Y(5) = PI/3.
    ENDIF
    IF(IOD.EQ.1) THEN
        Y(2) = Y(3)
        Y(3) = Y(5)
        Y(4) = Y(6)
        Y(5) = Y(7)
    ENDIF
    IF(IOD.EQ.2) THEN
        TEMP = Y(2)
        Y(1) = TEMP
        Y(2) = (1 + TEMP**2)**0.5
        Y(3) = Y(4)
        Y(4) = ATAN(TEMP)
        Y(5) = Y(4)
    ENDIF
    IF(IOD.EQ.4) THEN
        TEMP = Y(2)
        Y(2) = (1 + Y(1)**2)**0.5
        Y(3) = TEMP
        Y(4) = ATAN(Y(1))
        Y(5) = Y(4)
    ENDIF
    N = 5
305 XGUESS(1) = Y(1)-I*0.2
    XGUESS(2) = Y(2)-I*0.2
    XGUESS(3) = Y(3)
    XGUESS(4) = Y(4)-I*0.1
    XGUESS(5) = Y(5)-I*0.1
    CALL NEQNF(FCN3,ERREL,N,ITMAX,XGUESS,X,FORM)
    IF(X(1).GE.0.AND.X(2).GE.0

```

```

1 .AND.X(2).LE.(1+4*OI**2)**0.5.AND.X(3).GE.0
1 .AND.X(3).LE.6.2832.AND.X(5).GE.0.AND.X(5).LE.X(4).AND.
1 X(4).LE.1.5708) THEN
    IOD=3
    DO 350 K=1,N
    Y(K)=X(K)
350 CONTINUE
    X(1)=Y(1)
    X(2)=Y(2)
    X(3)=2*PI-Y(3)
    X(4)=1.5*PI-X(3)/2.+BT-WTS
    X(5)=Y(5)
    X(6)=Y(4)
    X(7)=0.
    X(8)=0.
    IF(X(3).GE.PI) THEN
        GA=(-PI+X(3))/2.
        IF(X(1)*SIN(GA).GT.OI) THEN
            IDD=31
        ELSE
            IDD=32
        ENDIF
    ELSE

```

FORTRAN Program for Calculating Trajectory Parameters Above Resonant Frequency

```

C *****
C *****
C ***** PROGRAM : PC10PAR.FOR
C ***** FUNCTION : CALCULATE THE PARAMETERS FOR EQUILIBRIUM STATE
C *****          TRAJECTORIES. ION FIXED, PULSE WIDTH VARYING.
C *****
C *****
C *****
C
DIMENSION X(8), XGUESS(8), Y(8)
EXTERNAL FCN1, FCN2A, FCN3
COMMON WN, OI, PI, BT, WTS
PI=4.*ATAN(1.)
ERREL=0.0001
ITMAX=200
10 READ(5,*) WN,OI,SN
IF(WN.LE.0) STOP
WRITE(6,111) WN, OI
IC=1
WTS=PI/WN
CALL BDY(BA1,BA2,BC1,BC2)
BT=WTS
20 IF(BT.GT.BA1) THEN
ID=1
ELSE
IF(BT.GT.BA2) THEN
ID=21
ELSE
IF(BT.GT.BC1) THEN
ID=1
ELSE
IF(BT.GT.BC2) THEN
ID=3
ELSE
ID=5
ENDIF
ENDIF
ENDIF
ENDIF
ENDIF
IF(ID.EQ.1) GO TO 100
IF(ID.EQ.21) GO TO 2100
IF(ID.EQ.3) GO TO 300
IF(ID.EQ.5) GO TO 500
100 IF(IC.EQ.1) THEN
CALL INITIAL1(XGUESS)
IC=0
ELSE
IF(IOD.EQ.21) THEN
XGUESS(1)=(1+Y(2)**2)**0.5
XGUESS(2)=Y(2)
XGUESS(3)=Y(3)
XGUESS(4)=ACOS(1/XGUESS(1))
XGUESS(5)=XGUESS(4)
XGUESS(6)=Y(5)

```

```

        XGUESS(7) = Y(6)
        XGUESS(8) = Y(7)
        ELSE
        DO 110, K = 1,8
110     XGUESS(K) = Y(K)
        ENDIF
        ENDIF
        N = 8
        CALL NEQNF(FCN1,ERREL,N,ITMAX,XGUESS,X,FNORM)
        IOD = 1
        DO 120, K = 1,8
120     Y(K) = X(K)
        IF(X(5).GE.PI) THEN
            GA = PI-WTS-X(6) + BT
            IF(X(2)*SIN(GA).GE.OI) THEN
                IDD = 11
            ELSE
                IDD = 12
            ENDIF
        ELSE
            IF(X(6).LE.PI) THEN
                IF(X(3)*SIN(X(7)).GE.OI) THEN
                    IDD = 13
                ELSE
                    IDD = 14
                ENDIF
            ELSE
                IDD = 15
            ENDIF
        ENDIF
        BS = BT*180./WTS
        WRITE(6,1000) ID, IDD, BS, (X(K),K = 1,8)
        GO TO 999
2100    IF(IOD.EQ.1) THEN
            XGUESS(1) = Y(2) + 2*OI
            XGUESS(2) = Y(2)
            XGUESS(3) = Y(3)
            XGUESS(4) = 0.
            XGUESS(5) = Y(6)
            XGUESS(6) = Y(7)
            XGUESS(7) = Y(8)
        ELSE
            DO 2110, K = 1,7
2110     XGUESS(K) = Y(K)
        ENDIF
        N = 7
        CALL NEQNF(FCN2A,ERREL,N,ITMAX,XGUESS,X,FNORM)
        IOD = 21
        DO 2120, K = 1,N
2120     Y(K) = X(K)
        IF(X(5).LE.PI) THEN
            IF(X(3)*SIN(X(6)).GE.OI) THEN
                IDD = 23
            ELSE
                IDD = 24
            ENDIF
        ELSE
            IDD = 25
        ENDIF

```

```

ENDIF
BS = BT*180./WTS
X(8) = 0.
WRITE(6,1000) ID, IDD, BS, (X(K), K = 1,8)
GO TO 999
300 IF(IC.EQ.1) THEN
    CALL INITIAL3(XGUESS)
    IC = 0
ELSE
    IF(IOD.EQ.1) THEN
        XGUESS(1) = Y(2)
        XGUESS(2) = Y(3)
        XGUESS(3) = Y(5)
        XGUESS(4) = Y(6)
        XGUESS(5) = Y(7)
        XGUESS(6) = Y(8)
    ELSE
        IF(IOD.EQ.21) THEN
            BT = BT + WTS/SN-0.005
            GO TO 20
        ENDIF
        DO 310, K = 1,6
310     XGUESS(K) = Y(K)
    ENDIF
ENDIF
N = 6
CALL NEQNF(FCN3,ERREL,N,ITMAX,XGUESS,X,FNORM)
IOD = 3
DO 320, K = 1,N
320 Y(K) = X(K)
    IF(X(3).GE.PI) THEN
        GA = (X(3)-PI)/2.
        IF(X(1)*SIN(GA).GE.O1) THEN
            IDD = 31
        ELSE
            IDD = 32
        ENDIF
    ELSE
        IF(X(4).LE.PI) THEN
            IF(X(2)*SIN(X(5)).GE.O1) THEN
                IDD = 33
            ELSE
                IF(X(2)*SIN(X(6)).GT.O1) THEN
                    IDD = 34
                ELSE
                    IDD = 36
                ENDIF
            ENDIF
        ELSE
            IF(X(2)*SIN(X(6)).GT.O1) THEN
                IDD = 35
            ELSE
                IDD = 37
            ENDIF
        ENDIF
    ENDIF
ENDIF
BS = BT*180./WTS
X(7) = 0.

```

```

X(8)=0.
WRITE(6,1000) ID, IDD, BS, (X(K), K = 1,8)
GO TO 999
500 IDD = 55
    N = 2
    X(1) = BT
    X(2) = WTS - BT
    BS = BT * 180. / WTS
    DO 505, K = 3,8
505 X(K) = 0.
    WRITE(6,1000) ID, IDD, BS, (X(K), K = 1,8)
999 IF(BT.EQ.0) GO TO 10
    BT = BT - WTS / SN
    IF(BT.LT.0) BT = 0
    GO TO 20
111 FORMAT(1X,2F10.5)
1000 FORMAT(1X,I2,1X,I2,F10.4,8F7.4)
    END
C
C *****
C *****
C *****
C
SUBROUTINE BDY(BA1,BA2,BC1,BC2)
COMMON WN, OI, PI, BT, WTS
10 A = ACOS(1-OI**2)
    B = ACOS((1 + OI**2)/(1 + 4*OI**2)**0.5)
    C = ACOS(1/(1 + 4*OI**2)**0.5)
    WN1 = PI/(A + B + C)
    WN2 = PI/(2*OI)
    IF(WN.GE.WN2) THEN
        BC1 = WTS
        BC2 = WTS
    ELSE
        IF(WN.GE.WN1) THEN
            BC1 = WTS
            BC2 = 2*OI
        ELSE
            BC2 = 2*OI
            A = ACOS(-2*OI**2 + (1 + 4*OI**2)**0.5)
            B = ACOS(1/(1 + 4*OI**2)**0.5)
            WN3 = PI/(0.5*(PI + A) + B)
            IF(WN.GE.WN3) THEN
                RH = (2**0.5)*OI
                RL = (1 + 4*OI**2)**0.5 - 1
                R = (RH + RL)/2.
                CALL FQBDIII(R,AL,BE1,BE2,GA1,GA2)
                WNC = PI/(AL + BE1 - BE2 + GA2 + GA1)
                IF(ABS(WNC - WN).LE.1.E-4) THEN
                    BC1 = (GA2 + GA1 + AL)
                ELSE
                    IF(WNC.GT.WN) THEN
                        RH = R
                    ELSE
                        RL = R
                    ENDIF
                    GO TO 15
                ENDIF
            ENDIF
        ENDIF
    ENDIF
15
    ENDIF

```

```

ELSE
  RH = 2*OI
  RL = (1 + 4*OI**2)**0.5-1
25  R = (RH + RL)/2.
  CALL FQBDIII(R,AL,BE1,BE2,GA1,GA2)
  WNC = PI/(AL + BE1 + BE2 + GA2-GA1)
  IF(ABS(WNC-WN).LE.1.E-4) THEN
    BC1 = (GA2-GA1 + AL)
  ELSE
    IF(WNC.GT.WN) THEN
      RL = R
    ELSE
      RH = R
    ENDIF
    GO TO 25
  ENDIF
ENDIF
ENDIF
ENDIF
ENDIF
CALL BDIIA(BA1,BA2)
RETURN
END
C
C *****
C *****
C *****
C
SUBROUTINE FQBDIII(R1,AL,BE1,BE2,GA1,GA2)
IMPLICIT REAL*4 (A-H,O-Z)
COMMON WN, OI, PI, BT, WTS
R2 = (1 + 4*OI**2)**0.5
AL = ACOS(1-0.5*R1**2)
BE1 = (PI-AL)*0.5
BE2 = PI-ACOS((1 + R1**2-R2**2)/(2*R1))
GA1 = ACOS((1 + R2**2-R1**2)/(2*R2))
GA2 = ACOS(1/R2)
RETURN
END
C
C *****
C *****
C *****
C
SUBROUTINE BDIIA(BA1,BA2)
IMPLICIT REAL*4 (A-H,O-Z)
COMMON WN, OI, PI, BT, WTS
11 IF(OI.GE.0.5) THEN
  BA1 = WTS
  BA2 = WTS
  RETURN
ENDIF
R2A1 = 2*OI**2/(1-2*OI)
CALL FQIIA(R2A1,AL1,AL2,ET2,WA1,WA11)
R2 = R2A1 + 25.
12 CALL FQIIA(R2,AL1,AL2,ET2,WNC1,WNC2)
IF(WNC1.GE.WA1) THEN
  R2 = R2*2.
  GO TO 12

```

```

ENDIF
R2A2 = R2
WA2 = WNC1
RH = R2A2
RL = R2A1
14 R2 = (RH + RL) / 2.
R2P = R2 + 1.E-4
CALL FQIIA(R2,AL1,AL2,ET2,WNC1,WNC2)
CALL FQIIA(R2P,AL1,AL2,ET2,WNC1,WNC2)
IF(ABS(RH-RL).LE.1.E-4) THEN
  R2AMAX = R2
  WAMAX = WNC1
ELSE
  IF(WNC1.LE.WNC2) THEN
    RL = R2
  ELSE
    RH = R2
  ENDIF
  GO TO 14
ENDIF
IF(WN.GE.WAMAX) THEN
  BA1 = WTS
  BA2 = WTS
  RETURN
ENDIF
IF(WN.GE.WA1) THEN
  RH = R2A2
  RL = R2AMAX
22 R2 = (RH + RL) / 2.
CALL FQIIA(R2,AL1,AL2,ET2,WNC1,WNC2)
IF(ABS(RH-RL).LE.1.E-4) THEN
  BA1 = (AL2 + AL1)
ELSE
  IF(WNC1.GT.WN) THEN
    RL = R2
  ELSE
    RH = R2
  ENDIF
  GO TO 22
ENDIF
RH = R2AMAX
RL = R2A1
24 R2 = (RH + RL) / 2.
CALL FQIIA(R2,AL1,AL2,ET2,WNC1,WNC2)
IF(ABS(RH-RL).LE.1.E-4) THEN
  BA2 = (AL2 + AL1)
ELSE
  IF(WNC1.GT.WN) THEN
    RH = R2
  ELSE
    RL = R2
  ENDIF
  GO TO 24
ENDIF
ELSE
  IF(WN.GE.WA2) THEN
    R2A3 = R2A2
  ELSE

```



```

26      R2=R2A2*2
      CALL FQIIA(R2,AL1,AL2,ET2,WNC1,WNC2)
      IF(WN.GT.WNC1) THEN
          R2A3= R2
          ELSE
          R2= R2*2
          GO TO 26
      ENDIF
      ENDIF
      RH= R2A3
      RL= R2AMAX
28      R2=(RH+RL)/2.
      CALL FQIIA(R2,AL1,AL2,ET2,WNC1,WNC2)
      IF(ABS(RH-RL).LE.1.E-4) THEN
          BA1=(AL2+AL1)
          ELSE
          IF(WNC1.GT.WN) THEN
              RL= R2
              ELSE
              RH= R2
          ENDIF
          GO TO 28
      ENDIF
      R2= R2A1 + 5.
32      CALL FQIIA(R2,AL1,AL2,ET2,WNC1,WNC2)
      IF(WNC2.LE.WN) THEN
          R2A4= R2
          ELSE
          R2= R2*2.
          GO TO 32
      ENDIF
      RH= R2A4
      RL= R2A1
34      R2=(RH+RL)/2.
      CALL FQIIA(R2,AL1,AL2,ET2,WNC1,WNC2)
      IF(ABS(RH-RL).LE.1.E-4) THEN
          BA2=(AL2-AL1)
          ELSE
          IF(WNC2.GT.WN) THEN
              RL= R2
              ELSE
              RH= R2
          ENDIF
          GO TO 34
      ENDIF
      ENDIF
      ENDIF
      RETURN
      END
C
C *****
C *****
C *****
C
SUBROUTINE FQIIA(R2,AL1,AL2,ET2,WNC1,WNC2)
IMPLICIT REAL*4 (A-H,O-Z)
COMMON WN, OI, PI, BT, WTS
R3= ((R2+2*OI)**2+ 1.)**0.5
AL2= ACOS(1/R3)

```

```

AL1 = ACOS((1 + R3**2 - R2**2)/(2*R3))
ET1 = 2*PI - ACOS((1 + R2**2 - R3**2)/(2*R2))
ET2 = 2*PI - ET1
WNC1 = PI/(AL2 + AL1 + 1.5*PI - ET1)
WNC2 = PI/(AL2 - AL1 + 1.5*PI - ET2)
RETURN
END

```

C
C
C
C
C

```

SUBROUTINE INITIAL1(X)
IMPLICIT REAL*4 (A-H,O-Z)
DIMENSION X(8)
COMMON WN, OI, PI, BT, WTS
RMAX = 10.

```

```

601 CALL ICFREQ1(RMAX,R3,RO,SI,AL1,AL2,WNC)
IF(WNC.GT.WN) THEN
  RMAX = RMAX*2.
  GO TO 601

```

```

ENDIF
RA = RMAX
RB = 1.

```

```

611 R = (RA + RB)/2.
CALL ICFREQ1(R,R3,RO,SI,AL1,AL2,WNC)
IF(ABS(WNC-WN).LE.0.0001) THEN
  X(1) = R
  X(2) = (1 + R**2 - 2*R*COS(SI))**0.5
  X(3) = R3
  X(4) = RO
  X(5) = SI
  X(6) = PI + ACOS((1 + X(2)**2 - R**2)/(2*X(2)))
  X(7) = -AL1
  X(8) = AL2
  RETURN

```

```

ELSE
  IF(WNC.LT.WN) THEN
    RA = R
  ELSE
    RB = R
  ENDIF
  GO TO 611

```

```

ENDIF
END

```

C
C
C
C
C

```

SUBROUTINE INITIAL3(X)
IMPLICIT REAL*4 (A-H,O-Z)
DIMENSION X(8)
COMMON WN, OI, PI, BT, WTS
RA = (1. + 4.*OI**2)**0.5
RB = 1.

```

```

622 R = (RA + RB)/2.
CALL ICFREQ3(R,SI,AL1,AL2,WNC)

```

```

IF(ABS(WNC-WN).LE.0.0001) THEN
  X(1)=(2.-2.*COS(SI))**0.5
  X(2)=R
  X(3)=SI
  X(4)=1.5*PI-0.5*SI
  X(5)=-AL1
  X(6)=AL2
  RETURN
ELSE
  IF(WNC.LT.WN) THEN
    RA=R
  ELSE
    RB=R
  ENDIF
  GO TO 622
ENDIF
END

```

C
C
C
C
C

```

SUBROUTINE ICFREQ1(R1,R3,RO,SI,AL1,AL2,WNC)
IMPLICIT REAL*4 (A-H,O-Z)
COMMON WN, OI, PI, BT, WTS
R3=(1+(2*OI+(R1**2-1)**0.5)**2)**0.5
SI=ACOS((4+R1**2-R3**2)/(4*R1))
RO=ACOS(1/R1)
AL1=ACOS((4+R3**2-R1**2)/(4*R3))
AL2=ACOS(1/R3)
WNC=PI/(AL1+AL2+SI-RO)
RETURN
END

```

C
C
C
C
C

```

SUBROUTINE ICFREQ3(R,SI,AL1,AL2,WNC)
IMPLICIT REAL*4 (A-H,O-Z)
REAL*4 LK
COMMON WN, OI, PI, BT, WTS
SI=ACOS((5-R**2)/4.)
AL1=ACOS((3+R**2)/(4*R))
AL2=ACOS(1/R)
LK=2*OI-(R**2-1)**0.5
WNC=PI/(LK+AL1+AL2+SI)
RETURN
END

```

C
C
C
C
C

```

SUBROUTINE FCN1(X,F,N)
IMPLICIT REAL*4 (A-H,O-Z)
DIMENSION X(N), F(N)
COMMON WN, OI, PI, BT, WTS

```

```

F(1) = X(1)*COS(X(4))-1
F(2) = 2*X(1)*COS(2*PI-X(5))-1-X(1)**2 + X(2)**2
F(3) = X(3)*COS(X(8))-1
F(4) = 2*X(3)*COS(X(7))-1-X(3)**2 + X(2)**2
F(5) = 2*X(2)*COS(PI-WTS-X(6) + BT)-1-X(2)**2 + X(1)**2
F(6) = 2*X(2)*COS(X(6))-1-X(2)**2 + X(3)**2
IF(X(1).LT.1) THEN
  X(1) = 1.
ENDIF
F(7) = X(3)**2-1-(2*OI + (X(1)**2-1)**0.5)**2
F(8) = X(8)-X(7) + X(5)-X(4)-BT
RETURN
END

```

C
C
C
C
C

```

*****
*****
*****

```

```

SUBROUTINE FCN2A(X,F,N)
IMPLICIT REAL*4 (A-H,O-Z)
DIMENSION X(N), F(N)
COMMON WN, OI, PI, BT, WTS
F(1) = X(1)-X(2)-2*OI
F(2) = 2*X(3)*COS(X(7))-1-X(3)**2 + X(1)**2
F(3) = 2*X(3)*COS(X(6))-1-X(3)**2 + X(2)**2
F(4) = 2*X(2)*COS(X(5))-1-X(2)**2 + X(3)**2
F(5) = 2*X(1)*COS(X(4) + 0.5*PI)-1-X(1)**2 + X(3)**2
F(6) = 1.5*PI-X(5)-X(6) + X(7) + X(4)-WTS
F(7) = X(7)-X(6)-BT
RETURN
END

```

C
C
C
C
C

```

*****
*****
*****

```

```

SUBROUTINE FCN3(X,F,N)
IMPLICIT REAL*4 (A-H,O-Z)
DIMENSION X(N), F(N)
COMMON WN, OI, PI, BT, WTS
F(1) = 2*COS(X(3))-2 + X(1)**2
F(2) = 2*X(1)*COS(X(4))-1-X(1)**2 + X(2)**2
F(3) = X(2)*COS(X(6))-1
F(4) = 2*X(2)*COS(X(5))-1-X(2)**2 + X(1)**2
IF(X(2).LT.1) THEN
  X(2) = 1.00
ENDIF
F(5) = X(6)-X(5) + 2*OI-(X(2)**2-1)**0.5 + X(3)-BT
F(6) = 1.5*PI-X(4)-0.5*X(3)-WTS + BT
RETURN
END

```



```

RC = RMSI(R3,A,B,OI,4)
AC = AVV(R3,A,B,OI,4)
VAV = (AA + AB + AC)/WTS
ILRMS = ((RA + RB + RC)/WTS)**0.5
IF(IDD.EQ.11) THEN
  VCPK = 1 + R1
  IQ1OFF = 0.
  IQ2OFF = 0.
  IQ1ON = R2*SIN(GA)-OI
  IQ2ON = R3*SIN(AL1)-OI
  XX = PI-ASIN(OI/R1)
  B = PI-RO
  A = PI-XX
  RAA = RMSI(R1,A,B,OI,2)
  IQ1RMS = ((RAA + RB + RC)/WTS)**0.5
  IQ2RMS = ((RAA + RC)/WTS)**0.5
  B = -(PI-XX)
  A = SI-PI
  DA = AVI(R1,A,B,OI,2)
  B = -GA
  A = PI-ET
  DB = AVI(R2,A,B,OI,3)
  ID1AV = -DA/WTS
  ID2AV = -(DA + DB)/WTS
ELSE
  IF(IDD.EQ.12.OR.IDD.EQ.13) THEN
    IF(IDD.EQ.12) THEN
      VCPK = 1 + R1
      ELSE
        VCPK = R2
      ENDIF
      IQ1OFF = OI + R1*SIN(SI)
      IQ2OFF = 0.
      IQ1ON = 0.
      IQ2ON = R3*SIN(AL1)-OI
      Y = ASIN(OI/R2)
      B = -Y
      A = PI-ET
      RBB = RMSI(R2,A,B,OI,3)
      IQ1RMS = ((RA + RBB + RC)/WTS)**0.5
      B = -GA
      A = Y
      RBB = RMSI(R2,A,B,OI,3)
      IQ2RMS = ((RA + RBB + RC)/WTS)**0.5
      B = -GA
      A = Y
      DA = AVI(R2,A,B,OI,3)
      B = -Y
      A = PI-ET
      DB = AVI(R2,A,B,OI,3)
      ID1AV = DA/WTS
      ID2AV = -DB/WTS
    ELSE
      IF(IDD.EQ.14) THEN
        VCPK = R2
        ELSE
          VCPK = R3-1
        ENDIF
    ENDIF

```

```

IQ1OFF = OI + R1*SIN(SI)
IQ2OFF = OI - R3*SIN(AL1)
IQ1ON = 0.
IQ2ON = 0.
Z = ASIN(OI/R3)
B = -Z
A = AL2
RCC = RMSI(R3,A,B,OI,4)
IQ1RMS = ((RA + RCC)/WTS)**0.5
IQ2RMS = ((RA + RB + RCC)/WTS)**0.5
B = -GA
A = PI-ET
DA = AVI(R2,A,B,OI,3)
B = -AL1
A = Z
DB = AVI(R3,A,B,OI,4)
ID1AV = (DA + DB)/WTS
ID2AV = DB/WTS
ENDIF
ENDIF
GO TO 999
200 R1 = X(1)
R2 = X(2)
RO = X(3)
SI = X(4)
AL = X(5)
GA = (1-1/WN)*PI-AL + BT
R3 = R2-2*OI
IF(AL.LT.0.AND.R3*SIN(-AL).GT.OI) IDD = 29
B = 0.5*PI
A = -AL
RA = RMSI(R3,A,B,OI,3)
AA = AVV(R3,A,B,OI,3)
B = PI-RO
A = SI-PI
RB = RMSI(R1,A,B,OI,2)
AB = AVV(R1,A,B,OI,2)
B = -GA
A = 0.5*PI
RC = RMSI(R2,A,B,OI,3)
AC = AVV(R2,A,B,OI,3)
VAV = (AA + AB + AC)/WTS
ILRMS = ((RA + RB + RC)/WTS)**0.5
IF(IDD.EQ.21) THEN
  XX = ASIN(OI/R1)
  B = PI-RO
  A = XX
  RBB = RMSI(R1,A,B,OI,2)
  IQ1RMS = ((RA + RBB + RC)/WTS)**0.5
  IQ2RMS = (RBB/WTS)**0.5
  B = 0.5*PI
  A = -AL
  DA = AVI(R3,A,B,OI,3)
  B = -XX
  A = SI-PI
  DB = AVI(R1,A,B,OI,2)
  B = -GA
  A = 0.5*PI

```

```

DC = AVI(R2,A,B,OI,3)
ID1AV = -DB/WTS
ID2AV = (DA-DB-DC)/WTS
VCPK = 1 + R1
IQ1OFF = 0.
IQ2OFF = 0.
IQ1ON = R2*SIN(GA)-OI
IQ2ON = R1*SIN(RO) + OI
ELSE
IF(IDD.EQ.22.OR.IDD.EQ.23) THEN
  IF(IDD.EQ.22) THEN
    VCPK = 1 + R1
  ELSE
    VCPK = R2
  ENDIF
  Y = ASIN(OI/R2)
  B = -Y
  A = 0.5*PI
  RCC = RMSI(R2,A,B,OI,3)
  IQ1RMS = ((RA + RB + RCC)/WTS)**0.5
  B = -GA
  A = Y
  RCC = RMSI(R2,A,B,OI,3)
  IQ2RMS = ((RB + RCC)/WTS)**0.5
  B = PI/2.
  A = -AL
  DA = AVI(R3,A,B,OI,3)
  B = -GA
  A = Y
  DCC = AVI(R2,A,B,OI,3)
  ID1AV = DCC/WTS
  B = -Y
  A = PI/2.
  DCC = AVI(R2,A,B,OI,3)
  ID2AV = (DA-DCC)/WTS
  IQ1OFF = R2*SIN(-GA) + OI
  IQ2OFF = 0.
  IQ1ON = 0.
  IQ2ON = R1*SIN(RO) + OI
ELSE
  VCPK = R2
  Y = ASIN(OI/R3)
  B = PI/2.
  A = Y
  RAA = RMSI(R3,A,B,OI,3)
  Z = ASIN(OI/R1)
  B = PI + Z
  A = SI-PI
  RBB = RMSI(R1,A,B,OI,2)
  YY = ASIN(OI/R2)
  B = -YY
  A = PI/2.
  RCC = RMSI(R2,A,B,OI,3)
  IQ1RMS = ((RAA + RBB + RCC)/WTS)**0.5
  B = -Y
  A = -AL
  RAA = RMSI(R3,A,B,OI,3)
  B = -GA

```



```

A = YY
RCC = RMSI(R2,A,B,OI,3)
IQ2RMS = ((RAA + RBB + RCC)/WTS)**0.5
B = -Y
A = -AL
DA = AVI(R3,A,B,OI,3)
B = PI-RO
A = PI+Z
DB = AVI(R1,A,B,OI,2)
B = -GA
A = YY
DC = AVI(R2,A,B,OI,3)
ID1AV = (-DA-DB + DC)/WTS
B = PI/2.
A = Y
DA = AVI(R3,A,B,OI,3)
B = -YY
A = PI/2.
DC = AVI(R2,A,B,OI,3)
ID2AV = (DA-DB-DC)/WTS
IQ1OFF = R2*SIN(-GA) + OI
IQ2OFF = 0.
IQ1ON = 0.
IQ2ON = 0.
ENDIF
ENDIF
GO TO 999
2100 R1 = X(1)
R2 = X(2)
R3 = X(3)
RO = X(4)
ET = X(5)
AL1 = X(6)
AL2 = X(7)
B = 0.5*PI
A = -(ET-PI)
RA = RMSI(R2,A,B,OI,3)
AA = AVV(R2,A,B,OI,3)
B = -AL1
A = AL2
RB = RMSI(R3,A,B,OI,4)
AB = AVV(R3,A,B,OI,4)
B = -(0.5*PI-RO)
A = 0.5*PI
RC = RMSI(R1,A,B,OI,3)
AC = AVV(R1,A,B,OI,3)
VAV = (AA + AB + AC)/WTS
ILRMS = ((RA + RB + RC)/WTS)**0.5
IF(IDD.EQ.23) THEN
XX = ASIN(OI/R2)
B = -XX
A = PI-ET
RAA = RMSI(R2,A,B,OI,3)
IQ1RMS = ((RAA + RB)/WTS)**0.5
B = 0.5*PI
A = XX
RAA = RMSI(R2,A,B,OI,3)
IQ2RMS = ((RAA + RB + RC)/WTS)**0.5

```

```

DA = AVI(R2,A,B,OI,3)
B = -(0.5*PI-RO)
A = 0.5*PI
DC = AVI(R1,A,B,OI,3)
ID1AV = (DA-DC)/WTS
B = -XX
A = PI-ET
DA = AVI(R2,A,B,OI,3)
ID2AV = -DA/WTS
VCPK = R2
IQ1OFF = R3*SIN(AL2)-OI
IQ2OFF = 0.
IQ1ON = 0.
IQ2ON = R3*SIN(AL1)-OI
ELSE
IF(IDD.EQ.24) THEN
  VCPK = R2
  ELSE
  VCPK = R3-1.
ENDIF
Y = ASIN(OI/R3)
B = -Y
A = AL2
RBB = RMSI(R3,A,B,OI,4)
IQ1RMS = (RBB/WTS)**0.5
IQ2RMS = ((RA + RBB + RC)/WTS)**0.5
B = 0.5*PI
A = PI-ET
DA = AVI(R2,A,B,OI,3)
B = -AL1
A = Y
DB = AVI(R3,A,B,OI,4)
B = -(0.5*PI-RO)
A = 0.5*PI
DC = AVI(R1,A,B,OI,3)
ID1AV = (DA + DB-DC)/WTS
ID2AV = DB/WTS
IQ1OFF = R3*SIN(AL2)-OI
IQ2OFF = R3*SIN(-AL1) + OI
IQ1ON = 0.
IQ2ON = 0.
ENDIF
GO TO 999
300 R1 = X(1)
R2 = X(2)
SI = X(3)
ET = X(4)
AL1 = X(5)
AL2 = X(6)
LK = 2*OI-(R2**2-1)**0.5
GA = (-PI + SI)/2.
B = PI
A = SI-PI
RA = RMSI(1.,A,B,OI,2)
AA = AVV(1.,A,B,OI,2)
B = -GA
A = PI-ET
RB = RMSI(R1,A,B,OI,3)

```

```

AB = AVV(R1,A,B,OI,3)
B = -AL1
A = AL2
RC = RMSI(R2,A,B,OI,4)
AC = AVV(R2,A,B,OI,4)
VAV = (AA + AB + AC)/WTS
OI1 = (R2**2-1)**0.5-OI
OI2 = OI
RD = LK*(OI2**2 + OI1**2 + OI1*OI2)/3.
VAV = (AA + AB + AC)/WTS
ILRMS = ((RA + RB + RC + RD)/WTS)**0.5
IF(IDD.EQ.31) THEN
  VCPK = 2.
  IQ1OFF = 0.
  IQ2OFF = 0.
  IQ1ON = -SIN(SI)-OI
  IQ2ON = R2*SIN(AL1)-OI
  Y = ASIN(OI)
  B = PI
  A = Y
  RAA = RMSI(1.,A,B,OI,2)
  IQ1RMS = ((RAA + RB + RC + RD)/WTS)**0.5
  IQ2RMS = ((RAA + RC + RD)/WTS)**0.5
  B = -Y
  A = SI-PI
  DA = AVI(1.,A,B,OI,2)
  B = -GA
  A = PI-ET
  DB = AVI(R1,A,B,OI,3)
  ID1AV = -DA/WTS
  ID2AV = -(DA + DB)/WTS
ELSE
  IF(IDD.EQ.32.OR.IDD.EQ.33) THEN
    IF(IDD.EQ.32) THEN
      VCPK = 2.
    ELSE
      VCPK = R1
    ENDIF
    IQ1OFF = OI-R1*SIN(GA)
    IQ2OFF = 0.
    IQ1ON = 0.
    IQ2ON = R2*SIN(AL1)-OI
    Y1 = ASIN(OI/R1)
    B = -Y1
    A = PI-ET
    RBB = RMSI(R1,A,B,OI,3)
    IQ1RMS = ((RA + RBB + RC + RD)/WTS)**0.5
    B = -GA
    A = Y1
    RBB = RMSI(R1,A,B,OI,3)
    IQ2RMS = ((RA + RBB + RC + RD)/WTS)**0.5
    B = -GA
    A = Y1
    DA = AVI(R1,A,B,OI,3)
    B = -Y1
    A = PI-ET
    DB = AVI(R1,A,B,OI,3)
    ID1AV = DA/WTS

```

```

ID2AV = -DB/WTS
ELSE
IF(IDD.EQ.34.OR.IDD.EQ.36) THEN
  VCPK = R1
  ELSE
  VCPK = R2-1
ENDIF
IQ1OFF = OI-R1*SIN(GA)
IQ2OFF = OI-R2*SIN(AL1)
IQ1ON = 0.
IQ2ON = 0.
IF(R2*SIN(AL2).GT.OI) THEN
  Z = ASIN(OI/R2)
  B = -Z
  A = AL2
  RCC = RMSI(R2,A,B,OI,4)
  IQ1RMS = ((RA + RCC + RD)/WTS)**0.5
  IQ2RMS = ((RA + RB + RCC + RD)/WTS)**0.5
  B = -GA
  A = PI-ET
  DA = AVI(R1,A,B,OI,3)
  B = -AL1
  A = Z
  DB = AVI(R2,A,B,OI,4)
  ID1AV = (DA + DB)/WTS
  ID2AV = DB/WTS
ELSE
  RDD = OI**3/3.
  IQ1RMS = ((RA + RDD)/WTS)**0.5
  IQ2RMS = ((RA + RB + RDD)/WTS)**0.5
  B = -GA
  A = PI-ET
  DA = AVI(R1,A,B,OI,3)
  B = -AL1
  A = AL2
  DB = AVI(R2,A,B,OI,4)
  DC = (OI-R2*SIN(AL2))**2/2.
  ID1AV = (DA + DB + DC)/WTS
  ID2AV = (DB + DC)/WTS
ENDIF
ENDIF
ENDIF
GO TO 999
400 R1 = X(1)
SI = X(2)
TH = X(3)
LK = 2*OI-R1
GA = (-PI + SI)/2.
B = PI
A = SI-PI
RA = RMSI(1.,A,B,OI,2)
AA = AVV(1.,A,B,OI,2)
B = -GA
A = PI/2.
RB = RMSI(R1,A,B,OI,3)
AB = AVV(R1,A,B,OI,3)
RC = (OI-LK)**2*TH
AC = 0.

```

```

O11 = (OI-LK)
O12 = OI
RD = LK*(O11**2 + O12**2 + O11*O12)/3.
AD = 0.
VAV = (AA + AB)/WTS
ILRMS = ((RA + RB + RC + RD)/WTS)**0.5
IF(IDD.EQ.41) THEN
  XX = ASIN(OI)
  B = PI
  A = XX
  RAA = RMSI(1.,A,B,OI,2)
  IQ1RMS = ((RAA + RB + RC + RD)/WTS)**0.5
  IQ2RMS = ((RAA + RD)/WTS)**0.5
  B = -XX
  A = SI-PI
  DA = AVI(1.,A,B,OI,2)
  B = -GA
  A = PI/2.
  DB = AVI(R1,1,B,OI,3)
  DC = TH*(OI-LK)
  ID1AV = -DA/WTS
  ID2AV = (-DA-DB + DC)/WTS
  VCPK = 2.
  IQ1OFF = 0.
  IQ2OFF = 0.
  IQ1ON = SIN(2*PI-SI)-OI
  IQ2ON = OI-LK
ELSE
IF(IDD.EQ.42.OR.IDD.EQ.43) THEN
  IF(IDD.EQ.42) THEN
    VCPK = 2.
    ELSE
    VCPK = R1
  ENDIF
  Y = ASIN(OI/R1)
  B = -Y
  A = PI/2.
  RBB = RMSI(R1,A,B,OI,3)
  IQ1RMS = ((RA + RBB + RC + RD)/WTS)**0.5
  B = -GA
  A = Y
  RBB = RMSI(R1,A,B,OI,3)
  IQ2RMS = ((RA + RBB + RD)/WTS)**0.5
  B = -GA
  A = Y
  DBB = AVI(R1,A,B,OI,3)
  ID1AV = DBB/WTS
  B = -Y
  A = PI/2.
  DBB = AVI(R1,A,B,OI,3)
  DC = TH*(OI-LK)
  ID2AV = (-DBB + DC)/WTS
  IQ1OFF = SIN(SI) + OI
  IQ2OFF = 0.
  IQ1ON = 0.
  IQ2ON = OI-LK
ELSE
  VCPK = R1

```

```

      IQ1OFF = SIN(SI) + OI
      IQ2OFF = LK - OI
      IQ1ON = 0.
      IQ2ON = 0.
      RDD = OI**3/3.
      IQ1RMS = ((RA + RDD)/WTS)**0.5
      IQ2RMS = ((RA + RB + RC + RDD)/WTS)**0.5
      B = -GA
      A = PI/2.
      DB = AVI(R1,A,B,OI,3)
      DC = (LK - OI)*TH
      DDD = (LK - OI)**2/2.
      ID1AV = (DB + DC + DDD)/WTS
      ID2AV = DDD/WTS
    ENDIF
  ENDIF
  GO TO 999
500 LK = BT
   PHI = WTS - BT
   VAV = 0.
   RA = LK**3/24.
   RB = LK**2*PHI/4.
   RC = LK**3/24.
   ILRMS = ((RA + RB + RC)/WTS)**0.5
   IQ1RMS = (RA/WTS)**0.5
   IQ2RMS = ((RA + RB)/WTS)**0.5
   ID1AV = (LK*PHI/2. + LK**2/8.)/WTS
   ID2AV = (LK**2/8.)/WTS
   IQ1OFF = LK/2.
   IQ2OFF = LK/2.
   VCPK = 0.
   IQ1ON = 0.
   IQ2ON = 0.
999 WRITE(6,3000) BS, VAV, ILRMS, VCPK
   WRITE(7,3000) BS, IQ1RMS, ID1AV, IQ1OFF, IQ1ON
   WRITE(8,3000) BS, IQ2RMS, ID2AV, IQ2OFF, IQ2ON
   IF(BT.EQ.0.AND.OI.EQ.1.0) STOP
   IF(BT.EQ.0) GO TO 10
   GO TO 15
3000 FORMAT(1X,5F14.5)
2000 FORMAT(1X,I2,1X,I2,F10.4,8F7.4)
1000 FORMAT(2F14.5)
  END
C
C *****
C *****
C *****
C
  FUNCTION RMSI(R,AL,BE,OI,IC)
  IF(IC.EQ.2.OR.IC.EQ.3.OR.IC.EQ.4) THEN
    RMSI = OI**2*(AL + BE) - 2*R*OI*(COS(BE) - COS(AL))
  1    + 0.5*R**2*(AL + BE - 0.5*SIN(2*BE) - 0.5*SIN(2*AL))
  ELSE
    IF(IC.EQ.5.OR.IC.EQ.6.OR.IC.EQ.1) THEN
      RMSI = OI**2*(AL + BE) + 2*R*OI*(COS(BE) - COS(AL))
  1    + 0.5*R**2*(AL + BE - 0.5*SIN(2*BE) - 0.5*SIN(2*AL))
    ELSE
      RMSI = -9999.

```

```
ENDIF
ENDIF
RETURN
END
```

```
C
C
C
C
C
```

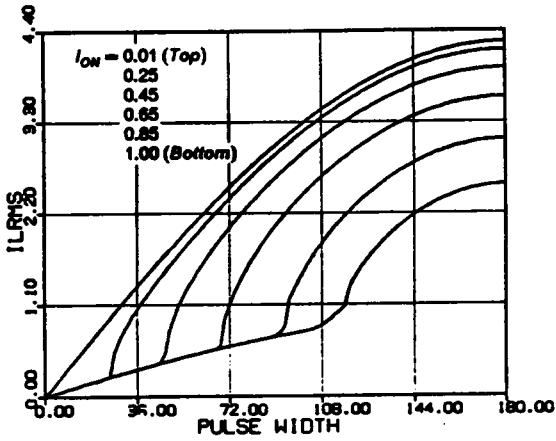
```
FUNCTION AVI(R,AL,BE,OI,IC)
IF(IC.EQ.2.OR.IC.EQ.3.OR.IC.EQ.4) THEN
  AVI = OI*(AL + BE) + R*(COS(AL)-COS(BE))
ELSE
  IF(IC.EQ.5.OR.IC.EQ.6.OR.IC.EQ.1) THEN
    AVI = -OI*(AL + BE) + R*(COS(AL)-COS(BE))
  ELSE
    AVI = -999.
  ENDIF
ENDIF
RETURN
END
```

```
C
C
C
C
C
```

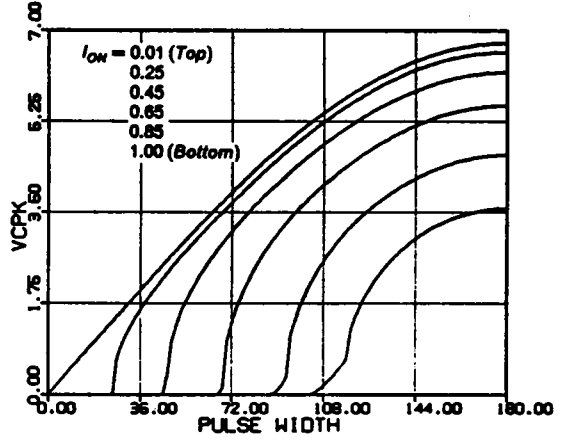
```
FUNCTION AVV(R,AL,BE,OI,IC)
IF(IC.EQ.1.OR.IC.EQ.2) THEN
  AVV = (AL + BE) + R*(SIN(AL) + SIN(BE))
ELSE
  IF(IC.EQ.3.OR.IC.EQ.6) THEN
    AVV = R*(SIN(AL) + SIN(BE))
  ELSE
    IF(IC.EQ.4.OR.IC.EQ.5) THEN
      AVV = -(AL + BE) + R*(SIN(AL) + SIN(BE))
    ELSE
      AVI = -999.
    ENDIF
  ENDIF
ENDIF
RETURN
END
```

APPENDIX C.6

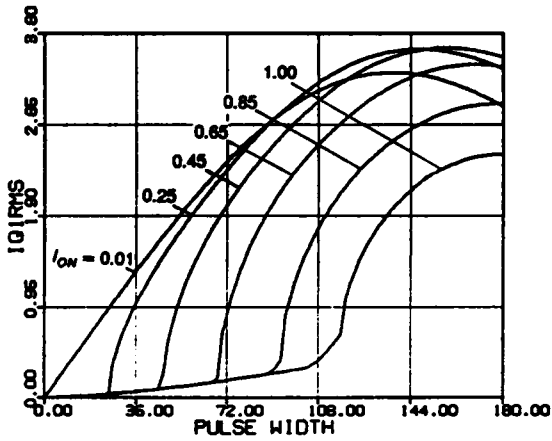
DC CHARACTERISTICS BELOW RESONANT FREQUENCY



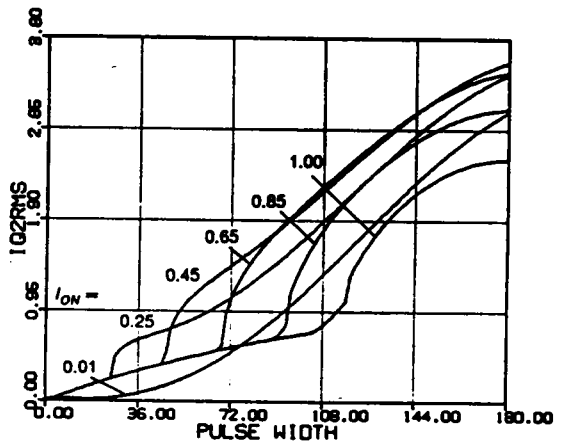
• *RMS inductor current*



• *Peak capacitor voltage*

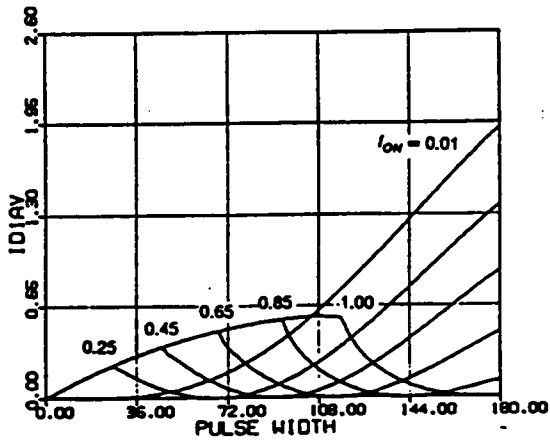


• *RMS switch current (Q1,Q3)*

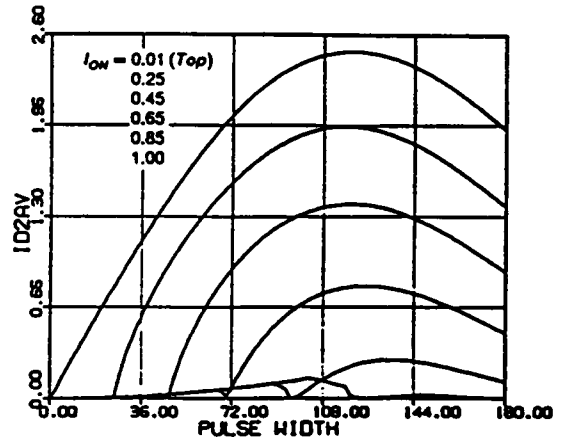


• *RMS switch current (Q2,Q4)*

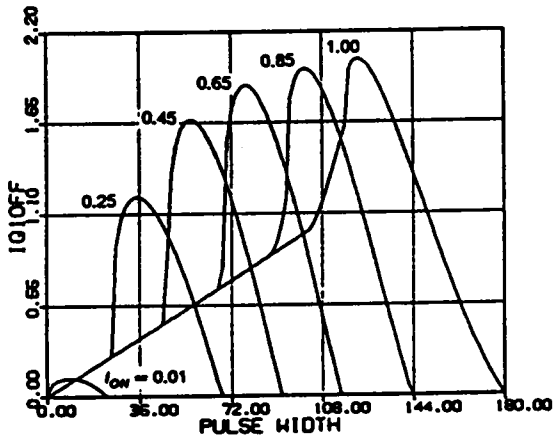
Figure C.6.1 DC Characteristics for $\omega_{SN} = 0.9$



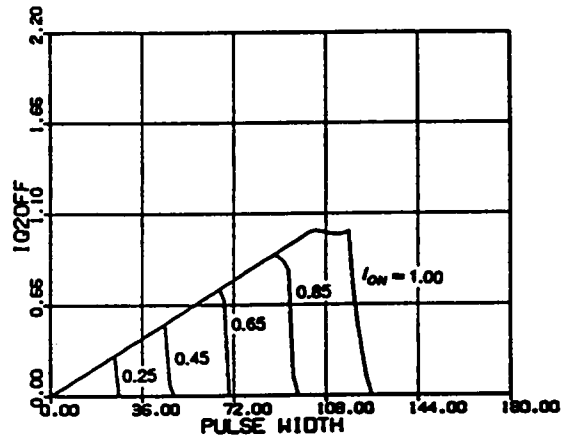
• Average diode current (D1,D3)



• Average diode current (D2,D4)

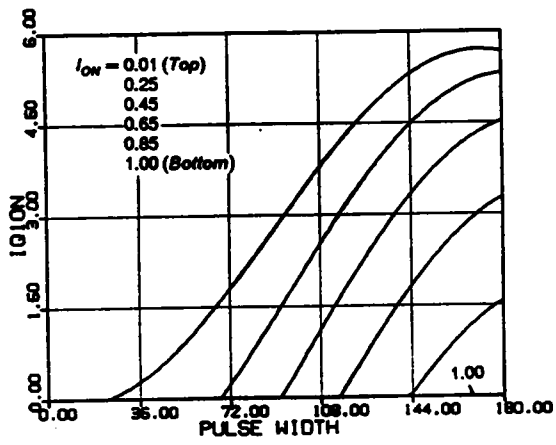


• Switch turn-off current (Q1,Q3)

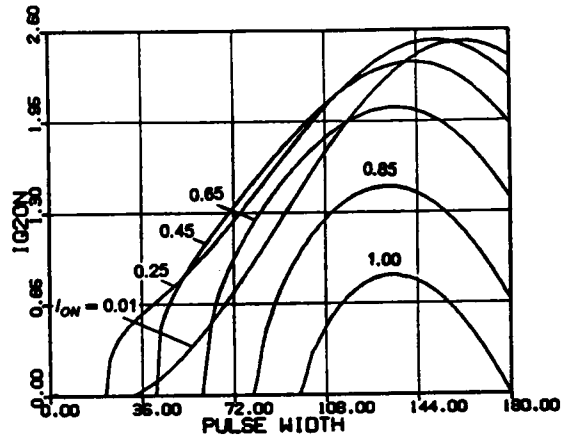


• Switch turn-off current (Q2,Q4)

Figure C.6.1 Continued



• Switch turn-on current ($Q1, Q3$)

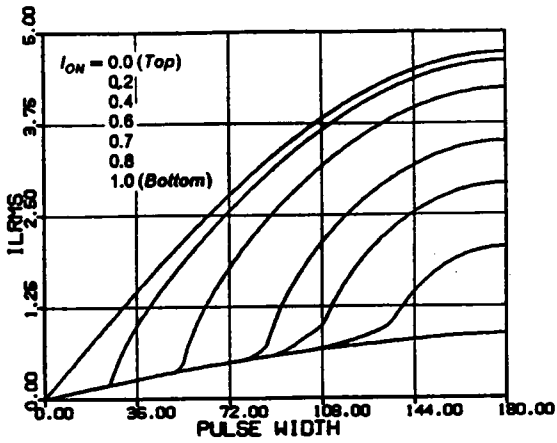


• Switch turn-on current ($Q2, Q4$)

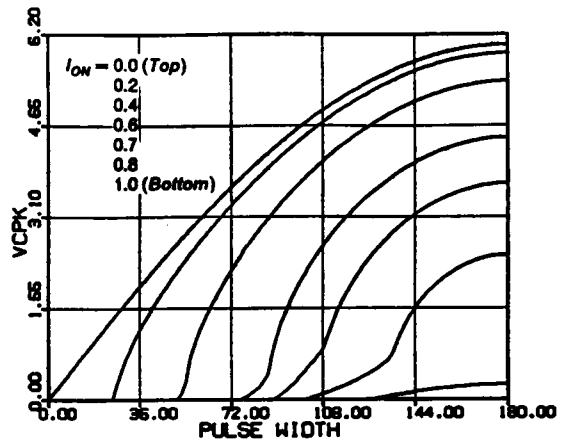
Figure C.6.1 Continued

APPENDIX C.7

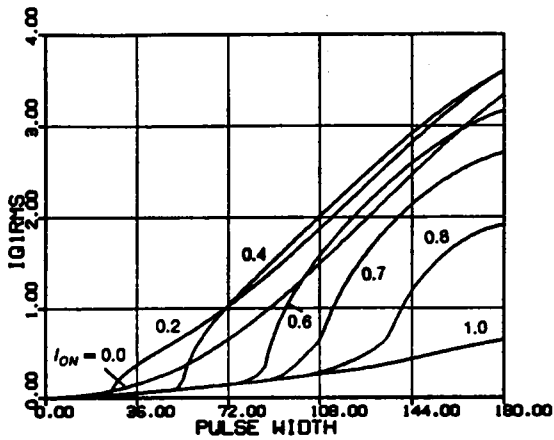
DC CHARACTERISTICS ABOVE RESONANT FREQUENCY



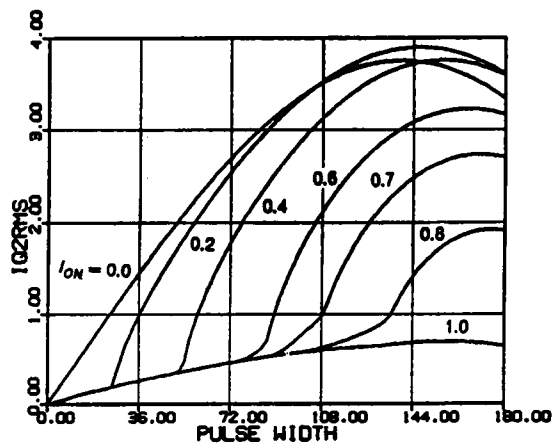
• *RMS inductor current*



• *Peak capacitor voltage*

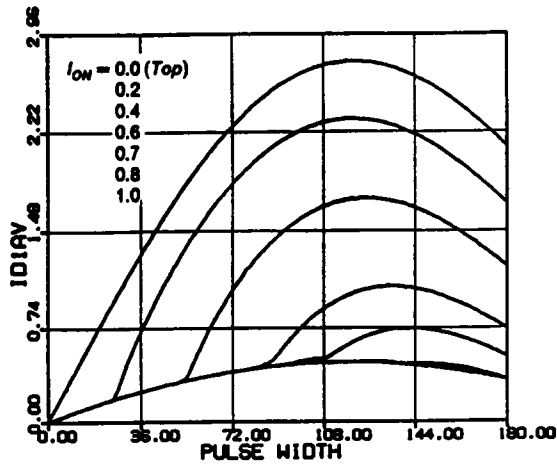


• *RMS switch current (Q1,Q3)*

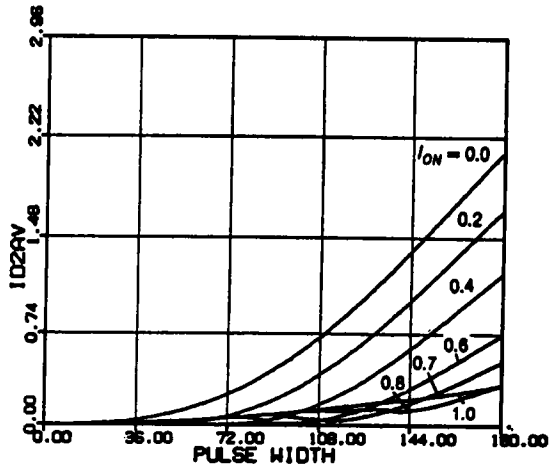


• *RMS switch current (Q2,Q4)*

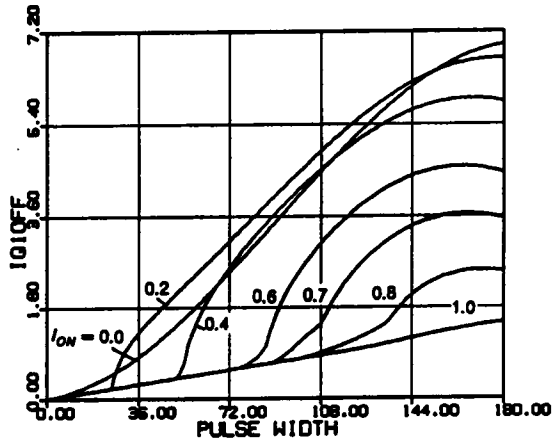
Figure C.7.1 DC Characteristics for $\omega_{SN} = 1.1$



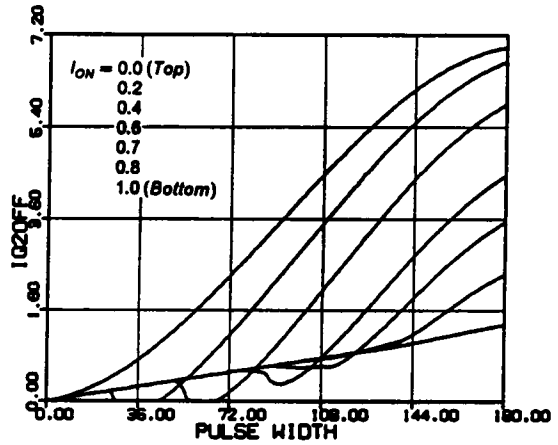
• Average diode current ($D1, D3$)



• Average diode current ($D2, D4$)

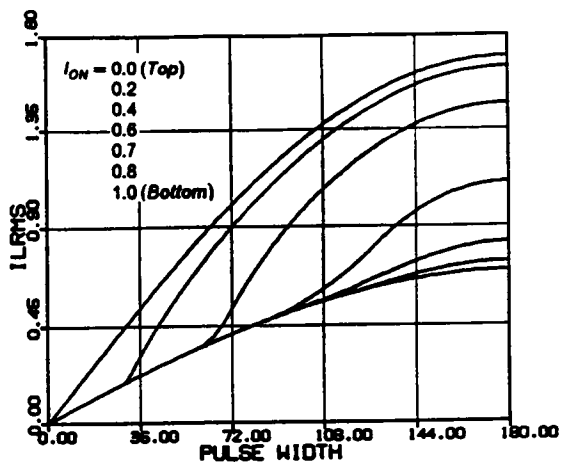


• Switch turn-off current ($Q1, Q3$)

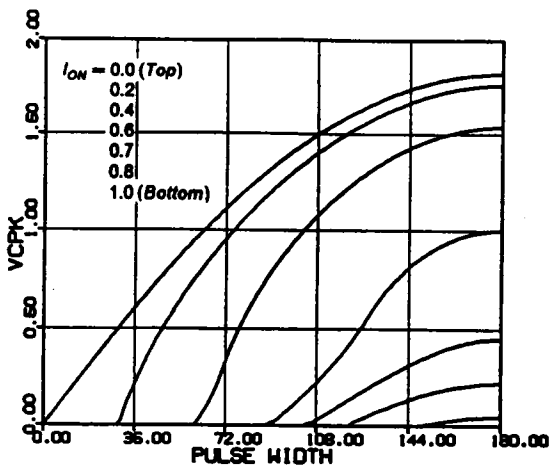


• Switch turn-off current ($Q2, Q4$)

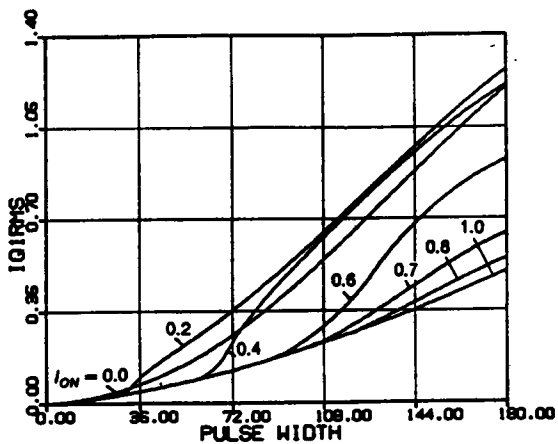
Figure C.7.1 Continued



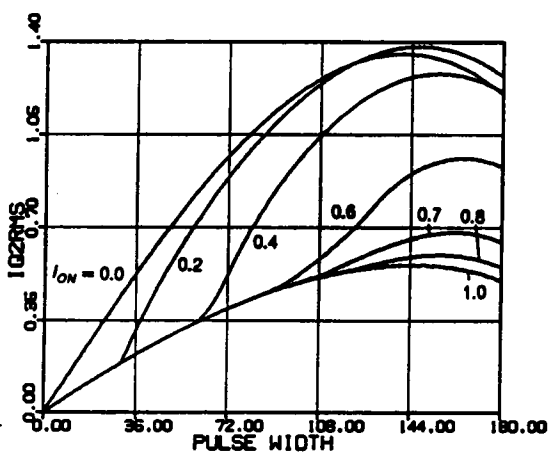
• RMS inductor current



• Peak capacitor voltage

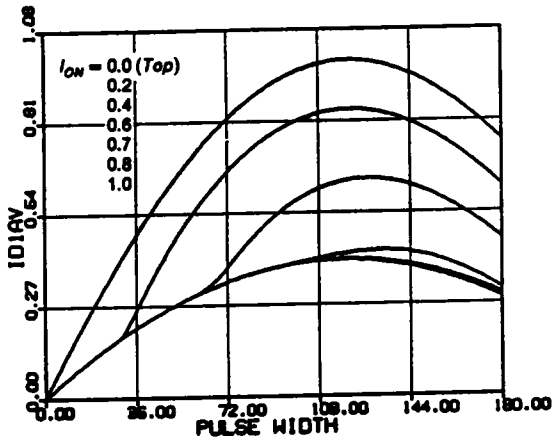


• RMS switch current (Q1,Q3)

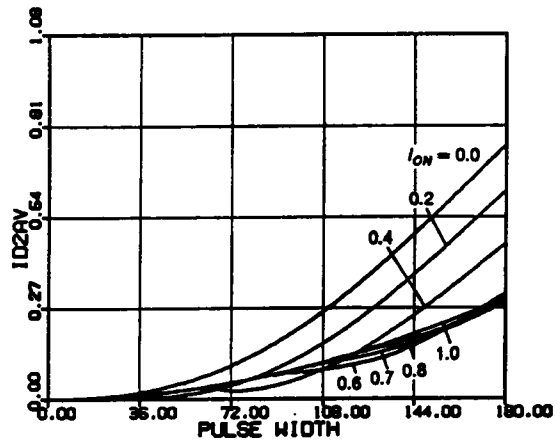


• RMS switch current (Q2,Q4)

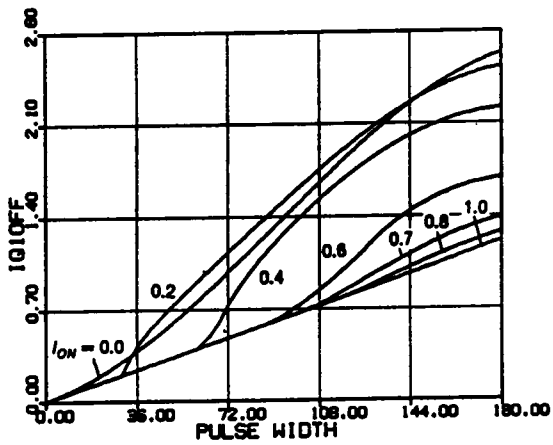
Figure C.7.2 DC Characteristics for $\omega_{SN} = 1.3$



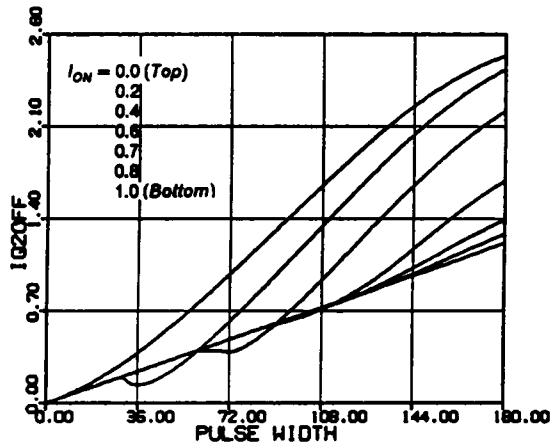
• Average diode current (D1,D3)



• Average diode current (D2,D4)

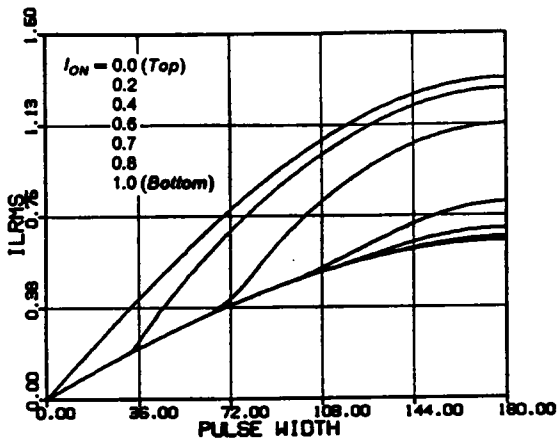


• Switch turn-off current (Q1,Q3)

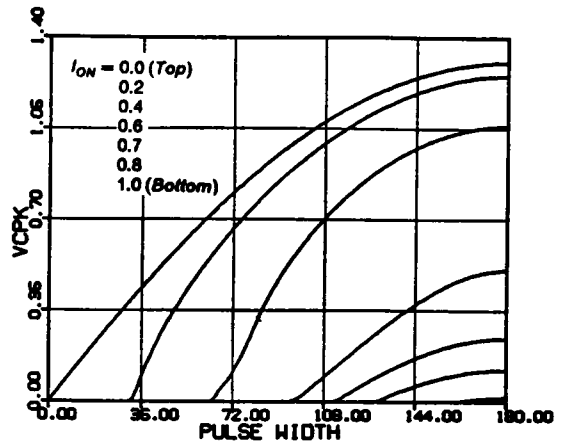


• Switch turn-off current (Q2,Q4)

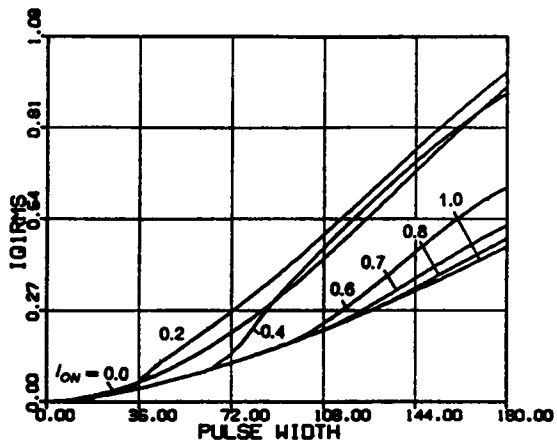
Figure C.7.2 Continued



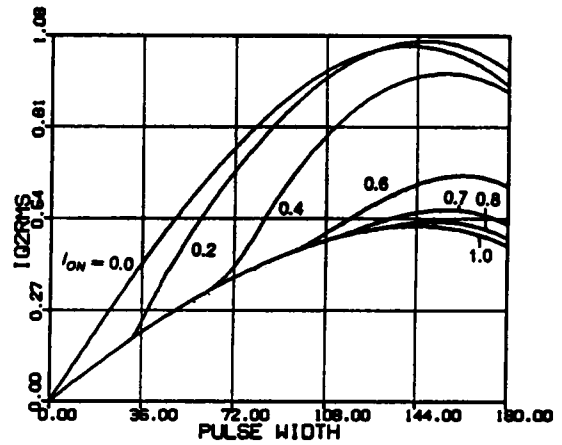
• RMS inductor current



• Peak capacitor voltage

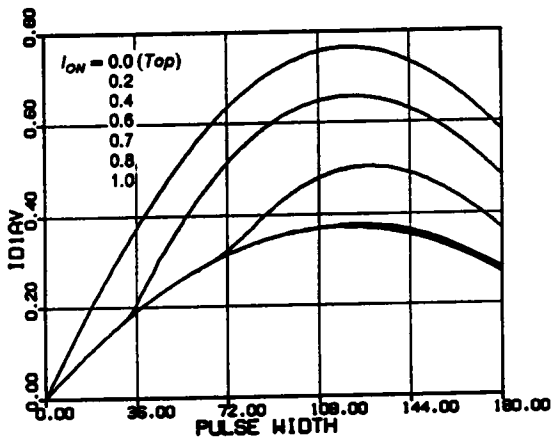


• RMS switch current ($Q1, Q3$)

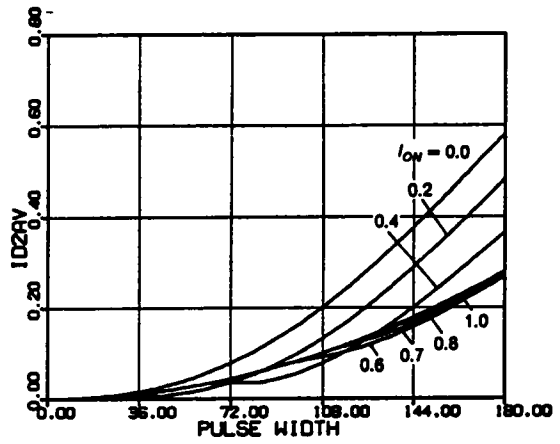


• RMS switch current ($Q2, Q4$)

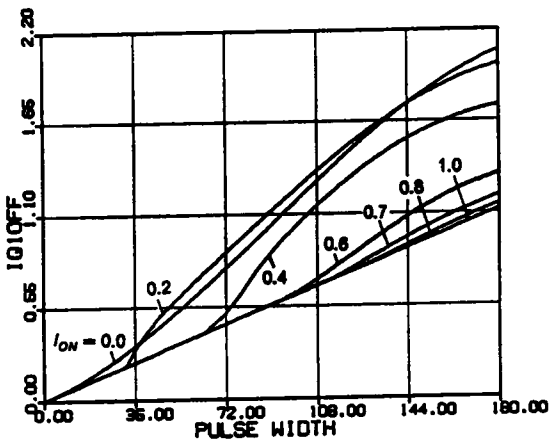
Figure C.7.3 DC Characteristics for $\omega_{SN} = 1.4$



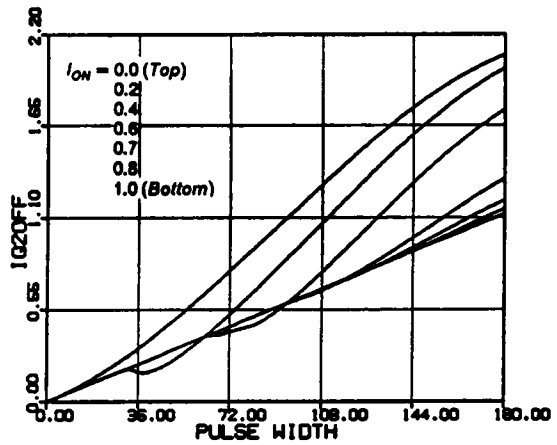
• Average diode current (D1,D3)



• Average diode current (D2,D4)



• Switch turn-off current (Q1,Q3)



• Switch turn-off current (Q2,Q4)

Figure C.7.3 Continued

APPENDIX C.8

GENERATION OF CIRCUIT WAVEFORMS OF A CM-PRC

Fortran Program for Generating Capacitor Voltage and Inductor Current Waveforms (for Both Below and Above Resonant Frequency)

```

C *****
C *****
C ***** PROGRAM : PCWAVE.FOR
C ***** FUNCTION : GENERATE DATA FOR PLOTTING WAVEFORMS AND STATE
C ***** TRAJECTORIES OF A CM-PRC. THE PROGRAM CAN BE
C ***** USED FOR BOTH BELOW AND ABOVE RESONANT FREQUENCY
C ***** CASES.
C *****
C *****
C *****
C *****
REAL ILN, VCN, LK
DIMENSION X(8)
PI=4.*ATAN(1.)
10 READ(5,*) WN, OI
IF(WN.LT.0) STOP
11 READ(5,1000) ID,IDD,BS,(X(K), K = 1,8)
WTS=PI/WN
BT=(BS/180)*WTS
DT=WTS/200.
WT=0.
YT=0.
IF(ID.EQ.1) GO TO 100
IF(ID.EQ.2) GO TO 200
IF(ID.EQ.21) GO TO 2100
IF(ID.EQ.3) GO TO 300
IF(ID.EQ.4) GO TO 400
IF(ID.EQ.5) GO TO 500
100 R1=X(1)
R2=X(2)
R3=X(3)
RO=X(4)
SI=X(5)
ET=X(6)
AL1=X(7)
AL2=X(8)
GA=(1-1/WN)*PI-ET+BT
T=PI-GA
101 IF(T.LE.ET) GO TO 102
ILN=R2*SIN(T)-OI
VCN=R2*COS(T)
WRITE(6,2000) WT,VCN,ILN
WRITE(7,2000) WT,ILN
T=T-DT
WT=WT+DT*180/WTS
GO TO 101
102 T=PI-AL1
YT=YT+(PI-GA-ET)
WT=WT+180*WN/PI
103 IF(T.LT.(PI-AL2)) GO TO 104

```

```

ILN = R3*SIN(T)-OI
VCN = R3*COS(T) + 1
WRITE(6,2000) WT,VCN,ILN
WRITE(7,2000) WT,ILN
T = T-DT
WT = WT + DT*180/WTS
GO TO 103
104 T = PI-RO
YT = YT + (AL2-AL1)
WT = YT*180*WN/PI
105 IF(T.LT.(PI-SI)) GO TO 106
ILN = R1*SIN(T) + OI
VCN = R1*COS(T) + 1
WRITE(6,2000) WT,VCN,ILN
WRITE(7,2000) WT,ILN
T = T-DT
WT = WT + DT*180/WTS
GO TO 105
106 T = -GA
YT = YT + (SI-RO)
WT = YT*180*WN/PI
107 IF(T.LT.(-PI + ET)) GO TO 108
ILN = R2*SIN(T) + OI
VCN = R2*COS(T)
WRITE(6,2000) WT,VCN,ILN
WRITE(7,2000) WT,ILN
T = T-DT
WT = WT + DT*180/WTS
GO TO 107
108 T = -AL1
YT = YT + (PI-GA-ET)
WT = YT*180*WN/PI
109 IF(T.LT.-AL2) GO TO 110
ILN = R3*SIN(T) + OI
VCN = R3*COS(T)-1
WRITE(6,2000) WT,VCN,ILN
WRITE(7,2000) WT,ILN
T = T-DT
WT = WT + DT*180/WTS
GO TO 109
110 T = -RO
YT = YT + (AL2-AL1)
WT = YT*180*WN/PI
111 IF(T.LT.(-SI)) GO TO 112
ILN = R1*SIN(T)-OI
VCN = R1*COS(T)-1
WRITE(6,2000) WT,VCN,ILN
WRITE(7,2000) WT,ILN
T = T-DT
WT = WT + DT*180/WTS
GO TO 111
112 T = PI-GA
YT = YT + (SI-RO)
WT = YT*180*WN/PI
113 IF(T.LT.ET) GO TO 10
ILN = R2*SIN(T)-OI
VCN = R2*COS(T)
WRITE(6,2000) WT,VCN,ILN
WRITE(7,2000) WT,ILN
T = T-DT
WT = WT + DT*180/WTS

```

```

GO TO 113
200 R1 = X(1)
    R2 = X(2)
    RO = X(3)
    SI = X(4)
    AL = X(5)
    GA = (1-1/WN)*PI-AL + BT
    T = PI-GA
201 IF(T.LT.(PI/2.)) GO TO 202
    ILN = R2*SIN(T)-OI
    VCN = R2*COS(T)
    WRITE(6,2000) WT,VCN,ILN
    WRITE(7,2000) WT,ILN
    T = T-DT
    WT = WT + DT*180/WTS
    GO TO 201
202 T = PI/2.
    YT = YT + (PI/2.-GA)
    WT = YT*180*WN/PI
203 IF(T.LT.AL) GO TO 204
    ILN = (R2-2*OI)*SIN(T) + OI
    VCN = (R2-2*OI)*COS(T)
    WRITE(6,2000) WT,VCN,ILN
    WRITE(7,2000) WT,ILN
    T = T-DT
    WT = WT + DT*180/WTS
    GO TO 203
204 T = PI-RO
    YT = YT + (PI/2.-AL)
    WT = YT*180*WN/PI
205 IF(T.LT.(PI-SI)) GO TO 206
    ILN = R1*SIN(T) + OI
    VCN = R1*COS(T) + 1
    WRITE(6,2000) WT,VCN,ILN
    WRITE(7,2000) WT,ILN
    T = T-DT
    WT = WT + DT*180/WTS
    GO TO 205
206 T = -GA
    YT = YT + (SI-RO)
    WT = YT*180*WN/PI
207 IF(T.LT.-PI/2.) GO TO 208
    ILN = R2*SIN(T) + OI
    VCN = R2*COS(T)
    WRITE(6,2000) WT,VCN,ILN
    WRITE(7,2000) WT,ILN
    T = T-DT
    WT = WT + DT*180/WTS
    GO TO 207
208 T = -PI/2.
    YT = YT + (PI/2.-GA)
    WT = YT*180*WN/PI
209 IF(T.LT.(-PI + AL)) GO TO 210
    ILN = (R2-2*OI)*SIN(T)-OI
    VCN = (R2-2*OI)*COS(T)
    WRITE(6,2000) WT,VCN,ILN
    WRITE(7,2000) WT,ILN
    T = T-DT
    WT = WT + DT*180/WTS
    GO TO 209
210 T = -RO

```

```

YT = YT + (PI/2.-AL)
WT = YT*180*WN/PI
211 IF(T.LT.(-SI)) GO TO 212
ILN = R1*SIN(T)-OI
VCN = R1*COS(T)-1
WRITE(6,2000) WT,VCN,ILN
WRITE(7,2000) WT,ILN
T = T-DT
WT = WT + DT*180/WTS
GO TO 211
212 T = PI-GA
YT = YT + (SI-RO)
WT = YT*180*WN/PI
213 IF(T.LT.(PI/2.)) GO TO 10
ILN = R2*SIN(T)-OI
VCN = R2*COS(T)
WRITE(6,2000) WT,VCN,ILN
WRITE(7,2000) WT,ILN
T = T-DT
WT = WT + DT*180/WTS
GO TO 213
2100 R1 = X(1)
R2 = X(2)
R3 = X(3)
RO = X(4)
ET = X(5)
AL1 = X(6)
AL2 = X(7)
T = -0.5*PI + RO
2101 IF(T.LT.(-PI/2.)) GO TO 2102
ILN = R1*SIN(T) + OI
VCN = R1*COS(T)
WRITE(6,2000) WT,VCN,ILN
WRITE(7,2000) WT,ILN
T = T-DT
WT = WT + DT*180/WTS
GO TO 2101
2102 T = -PI/2.
YT = YT + RO
WT = YT*180*WN/PI
2103 IF(T.LT.(ET-2*PI)) GO TO 2104
ILN = (R1-2*OI)*SIN(T)-OI
VCN = (R1-2*OI)*COS(T)
WRITE(6,2000) WT,VCN,ILN
WRITE(7,2000) WT,ILN
T = T-DT
WT = WT + DT*180/WTS
GO TO 2103
2104 T = -PI-AL1
YT = YT + (1.5*PI-ET)
WT = YT*180*WN/PI
2105 IF(T.LT.(-PI-AL2)) GO TO 2106
ILN = R3*SIN(T)-OI
VCN = R3*COS(T) + 1
WRITE(6,2000) WT,VCN,ILN
WRITE(7,2000) WT,ILN
T = T-DT
WT = WT + DT*180/WTS
GO TO 2105
2106 T = 0.5*PI + RO
YT = YT + (AL2-AL1)

```

```

WT = YT*180*WN/PI
2107 IF(T.LT.PI/2.) GO TO 2108
ILN = R1*SIN(T)-OI
VCN = R1*COS(T)
WRITE(6,2000) WT,VCN,ILN
WRITE(7,2000) WT,ILN
T = T-DT
WT = WT + DT*180/WTS
GO TO 2107
2108 T = PI/2.
YT = YT + RO
WT = YT*180*WN/PI
2109 IF(T.LT.(ET-PI)) GO TO 2110
ILN = (R1-2*OI)*SIN(T) + OI
VCN = (R1-2*OI)*COS(T)
WRITE(6,2000) WT,VCN,ILN
WRITE(7,2000) WT,ILN
T = T-DT
WT = WT + DT*180/WTS
GO TO 2109
2110 T = -AL1
YT = YT + (1.5*PI-ET)
WT = YT*180*WN/PI
2111 IF(T.LT.(-AL2)) GO TO 2112
ILN = R3*SIN(T) + OI
VCN = R3*COS(T)-1
WRITE(6,2000) WT,VCN,ILN
WRITE(7,2000) WT,ILN
T = T-DT
WT = WT + DT*180/WTS
GO TO 2111
2112 T = -0.5*PI + RO
YT = YT + (AL2-AL1)
WT = YT*180*WN/PI
2113 IF(T.LT.(-PI/2.)) GO TO 2114
ILN = R1*SIN(T) + OI
VCN = R1*COS(T)
WRITE(6,2000) WT,VCN,ILN
WRITE(7,2000) WT,ILN
T = T-DT
WT = WT + DT*180/WTS
GO TO 2113
300 R1 = X(1)
R2 = X(2)
SI = X(3)
ET = X(4)
AL1 = X(5)
AL2 = X(6)
GA = 0.5*(-PI + SI)
LK = 2*OI-(R2**2-1)**0.5
T = PI-GA
301 IF(T.LT.ET) GO TO 302
ILN = R1*SIN(T)-OI
VCN = R1*COS(T)
WRITE(6,2000) WT,VCN,ILN
WRITE(7,2000) WT,ILN
T = T-DT
WT = WT + DT*180/WTS
GO TO 301
302 T = PI-AL1
YT = YT + (PI-ET-GA)

```

```

WT = YT*180*WN/PI
303 IF(T.LT.(PI-AL2)) GO TO 304
ILN = R2*SIN(T)-OI
VCN = R2*COS(T)+1.
WRITE(6,2000) WT,VCN,ILN
WRITE(7,2000) WT,ILN
T = T-DT
WT = WT + DT*180/WTS
GO TO 303
304 T = 0.
YT = YT + (AL2-AL1)
WT = YT*180*WN/PI
305 IF(T.GT.LK) GO TO 306
ILN = OI-LK + T
VCN = 0.
WRITE(6,2000) WT,VCN,ILN
WRITE(7,2000) WT,ILN
T = T + DT
WT = WT + DT*180/WTS
GO TO 305
306 T = PI
YT = YT + LK
WT = YT*180*WN/PI
307 IF(T.LT.(PI-SI)) GO TO 308
ILN = SIN(T) + OI
VCN = COS(T) + 1
WRITE(6,2000) WT,VCN,ILN
WRITE(7,2000) WT,ILN
T = T-DT
WT = WT + DT*180/WTS
GO TO 307
308 T = -GA
YT = YT + SI
WT = YT*180*WN/PI
309 IF(T.LT.(ET-PI)) GO TO 310
ILN = R1*SIN(T) + OI
VCN = R1*COS(T)
WRITE(6,2000) WT,VCN,ILN
WRITE(7,2000) WT,ILN
T = T-DT
WT = WT + DT*180/WTS
GO TO 309
310 T = -AL1
YT = YT + (PI-ET-GA)
WT = YT*180*WN/PI
311 IF(T.LT.-AL2) GO TO 312
ILN = R2*SIN(T) + OI
VCN = R2*COS(T)-1
WRITE(6,2000) WT,VCN,ILN
WRITE(7,2000) WT,ILN
T = T-DT
WT = WT + DT*180/WTS
GO TO 311
312 T = 0.
YT = YT + (AL2-AL1)
WT = YT*180*WN/PI
313 IF(T.GT.LK) GO TO 314
ILN = -OI + LK-T
VCN = 0.
WRITE(6,2000) WT,VCN,ILN
WRITE(7,2000) WT,ILN

```

```

T = T + DT
WT = WT + DT*180/WTS
GO TO 313
314 T = 0.
YT = YT + LK
WT = YT*180*WN/PI
315 IF(T.LT.(-SI)) GO TO 316
ILN = SIN(T)-OI
VCN = COS(T)-1
WRITE(6,2000) WT,VCN,ILN
WRITE(7,2000) WT,ILN
T = T-DT
WT = WT + DT*180/WTS
GO TO 315
316 T = PI-GA
YT = YT + SI
WT = YT*180*WN/PI
317 IF(T.LT.ET) GO TO 10
ILN = R1*SIN(T)-OI
VCN = R1*COS(T)
WRITE(6,2000) WT,VCN,ILN
WRITE(7,2000) WT,ILN
T = T-DT
WT = WT + DT*180/WTS
GO TO 317
400 R1 = X(1)
SI = X(2)
TH = X(3)
LK = 2*OI-R1
GA = 0.5*(-PI + SI)
T = PI-GA
401 IF(T.LT.PI/2.) GO TO 402
ILN = R1*SIN(T)-OI
VCN = R1*COS(T)
WRITE(6,2000) WT,VCN,ILN
WRITE(7,2000) WT,ILN
T = T-DT
WT = WT + DT*180/WTS
GO TO 401
402 T = 0.
YT = YT + (0.5*PI-GA)
WT = YT*180*WN/PI
403 IF(T.GT.TH) GO TO 404
ILN = OI-LK
VCN = 0.
WRITE(6,2000) WT,VCN,ILN
WRITE(7,2000) WT,ILN
T = T + DT
WT = WT + DT*180/WTS
GO TO 403
404 T = 0.
YT = YT + TH
WT = YT*180*WN/PI
405 IF(T.GT.LK) GO TO 406
ILN = OI-LK + T
VCN = 0.
WRITE(6,2000) WT,VCN,ILN
WRITE(7,2000) WT,ILN
T = T + DT
WT = WT + DT*180/WTS
GO TO 405

```

```

406 T=PI
   YT=YT+LK
   WT=YT*180*WN/PI
407 IF(T.LT.(PI-SI)) GO TO 408
   ILN=SIN(T)+OI
   VCN= COS(T)+1
   WRITE(6,2000) WT,VCN,ILN
   WRITE(7,2000) WT,ILN
   T=T-DT
   WT=WT+DT*180/WTS
   GO TO 407
408 T=-GA
   YT=YT+SI
   WT=YT*180*WN/PI
409 IF(T.LT.-PI/2.) GO TO 410
   ILN=R1*SIN(T)+OI
   VCN=R1*COS(T)
   WRITE(6,2000) WT,VCN,ILN
   WRITE(7,2000) WT,ILN
   T=T-DT
   WT=WT+DT*180/WTS
   GO TO 409
410 T=0.
   YT=YT+(0.5*PI-GA)
   WT=YT*180*WN/PI
411 IF(T.GT.TH) GO TO 412
   ILN=-OI+LK
   VCN=0.
   WRITE(6,2000) WT,VCN,ILN
   WRITE(7,2000) WT,ILN
   T=T+DT
   WT=WT+DT*180/WTS
   GO TO 411
412 T=0.
   YT=YT+TH
   WT=YT*180*WN/PI
413 IF(T.GT.LK) GO TO 414
   ILN=-OI+LK-T
   VCN=0.
   WRITE(6,2000) WT,VCN,ILN
   WRITE(7,2000) WT,ILN
   T=T+DT
   WT=WT+DT*180/WTS
   GO TO 413
414 T=0.
   YT=YT+LK
   WT=YT*180*WN/PI
415 IF(T.LT.(-SI)) GO TO 416
   ILN=SIN(T)-OI
   VCN= COS(T)-1
   WRITE(6,2000) WT,VCN,ILN
   WRITE(7,2000) WT,ILN
   T=T-DT
   WT=WT+DT*180/WTS
   GO TO 415
416 T=(PI-GA)
   YT=YT+SI
   WT=YT*180*WN/PI
417 IF(T.LT.PI/2.) GO TO 418
   ILN=R1*SIN(T)-OI
   VCN=R1*COS(T)

```



```

WRITE(6,2000) WT,VCN,ILN
WRITE(7,2000) WT,ILN
T = T - DT
WT = WT + DT*180/WTS
GO TO 417
418 T = 0.
YT = YT + (0.5*pi-GA)
WT = YT*180*WN/PI
419 IF(T.GT.TH) GO TO 10
ILN = OI-LK
VCN = 0.
WRITE(6,2000) WT,VCN,ILN
WRITE(7,2000) WT,ILN
T = T + DT
WT = WT + DT*180/WTS
GO TO 419
500 LK = BT
TH = PI/WN-BT
T = 0.
501 IF(T.GT.TH) GO TO 502
ILN = -LK/2.
VCN = 0.
WRITE(6,2000) WT,VCN,ILN
WRITE(7,2000) WT,ILN
T = T + DT
WT = WT + DT*180/WTS
GO TO 501
502 T = 0.
YT = YT + TH
WT = YT*180*WN/PI
503 IF(T.GT.LK) GO TO 504
ILN = T-LK/2.
VCN = 0.
WRITE(6,2000) WT,VCN,ILN
WRITE(7,2000) WT,ILN
T = T + DT
WT = WT + DT*180/WTS
GO TO 503
504 T = 0.
YT = YT + LK
WT = YT*180*WN/PI
505 IF(T.GT.TH) GO TO 506
ILN = LK/2.
VCN = 0.
WRITE(6,2000) WT,VCN,ILN
WRITE(7,2000) WT,ILN
T = T + DT
WT = WT + DT*180/WTS
GO TO 505
506 T = 0.
YT = YT + TH
WT = YT*180*WN/PI
507 IF(T.GT.LK) GO TO 508
ILN = LK/2.-T
VCN = 0.
WRITE(6,2000) WT,VCN,ILN
WRITE(7,2000) WT,ILN
T = T + DT
WT = WT + DT*180/WTS
GO TO 507
508 T = 0.

```

```
YT = YT + LK
WT = YT * 180 * WN / PI
509 IF (T.GT.TH) GO TO 10
ILN = -LK / 2.
VCN = 0.
WRITE(6,2000) WT,VCN,ILN
WRITE(7,2000) WT,ILN
T = T + DT
WT = WT + DT * 180 / WTS
GO TO 509
1000 FORMAT(I2,1X,I2,F10.4,8F7.4)
2000 FORMAT(4F14.5)
END
```

**The vita has been removed from
the scanned document**